STUDY OF THE SUPERCRITICAL EXTRACTION OF FLAVONOIDS FROM DISTILLATION RESIDUES OF PHENYLPROPANOID-PRODUCING PLANTS

ÁNDERSON JULIÁN ARIAS VELANDIA

UNIVERSIDAD INDUSTRIAL DE SANTANDER
FACULTAD DE INGENIERÍAS FÍSICOQUÍMICAS
ESCUELA DE INGENIERÍA QUÍMICA
BUCARAMANGA
2021

STUDY OF THE SUPERCRITICAL EXTRACTION OF FLAVONOIDS FROM DISTILLATION RESIDUES OF PHENYLPROPANOID-PRODUCING PLANTS

ÁNDERSON JULIÁN ARIAS VELANDIA

A thesis submitted in fulfillment of the requirements
for the degree of Doctor of Philosophy in Chemical Engineering

Directors
Dr. Jairo René MARTÍNEZ-MORALES
Dr. Elena STASHENKO

UNIVERSIDAD INDUSTRIAL DE SANTANDER
FACULTAD DE INGENIERÍAS FÍSICOQUÍMICAS
ESCUELA DE INGENIERÍA QUÍMICA
BUCARAMANGA
2021

DEDICATORY

To my parents and wife.

ACKNOWLEDGEMENTS

Financial support from Universidad Industrial de Santander through VIE project number 1872, calls for student mobility 2013-2016, and CROM-MASS; Patrimonio Autónomo Fondo Nacional de Financiamiento para la Ciencia, la Tecnología y la Innovación, Francisco José de Caldas, through contract RC 0572-2012; CASSS through its Travel Reimbursement Grant for the 22nd International Symposium on Separation Sciences, and AGCI Chile through the student and academic mobility program of the Pacific Alliance are acknowledged. Author acknowledge the economic support of Departamento Administrativo de Ciencia, Tecnología e Innovación de Colombia (COLCIENCIAS) through the Ph.D. Scholarship, Call 567 of 2012.

Supervisors, Prof. Elena Stashenko and Prof. Jairo René Martínez, are especially gratefully acknowledged for their work to train me as a scientific, citizen, autonomous, thinking, and rational individual. Their teachings transcended the strictly academic and transformed my way of perceiving and understanding nature and our interaction with it. My eternal gratitude, respect, and admiration. I'm not sure if I'll ever be as good a scientist as they are. Prof. José M. del Valle and Prof. Juan de la Fuente are gratefully acknowledged for their guidance, motivating effect, and exceptional expert support in my doctoral research internship in Chile. Ayleen Acuña and the UIS Chemical Engineering Professors: Cisóstomo Barajas, Débora Nabarlatz, Ramiro Martínez, and Carlos Muvdi are gratefully acknowledged for their teachings and support overcoming the consequences of the accident that hampered the normal development of my Ph.D. study.

Diego Castiblanco is gratefully acknowledged for their contribution with the experimental development of Tables 5 and 7. Andrea Gómez and Giocarlo Vásquez are gratefully acknowledged for their contribution with the experimental development of Tables 8 - 10. Sergio Rincón, Luz Díaz and Andrés Cáceres are gratefully acknowled-

ged for their contribution with the experimental development of Appendix 4. Andrés Cáceres is gratefully acknowledged for their contribution with the experimental development of Table 17, Fig. 20 - 22, Table 18, and Fig. 23. Adolfo Cabrera and Alex Shultz are gratefully acknowledged for their support in the experimental measurement of nobiletin and pinocembrin (in extract) solubilities. Yuri Córdoba and Jésica Mejía are gratefully acknowledged for their contribution with the analytic chemistry necessary to produce Table 12 and Figure 15. Sergio Rivero, Sergio Beltrán, Andrés Cáceres and Prof. Omar Gélvez are gratefully acknowledged for their support in the technological development of the work. Daniel Casas and Adolfo Cabrera are gratefully acknowledged for their support in the mathematical development of the work.

CONTENTS

LIST OF FIGURES

pg.

---

[1] Tom O'Haver. *Curve fitting B: Multicomponent Spectroscopy*. `http://terpconnect.umd.edu/~toh/spectrum/CurveFittingB.html`. Accedido: 2020-02-03. 2014.

[2] José M. del Valle y Freddy a. Urrego. «Free solute content and solute-matrix interactions affect apparent solubility and apparent solute content in supercritical CO2 extractions. A hypothesis paper». En: *Journal of Supercritical Fluids* 66 (2012), págs. 157-175. DOI: `10.1016/j.supflu.2011.10.006`.

LIST OF TABLES

LIST OF APPENDICES

ABBREVIATIONS

ext	**ext**ract
m	**m**ixture of CO_2 and EtOH, pseudo-component
sc	**s**uper**c**ritical
sol	**sol**ute
solv	**solv**ent
subs	**subs**trate
BIC	**B**roken and **I**ntact **C**ells model
CLS	**C**lassical **L**east **S**quares
CM	**C**hopped **M**aterial
CW	**C**uticular **W**axes
DS	**D**ata **S**et
ED	**E**xternal **D**iameter
EIEC	**E**quilibrium **I**ntegral **E**xtraction **C**urves
EtOH	**Et**thanol (C_2H_5**OH**)
`Gn`	**G**alangi**n**
ID	**I**nner **D**iameter
IEC	**I**ntegral **E**xtraction **C**urves
ILS	**I**nverse **L**east **S**quares
`Intf`	**Int**er**f**erence
L	**L**ength
LG	***L**ippia **g**raveolens*
LO	***L**ippia **o**riganoides*
LOC	***L**ippia **o**riganoides* **c**arvacrol-rich chemotype
LOP	***L**ippia **o**riganoides* **p**hellandrene-rich chemotype

LOT	***L**ippia **o**riganoides* **t**hymol-rich chemotype
LP	**L**arge **P**ellets, 4 mm
LOO	**L**eave **O**ne **O**ut crossing validation method
MeOH	**Me**thanol (CH_3**OH**)
Pn	**P**inocembri**n**
PSRK	**P**redictive **S**oave-**R**edlich-**K**wong EoS
RSD	**R**elative **S**tandard **D**eviation
Sep	**Sep**arator
SP	**S**mall **P**ellets, 2.5 mm

CONSTANTS

CO_2 hard-sphere diameter	$\sigma_{CO_2} = 3.26\,\text{Å}$
EtOH hard-sphere diameter	$\sigma_{EtOH} = 4.24\,\text{Å}$
CO_2 minimum dual potential energy per Boltzmann constant	$(\epsilon/k)_{CO_2} = 500.71\,\text{K}$
EtOH minimum dual potential energy per Boltzmann constant	$(\epsilon/k)_{EtOH} = 1291.41\,\text{K}$
CO_2 normal-boiling molar volume	$v_{\mathrm{b}_{CO_2}} = 33.32\,\text{cm}^3\,\text{mol}^{-1}$
EtOH normal-boiling molar volume	$v_{\mathrm{b}_{EtOH}} = 62.52\,\text{cm}^3\,\text{mol}^{-1}$

SYMBOLS

a_0	specific surface area per unit volume of extraction bed	m^{-1}
a_s	specific area between the regions of intact and broken cells	m^{-1}
$\boldsymbol{b}$	model parameter matrix	$\mathrm{mol\,L}^{-1}$
$\boldsymbol{c}$	matrix of unknown concentration	$\mathrm{mol\,L}^{-1}$
d	diameter	mm
d_p	particle diameter or particle size	µm,mm
$\boldsymbol{e}$	vector or matrix of noise	$\mathrm{mol\,L}^{-1}$
e_i	yield of component (i)	$\mathrm{g_{sol}/kg_{subs}}$
f_2^{solid}	solid phase fugacity of the solute	MPa
f_2^F	fugacity of the solute in the supercritical phase	MPa
h	height or axial co-ordinate	mm,cm,m
j_f	flux from broken cells to solvent	$\mathrm{kg\,m}^{-3}\,\mathrm{s}^{-1}$
j_s	flux from intact cells to broken cells	$\mathrm{kg\,m}^{-3}\,\mathrm{s}^{-1}$
k_s	solid-phase mass transfer coefficient	s
k_f	fluid-phase mass transfer coefficient	s
$\boldsymbol{r}$	matrix of measured absorbance data	unitless
r	grinding efficiency (fraction of broken cells)	unitless
t	time	$\mathrm{mín}$,s
t_r	solvent residense time (H/U)	s

v_{bm}	normal-boiling molar volume of the solvent mixture	$\mathrm{cm^3\,mol^{-1}}$
v_{b1}	normal-boiling molar volume of pinocembrin	$\mathrm{cm^3\,mol^{-1}}$
v_2^{solid}	molar volume of the solid	$\mathrm{cm^3\,mol^{-1}}$
w	weight	kg
x_{t}	transition concentration	$\mathrm{kg_{sol}/kg_{subs}}$
x_{u}	concentration in the untreated solid or solute available in substrate	$\mathrm{kg_{sol}/kg_{subs}}$
x_1	concentration in broken cells	$\mathrm{kg_{sol}/kg_{subs}}$
$x_{1,0}$	initial concentration in broken cells	$\mathrm{kg_{sol}/kg_{subs}}$
x_2	concentration in intact cells	$\mathrm{kg_{sol}/kg_{subs}}$
y	fluid-phase concentration	$\mathrm{kg_{sol}/kg_{solv}}$
y_2	solubility of pinocembrin or nobiletin	$\mathrm{mol_{Pn}/mol_{CO_2}}$
y_{s}	saturation concentration or solubility	$\mathrm{kg_{sol}/kg_{solv}}$
y_0	initial fluid-phase concentration	$\mathrm{kg_{sol}/kg_{solv}}$
A_2	chromatographic peak area of CO_2-rich phase sample	$\mathrm{mAU^2}$
A_{S2}	chromatographic peak area of a standard	$\mathrm{mAU^2}$
C_{S2}	concentration of standard for calibration	$\mathrm{mol\,cm^{-3}}$
$D_{1\mathrm{m}}$	binary diffusivity parameter (D_{12})	$\mathrm{m^2\,s^{-1}}$
E	percent ethanol	wt $\%$
F	flow of CO_2	$\mathrm{g/\,mín}$
H	extraction bed length	m
J_{f}	dimensionless flux to broken cells to solvent $(j_{\mathrm{f}} t_{\mathrm{r}}/\rho_{\mathrm{f}} \epsilon y_0)$	unitless

J_{s}	dimensionless flux to intact cells to broken cells $(j_{\mathrm{s}} t_{\mathrm{r}} / \rho_{\mathrm{s}} (1-\epsilon) x_{1,0})$	unitless
K	partition or equilibrium coefficient	unitless
$\overline{K}$	partition constant in dimensionless model equation $(K x_{1,0}/y_0)$	unitless
M_{d}	dry basis moisture	$\%$
P	pressure	bar, MPa
P_2^{s}	sublimation pressure of the pure solid	MPa
Q^2	prediction coefficient	unitless
$\boldsymbol{R}$	array of spectra of mixtures of flavonoids	unitless
R^2	determination coefficient	unitless
Re	Reynolds number	unitless
$\boldsymbol{S}$	matrix of pure spectrum for each analyte	unitless
Sc	Schmidt number	unitless
Sh	Sherwood number	unitless
T	temperature	℃,K
U	intersticial fluid velocity	$\mathrm{m\,s^{-1}}$
V_{IV}	Volume of sampler loop of the equilibrium cell	µL
V_{S}	Volume of sampler loop of the HPLC injector	µL
X_{t}	dimensionless transition concentration $(x_{\mathrm{t}}/x_{1,0})$	unitless
X_1	dimensionless concentration in broken cells $(x_1/x_{1,0})$	unitless
X_2	dimensionless concentration in intact cells $(x_2/x_{1,0})$	unitless

Y	dimensionless fluid-phase concentration (y/y_0)	unitless
Y^*	dimensionless equilibrium fluid-phase concentration	unitless
Y_s	dimensionless solubility (y_s/y_0)	unitless
ρ_b	bulk density	$\mathrm{kg\,m^{-3}}$
ρ_f	fluid density	$\mathrm{kg\,m^{-3}}$
ρ_s	solid density	$\mathrm{kg\,m^{-3}}$
τ	dimensionless time (t/t_r)	unitless
ϵ	bed void fraction or porosity	unitless
γ	solvent-to-matrix ratio in the bed ($\rho_\mathrm{f}\epsilon/\left[\rho_\mathrm{s}(1-\epsilon)\right]$	$\mathrm{kg_{solv}/kg_{subs}}$
Γ	initial solute distribution between solvent and broken cells ($\gamma y_0/r x_{1,0}$)	unitless
Θ_e	dimensionless external mass transfer resistance ($\epsilon/(k_\mathrm{f} a_0 t_\mathrm{r})$)	unitles
Θ_i	dimensionless internal mass transfer resistance ($(1-\epsilon)/(k_\mathrm{s} a_0 t_\mathrm{r})$)	unitless
Φ	dimensionless extraction yield	unitless
φ_2^S	fugacity coefficient at sublimation pressure	unitless
φ_2^F	fugacity coefficient of fluid phase	unitless

RESUMEN

TÍTULO: ESTUDIO DE LA EXTRACCIÓN SUPERCRÍTICA DE FLAVONOIDES A PARTIR DE RESIDUOS DE DESTILACIÓN DE PLANTAS PRODUCTORAS DE FENIL-PROPANOIDES [*]

AUTOR: ÁNDERSON JULIÁN ARIAS VELANDIA [**]

PALABRAS CLAVE: EXTRACCIÓN SUPERCRÍTICA, LIPPIA ORIGANOIDES, LIPPIA GRAVEOLENS, EQUILIBRIO DE FASES, CINÉTICA, VALORIZARIZACIÓN DE RESIDUOS.

DESCRIPCIÓN:

Las plantas productoras de fenilpropanoides son materia prima de condimentos y aceites esenciales (AE) útiles en aplicaciones industriales. La *Lippia origanoides* y *L. graveolens* son las especies americanas de mayor interés comercial. El proceso de obtención de sus AEs deja compuestos bioactivos retenidos en el sustrato; porque las plantas, además de los AEs, contienen en sus estructuras celulares flavonoides como la pinocembrina (**Pn**). La **Pn** es un compuesto activo para el tratamiento de la hemorragia cerebral y la fibrosis pulmonar. Por lo tanto, existe una clara oportunidad con los subproductos de la destilación de estas plantas para aumentar las ganancias; esto si además de los AEs, se extraen y comercializan oleorresinas ricas en flavonoides. Para valorizar el proceso se requiere caracterizar el sustrato y describir matemáticamente las operaciones unitarias complementarias necesarias para lograr el aprovechamiento integral del material vegetal. De todas las operaciones unitarias viables para complementar el proceso, este trabajo se enfocó en el estudio de la extracción con CO_2 supercrítico modificado con EtOH, debido a la capacidad de la técnica para controlar la solvatación y la selectividad del CO_2. Determinar el potencial de valorización de los residuos posdestilados en la producción conjunta de AE y flavonoides; determinar los límites impuestos por los equilibrios de fase entre la interacción soluto, matriz y solvente, y determinar la cinética de extracción supercrítica de flavonoides y oleorresina son temas que el lector encontrará desarrollados en los capítulos de este libro. El trabajo buscó contribuir a incrementar la competitividad de la industria de AEs proporcionando elementos de decisión relevantes sobre la viabilidad técnica de la extracción supercrítica para complementar el proceso de extracción de AEs.

---

[*] Tesis Doctoral

[**] Facultad de Ingenierías Fisico-Químicas. Escuela de Ingeniería Química. Director: Jairo René MARTÍNEZ MORALES. Codirectora: Elena E. STASHENKO.

ABSTRACT

TITLE: : STUDY OF THE SUPERCRITICAL EXTRACTION OF FLAVONOIDS FROM DISTILLATION RESIDUES OF PHENYLPROPANOID-PRODUCING PLANTS [*]

AUTHOR: ÁNDERSON JULIÁN ARIAS VELANDIA [**]

KEYWORDS: SUPERCRITICAL EXTRACTION, LIPPIA ORIGANOIDES, LIPPIA GRAVEOLENS, PHASE EQUILIBRIA, KINETICS, RESIDUE VALORIZARIZATION.

DESCRIPTION:

Phenylpropanoid-producing plants are raw materials for production of culinary seasonings and essential oils (EOs) useful in different industries. *Lippia origanoides* and *L. graveolens* are the American species of greatest commercial interest in market due to their phenylpropanoids. In Central-South America, at least 4.000 t/year are produced and sold. The process of obtaining EOs, leaves behind valuable post-distillation residues because plants also contain flavonoids such as pinocembrin (**Pn**) in their cellular structures. **Pn** is an active compound proven in drugs for the treatment of cerebral hemorrhage and pulmonary fibrosis. Considering this, industry has a clear opportunity with distillation by-products to increase their profit by extracting and commercializing flavonoids-rich oleoresin. Evidence that indicates the integration of process stages, beyond distillation and waste treatment, to increase the profitability was not found in the open literature. Moving in this direction requires characterizing the substrate and describing mathematically the complementary unit operations necessary to achieve an integral use. Of all viable unit operations to complement the extractive process, we focus on the study of EtOH-modified supercritical $scCO_2$ extraction due to the process capability to control the solvation and the selectivity of $scCO_2$ by tuning the operating conditions and the polarity modifier. Besides, it is considered human-health and environmentally friendly. To determine the potential valorization of some post-distillation residues of *Lippia* species in the joint production of EOs and flavonoids; determining the limits imposed by the phase equilibria between the solute, matrix, and sc-solvent interaction, and determining the sc-extraction kinetics of flavonoids and oleoresin are topics that reader will find developed in chapters of this book. The work sought to contribute to increasing the competitiveness of the EOs industry by providing relevant decision elements on the technical feasibility of including sc-extraction as a unit operation that complements the EOs extraction process.

---

[*] Doctoral Thesis

[**] Facultad de Ingenierías Físico-Químicas. Escuela de Ingeniería Química. Director: Jairo René MARTÍNEZ MORALES. Co-director: Elena E. STASHENKO.

INTRODUCTION

eig

Essential oils (EOs) represented a market of *ca.* 9 billion USD in the world in 2019. It is expected to reach 11.19 billion USD by 2022, with an annual growth rate of 8.7 % from 2016 to 2022 [1]. EOs rich in phenylpropanoids thymol and carvacrol are part of that market and are sold at 82 EUR/kg for thyme EO (*Thymus vulgaris*, 37 to 55 wt % thymol and 1 to 6 wt % carvacrol, [2]) or *ca.* 128 EUR/kg for Mediterranean oregano EO (*Origanum vulgare*, 22 to 65 wt % thymol and 18 to 75 wt % carvacrol, [3]), according to July-August 2019 reports of the European harvests, [4]. In the American continent, phenylpropanoid-rich EOs are produced and exported. They are distilled from some endemic species of the *Lippia* genus. EOs of species such as *Lippia origanoides* (53 to 61 wt % thymol and 44 to 52 wt % carvacrol, [5][6]) and *Lippia graveolens* (0 to 60 wt %

---

1 Verma Preksha. *Allied Market Research. Essential Oil Market Size, Share, Essential Oil Industry Trends*. 2016.

2 International Organization for Standardization. *ISO 19817:2017 - Essential oil of thyme Thymus vulgaris L. and Thymus zygis L.], thymol type*. 2017.

3 L D'Antuono. «Variability of Essential Oil Content and Composition of *Origanum vulgare* L. Populations from a North Mediterranean Area (Liguria Region, Northern Italy)». En: *Annals of Botany* 86.3 (2000), págs. 471-478. DOI: 10.1006/anbo.2000.1205.

4 Ultra International B.V. *Essential Oils Market Report - Summer 2019*. Inf. téc. Spijkenisse: Ultra International B.V., 2019, pág. 37.

5 Elena E. Stashenko *y col.* «*Lippia origanoides* chemotype differentiation based on essential oil GC-MS and principal component analysis». En: *Journal of Separation Science* 33.1 (2010), págs. 93-103. DOI: 10.1002/jssc.200900452.

6 Jairo Martínez, Juliana Agudelo y Elena Stashenko. «Criterio de calidad para *Lippia alba* y *Lippia origanoides* en aceites esenciales». En: *Vitae*. Ed. por Gloria Holguín Martínez. Vol. 18. 2 (2). Medellín: Vitae., 2011, S295.

thymol and 0 to 78 wt % carvacrol, [78]) are sold in international markets between 120-150 USD/kg [9].The prospect is especially promising so that countries in Central and South America, such as Mexico and Colombia, where the plant is native, can benefit economically from its commercialization.

EOs are commonly extracted by entrainer effects of steam, which strictly removes volatile substances from the botanical substrate, leaving retained compounds in the substrate, such as heavy terpenes, free fatty acids, oleoresins, and pigments, among others [10]. These solid residues may have a valorization potential depending on the plants benefits. *L. origanoides* and *L. graveolens*, in addition to EOs, contain flavonoids in their cellular structures. These minority substances have been co-extracted with oleoresin through hydroalcoholic or supercritical (sc) extractions [111213]. Depen-

---

[7] Violeta Acosta Arriola. «Variación en la composición química del aceite esencial de *Lippia graveolens*, en poblaciones silvestres de Yucatán, y su relación con factores edafoclimáticos». Tesis doct. Centro de Investigación científica de Yucatán, 2013, pág. 77.

[8] Daniela A. Martínez-Natarén *y col.* «Essential oil Yield Variation Within and Among Wild Populations of Mexican Oregano (*Lippia graveolens* H.B.K.-Verbenaceae), and its Relation to Climatic and Edaphic Conditions». En: *Journal of Essential Oil Bearing Plants* 15.4 (ene. de 2012), págs. 589-601. DOI: 10.1080/0972060X.2012.10644093.

[9] Delegación SADER San Luis Potosí. *Crea INIFAP nueva tecnología para la producción de orégano resistente a fenómenos climáticos*. 2013.

[10] H Brogle. «CO2 in solvent extraction». En: *Chemistry and Industry* 19 (1982), págs. 385-390.

[11] Suzana Guimaraes Leitão *y col.* «Counter-current chromatography with off-line detection by ultra high performance liquid chromatography/high resolution mass spectrometry in the study of the phenolic profile of *Lippia origanoides*». En: *Journal of Chromatography A* 1520 (oct. de 2017), págs. 83-90. DOI: 10.1016/J.CHROMA.2017.09.004.

[12] LIn Long-Ze *y col.* «Identification and quantification of flavonoids of Mexican oregano (*Lippia graveolens*) by LC-DAD-ESI/MS analysis». En: *Journal of Food Composition and Analysis* 20.5 (2007), págs. 361-369. DOI: 10.1016/j.jfca.2006.09.005.

[13] E E Stashenko *y col.* «Chromatographic and mass spectrometric characterization of essential oils and extracts from *Lippia* (Verbenaceae) aromatic plants». En: *Journal of Separation Science* 36.1 (2013), págs. 192-202. DOI: 10.1002/jssc.201200877.

ding on the amount of these molecules retained in post-distillation substrate, it is possible to add value to the process by including a solid-liquid extraction step, as has already been shown to be convenient for other by-products of the EOs-industry [14][15].

Pinocembrin (Pn) is one of those flavonoids extracted from *L. origanoides* and *L. graveolens*. Pn appears in recent patents as an active compound in medications for treatment of cerebral hemorrhage [16] and pulmonary fibrosis [17], due to its proven effectiveness against such ailments [18][19][20]. The amount of Pn in *L. origanoides* ($30 \pm 1 \mathrm{mg/g_{DW}}$, Dry Weigh, [13]) is notably higher than that found in other commercial

---

[14] A. Navarrete *y col.* «Valorization of solid wastes from essential oil industry». En: *Journal of Food Engineering* 104.2 (mayo de 2011), págs. 196-201. DOI: 10.1016/J.JFOODENG.2010.10.033.

[15] R. Sánchez-Vioque *y col.* «Polyphenol composition and antioxidant and metal chelating activities of the solid residues from the essential oil industry». En: *Industrial Crops and Products* 49 (ago. de 2013), págs. 150-159. DOI: 10.1016/J.INDCROP.2013.04.053.

[16] Guanhua Du *y col. Applications of pinocembrin in preparing anti-cerebral hemorrhage medicament*. 2018.

[17] Yang Cheng *y col. Pinocembrin is in preparation for treating the application in pulmonary fibrosis disease drug*. 2019.

[18] Xi Lan *y col.* «Pinocembrin protects hemorrhagic brain primarily by inhibiting toll-like receptor 4 and reducing M1 phenotype microglia». En: *Brain, Behavior, and Immunity* 61 (2017), págs. 326-339. DOI: 10.1016/J.BBI.2016.12.012.

[19] Azhar Rasul *y col.* «Pinocembrin: A novel natural compound with versatile pharmacological and biological activities». En: *BioMed Research International* 2013.2013 (2013), págs. 1-9. DOI: 10.1155/2013/379850.

[20] Wenzhu Wang *y col.* «Using functional and molecular MRI techniques to detect neuroinflammation and neuroprotection after traumatic brain injury». En: *Brain, Behavior, and Immunity* 64 (2017), págs. 344-353. DOI: 10.1016/J.BBI.2017.04.019.

natural sources (0.6 to 2.5 m/g_{DW}, [21][22]) and cultures recently identified as promising for their extraction (15 and 18 mg/g_{DW}, [23]). Since Pn is still stable at 200 °C [24], the industry of *L. origanoides* and *L. graveolens* EOs has a clear opportunity with distillation by-producs to increase their profit by extracting, in addition to phenylpropanoid-rich EOs, flavonoid-rich oleoresin.

Although at least 4000 t/year of fresh-, dry-plant material and EOs from *Lippia* spp. are produced and commercialized by Central America, no evidence was found in the open literature to demonstrate implementation of process stages beyond distillation and waste treatment to increase economic profit. This is possibly because it is still necessary to deepen in knowledge of raw matter and description of complementary extractive stages. From the application area of chemical engineering, it is possible to contribute providing useful knowledge for decision-making. Process design, planning, and operation parameters are relevant information obtainable from this knowledge area that complement the comprehensive extraction process of other promising ingredients from *Lippia* spp. Description of EOs composition standardization process, determination of valorization potential of some *Lippia* species in the joint production of EOs and flavonoids, determination of phase equilibria and kine-

---

[21] Aifeng Li, Ailing Sun y Renmin Liu. «Preparative isolation and purification of three flavonoids from the chinese medicinal plant *Alpinia katsumadai* hayata by high-speed counter-current chromatography». En: *Journal of Liquid Chromatography & Related Technologies* 35.20 (ene. de 2012), págs. 2900-2909. DOI: 10.1080/10826076.2011.643523.

[22] Norio Yamamoto *y col.* «Cardamonin stimulates glucose ptake through translocation of glucose transporter-4 in L6 myotubes». En: *Phytotherapy Research* 25.8 (2011), págs. 1218-1224. DOI: 10.1002/ptr.3416.

[23] Jason Q.D. Goodger *y col.* «*Eucalyptus* subgenus *Eucalyptus* (Myrtaceae) trees are abundant sources of medicinal pinocembrin and related methylated flavanones». En: *Industrial Crops and Products* 131 (mayo de 2019), págs. 166-172. DOI: 10.1016/J.INDCROP.2019.01.050.

[24] Xu Yang *y col.* «Pinocembrinâ€"lecithin complex: Characterization, solubilization, and antioxidant activities». En: *Biomolecules* 8.2 (2018), pág. 41. DOI: 10.3390/biom8020041.

tics of sc-extraction of flavonoids are topics developed in this work, and will surely contribute to increasing competitiveness of EOs-industry in the future.

From the viable unit operations to complement the extraction process of *L. origanoides* EOs, this work limited its scope to study in depth ethanol (EtOH)-modified $scCO_2$ extraction. An efficient extractive process of phenolic compounds from botanical substrates [25] has been demonstrated for antioxidants recovery from different substrates [26][27]. Solvation power and selectivity of the $scCO_2$ can be tuned by extraction conditions and selection of a polar-modifier [28]. Selectivity is improved by EtOH addition because its polarity in mixture with $scCO_2$ enhance the extraction of aglycones such as Pn, in comparison with other phenolic compounds and their derivatives [29][30][31]. Furthermore, $scCO_2$ extraction is considered environmentally friendly.

---

[25] Beatriz Díaz-Reinoso *y col.* «Supercritical CO2 extraction and purification of compounds with antioxidant activity». En: *Journal of Agricultural and Food Chemistry* 54.7 (2006), págs. 2441-2469. DOI: 10.1021/jf052858j.

[26] Sara López-Sebastián *y col.* «Dearomatization of antioxidant rosemary extracts by treatment with supercritical carbon dioxide». En: *Journal of Agricultural and Food Chemistry* 46.1 (1998), págs. 13-19. DOI: 10.1021/jf970565n.

[27] Karin Schwarz, Waldemar Ternes y Eberhard Schmauderer. «Antioxidative constituents of *Rosmarinus officinalis* and *Salvia officinalis*». En: *Zeitschrift fur Lebensmittel-Untersuchung und -Forschung* 195.2 (ago. de 1992), págs. 104-107. DOI: 10.1007/BF01201767.

[28] B. Klejdus *y col.* «Hyphenated technique for the extraction and determination of isoflavones in algae: Ultrasound-assisted supercritical fluid extraction followed by fast chromatography with tandem mass spectrometry». En: *Journal of Chromatography A* 1217.51 (2010), págs. 7956-7965. DOI: 10.1016/J.CHROMA.2010.07.020.

[29] Markus Ganzera. «Supercritical fluid chromatography for the separation of isoflavones». En: *Journal of Pharmaceutical and Biomedical Analysis* 107 (mar. de 2015), págs. 364-369. DOI: 10.1016/J.JPBA.2015.01.013.

[30] Juliana Paes *y col.* «Extraction of phenolic compounds and anthocyanins from blueberry (*Vaccinium myrtillus* L.) residues using supercritical CO2 and pressurized liquids». En: *The Journal of Supercritical Fluids* 95 (nov. de 2014), págs. 8-16. DOI: 10.1016/J.SUPFLU.2014.07.025.

[31] M. Solana *y col.* «A comparison between supercritical fluid and pressurized liquid extraction methods for obtaining phenolic compounds from *Asparagus officinalis* L». En: *The Journal of*

Tasks inherent to the proposed study would require such a large amount of experiments and sample analysis that two technological strategies were preliminarily developed. This implied advances in extraction and quantification technologies for our research group. The first was to reduce the operating costs of the sc-extraction, which was addressed by modifying the available extraction system to semi-batch operation, adding a fractionation and CO_2 recirculation stages. In this way, the extraction capacity was doubled in time and production cost was reduced from 26 to 11 USD/extraction. Chapter 2 mentions the applications of the modified system. Regarding the recirculation system, an international patent written by the authors and granted to the Universidad Industrial de Santander is attached in Appendix 1.The second technological development was a validated methodology with their figures of merit for instrumental multi-component quantification of flavonoids in extracts. Given the number of samples to be processed, an instrumental analysis methodology based on UV-Vis spectroscopy and chemometric methods was implemented to avoid chromatographic separation and to reduce solvent- and time-consumption in quantification. The methodology was validated and compared with the HPLC-DAD results. Its application in this work is mentioned in Chapter 4 and summary details of its implementation are attached in Appendix 2. A manuscript on this subject is being prepared for submission to an international scientific journal.

Chapter 3 presents a study of potential valorization of solid residues from distillation of four *Lippia* chemotypes using sc-extraction. Sc-extraction yields were compared with results from solid-liquid extraction and another botanical source of pinocembrin. The effects of extraction conditions over yields were discussed and optimized at pilot scale. The results of this section were conclusive regarding the potential of each substrate as a function of the extractable EO and oleoresins. From this section, an

---

Supercritical Fluids 100 (mayo de 2015), págs. 201-208. DOI: 10.1016/J.SUPFLU.2015.02.014.

article was published in the *Industrial Crops and Products* Journal, *cf.* Appendix 3.

In Chapter 4, phase equilibria for the sc-extraction application were studied. Two approaches were considered, namely, the thermodynamic one, where solubility of Pn was measured and modeled, and the operational, where solvent, solute, and substrate interactions were measured and modeled. Limits imposed by phase equilibria will be important in the future basic design of the *L. origanoides* and *L. graveolens* extraction process. A manuscript is currently being prepared for the *Journal of Supercritical Fluids* with this chapter results.

In Chapter 5, the kinetics of oleoresin and flavonoid extraction from *Lippia* spp. substrates were studied. Here, in addition to the chopped substrates, the effect of their pelletization on yield and shape of extraction curves was considered. The models developed will be relevant in future optimization *via* mathematical simulation and economic feasibility studies. A manuscript is currently being prepared for the *Journal of Supercritical Fluids* with this chapter results.

Although there is no dedicated chapter in this book, the authors took advantage of the OEs obtained in the step before sc-extraction to study fractional distillation and to describe the standardization process of *L. origanoides* EOs. A methodology was developed to solve and validate a batch distillation model applicable to EOs. This methodology can be extended to other EOs of industrial interest to support the rectification processes. Details of this non-aligned with sc-extraction work were published in the *Computers and Chemical Engineering* Journal, *cf.* Appendix 4. From literature information, previous work carried out in our research group, and results of this work up to this point, enough information was collected to propose a configuration of consecutive unit operations that would achieve a method for making full use of *L. origanoides*. Details and descriptions are detailed in an international patent written by the authors and granted to the Universidad Industrial de Santander, *cf.* Appendix 5.

The author hopes that the reader of the following pages will find useful information

related to the technical feasibility of sc-extraction of by-products from the *Lippia spp.* EOs-industry. The aim is to contribute to the progress of the state of the art and technological innovation with a holistic approach integrating processes that lead to making full use of botanical substrates. Other alternatives or complementary extraction and distillation stages, remain to be studied to complete the process integration. Only by knowing the mathematical approach and physicochemical parameters that describe the process will it be possible to plan and optimize an integrated plant. Sc-extraction is a relatively recent technique and their technological advances together with the discovery of new applications could increase the demand and their industrial uses.

1. STATE OF THE ART

1.1. *Lippia origanoides* and *Lippia graveolens*

Lippia origanoides K. (mountain oregano) and *Lippia graveolens* K. (Mexican oregano) belong to the Verbenaceae family and are aromatic shrubs native to Central America and the northern region of South America. They are raw materials for the production of culinary seasonings and essential oils (EOs) enriched in phenylpropanoids that are useful in the food, cosmetic, and pharmaceutical industries [32][33][34]. At least five chemotypes have been distinguished among these two (apparently the same) species [35][36][37], which differ in EO composition. *L. origanoides* is the second most studied specie of the *Lippia* genus, preceded by *Lippia alba* [38]. EOs are obtai-

---

[32] C. Hernandes *y col.* «*Lippia origanoides* essential oil: an efficient and safe alternative to preserve food, cosmetic and pharmaceutical products». En: *Journal of Applied Microbiology* 122.4 (2017), págs. 900-910. DOI: 10.1111/jam.13398.

[33] Antonia Lopes *y col. Formulção farmaceutica derivada de óleo essencial de Lippia origanoides H.B.K*. 2013.

[34] R E Ortiz *y col.* «Efecto del aceite esencial de orégano sobre el desempeño productivo de ponedoras y la estabilidad oxidativa de huevos enriquecidos con ácidos grasos poliinsaturados». Español. En: *Revista de la Facultad de Medicina Veterinaria y de Zootecnia* 64.1 (2017), págs. 61-70.

[35] Alessandra P. da Silva *y col.* «Tyrosinase inhibitory activity, molecular docking studies and antioxidant potential of chemotypes of *Lippia origanoides* (Verbenaceae) essential oils». En: *PLOS ONE* 12.5 (2017). Ed. por Jamshidkhan Chamani, e0175598. DOI: 10.1371/journal.pone.0175598.

[36] J. Maisch. «On some useful plants of the natural order of Verbenaceae.» En: *American Journal of Pharmacy* 57 (1885), págs. 189-199.

[37] Alcy F. Ribeiro *y col.* «Circadian and seasonal study of the cinnamate chemotype from *Lippia origanoides* Kunth». En: *Biochemical Systematics and Ecology* 55 (2014), págs. 249-259. DOI: 10.1016/J.BSE.2014.03.014.

[38] Cristina M. Pérez Zamora, Carola A. Torres y María B. Nuñez. «Antimicrobial Activity and Chemical Composition of Essential Oils from Verbenaceae Species Growing in South America». En:

ned by steam distillation, which leaves residual plant material that can be valorized. These plants, in addition to volatile compounds, also contain flavonoids that could be extracted as demonstrated for other byproducts from the essential oil industry [14][15].

1.1.1. Essential oils and extracts from *L. origanoides* and *L. graveolens*

Composition, bioactivity and applications of EOs The useful bioactive properties of "oregano" EOs are widely known. Their benefits are mainly attributed to the presence of two phenylpropanoids, namely, thymol and carvacrol. Phenylpropanoids are found throughout the plant kingdom, where they serve as essential components of a number of structural polymers, provide protection from ultraviolet light, defend against herbivores and pathogens, and mediate plant-pollinator interactions as floral pigments and scent compounds. Thymol and carvacrol have aroused interest in commercial applications such as food additive, preservative, or pest control agent, among others. The most widely known natural sources of thymol and carvacrol are thyme (*Thymus vulgaris*) and Mediterranean oregano (*Origanum vulgare*), both of Eurasian origin. Thymol and carvacrol contents in the EO of thyme (ISO 19817:2017) are 37 to 55 wt % and 1 to 6 wt %, [2], respectively, and 22 to 65 wt % and 18 to 75 wt %, respectively, for Mediterranean oregano [3]. *L. origanoides* and *L. graveolens*, meanwhile, are found in tropical America in various chemotypes. Thymol (53 to 61 wt %) and carvacrol (44 to 52 wt %) are the main components of the EO of these species [39][35]. The bioactivity of *Lippia origanoides* EO has been studied extensively in recent

---

Molecules 23.3 (2018). DOI: 10.3390/molecules23030544.

[39] Danilo R. Oliveira *y col.* «Chemical and antimicrobial analyses of essential oil of *Lippia origanoides* H.B.K». En: *Food Chemistry* 101.1 (2007), págs. 236-240. DOI: 10.1016/J.FOODCHEM.2006.01.022.

years, *e.g.* are antigenotoxic capacity against UV radiation [40], antimicrobial capacity due to the presence of compounds that increase or alter the permeability of the bacterial membrane [41][38], anti-Leishmania capacity with certain limitations of oral and cutaneous toxicity [42] and *in vitro* antiparasitic capacity against *Colossoma macropomum*, with limitations of application in native freshwater fish [43]. The addition of $200\,\mathrm{mg\,kg^{-1}}$ of EO to food stimulated the immune system and improved broiler growth [44]. The inclusion of *L. origanoides* EO in the diet of laying hens improved the time of oxidative stability of eggs stored at 4 ℃ 60 days [34]. Among other applications, [32], recently concluded that *L. origanoides* EO is an effective and safe preservative of

---

[40] J. L. Fuentes *y col.* «The SOS Chromotest applied for screening plant antigenotoxic agents against ultraviolet radiation». En: *Photochem. Photobiol. Sci.* 16 (9 2017), págs. 1424-1434. DOI: 10.1039/C7PP00024C.

[41] Sandra Layse F. Sarrazin *y col.* «Antimicrobial and Seasonal Evaluation of the Carvacrol-Chemotype Oil from *Lippia origanoides* Kunth.» En: *Molecules* 20.2 (2015), págs. 1860-1871. DOI: 10.3390/molecules20021860.

[42] Laura Neira *y col.* «Toxicidad, genotoxicidad y actividad anti-Leishmania de aceites esenciales obtenidos de cuatro (4) quimiotipos del género *Lippia*». En: *Boletín Latinoamericano y del Caribe de Plantas Medicinales y Aromáticas* 17.1 (2018), págs. 68-83.

[43] Bruna Viana Soares *y col.* «Antiparasitic, physiological and histological effects of the essential oil of *Lippia origanoides* (Verbenaceae) in native freshwater fish Colossoma macropomum». En: *Aquaculture* 469 (2017), págs. 72 -78. DOI: https://doi.org/10.1016/j.aquaculture.2016.12.001.

[44] Tomas Antonio Madrid-Garcés, Jaime Eduardo Parra-Suescún y Albeiro López-Herrera. «La inclusión de aceite esencial de orégano (*Lippia origanoides*) mejora parámetros inmunológicos en pollos de engorde». En: *Biotecnología en el Sector Agropecuario y Agroindustrial* 15 (dic. de 2017), págs. 75-83.

cosmetics and orange juice. [45], [46] and [47], showed that *L. origanoides* EO is a viable alternative for the control of diseases and pests.

Composition bioactivity and applications of extracts *L. origanoides* and *L. graveolens*, in addition to EOs, also contain flavonoids in their cellular structures. These minority substances have been co-extracted with the oleoresin obtainable through hydroalcoholic or supercritical (sc) extractions [111213]. Flavonoids have been detected in quantities of $\mathrm{mg/g_{subs}}$ (leaves and stems) for extractions with organic solvents or $scCO_2$. *E.g.*, the amount of Pn in the hydroalcoholic extract of *L. origanoides* phellandrene (LOP) chemotype ($30 \pm 1 \mathrm{mg/g_{DW}}$, Dry Weight, [13]), which is notably higher than what is found in other commercial natural sources (0.6 to $2.5\,\mathrm{m/g_{DW}}$, [2122]) and cultures recently identified as promising for their extraction (15 and $18\,\mathrm{mg/g_{DW}}$, [23]). Other very common dietary flavonoids identified in extracts are: naringenin, which is one of the main flavanones obtainable from grapefruit [48], galangin, quercetin which are the most common flavonols in diet; as well as apigenin and luteolin are the most common flavones [49]. Flavonoid extraction is frequently performed by conventional

---

[45] Josiana M. Mar *y col.* «*Lippia origanoides* essential oil: An efficient alternative to control *Aedes aegypti*, *Tetranychus urticae* and *Cerataphis lataniae*». En: *Industrial Crops and Products* 111 (2018), págs. 292 -297. DOI: https://doi.org/10.1016/j.indcrop.2017.10.033.

[46] Natalia Ríos, Elena E Stashenko y Jonny E Duque. «Evaluation of the insecticidal activity of essential oils and their mixtures against *Aedes aegypti* (Diptera: Culicidae)». En: *Revista Brasileira de Entomologia* 61.4 (2017), págs. 307-311.

[47] Maria Alcalá-Orozco *y col.* «Actividad repelente de los aceites esenciales de *Elettaria cardamomum*, *Salvia officinalis* y *Lippia origanoides* Carvacrol contra dos insectos plagas de productos almacenados». En: *2017*. 2017.

[48] S Kawaii *y col.* «Quantitation of flavonoids constituents in Citrus fruits». En: *Journal of Agricultural and Food Chemistry* 47 (1999), págs. 3565-3571.

[49] Iris Erlund. «Review of the flavonoids quercetin, hesperetin, and naringenin. Dietary sources, bioactivities, bioavailability, and epidemiology». En: *Nutrition Research* 24.10 (2004), págs. 851-874. DOI: 10.1016/j.nutres.2004.07.005.

solvent extraction followed by fractionation methods.

All these molecules posses important antioxidant, photo-resistant and antimicrobial capacities. Flavonoids contain in their chemical structure phenolic hydroxyl groups good for iron and other transition metals chelation, which confers them a great antioxidant capacity [50][51]. Flavonoids are essentials in protection against the oxidative damage phenomenon and have therapeutic effects in a number of pathologies, including ischemic heart disease and arteriosclerosis among others [52][53]. Several research results have shown the potential applications of Pn in *in vitro* and *in vivo* experiments, furthermore it is nontoxic and non-mutagenic to male Wistar rats within the 1 to $100\,\mathrm{mg/kg_{weigth}}$ [19]. Pn appears in recent patents as an active compound in medications for treatment of cerebral hemorrhage [16] and pulmonary fibrosis [17], due to its proven effectiveness against such ailments [18][20]. Ming y Towers found that $100\,\mu g_{Pn}/mL_{solv}$ exhibited antifungal activity against *Candida albicans* by interfering energy homeostasis [54]. Park *y col.* found that propolis with the highest amounts of pinocembrin and galangin (Gn) have inhibition on growth of *Streptococcus mutans* [55]. In addition to Pn, Gn has also been found in several studies as one of the most

---

[50] B Havsteen. «Flavonoids, a class of natural products of high pharmacological potency». En: *Biochemical Pharmacology* 32.7 (1983), págs. 1141-1148.

[51] William Peres. «Radicais Livres em nïveis biológicos». En: *Pelotas: Ed. Universidade Cat{ó}lica de Pelotas* (1994), págs. 49-81.

[52] Meishiang Jang *y col.* «Cancer chemopreventive activity of resveratrol, a natural product derived from grapes». En: *Science* 275.5297 (1997), págs. 218-220.

[53] Cecil R Pace-Asciak *y col.* «The red wine phenolic trans - resveratrol and quercetin block human platelet aggregation and eicosanoid synthesis: Implications for protection against coronary heart disease». En: *Clinica Chimica Acta* 235.2 (1995), págs. 207-219.

[54] Dong Sheng Ming y G H Neil Towers. «Antifungal Activity of Benzoic Acid Derivatives from *Piper lanceaefolium*». En: 604 (2002), págs. 62-64.

[55] Yong K Park *y col.* «Antimicrobial Activity of Propolis on Oral Microorganisms». En: 36 (1998), págs. 24-28.

abundant flavonoids in extracts from Mexican oregano, [125657]. It also has been reported as a cancer chemo preventive, antimicrobial, antioxidant and antiviral agent [585960]. Specifically, it has shown growth inhibition of human lung cancer cells [61] and suppressor activity in human ovarian cancer cells [56].

Despite the significant amount of flavonoids found in the LOP sc-extract, they are minority compared to co-extracted compounds such as fatty acids, waxes, pigments, and resinoids among others [62]. In fact, Reverchon describes whole extracts from botanical plants composition as two families of compounds: essential oils (EOs) and cuticular waxes (CW) [62], this because some extractive techniques in addition to steam distillation can also extract volatile compounds by entrainer or solubilization effects. CW have been reported in several works as the second major family of constituent after volatile compounds to be extracted. CWs are extracted through a different mass

---

[56] A.M. García-Bores *y col.* « *Lippia graveolens* photochemopreventive effect against UVB radiation-induced skin carcinogenesis». En: *Journal of Photochemistry & Photobiology, B: Biology* 167 (2017), págs. 72-81. DOI: 10.1016/j.jphotobiol.2016.12.014.

[57] Teresa Soledad Cid-Pérez *y col. Mexican Oregano (Lippia berlandieri and Poliomintha longiflora) Oils*. Elsevier Inc., 2016, págs. 551-560. DOI: 10.1016/B978-0-12-416641-7.00063-8.

[58] Moon Y. Heo, Su J. Sohn y William W. Au. «Anti-genotoxicity of galangin as a cancer chemopreventive agent candidate». En: *Mutation Research - Reviews in Mutation Research* 488.2 (2001), págs. 135-150. DOI: 10.1016/S1383-5742(01)00054-0.

[59] A Russo, R Longo y A Vanella. «Antioxidant activity of propolis: role of caffeic acid phenethyl ester and galangin.» En: *Fitoterapia* 73 Suppl 1 (2002), S21-9.

[60] J.J.M. Meyer *y col.* «Antiviral activity of galangin isolated from the aerial parts of *Helichrysum aureonitens*». En: *Journal of Ethnopharmacology* 56.2 (1997), págs. 165-169. DOI: 10.1016/S0378-8741(97)01514-6.

[61] D K Patel *y col.* «Pharmacological and bioanalytical aspects of galangin-a concise report». En: *Asian Pacific Journal of Tropical Biomedicine* 2.1 (2012), S449-S455. DOI: 10.1016/S2221-1691(12)60205-6.

[62] Ernesto Reverchon. «Fractional Separation of SCF Extracts from *Marjoram* Leaves : Mass Transfer and Optimization». En: *Journal of Supercritical Fluids* 5 (1992), págs. 256-261.

transfer mechanism [63]. The outer layer of botanical plants is covered by CWs as a waterproof to diminish water loss from leaves. Constituents of this wax have been reported as long chain aliphatic acids, long-chain n-alkanes (n-C_{25} to n-C_{35}), olefins and flavonoids [646566]. Researches that applied discriminant analysis to the composition of long-chain alkanes extracted from leaves of the Verbenaceae plant family showed, in average for a sample of seven plants, that the main cuticular waxes (CW) present in the extracts are: hentriacontane ($C_{31}H_{64}$, $17.9\,\mathrm{wt}\,\%$), tritriacontane ($C_{33}H_{68}$, $30.9\,\mathrm{wt}\,\%$) and pentatriacontane ($C_{35}H_{72}$, $16.1\,\mathrm{wt}\,\%$) [67].

1.1.2. Economic value and potential valorization of extraction process EOs represented a market of *ca.* 9 billion USD in the world in 2019. It is expected to reach 11.19 billion USD by 2022, with an annual growth rate of $8.7\ \%$ from 2016 to 2022 [1]. EOs rich in phenylpropanoids thymol and carvacrol are part of that market and are sold at 82 EUR/kg for thyme EO or *ca.* 128 EUR/kg for Mediterranean oregano EO, according to July-August 2019 reports of the European harvests, [4]. In the American

---

[63] B. Mira *y col.* «Supercritical CO2 extraction of essential oil from orange peel. Effect of operation conditions on the extract composition». En: *Journal of Supercritical Fluids* 14.2 (1999), págs. 95-104. DOI: 10.1016/S0896-8446(98)00111-9.

[64] Egon Stahl *y col.* «Anwendungen verdichteter Gase zur Extraktion und Raffination». En: *Verdichtete Gase zur Extraktion und Raffination*. Springer Berlin Heidelberg, 1987, págs. 82-241. DOI: 10.1007/978-3-662-10763-8_4.

[65] Ernesto Reverchon, Pietro Russo y Alberto Stassi. «Solubilities of solid octacosane and triacontane in supercritical carbon dioxide». En: *Journal of Chemical & Engineering Data* 38.3 (jul. de 1993), págs. 458-460. DOI: 10.1021/je00011a034.

[66] Hafiz Muhammad Ahmad, Mahmood-Ur Rahman y Qurban Ali. «Plant cuticular waxes: a review on functions, composition, biosyntheses mechanism and transportation». En: *Industrial & Engineering Chemistry Research* 12 (2015), págs. 4861-4870.

[67] M. Maffei. «Discriminant analysis of leaf wax alkanes in the Lamiaceae and four other plant families». En: *Biochemical Systematics and Ecology* 22.7 (oct. de 1994), págs. 711-728. DOI: 10.1016/0305-1978(94)90057-4.

continent, phenylpropanoid-rich EOs from *L. origanoides* and *L. graveolens* are also produced and exported. They are sold in international markets between 120-150 USD/kg [9]. The useful bioactive EOs properties have aroused interest in commercial applications such as food additive, preservative, or pest control agent, among others. *E.g.* multinational food company Du Pont markets Enviva EO, which is thymol- and cinnamaldehyde-rich EO encapsulated in maltodextrin, as a food product for production of pigs and laying hens. The prospect is especially promising so that countries in Central and South America, such as Mexico and Colombia, where the plant is native, can benefit economically from its production and commercialization.

The oregano EOs, as mentioned before, are commonly extracted by entrainer effects of steam, which strictly removes volatile substances from the botanical substrate, leaving retained compounds in the substrate, such as heavy terpenes, free fatty acids, oleoresins, and pigments, among others [10]. These solid residues may have a valorization potential given the retained flavonoids which would still be on the substrate. Pn and other flavonoids should remain stable during steam distillation process because there is no variation in the thermogram line of pinocembrin from 50 ℃ to the endothermic peak starting at *ca.* 204 ℃ for its melting [24]. Not only should Pn and other thermoresistant flavonoids remain intact during the steam distillation, but the modification of the plant material structure during steam distillation would favor subsequent mass transfer and improve extraction yield as compared with non-distillation substrate if an extraction were made with the solid residue [14]. Considering this, the industry of *L. origanoides* and *L. graveolens* EOs has a clear opportunity with distillation by-products to increase its profit by extracting, in addition to phenylpropanoid-rich EOs, flavonoids-rich oleoresin.

Another opportunity to increase the profit of this industry is increase the EOs value through its rectification. The composition variation of the EOs obtained at the same extraction conditions from the same plants, is due to the vegetative harvest cy-

cle, the agricultural conditions of the growth and the post-harvest treatment, among other causes [6869]. To carry out the formulation of industrial products based on EOs, it is indispensable to standardize their composition. It may even be of interest to isolate single, high-purity compounds. This is carried out by separation operations, of which distillation is one of the oldest and most commonly used [70]. Fractionation of EOs by distillation processes, although few in the literature, has been applied in different ways to increase the economic value of EOs. Although there is nonexposed in this book, the authors took advantage of the *L. origanoides* OEs to study fractional distillation and describe its standardization process. Details of this work were published in the *Computers and Chemical Engineering* Journal, *cf.* Appendix 4. A configuration of consecutive unit operations that would achieve a method for making full use of *L. origanoides* is described in an international patent written by the authors and granted to the Universidad Industrial de Santander, *cf.* Appendix 5.

1.2. Scalable flavonoid extraction processes

Flavonoids extraction is frequently performed by conventional solvent extraction followed by fractionation methods. Large amounts of organic solvent and long extraction periods are drawbacks of this process, which is sometimes assisted with ultrasound or microwave heating to increase extraction yields. An extraction alternative that has

---

[68] Paula C. Santos-Gomes y Manuel Fernandes-Ferreira. «Organ- and Season-Dependent Variation in the Essential Oil Composition of Salvia officinalis L. Cultivated at Two Different Sites». En: *J. Agric. Food Chem.* 49 (2001), págs. 2908-2916. DOI: 10.1021/JF001102B.

[69] Isa Telci, Ibrahim Demirtas y Ayse Sahin. «Variation in plant properties and essential oil composition of sweet fennel (<i>Foeniculum vulgare<i/> Mill.) fruits during stages of maturity». En: *Industrial Crops and Products* 30.1 (jul. de 2009), págs. 126-130. DOI: 10.1016/J.INDCROP.2009.02.010.

[70] Eugeny Y. Kenig *y col.* «Modeling of Distillation Processes». En: *Distillation*. Boston: Academic Press, 2014. Cap. 10, págs. 383 -436. DOI: 10.1016/B978-0-12-386547-2.00010-7.

sparked interest is supercritical (sc) fluid extraction. $ScCO_2$ extraction can be a very efficient process for the recovery of vegetable extracts with antioxidant activity [25]. Studies carried out considering the amount of raw materials, antioxidant activity results, and operative conditions show the advantages of this technique specially regarding recovery of antioxidant compounds [2627]. Solvation power and selectivity of the $scCO_2$ can be tuned by extraction conditions and selection of a polarity modifier [28]. The entrainer effects by addition of co-solvents have been observed for botanical materials when comparing $scCO_2$ with solid-liquid extractive techniques using hydro-alcoholic mixtures, or when water is included as a polarity modifier of $scCO_2$. Selectivity is improved by EtOH addition because its polarity in mixture with $scCO_2$ enhances extraction of aglycones such as Pn, in comparison with other phenolic compounds and their derivatives. [293031]. $ScCO_2$ extraction is also considered an environmentally friendly process that leaves no trace of solvent in the extract.

The main limitations of the industrial-scale implementation of sc-extraction are the high costs of investment and operation [71]. The alternatives that allow obtaining extracts at a lower cost are increasing production capacity over time and CO_2 recirculation. Only a recirculation system can decrease solvent losses to 2 % compared to 100 % of the extraction without recirculation [72]. The convenience of installing additional valves and separators has also been demonstrated, to carry out the fractionation process in line with the extraction according to the $scCO_2$ solubilities of extract constituents [73]. Some research groups have chosen to design and implement devices

---

[71] Luca Fiori. «Supercritical extraction of grape seed oil at industrial-scale: Plant and process design, modeling, economic feasibility». En: *Chemical Engineering and Processing: Process Intensification* 49.8 (2010), págs. 866-872. DOI: 10.1016/J.CEP.2010.06.001.

[72] C A Passey. «Commercial feasibility of a supercritical extraction plant for making reduced-calorie peanuts». En: *Supercritical Fluid Processing of Food and Biomaterials*. Ed. por S.S.H. Rizvi. 1.ª ed. London, UK: Blakie Academic & Professional, 1994, págs. 223-243.

[73] José M. del Valle, Juan C. de la Fuente y Damian A. Cardarelli. «Contributions to supercritical

and accessories necessary to improve the systems purchased on the market, as they propose process improvements based on their results. Such is the case of our research group that modified an extraction system (*Thar Technology*, Pittsburgh, PA, USA, Model SFE-2000-2-FMC50) to operate semi-batch, with a new fractionation stage and another of recirculation of CO_2. Regarding the recirculation system, an international patent written by the authors and granted to the Universidad Industrial de Santander is attached in Appendix 1.

Sc extraction is a promising process for obtaining compounds of interest selectively, but it has the disadvantage that the cost of its study and its implementation on an industrial scale is high for now. However, it is convenient to carry out studies on its potential application in new extraction processes while continuing to develop technologies that reduce the production cost.

1.3. Approach to experimental study of process valorization

Theoretically, a certain number of factors have simultaneous effects on a process. The application of an experimental design is the most effective way to identify and optimize the significant factors. In a problem like the one that represents the valorization of post-distillation solid residues from *L. origanoides* given the recovery potential of the bioactive molecules retained in the substrate, the experimental designs help as overview in the context of the technological limitations of the available methods or equipment. The experiment's result range and the effects of the factors on the observables are relevant results that, contrasted with the benchmarks of the study objective, provide information for decision-making. The extraction yield and selectivity on extraction process may depend on humidity, particle size (d_{p}), pressure (P),

---

extraction of vegetable substrates in Latin America». En: *Journal of Food Engineering* 67.1-2 (2005), págs. 35-57. DOI: 10.1016/J.JFOODENG.2004.05.051.

temperature (T), superficial velocity of the solvent (CO_2 for sc-extraction), the modifier type and percentage (E), and treatment time (t). Due to the large number of variables, experimental screening designs are a fundamental approach before studying in-depth models to describe extraction curves and allow scaling-up, and cost analysis [74][75].

Extractions with sc-fluids depend on the intrinsic nature of the fluid given by temperature and pressure, and some extrinsic characteristics such as type of matrix, interaction with the interest compound and many other environmental effects. In this way, greater degrees of freedom can be obtained in sc-extraction than with other conventional extraction methods, which means that there will be a greater number of adjustable variables that will make this process unique, sensitive and specific compared to conventional extraction methods [76].

Based on the scope, all designs can be categorized into two main groups: screening- and optimization-designs. The most widely used in sc-extraction for screening are Full Factorial, Fractional Factorial and Plackett-Burman designs. Taguchi design, Composite Central and Box-Behnken are the common designs for optimization. Choosing a convenient design, performing experimental tests, analyzing and interpreting the data, are the common stages crucial to carry out a successful experimental design [75]. Fig. 1 shows a methodological flowchart proposal based on the state of art to experimentally develop a modeling and optimization study of variables that govern the extraction process.

---

[74] Eduardo L.G. Oliveira, Armando J.D. Silvestre y Carlos M. Silva. «Review of kinetic models for supercritical fluid extraction». En: *Chemical Engineering Research and Design* 89.7 (jul. de 2011), págs. 1104-1117. DOI: 10.1016/J.CHERD.2010.10.025.

[75] K.M. Sharif *y col.* «Experimental design of supercritical fluid extraction–A review». En: *Journal of Food Engineering* 124 (2014), págs. 105-116. DOI: 10.1016/J.JFOODENG.2013.10.003.

[76] Marcel Caude y Didier Thiebaut. *Practical supercritical fluid chromatography and extraction*. Harwood Academic Publishers, 1999, pág. 442.

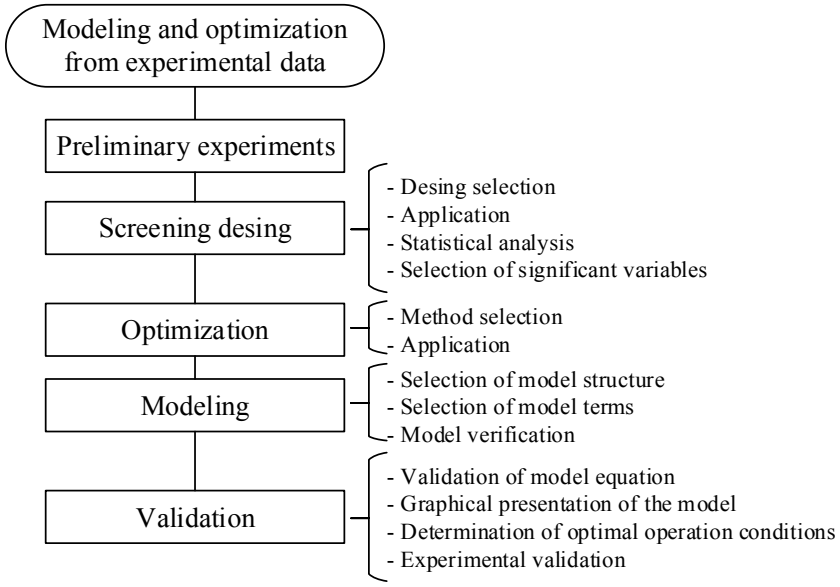

Figura 1. Methodology of experimental design.

Usually, preliminary experiments are made to determine experimental error and to estimate operation intervals of the experimental region. The experimental error can be assessed through a reproducibility measure as RSD, whose value less than 10 % is acceptable for bio-separations processes. Although a large number of factors influence the sc-extraction process, some of these have no significant effect. Screening for significant effects is the primary objective of experimental designs. Screening designs are used to determine the most important factors and their binary interactions from all potential factors. These types of design can examine quantitatively, qualitatively and simultaneously, related factors [77]. Optimization is another experimental design practice that confirms conditions or optimal region of experiments. The optimization approach usually begins with a screening design to select the important factors and then an optimization design such as those already mentioned. Sharif

[77] Bieke Dejaegher e Yvan Vander Heyden. «Experimental designs and their recent advances in set-up, data interpretation, and analytical applications». En: *Journal of Pharmaceutical and Biomedical Analysis* 56.2 (2011), págs. 141-158.

y col. included in their review a compilation of experimental designs applied in the literature to the sc-extraction from 2000 to 2014 [75].

One of the main aspects that should be considered in sc-extraction is the extraction optimization. The use of the optimum values for the different variables influencing the sc-extractions could significantly enhance the recovery or extraction yield of a target compound. With the aim to effectively optimize these variables, different approaches have been applied. Those strategies can be grouped in phase equilibrium strategies and experimental design statistical optimization. Phase equilibrium and mass transfer are not modelling problems; they are limit stages of the process that can justify the results. Therefore, it is very important to organize the experiments based on these fundamentals, to contribute to the understanding of the extraction problem. Despite of the valuable information obtained by phase equilibrium engineering, it is a common practice to optimize the processes using experimental designs and statistical modelling [78]. The use of experimental designs is one of the most common strategies when it comes to set up robust extraction methods [79].

Optimization problems in process design usually coincide with maximizing or minimizing a given objective function. When the function is not known the way to know the response-value is through direct measurement and experimentation. Commonly used experimental optimization designs dictate an exact number of experiments necessary to acquire information about the variables- and their interaction-effect on the response. With this information, multivariate models are constructed and represented by a response surface. After that, the optimal conditions predicted by the model

---

[78] Miguel Herrero *y col.* «Supercritical fluid extraction: Recent advances and applications». En: *Journal of Chromatography A* 1217.16 (2010), págs. 2495-2511. DOI: 10.1016/J.CHROMA.2009.12.019.

[79] Federica Bianchi y Maria Careri. «Experimental Design Techniques for Optimization of Analytical Methods. Part I: Separation and Sample Preparation Techniques». En: *Current Analytical Chemistry* 4.1 (2008), págs. 55-74. DOI: 10.2174/157341108783339070.

are found and validated. The latter is a stage that was found to be scarcely applied in the consulted literature. An alternative experimental optimization design exist that does not use an exact number of experiments but follows a specific search pattern. This is the simplex centroid design (SCD) [80]. The use of SCD in sc-extraction literature is not common, despite the refined methodology that proposes to find the optimal conditions. Using SCD is not necessary to build a multivariate model to generate response surfaces because experiments *per se* are optimization iterations. To generate a response surface with the experiments is also possible, but the stage of optimal conditions validation is not necessary because the design finishes with an experimental evaluation of the "simplex" that contains them.

In a query made with the Scopus database, only nine articles about sc-extraction application using SCD were found between 1990-2018 compared to more than 300 found for the conventional response surface methodology. [81], made the most recent work consulted in the same period. Most of the articles consulted using SCD carried out a screening design before the SCD. Among the works consulted, [82] stands out as the one with the best experimental approach since consecutively performs the preliminary experiments, the screening of the variables and the subsequent optimization-validation through an SCD.

---

[80] Robin M Smith. «Optimization». En: *Chemical process: design and integration*. John Wiley & Sons, 2005. Cap. 3, págs. 35-56.

[81] Asghar Safaralie, Shohreh Fatemi y Alireza Salimi. «Experimental design on supercritical extraction of essential oil from valerian roots and study of optimal conditions». En: *Food and Bioproducts Processing* 88.2-3 (jun. de 2010), págs. 312-318. DOI: 10.1016/J.FBP.2009.02.002.

[82] Giovanni Maio *y col.* «Supercritical Fluid Extraction of Some Chlorinated Benzenes and Cyclohexanes from Soil: Optimization with Fractional Factorial Design and Simplex». En: *Analytical Chemistry* 69.4 (1997), págs. 601-606. DOI: 10.1021/ac960349y.

1.4. Analytical methodologies for multicomponent quantification of extracts

To study the sc-extraction of minority compounds such as flavonoids from botanical substrates, it is essential to have a reliable methodology and measurement instruments for their identification and quantification. Since the response monitored in the sc-extraction experiments are concentration as a function of time, it is convenient to use analytical methods that avoid chromatographic separation to save solvent- and time-consumption.

UV–Vis spectrophotometry is considered a simple technique useful for the analysis and characterization of individual compounds but with limited applications in the field of complex media analysis. Colorimetric- [83] and Folin-Ciocalteu [84] methods use UV-Vis spectroscopy to quantify flavonoids and phenolic compounds. These methods have been widely and successfully used in the literature, but do not quantify substances individually. UV-Vis spectroscopy can be criticized for its low sensitivity and low selectivity; however, when it comes to real technological solutions engineers don't rule it out. Low sensitivity could be irrelevant if there is enough concentration of analytes in the sample, as is usual for minority compounds in extracts obtained from promising substrates. And low selectivity caused by overlapping of the extract constituents spectral signatures can be elegantly circumvented using modern che-

---

[83] Chia-Chi Chang *y col.* «Estimation of Total Flavonoid Content in Propolis by Two Complementary Colorimetric Methods». En: *Journal of Food and Drug Analysis* 10.3 (2002), págs. 178-182.

[84] Vernon L. Singleton, Rudolf Orthofer y Rosa M. Lamuela-Raventós. «Analysis of total phenols and other oxidation substrates and antioxidants by means of folin-ciocalteu reagent». En: *Methods in Enzymology* 299 (1998), págs. 152-178. DOI: 10.1016/S0076-6879(99)99017-1. arXiv: arXiv:1011.1669v3.

mometric tools [8586]. Most of the related studies reported so far, apply basic chemometric procedures with simple mathematical procedures that have shown quite convincing results. With the application in industrial environments and the advancement of sophisticated and specialized multivariate methods, UV-Vis spectroscopy can become one more success story of chemometrics along with NIR spectroscopy [85].

Multivariate methods estimate concentration of individual substances by transforming non-selective signals (*i.e.*, absorption spectra) into specific concentration values for multicomponent mixtures [87]. To estimate concentration, the spectral signatures of the reference substances are used as model calibration data. This procedure is known as multivariate calibration and its application requires prior knowledge of the extract constituents by chromatographic identification or by another analytical method. Fig 2 shows an example of overlapped spectra in a mixture. The resulting spectrum is the line fitted to the points. The colored lines are the individual spectra of the extract constituents. Regression and Curve resolution techniques are the mathematical methodologies usually applied to the absorption spectroscopy data [88]. Some methods most frequently found in literature are Classical Least Squares (CLS), Inver-

---

[85] Dmitry Kirsanov *y col.* «UV–Vis spectroscopy with chemometric data treatment: an option for online control in nuclear industry». En: *Journal of Radioanalytical and Nuclear Chemistry* 312.3 (2017), págs. 461-470. DOI: 10.1007/s10967-017-5252-8.

[86] Rolf Manne. «On the resolution problem in hyphenated chromatography». En: *Chemometrics and Intelligent Laboratory Systems* 27.1 (1995), págs. 89 -94. DOI: https://doi.org/10.1016/0169-7439(95)80009-X.

[87] Alejandro C. Olivieri *y col.* «Uncertainty estimation and figures of merit for multivariate calibration (IUPAC Technical Report)». En: *Pure and Applied Chemistry* 78.3 (ene. de 2006), págs. 633-661. DOI: 10.1351/pac200678030633.

[88] Victor Abrahamsson, Firas Jumaah y Charlotta Turner. «Continuous multicomponent quantification during supercritical fluid extraction applied to microalgae using in-line UV/Vis absorption spectroscopy and on-line evaporative light scattering detection». En: *The Journal of Supercritical Fluids* 131 (ene. de 2018), págs. 157-165. DOI: 10.1016/J.SUPFLU.2017.09.014.

se Last Squares (ILS) and partial least squares for the regression-techniques family, and Multivariate Curve Resolution by Alternating Least Squares (MCR-ALS), Parallel Factor Analysis (PARAFAC2) and Artificial Neural Networks (ANN) for the family of Curve resolution techniques.

Figura 2. Analysis of mixture of peaks by multiple regression. Colored bands are true and measured components. Taken from [89]

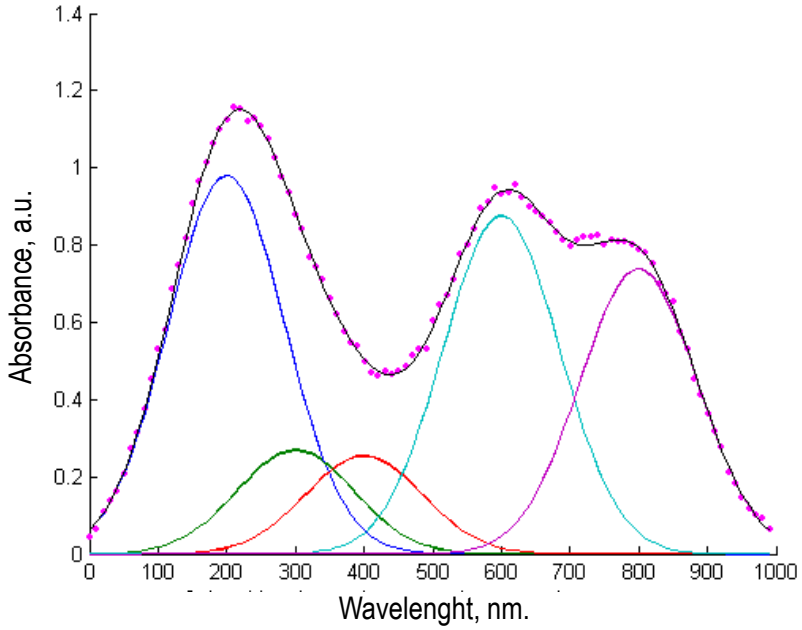

There are many examples of the application of multivariate calibration in the literature for extraction of valuable compounds. *E.g.* [90] employed UV–Vis spectrometry and multivariate calibration as a rapid and reliable tool for simultaneous quantification of ternary mixtures of phenolic acids in fruit juice. They employed the same methodology to propose a simple, inexpensive and sensitive kinetic spectrophotometric method developed for the simultaneous determination of three flavonoids: catechin,

---

[90] Rouhollah Khani, Reza Rahmanian y Naser Valipour Motlagh. «UVâ€“Visible Spectrometry and Multivariate Calibration as a Rapid and Reliable Tool for Simultaneous Quantification of Ternary Mixture of Phenolic Acids in Fruit Juice Samples». En: *Food Analytical Methods* 9.5 (2016), págs. 1112-1119. DOI: 10.1007/s12161-015-0287-3.

quercetin and naringenin, in fruit samples. [88] for their part, applied multivariate calibration to implement a quantitative methodology based on in-line UV-Vis absorption spectroscopy and on-line evaporative light scattering detection for sc-extraction. The method was developed to simultaneously quantify *in situ* the concentration of carotenoids, chlorophyll A, ergosterol and total lipids extracted from microalgae.

Based on the application of the [91] work, which exposes complex mechanisms in chemical engineering processes using specifically configured optical measurement techniques, it will be possible to see many of these methods applied at high-pressure processes shortly. However, together with technological advances, it is necessary to overcome the limitations associated with the analytical methodology that allows developing and validating models with acceptable figures of merit, such as precision, analytical sensitivity, adjustment, linearity, residual prediction deviation, detection, and quantification limits. Given the high heterogeneity of the samples to be analyzed, in some studies, it is necessary to propose strategies to optimize the calibration and validation data sets as [92] did by outlier elimination based on leverage and non-modelled residuals in spectral data.

The implementation of an analytical methodology for the simultaneous multicomponent quantification of extracts requires the technological measurement tool, a multivariate quantification methodology and the validation of the results. The latter treated with little rigor in the consulted literature.

---

[91] Andreas Braeuer. *In situ Spectroscopic Techniques at High Pressure*. Ed. por Erdogan Kiran. 1.ª ed. Vol. 7. Amsterdam: Elsevier, 2015, págs. 1-394.

[92] Dayane Aparecida dos Santos *y col.* «Multiproduct, Multicomponent and Multivariate Calibration: a Case Study by Using Vis-NIR Spectroscopy». En: *Food Analytical Methods* 11.7 (2018), págs. 1915-1919. DOI: 10.1007/s12161-017-1099-4.

1.5. Phase equilibria

The design of processes using sc-solvents is strongly dependent on the phase equilibrium scenario, which is highly sensitive to changes in operating conditions. Therefore, phase equilibrium engineering plays a key role in the synthesis and design of these processes [78]. Phase equilibrium engineering is the systematic application of phase equilibrium knowledge to process development [93]. This knowledge comprises data banks, experimental data, phenomenological phase behaviour, thermodynamic analysis, and mathematical modeling procedures for phase equilibrium process calculations. There is still a considerable lack of data because experimental determination of phase equilibria in sc-fluids is tedious, time-consuming, expensive and often even not reported in the literature because the scatter of the experimental values is big and unacceptable [94].

According to Brennecke y Eckert “any really widespread applications of sc-fluid extraction in the future are highly dependent on the ability of engineers to model and predict phase equilibria in the complex systems represented” (p. 1409, [95]). Each sc-application has a set of specifications and physical restrictions. Rigorous simulations of equilibrium stage separations at near-critical conditions are needed for the design and optimization of sc-processes. However, equilibrium calculations in the near-critical region can present serious convergence difficulties [78], even more when it comes to multi-component phase equilibria.

---

[93] Jose L Martinez. *Supercritical fluid extraction of nutraceuticals and bioactive compounds*. CRC Press, 2007.

[94] Helena Sovová, Marie Sajfrtová y Roumiana P. Stateva. «A novel model for multicomponent supercritical fluid extraction and its application to *Ruta graveolens*». En: *The Journal of Supercritical Fluids* 120 (feb. de 2017), págs. 102-112. DOI: 10.1016/J.SUPFLU.2016.10.008.

[95] Joan F. Brennecke y Charles A. Eckert. *Phase equilibria for supercritical fluid process design*. 1989. DOI: 10.1002/aic.690350902.

1.5.1. Solute-solvent equilibria Sc-extracts (solute) from botanical substrates are mainly constituted by CW and other already mentioned minor compounds what would be by definition a multi-component system. The concentration of the whole extract in the extraction solvent under equilibrium conditions and enough mass to saturate is called apparent solubility, an important parameter that controls the extraction kinetics and affects the extract production cost [96]. For now, it is impossible to model and predict the true solubility of this complex system, but some authors have recently addressed the problem by simplifying the system using strategies of grouping the components into families of molecules. This strategy relies heavily on experimental information and the modeling of the solubility of binary systems that are measured in the laboratory from pure substances and are known as thermodynamic solubility. Similar extracts constituents can be grouped and represented by a single molecule (pseudo-component) that presumably describe the thermodynamic behavior of their family in a simplified system. *E.g.* If the object of study are flavonoids but the main extract components are CW. Therefore, the system can be simplified to three components, *i.e.*, $scCO_2$, a representative molecule of the CW (majority compounds), and other for the flavonoid family (minority and valuable compounds).

Sovova *et al.* recently considered whether it is appropriate to use the solubility estimate of the most abundant long-chain alkane mixture in the extract to model the solubility of the extract in $scCO_2$. The authors modeled the extraction of mint from [97] data representing the extract as a mixture of 2 (C_{33} and C_{31}), and 3 (C_{29}, C_{31} and C_{33}) long-chain alkanes. Although the discussion about the convenience of this ap-

---

[96] Helena Sovová. «Apparent Solubility of Natural Products Extracted with Near-Critical Carbon Dioxide». En: *American Journal of Analytical Chemistry* 3 (2012), págs. 958-965.

[97] Bhupesh C. Roy *y col.* «Supercritical CO2 Extraction of Essential Oils and Cuticular Waxes from Peppermint Leaves». En: *Journal of Chemical Technology & Biotechnology* 67.1 (1996), págs. 21-26. DOI: 10.1002/(SICI)1097-4660(199609)67:1<21::AID-JCTB522>3.0.CO;2-0.

proach remains open, they found that changes in modeling of the extraction curve can be predicted quite well considering solubility of these n-alkanes in the mixture. In sc-extraction of a mixture of long-chain alkanes, the solubility in $scCO_2$ decreases with increasing length of the carbon chain. Authors also have shown that, if a mixture of such hydrocarbons should be represented by one component in a model for SFE, then the carbon chain of that component should be slightly longer than the average chain length in the mixture [94][98].

In the literature, there are many data about solubility of long-chain hydrocarbons in sc CO_2, but not for the great diversity of flavonoids found in nature. Solubility data for binary, ternary, or multi-component solid mixtures is still very limited. [99], and [100] are authors who have compiled solubility data between 2005 and 2017. In summary, they published a compendium of ca. 600 different solid compounds, most of which are biological and pharmaceutical compounds. Most of the reported data correspond to solute-$scCO_2$ binary systems, only 36 binary solid systems, five ternaries, and one quaternary have been investigated until 2017. To get closer to reality, it is still necessary to advance in the knowledge of the multi-component phase equilibrium, its thermodynamic description, modeling, and simplification strategies. Section 2.6.1 of this book describes a thermodynamic approach to multi-component modeling proposed by Sovová, Sajfrtová y Stateva and based on the well-known Parauznitz isofugacity equation.

---

[98] Helena Sovová y Roumiana P. Stateva. «New approach to modeling supercritical CO2 extraction of cuticular waxes: Interplay between solubility and kinetics». En: *Industrial and Engineering Chemistry Research* 54.17 (mayo de 2015), págs. 4861-4870. DOI: 10.1021/acs.iecr.5b00741.

[99] M Skerget, Željko Knez y Maša Knez-Hrnčič. «Solubility of solids in sub-and supercritical fluids: a review». En: *Journal of Chemical & Engineering Data* 56 (2011), págs. 694-719. DOI: 10.1021/je1011373.

[100] Željko Knez, Darija Cör y Maša Knez-Hrnčič. «Solubility of Solids in Sub- and Supercritical Fluids: A Review 2010-2017». En: *Journal of Chemical and Engineering Data* 63.4 (2018), págs. 860-884. DOI: 10.1021/acs.jced.7b00778.

1.5.2. Sorption equilibria In addition to solubility, other equilibrium parameters are relevant when the participation of the substrate in phase equilibria is considered. Typical extracts are complex mixtures of several interacting solutes, and solute-solute interactions affect the behaviour of the solubility of a constituent in the mixture as compared with the solubility of the pure counterpart [95]. The difference between apparent and thermodynamic solubilities can be explained by the interactions between solutes in complex extract mixtures as well as their interaction with the substrate. The maximal extraction yield from a biological tissue may be influenced by physical entrapment of solutes in the cellular structure, and there is no irrefutable experimental support to the claim that the yield is also negatively affected by solute-matrix interactions.

The approach of adopting expressions of adsorption isotherms to model the partitioning between the sample and the extraction phase has been shown to be suitable and does not necessarily complicate the models mathematically [101]. [102] made a compilation of such sorption expressions proposed until 2012 and remains valid to this day. Figure 3 shows a graphic representation of the approaches of the sorption models exposed by the authors. Del-Valle and Urrego (dVU) finish their work proposing a model that, at the cost of adding a new fitting parameter, describes a smooth and continuous function, universal enough to interpret data on CO_2 apparent solubility of volatile substances as well as the apparent solubility of vegetable oils from seeds, for which it was originally proposed [96]. The dVU sorption model is expended in sub-

---

[101] Camilo Pardo-Castaño, Manuel Velásquez y Gustavo Bolaños. «Simple models for supercritical extraction of natural matter». En: *Journal of Supercritical Fluids* 97 (2015), págs. 165-173. DOI: 10.1016/j.supflu.2014.09.044.

[102] José M. del Valle y Freddy a. Urrego. «Free solute content and solute-matrix interactions affect apparent solubility and apparent solute content in supercritical CO2 extractions. A hypothesis paper». En: *Journal of Supercritical Fluids* 66 (2012), págs. 157-175. DOI: 10.1016/j.supflu.2011.10.006.

section 2.6.1.

Figura 3. Comparison of sorption isotherm/isobar models presented in the del Valle y Urrego work. Taken from [103]

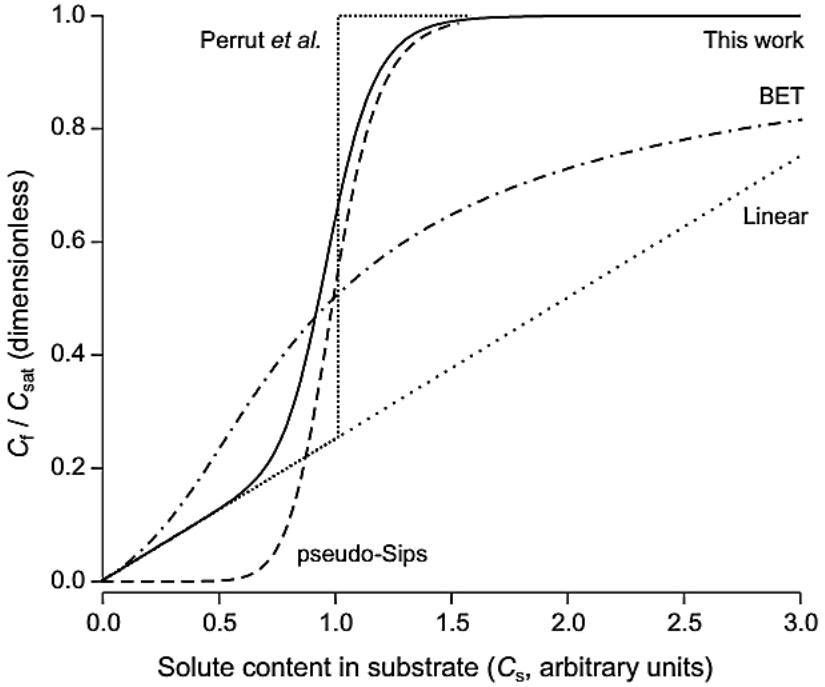

1.6. Kinetics of extraction

A number of kinetic mathematical models for sc-fluid extraction have been developed and proposed in the open literature as discussed in detail in several reviews [104][105]. Through matching the models against experimental extraction curves, the model parameters that are physically meaningful can be determined; in turn they cannot only

[104] José M. del Valle y Juan C. de la Fuente. «Supercritical CO2 Extraction of Oilseeds: Review of Kinetic and Equilibrium Models». En: *Critical Reviews in Food Science and Nutrition* 46.2 (mar. de 2006), págs. 131-160. DOI: 10.1080/10408390500526514.

[105] Zhen Huang, Xiao han Shi y Wei juan Jiang. *Theoretical models for supercritical fluid extraction*. 2012. DOI: 10.1016/j.chroma.2012.04.032.

depict the increase in extraction yield as a function of extraction time or solvent-to-feed ratio, but can also be used to predict large scale extraction curves as functions of the process variables. From this point of view, simple empirical models are of limited viability as their adjustable parameters, have no physical meanings and are not adequate for any predictions, even though they sometimes could deal with sc-fluid extraction curves very well [106].

There are various models employed to describe the sc-fluid extraction of oils or other compounds from plant material. All of them consider that the particles are packed inside an extractor column. The simplifying assumptions employed by most authors are: isothermal operation, negligible pressure drop across the extractor, and constant bed porosity and solid density along extraction. Furthermore, it is usually assumed that the solute loading in the sc-fluid is low and, therefore, fluid density, axial dispersion, and fluid velocity remain approximately constant. Such assumptions reduce the number of equations necessary to describe the extraction process to mass balances, equilibrium relations, and kinetics laws [74]. Four different models are described in the Oliveira, Silvestre y Silva work: linear driving force, shrinking core, broken plus intact cells, and a combination of the broken plus intact cells with shrinking core.

The broken and intact cells (BIC) approach proposed by [107], for mass transfer model of sc-extraction has shown good agreement with experimental results. This model considers substrate as particles that contain intact and broken cells. It is assumed that the extraction kinetics is fast or slow depending on whether the mass is transferred from the broken or intact cells respectively [74]. Sovová classified the extraction

---

[106] Zhen Huang. «Mass Transfer Models for Supercritical Fluid Extraction». En: *Food Engineering Series*. Springer, 2015, págs. 77-115. DOI: 10.1007/978-3-319-10611-3_3.

[107] Helena Sovová. «Mathematical model for supercritical fluid extraction of natural products and extraction curve evaluation». En: *The Journal of Supercritical Fluids* 33.1 (2005), págs. 35-52. DOI: 10.1016/J.SUPFLU.2004.03.005.

curves in four types from A to D, according to the regions of the discontinuous equilibrium function employed to describe the phase equilibrium stage.

1.7. Conclusion

Lippia origanoides K. and *Lippia graveolens* in addition to volatile compounds, also contain flavonoids in their celular structure that could be extracted. Considering this, the industry of *L. origanoides* and *L. graveolens* EOs has a clear opportunity with distillation by-producs to increase its profit by extracting, in addition to phenylpropanoid-rich EOs, flavonoids-rich oleoresin. Sc-extraction is a promising process to selectively obtain flavonoids. Evaluating the potential of its application in the valorization of solids residues from distillation of *Lippia* spp. is of great interest. The valorization study should be approached from a well-considered experimental strategy that allows identifying the factors with significant influence, optimizing them, and validating them within the experimental limits. Implementation of an analytical methodology for the simultaneous multicomponent quantification of extracts is necessary to achieve good experimental results. Modelling and simulation are important for process design purposes, particularly of sc-fluid extraction processes. Both, phase equilibrium and kinetic models have to be rigorously studied to build a reliable mathematical description of the phenomenon for simulation of sc-fluid extraction processes.

2. EXPERIMENTAL, MATERIALS AND METHODS

This chapter presents the experimental methodology and the modeling framework used in the present work. Fig. 4 shows a block diagram that summarizes all the methodology applied to achieve the results. The methodology is divided into three study sections. The first section (residues valorization study) focused on studying and selecting the variables that affect the sc-extraction of post-distillation *L. origanoides* chemotypes and *L. graveolens*. In this section, the sc-extraction of each substrate was also optimized and the best extracts were identified and quantified by rigorous chromatographic methods. The second section (study of phase equilibria) was applied with two approaches, *i.e.*, the phase equilibria between solutes and solvent (thermodynamic approach) and between solutes, solvent and support matrix (operational approach). In this stage, chemometrics tools were developed that allowed processing the large number of samples. Finally, the third section (kinetics study) delved into the kinetics of extraction joining the results of the phase equilibra with those of the mass transfer phenomena obtained fitting experimental extraction curves for the chopped and extruded substrates.

2.1. Plant material

2.1.1. Culture, harvest and distillation Different experimental lots of *L. graveolens* and three *L. origanoides* chemotypes (*i.e.*, thymol-, carvacrol- and phellandrene-rich chemotypes) were grown at the main campus (7°8′26.41″ N 73°7′10.45″ W, Bucaramanga, Colombia) and Barbosa campus (6°27′ N 75°19′59.99″ W, Barbosa, Colombia) of Universidad Industrial de Santander during the 2014 to 2016 period. The harvest collected each three months during these years, was steam distilled to remove essential oils that are not the subject of this work. A part of the steam distillation

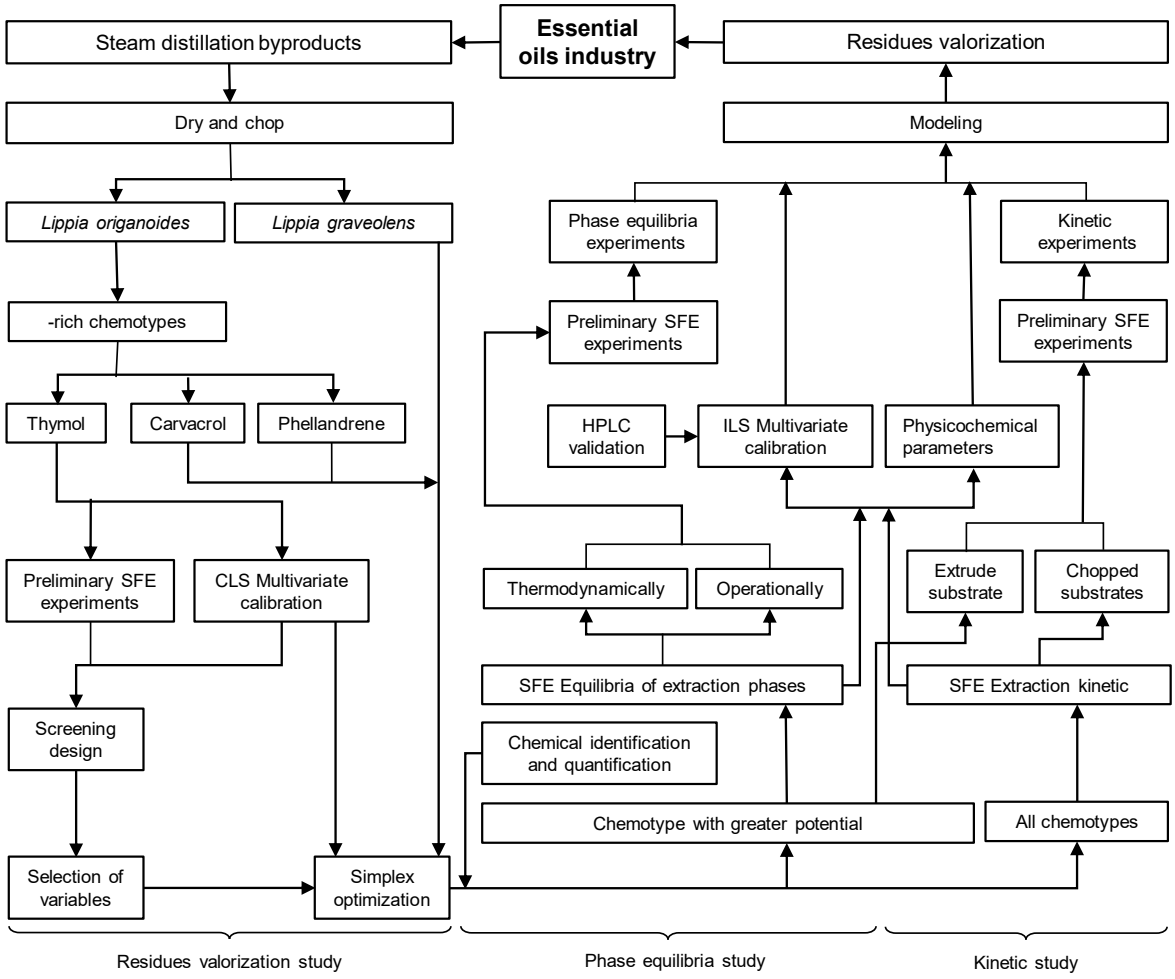

Figura 4. Block diagram of the methodology divided into three study sections.

residues was separated, dried in the shade and subsequently stored at controlled conditions. The remaining part of the waste was composted or used as a biofuel for other distillations.

2.1.2. Pretreatment

Particle size reduction Once there was enough raw material to make extractions, all the dried plant material was ground separately for each chemotype. Particle size was reduced in two steps, first with a chaff cutting machine PE800 *Penagos*

(Girón, Colombia) and then with a cutting mill *Retsch* SM100 (Haan, Germany). For *L. origanoides* thymol-rich chemotype, two exit grids were used, $0.5\,\mathrm{mm}$ and $2\,\mathrm{mm}$ openings, to use particle size as a variable for the screening design that is discussed in a following subsection. For the remaining chemotypes, the $2\,\mathrm{mm}$ opening exit grid was used. The chopped material was stored at $22\,℃$ in separate containers for each chemotype and particle size.

Microstructural disruption A part of the chopped material of *L. origanoides* phellandrene-rich chemotype was pretreated in a flat D-type PP85 pellet mill from *Pelletpros®* (Dubuque, USA) having exchangeable die openings (2.5 and $4\,\mathrm{mm}$ diameter). The extruded material was manually cut into cylindrical pellets having two sizes of unitary height (h)-to-diameter (d) ratio, *i.e.*, small pellets (**SP**, $h = d = 2.5\,\mathrm{mm}$) and large pellets (**LP**, $h = d = 4\,\mathrm{mm}$).

2.2. Sample analysis

2.2.1. Plant material A portable sieve shaker *CE Tyler* RX-24 (Cleveland, USA) was used to determine the particle size distribution of the chopped materials. A gas pycnometer *Quantacrome* Ultrapyc 1200e (Boynton Beach, USA) was used to determine the density ρ_s ($\mathrm{kg\,m^{-1}}$) of the solid chopped and extruded substrates using $99.9\,\mathrm{wt}\,\%$ nitrogen from *Air Liquide* (Santiago, Chile). The moisture was measured gravimetrically by removing water from samples of each post-distillation plant residue by drying in an WTC *Binder* convective oven (Tutlingen, Germany) set at $105\,℃$ for $24\,\mathrm{h}$. The total content of extract available in substrates was also measured gravimetrically by extracting samples using azeotropic ethanol-water mixture to exhaustion for $24\,\mathrm{h}$ (ca. $2\,\mathrm{cycles/h}$) in a $250\,\mathrm{mL}$ Soxhlet batch apparatus using $1:10$ $w_{\mathrm{subs}} : w_{\mathrm{solv}}$ ratio.

2.2.2. Extracts identification

UV spectroscopy A UV-Vis *Perkin-Elmer* Lambda 10 (Waltham, USA) spectrometer (speed 240 nm min^{-1}, smooth: 6) was used to obtain the UV-Vis spectral signal used in the residues valorization study for the CLS multivariate calibration. A UV-Vis miniature spectrophotometer (FLAME-S-UV-VIS-ES, 200 to 850 nm wavelengths range, 25 µm slit, 1:5 nm optical resolution (FWHM), L2 lens type and *Sony* ILX511b detector type) was used for the phase equilibria experiments by multivariate calibration. The spectrometer, deuterium and halogen light source (DH-2000-DUV, 190 to 2500 nm wavelength), fiber optic probes (QP455-025-XSR-BX, solarization resist, 180 to 900 nm) and collimator lens (74-UV,5 mm diameter, 10 mm focal length, 200 to 2000 nm wavelength) were obtained from *Ocean Optics* (Dunedin, USA). A UV quartz cuvette *SIGMA* C-9292 (Steinheim, Germany) was also used in the spectroscopic measurement. The UV spectrum was measured from 200 to 400 nm. This spectroscopic measurement setup, coupled to a high pressure visual cell for static solubility measurement, has been used and recently published by Pardo-Castaño and Bolaños [108][109]. Absorbance responses for extracts obtained from integral extraction curves (IEC) were taken at 287 nm in a *Shimadzu* UV mini-1240 spectrophotometer (Kyoto, Japan).

Gas chromatography Chromatographic analysis of fatty acids present in the sc-extract were performed as follows: 100 mg of extract was saponified with 2 mL of

---

[108] Camilo Pardo-Castaño *y col.* «Solubility of collinin and isocollinin in pressurized carbon dioxide: Synthesis, solubility parameters, and equilibrium measurements». En: *Journal of Chemical and Engineering Data* 64.9 (2019), págs. 3799-3810. DOI: 10.1021/acs.jced.9b00234.

[109] Camilo Pardo-Castaño y Gustavo Bolaños. «Solubility of chitosan in aqueous acetic acid and pressurized carbon dioxide-water: Experimental equilibrium and solubilization kinetics». En: *Journal of Supercritical Fluids* 151 (2019), págs. 63-74. DOI: 10.1016/j.supflu.2019.05.007.

KOH/MeOH 2 N (70 ℃, 10 $\mathrm{mín}$, stirring). Free fatty acids were derived to FAMEs using 3 mL of BF_3/MeOH (70 ℃, 5 $\mathrm{mín}$, stirring). FAMEs were extracted with 2 mL of n-hexane. One µL of the FAMEs was analyzed with a 7890A gas chromatograph (GC) (*Agilent Technologies*, Wilmington, DE) equipped with a flame ionization detector (FID) and a 7683B automatic injector. A fused silica DB23 capillary column (60 m L $\times$ 0.25 mm (ID), 0.25 µm d_p) was used. The oven temperature was programmed as follows: 50 ℃ for 1 $\mathrm{mín}$, increased to 175 ℃ at 25 ℃/ $\mathrm{mín}$, then increased to 230 ℃ at 4 ℃/ $\mathrm{mín}$, and kept at 230 ℃ for 7 $\mathrm{mín}$. The injection and detector temperatures were 250 ℃ and 280 ℃, respectively. The carrier gas was hydrogen at 33 cm s^{-1}. The split ratio was 1:50. FAME identification was based on retention times as compared with those of the standard FAME mixture. Results were expressed as percentage of peak area without any correction.

Liquid chromatography

UHPLC-ESI(+)-Orbitrap-MS A *Thermo Scientific* Exactive Plus LC-MS (Palo Alto, USA) system equipped with heated electrospray interface and orbitrap detection was employed for the determination and quantification of the highest-yield extract from each chemotype at the end of residues valorization study. A Hypersil GOLD aQ *Thermo Scientific* (Sunnyvale, USA; 100 mm L $\times$ 2.1 mm ID, 1.9 µm d_p) column was used. The column temperature was maintained at 35 ℃. A 0.2 $cm^3/$ $\mathrm{mín}$ mixture of water (A), acetonitrile (B), with 0.5 wt % formic acid each, was used as mobile phase with the following gradient program: 100 vol % A changed linearly to 100 vol % B in 8 $\mathrm{mín}$, maintained constant for 4 $\mathrm{mín}$, returned to 100 vol % A in 1 $\mathrm{mín}$ and remained unchanged for the last 3 $\mathrm{mín}$. The mass spectra were obtained in positive mode; injection volume: 1 µL; gas temperature: 350 ℃; drying gas: 7 L/ $\mathrm{mín}$ of N_2; nebulizer gas: 0.3 MPa; capillary voltage: 3.5 kV; mass range 100 to 1100 m/z. Mass spectra were acquired in the all-ion fragmentation mode for energies of 10, 20, 30 and

40 eV at the high-energy collision dissociation chamber. Chromatographic and mass spectrometric data were processed with *Xcalibur®* software, version 4.0. Compound identification was based on extracted ion chromatogram (EIC), exact masses, comparison with standard compounds, and fragment pattern interpretation.

HPLC with UV-Vis detectors An *Agilent Technologies* 1260 Infinity (Palo Alto, USA) chromatograph coupled to a diode array detector (DAD G1315D) and a multiple wave detector (G1365D) was used to validate the inverse multivariate calibration model by comparing the data obtained by HPLC quantification and the prediction of the ILS models. The separation of the constituents of the extracts was done in a C18 Gemini *Phenomenex* column (Torrance, USA), 25 cm L $\times$ 4.6 mm ID, 5 µm d_p. Detection of compounds was at 290 nm. The mobile phase was water (A, 0.5 wt $\%$ formic acid) and acetonitrile (B) with 1 mL/ mín volumetric flow and injection volume of 10 µL. The method was programmed at 0 mín: 98 vol $\%$ B, at 15 mín: 88 vol $\%$ B, 15 to 23 mín: 88 vol $\%$ B, 46 mín: 60 vol $\%$ B, 80 to 85 mín: 98 vol $\%$ B.

Perkin Elmer Series 200 HPLC (Shelton, USA) system, coupled to a Series 200 UV-Vis Detector, was interfaced with an equilibrium cell for measuring the solubility of Pn in CO_2+extract system at different P and T conditions. After reaching equilibrium, a 20 µL aliquot of the extract-saturated in CO2-rich phase was loaded into the loop of a six-port high-pressure injection *Rheodyne* 7010 valve (Rohnert Park, USA). The separation of the extract constituents dissolved in the CO_2-rich phase was done in a C18 Symmetry *Waters* column (Milford, USA), 25 cm L $\times$ 4.6 mm ID, 5 µm d_p. Detection of compounds was at 289 nm. The column temperature was maintained at 25 ℃. A 1 cm^3/ mín mixture of MeOH (A), water (B), was used as mobile phase with the following gradient program: 70 vol $\%$ A changed linearly to 100 vol $\%$ A in 8 mín, maintained constant for 4 mín, returned to 70 vol $\%$ A in 1 mín and remained unchanged for the last 3 mín.

2.3. Quantification

2.3.1. Multivariate Calibration Multivariate calibration is commonly used to determine the concentration of constituents in a mixture of analytes by means of spectral analysis. Here, the concentrations of the analytes are the predictor variables, and the absorbances at the different wavelengths are the response variables. The multivariate calibration method was used to transform the instrumental response of the spectrometers into useful concentration values, even given the several superpositions of the spectra of the *L. origanoides* and *L. graveolens* sc-extracts constituents. This methodology avoided using chemical separation techniques (e.g., chromatography) for the large number of experimental samples analyzed. The extract spectral signal was modeled as a sum of contributions from some flavonoids constituents of the sc-extract of post-distillation substrates. According to [13] and current studies by some of the same authors, these are: pinocembrin, galangin, naringenin, luteolin, and apigenin, which were purchased from *Sigma-Aldrich* (St. Louis, USA) as high purity standards ($> 98\,\text{wt}\,\%$).

Classical model The scope of the clasical least-squares (CLS) model is rather limited, since it requires the spectra of all contributing species to be measured or estimated from mixture spectra [87].The quantification method assumes a linear additive signal for the constituents, as represented mathematically by matrix Eq. 1:

$$\boldsymbol{r} = \boldsymbol{S}\boldsymbol{c} + \boldsymbol{e}, \tag{1}$$

where, $\boldsymbol{r}$ $(j \times k)$ is the measured absorbance data matrix (instrumental response of samples of unknown concentration, espectral value) with j wavelengths selected and k samples measured ($k = 3$ for triplicates), $\boldsymbol{S}$ $(j \times i)$ is the absorbance matrix of the pure-components, e.i., the spectra of the i flavonoids that represent the components,

that absorb UV-Vis radiation, present in the extract at the unit concentration. $\boldsymbol{S}$ is a matrix constructed from either measured pure spectrum of each standard of the flavonoids at a known concentration (direct mode) or estimated from the spectra of mixtures of the extract constituents (indirect mode) [110]. Finally, $\boldsymbol{c}$ $(i \times k)$ is the matrix of samples of unknown concentration and $\boldsymbol{e}$ $(j \times 1)$ is the vector of noise. To predict matrix concentration $\boldsymbol{c}$, the matrix expression of Eq. 2 is derived from matrix Eq. 1, where the superscript "+" denotes the pseudo-inverse operation (*i.e.*, $\boldsymbol{S}^{+} = \left(\boldsymbol{S}^{\boldsymbol{T}}\boldsymbol{S}\right)^{-1}\boldsymbol{S}^{\boldsymbol{T}}$), superscript "T" signifies transpose and hat over $\boldsymbol{c}$ indicates the ordinary least-squares (OLS) estimate of $\boldsymbol{c}$. The concentrations of all constituents of samples were obtained by fitting the pure-flavonoids signals $\boldsymbol{S}$ to the spectra of the measured samples $\boldsymbol{r}$ using OLS fit.

$$\hat{\boldsymbol{c}} = \boldsymbol{S}^{+}\boldsymbol{r} \tag{2}$$

The direct mode of CLS model was used in the residues valorization study of this work. A group of 44 wavelengths, which represent the variations in the spectral signals of the molecules, was conveniently selected to perform the calculations. Samples of extracts were measured in triplicate. Methanol (MeOH) was used as eluent of the samples and was supplied by *Mallinckrodt Baker Inc.* (Phillipsburg, USA).

Inverse model The inverse least squares (ILS) method was employed to determine extract flavonoid contents in phase equlibria and kinetics study of this work. The ILS method has an advantage compared to CLS because it minimizes errors during

---

[110] R D Bautista *y col.* «Simultaneous determination of diazepam and pyridoxine in synthetic mixtures and pharmaceutical formulations using graphical and multivariate calibration-prediction methods.» En: *Journal of pharmaceutical and biomedical analysis* 15.2 (1996), págs. 183-92. DOI: 10.1016/0731-7085(96)01844-4.

calibration [111], which is more convenient to deepen the study of thermodynamics and mass transfer phenomena of the extraction process. The multivariate inverse model for the prediction sample is:

$$\boldsymbol{c} = \boldsymbol{r}^{\boldsymbol{T}}\boldsymbol{b} + \boldsymbol{e}, \tag{3}$$

where $\boldsymbol{b}$ is the $j \times k$ model parameter matrix, *i.e.*, the multiple linear regression coefficients for each selected wavelength. The remaining symbols are as defined before. The estimate of $\boldsymbol{b}$ is obtained from calibration data, similar to the straight line fitting using in the external calibration methodology, but with data structures of higher complexity than scalars which is expressed using tensor algebra [112]:

$$\boldsymbol{c}_{\text{cal}} = \boldsymbol{R}^{\boldsymbol{T}}\boldsymbol{b} + \boldsymbol{e}, \tag{4}$$

where the subscript "cal" in $\boldsymbol{c}$ denotes the known concentration of flavonoids in calibration samples, $\boldsymbol{R}$ $(i \times j \times k)$ is an array that contains the spectra of mixtures of flavonoids of the calibration samples and $\boldsymbol{e}$ is now a matrix of noise. The interferences do not play an explicit role in Eq. 4. The ILS allowed to calibrate the flavonoids individually from the mixtures of the available or necessary standards for study, regardless of whether they represented all the constituents of the extract or all the interactions between the molecules (matrix effect). In other words, ILS can be a highly selective method for quantification of flavonoids of interest. This is a major advantage over the CLS, which requires that the number of standards used in the calibration be as close

---

[111] R. Torralba *y col.* «Speciation and simultaneous determination of arsenic(III), arsenic(V), monomethylarsonate and dimethylarsinate by atomic absorption using inverse least squares multivariate calibration». En: *Spectrochimica Acta Part B: Atomic Spectroscopy* 49.9 (ago. de 1994), págs. 893-899. DOI: 10.1016/0584-8547(94)80078-2.

[112] Eugenio Sanchez y Bruce R. Kowalski. «Tensorial resolution: A direct trilinear decomposition». En: *Journal of Chemometrics* 4.1 (ene. de 1990), págs. 29-45. DOI: 10.1002/cem.1180040105.

as possible to the constituents of the test extract [87].

As will be seen later in the results section, the phellandrene-rich chemotype was selected to further study phase equilibria and kinetics of the extraction process. The major flavonoids of EtOH-modified scCO$_2$ extract of *L. origanoides* phellandrene-rich chemotype are pinocembrin (Pn) and galangin (Gn). So the ILS method was selectively applied to those molecules. According to the IUPAC recommendation in 2001, "selectivity refers to the extent to which the method can be used to determine particular analytes in mixtures or matrices without interferences from other components of similar behavior" [113]. The interference (Intf), for our purpose, was defined as the mixtures of flavonoids that remain in a lesser proportion in the extract and the mixture of cuticular waxes that, although do not absorb the radiation in the UV-Vis region, contribute to the matrix effect. In this way, the samples of the sc-extract were represented as the mixture of three constituents, *i.e.*, Pn, Gn and Intf. This approach allowed to test different sets of data to find a better prediction of concentration comparing ILS with HPLC. Since it is not practical and virtually impossible to know the true value of Intf in the extract, the response factor for the Intf was an optimizable matrix within the array $\boldsymbol{R}$. Pure spectra for Pn, Gn and Intf were calculated using Eq. 5.

$$\boldsymbol{S} = \left(\boldsymbol{c}_{\text{cal}}\boldsymbol{c}_{\text{cal}}^{\boldsymbol{T}}\right)^{-1}\boldsymbol{c}_{\text{cal}}\boldsymbol{R} \tag{5}$$

Three data sets were prepared for calibration in MeOH as eluent (99.9 wt %, Merck, Darmstadt, Germany). First data set (DS1) were nine different mixtures of Pn and Gn standards assessed gravimetrically at: 21.6 and 10.7, 21.6 and 7.5, 21.6 and 4.3, 13 and 6.5, 13 and 4.5, 13 and 2.6, 4.4 and 2.1, 4.4 and 1.5, 4.4 and 0.9 $\mu g/g_{sln}$,

---

[113] Jörgen Vessman *y col.* «Selectivity in analytical chemistry (IUPAC Recommendations 2001)». En: *Pure and Applied Chemistry* 73.8 (ago. de 2001), págs. 1381-1386. DOI: 10.1351/pac200173081381.

respectively. DS1 does not consider Intf since mixtures were prepared by diluting standards of Pn and Gn in MeOH. Second data set (DS2) was prepared mixing a fixed concentration of extract ($2.55\,\mathrm{mg\,g^{-1}}$) with five diferent Pn and Gn mixture assessed gravimetrically at: 2.8 and 1.3, 5.6 and 2.6, 8.1 and 4.1, 10.8 and 5.5, 13.6 and 7.3 $\mu g/g_{sln}$, respectively. In DS2, the number of moles of Intf remained constants for all mixtures. Finally, the third data set (DS3) was prepared at three levels (2.6, 7.7 and $12.8\,mg_{extract}/g_{sln}$) of extract concentration. To measure the UV spectrum of DS2 and DS3, 100 µL of the HPLC prepared sample were diluted to 5 mL, because high concentration solutions cause deviations from linear behavior of absorbance response. All mixtures were prepared in triplicate.

In summary, 17 calibration mixture-samples in triplicate (51 points), grouped in three data sets (DS1-DS3) were used for ILS multivariate calibration. The approach to finding the models that best predict the concentration of Pn and Gn was to test the different sets of data individually and jointly comparing the results with those obtained by HPLC. Leave one out (LOO) cross-validation methodology was applied in order to determine the capability to predict concentration without the information of a point in triplicate for models. Prediction coefficient Q^2 was calculated as a measure of goodness of prediction achieved with the sets of calibration data.

2.3.2. Liquid chromatography

UHPLC-ESI(+)-Orbitrap-MS The external calibration methodology was employed for quantification using calibration curves of available standard substances (*i.e.* quercetin, luteolin, naringenin, apigenin, and pinocembrin) to relate concentration with chromatographic peak area [114]. The quantification of the molecules for which

[114] James N Miller y Jane Charlotte Miller. *Statistics and chemometrics for analytical chemistry*. Sixth. Pearson Education, 2010.

the standard substances were not available, was calculated from a surrogate (*i.e.*, kaempferol, *Sigma-Aldrich*, St. Louis, USA) with the method of internal standard [115].

HPLC with UV-Vis detectors The external calibration methodology was also employed for quantification in HPLC-DAD to compare results with those calculated by ILS method. DS1-DS3 were quantified by means of calibration curves of Pn and Gn standard substances that relate the concentration of the flavonoids in the sample with the corresponding chromatographic peak area. Each point of the curve was prepared three times from a stock solution containing Pn and Gn at the same mass concentration. The concentrations were 12.8, 38.3, 63.8, 102, 127.5, 255.1 and 510 $\mathrm{mg\,g^{-1}}$. Calibration curves were prepared and analyzed at the same chromatographic conditions at which DS1-DS3 were measured.

Values of solubility for Pn + sc-extract + CO_2 system were calculated using Eq. 6 [116] based on the chromatographic response (A_2, peak area) of a CO_2-rich phase sample ($V_{\mathrm{IV}} = 20\,\mu\mathrm{L}$, from the loop of the equilibrium cell) as compared to the chromatographic response of a standard reference solution (A_{S2} from $V_{\mathrm{S}} = 20\,\mu\mathrm{L}$ from the loop of the HPLC injector), of known concentration (C_{S2}) of nobiletin (for preliminary experiments) and Pn used for calibration purposes. Properties of CO_2, molar mass ($MW_{\mathrm{CO_2}}$) and specific volume at test conditions ($v_{\mathrm{CO_2}}$) was also necesary and calculated as a function of system temperature and pressure using the NIST database

---

[115] Luis Cuadros-Rodríguez *y col.* «Principles of analytical calibration/quantification for the separation sciences». En: *Journal of Chromatography A* 1158.1-2 (jul. de 2007), págs. 33-46. DOI: 10.1016/J.CHROMA.2007.03.030.

[116] Karina A. Araus *y col.* «Solubility of β-carotene in ethanol- and triolein-modified CO2». En: *The Journal of Chemical Thermodynamics* 43.12 (dic. de 2011), págs. 1991-2001. DOI: 10.1016/J.JCT.2011.07.013.

[117].

$$y_2 = \left(\frac{A_2/V_{\mathrm{IV}}}{A_{\mathrm{S2}}/V_{\mathrm{S}}}\right) C_{\mathrm{S2}} v_{\mathrm{CO_2}} MW_{\mathrm{CO_2}} \tag{6}$$

2.3.3. Cuticular waxes and `Intf` The present work did not have the scope of analytically quantifying, through some instrumental methodology, the co-extracted compounds such as fatty acids, waxes, pigments, resinoids, among others. The fatty acid analysis mentioned in subsection 2.2.2 was proposed as a preliminary and tentative identification of that family of molecules in a specific obtained extract. The analysis sought to confirm the presence of linear long-chain hydrocarbons and their fatty acids in the sc-extract of the studied substrates. These co-extracted with target flavonoids molecules, for our practical purposes, were grouped together with the interferences (`Intf`) previously defined as flavonoids that remain to a lesser extent in the extract. In this way, samples of the sc-extract were represented for mathematical purposes as the mixture of three constituents, *i.e.*, `Pn`, `Gn` and `Intf`. `Intf` was calculated by material balance and was the difference between the extract mass and the `Pn` and `Gn` mass predicted by multivariate calibration.

2.4. Supercritical extraction and phase equilibria

2.4.1. Supercritical extraction with ethanol-modified CO_2

Residues valorization study Before the extraction, the substrates were dried again on a tray in an *Indumegas* oven (Bucaramanga, Colombia) set at 60 ℃, for 12 h. The drying time was determined with a drying rate plot. Substrates (500 g for

---

[117] E. W. Lemmon, M. L. Huber y M.O. McLinden. *NIST Standard Reference Database 23: Reference Fluid Thermodynamic and Transport Properties (REFPROP), version 9.1*. Gaithersburg, 2013.

each experiment) were extracted in a one-pass pilot scale modified *Thar Instruments* SFE-2000–2-FMC50 equipment (Pittsburgh, USA) at corresponding conditions. The modified equipment consists of two extraction vessels in parallel ($2000\,\mathrm{cm}^3$ capacity each one, $d = 7.6\,\mathrm{cm}$ ID, $h = 43.9\,\mathrm{cm}$) equipped with heat transfer jackets; two pistons pumps (P200 for CO_2 and P50 for EtOH) from *Thar Technologies*; three separators ($500\,\mathrm{cm}^3$ capacity) equipped with heat transfer jackets, two of them in series and one for CO_2 discharge; an automated, and two manual back-pressure regulator valves from *Thar Technologies*. Fig. 5 shows the process diagram for the extraction system. During the development of this work the author also participated in the design and implementation of a CO_2 recirculation system coupled to the above-described pilot plant of sc-extraction. The details of the implementation of the recirculation system are shown in the international patent (Appendix 1) written by the author and presented together with other co-inventors on behalf of the Universidad Industrial de Santander to the World Intellectual Property Organization (WIPO).

The conditions used in the separators to obtain fractions, were $80\,\mathrm{bar}$ and $35\,℃$ in the first separator Sep1, atmospheric conditions and $20\,℃$ in the second separator Sep2, conditions similar to those used in a rosemary extraction study [118]. Extractions were carried out using $99.8\,\mathrm{wt}\,\%$ pure CO_2 from *Praxair* (Bucaramanga, Colombia) and industrial-quality EtOH from *Suquin* (96 %, Bucaramanga, Colombia). For these experiments, single samples were collected during the time of the extractions. The extracts from both separators were pooled and most of the solvent was removed on an R-Style rotary evaporator. The extract was completely cleaned of solvent in a subsequent stage of convective drying, using nitrogen flow. Dried extract samples were collected in pre-weighed glass vials and recovered extracts were assessed

---

[118] E Reverchon y F Senatore. «Isolation of rosemary oil: Comparison between hydrodistillation and supercritical CO2 extraction». En: *Flavour and Fragrance Journal* 7.4 (1992), págs. 227-230. DOI: 10.1002/ffj.2730070411.

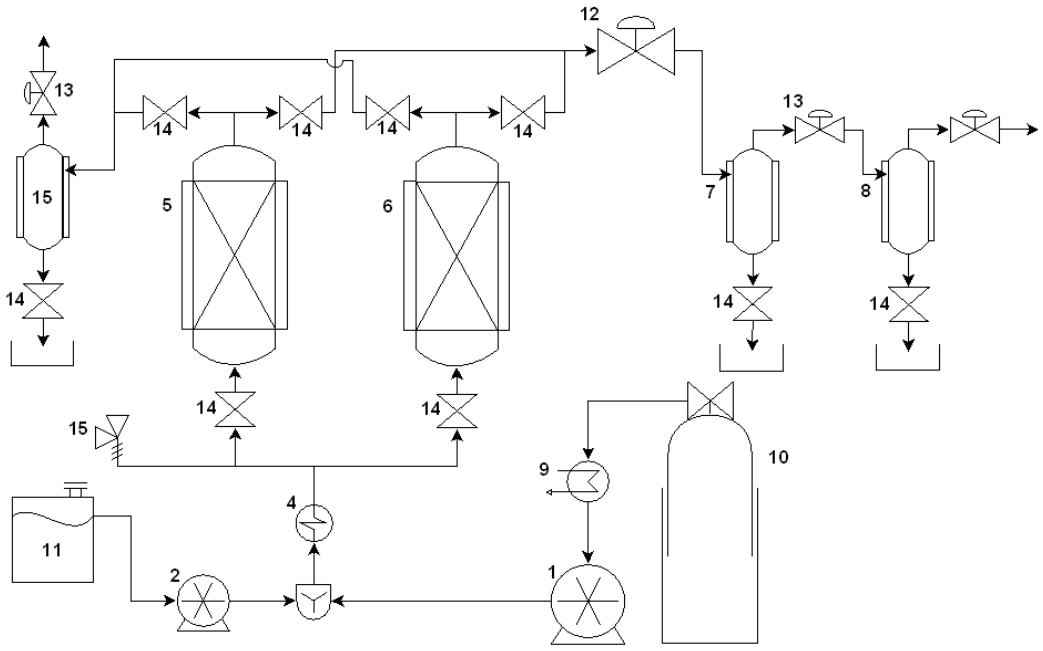

Figura 5. Schematic diagram of supercritical fluid extraction process used in residues valorization study. The system consists of: CO_2 pump (1), EtOH pump (2), mixer (3), heater (4), vessel I (5), vessel II (6), separator I (7), separator II (8), refrigerator (9), CO_2 feed (10), EtOH feed (11), ABPR (12), MBPR (13), on / off valves (14) and depressurizer (15).

gravimetrically. Samples were stored at $4\,°C$ in amber vials.

Kinetics study For each extraction, 20 to $40\,g$ of substrate were loaded into a extraction vessel ($50\,cm^3$ capacity, $d = 2\,cm$ ID, $h = 14.7\,cm$) from *Thar Technologies* (Pittsburgh, USA). Vessels were placed in a temperature-controlled air convection oven from *Thar Technologies* set at $50\,°C$. The one-pass system was fed with CO_2 + EtOH (mixture referred, for our purpose, as a pseudo-component m) by means of two piston pumps from *Thar Technologies* and the system pressure kept at the set value of $34\,MPa$ using an automated BP-2080 back-pressure regulator from *Jasco* (Tokyo, Japan). Extractions were carried out using $99.8\,wt\,\%$ pure CO_2 from *Air Liquide* (Santiago, Chile) and Pro-analysis-quality EtOH was purchased from *Merck*

(Darmstadt, Germany). The dynamic extraction was carried out during ca. 240 mín, at 20 g/ mín of CO_2 and 3 g/ mín of EtOH at 50 ℃ and 34 MPa (superficial velocity of m, U = 1.2 mm/s) that was fed in the bottom of the extraction vessel. The extract dissolved in EtOH were taken in glass vials every 5 mín during the first 20 mín, every 10 mín during the subsiding hour, and every half hour during the subsiding two and a half hours. Samples for spectroscopic analysis were prepared taking an aliquot of scEtOH-extract for each point of tha curve and then diluting in MeOH to complete 1 mL in volumetric flasks. scEtOH-extracts were transferred to pre-weighed Petri dishes and were dried in a convective hot air bath at 50 ℃: recovered extracts were assessed gravimetrically.

2.4.2. Supercritical phase equilibria

Measurement of the thermodynamic solubility The solubilities of sc-extract in $scCO_2$ (without substrate) were measured using a dynamic-analytical methodology in a modified version of the experimental apparatus described by [116], (Fig. 6). The experimental system consists of an stirred, 100 cm^3 (*TharTech*, Pittsburgh, USA) view-cell placed in a temperature-controlled air bath, with an syringe pump (Teledyne *ISCO* 260D, Lincoln, USA) to load CO_2 into the system and adjust system pressure, and with a gear pump (GAH-T23, *Eurotechnica*, Bargteheide, Germany) to recirculate the CO_2-rich phase and aid system equilibration, and to feed samples of the CO_2-rich phase to the HPLC system already coupled to the equilibration system. The system was complemented in this work by improving the equilibrium cell interface with on-line chromatography by adding a two-position, six-port high pressure switching valve 7010 *Rheodyne* (Rohnert Park, USA) to the system. With the new configuration, the operation of the system was simplified and some valves necessary for the cleaning and purging of the loop, the injection of the sample and to keep in equilibrium the cell were dispensed with. The configuration of two six-port valves, in

the coupling of sc-processes with HPLC, has also been used in the literature for the determination of explosives in vapor phases [119] and to control the progress of the reaction of synthetic organic materials [120], among other applications.

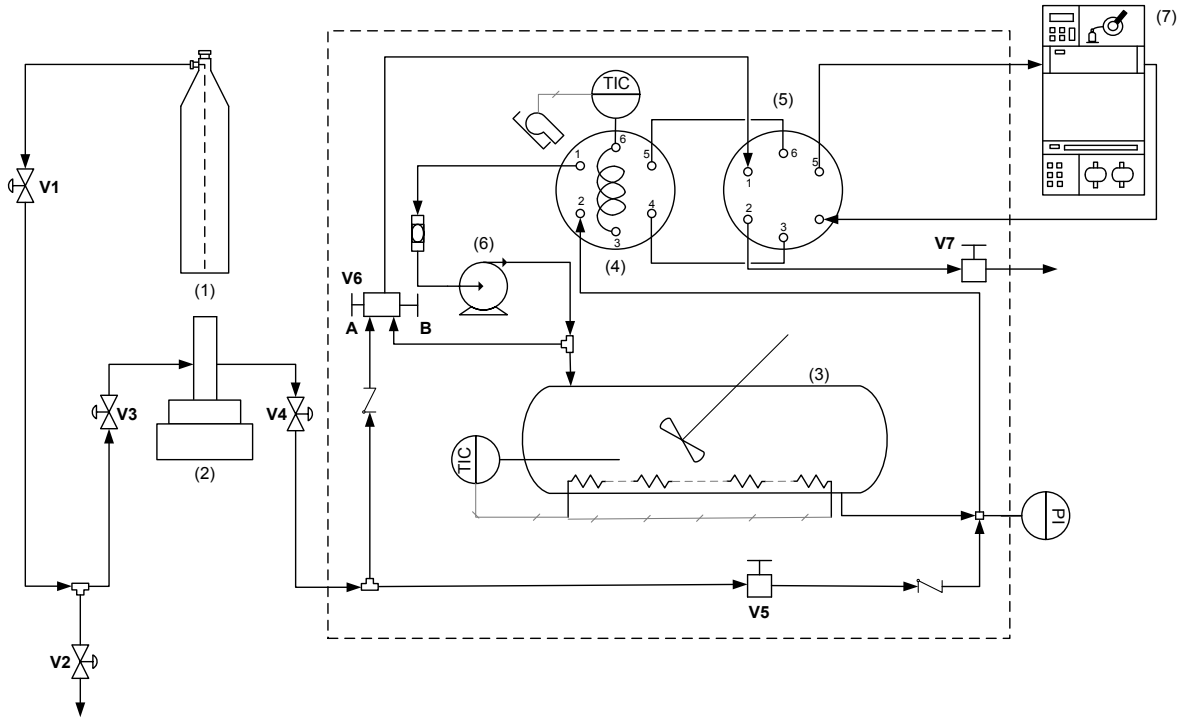

Figura 6. Schematic diagram of the experimental apparatus for solubility measurements. The main components of the system are the (1) CO_2 feed, (2) syringe pump, (3) 100 mL view-cell , (4) six-port high-pressure injection valve, (5) switching valve between the lines of pressurized CO_2 and mobile phase, (6) recirculation pump and (7) HPLC-DAD.

---

[119] Ramón Batlle *y col.* «On-line coupling of supercritical fluid extraction with high-performance liquid chromatography for the determination of explosives in vapour phases». En: *Journal of Chromatography A* 963.1-2 (jul. de 2002), págs. 73-82. DOI: 10.1016/S0021-9673(02)00136-X.

[120] Edward D. Ramsey *y col.* «Interfacing supercritical fluid reaction apparatus with on-line liquid chromatography: Monitoring the progress of a synthetic organic reaction performed in supercritical fluid solution». En: *Journal of Chromatography A* 1388 (abr. de 2015), págs. 141-150. DOI: 10.1016/J.CHROMA.2015.02.037.

Sorption equilibrium measurements Chopped post-distillation phellandrene-rich chemotype of *L. origanoides* was extracted using available instruments of a one-pass pilot scale Thar SFE-2000–2-FMC50 equipment, see section 2.4.1. The extraction vessel was $500\,\mathrm{cm}^3$ capacity ($d = 5.2\,\mathrm{cm}$ ID, $h = 24\,\mathrm{cm}$). The level of charged substrate inside extraction vessel (H) was $1/3$ of its h, to avoid channeling effects during extraction [88]. Over extraction vessel the electric jacket maintained the selected $\pm 1\,\mathrm{K}$ extraction temperature condition. Extraction pressure $\pm 0.1\,\mathrm{MPa}$ selected for each experiment was maintained through ABPR. For all experiments, CO_2 flow was set at $20\,\mathrm{g/\,mín}$, its value was controlled by a P200 pump in the flow mode which uses data from flowmeter *Siemens* Sitrans FC Mass 2100 (Munich, Germany) to regulate its RPM on-line. The P50 pump was operated in the fixed RPM mode, so EtOH flow was measured gravimetrically. Before dynamic extraction started, 10 minutes of static extraction were used. Fractions of equilibrium integral extraction curves (EIEC) were collected every $5\,\mathrm{mín}$ during the first $20\,\mathrm{mín}$ and subsequently every $20\,\mathrm{mín}$ to complete $300\,\mathrm{mín}$ in total. UV absorbance spectrum was measured for each fraction three times. Samples for spectroscopic analysis were prepared taking $20\,\mu\mathrm{L}$ of scEtOH-extract and then diluting in MeOH to complete $5\,\mathrm{mL}$ in volumetric flasks.

2.5. Experimental

2.5.1. Residues valorization study

Extraction reproducibility Six preliminary experiments with post-distillation substrate of thymol-rich chemotype were carried out to assess reproducibility (RSD <10 %). Triplicates with two different experimental conditions were performed and the variance found for these experiments was assumed as the variance of each experiment in the screening design.

Screening design The screening design was also performed only with the thymol-rich chemotype, so it was assumed that the independent variables of extraction affect in the same way all substrates studied, since in general terms it is considered that they come from the same plant. Six extraction variables were studied in the screening design: pressure (P), temperature (T), extraction time (t), CO_2 flow (F), particle size (d_p), and percent ethanol (E). Because the experiments were conducted in the same extraction vessel, it was preferred to use the variable F instead of the U_{CO_2}. On the other hand, the variable d_p refers to the exit grids opening the mill, not the real size of the particles. A $2^{(6-2)}$ fractional factorial design of resolution 4 was employed [121]. Table 3 shows the selected levels used, in accordance with the equipment constraints.

Table 3. Extraction variables values for 2^{6-2} fractional factorial design.

Factors	Symbol	Domain 1	Domain -1
Pressure, bar	P	400	80
Temperature, ℃	T	60	40
Flow, $\mathrm{g/\,mín}$ of CO_2	F	50	10
Particle size, mm	d_p	2	0.5
Extraction time, $\mathrm{mín}$	t	120	60
Percent ethanol, wt $\%$	E	10	0

Refers to the exit grids opening the mill, not the real size of the particles.

Optimization of extraction conditions The variables that showed significant influence in the screening design were experimentally modified according to the simplex optimization method proposed by [122], in order to find the extraction conditions

[121] NIST Sematech. *e-Handbook of Statistical Methods*. 2006.

[122] John A Nelder y Roger Mead. «A simplex method for function minimization». En: *The Computer Journal* 7.4 (1965), págs. 308-313. DOI: 10.1093/comjnl/7.4.308.

that produce the highest extraction yield of flavonoids in the selected experimental space. Few simplex optimization works on sc-extraction are found in the literature. However, it was considered more convenient approach for optimization because the search for the optimum is more refined compared to the widely used response surface methodology, and especially because the effects of the variables are already known from the screening experimental design of the previous stage. The top five experimental conditions in the screening design were used as initial point of the optimization. Three scalar parameters were specified to define a complete Nelder–Mead method (*i.e.*, reflection-, expansion- and contraction- coefficient) which were modified in their load according to the convenience to improve the experimental results.

2.5.2. Phase equilibria study

Thermodynamic solubility

Preliminary experiments and uncertainty To validate the results of the new configuration of the dynamic solubility measurement system (cf. subsection 2.4.2), preliminary experiments were carried out with nobiletin (>0.97 wt %, *CHEMOS GmbH*, Regenstauf, Germany), a solute whose solubility is known [123]. The solubility of solid nobiletin in $scCO_2$ was measured at 313 K and 323 K over a pressure range from (8.8 to 32.1 MPa). The cell was loaded with approximately 0.5 g of solid solute, then the residual air is removed by displacement with CO_2 from a gas cylinder, released with a vacuum pump and (*Welch Vacuum*, Skokie, USA), after that, CO_2 was loaded using the high pressure syringe pump. With both components loaded in the equili-

[123] Adolfo L. Cabrera *y col.* «Measuring and validation for isothermal solubility data of solid 2-(3,4-Dimethoxyphenyl)-5,6,7,8-tetramethoxychromen-4-one (nobiletin) in supercritical carbon dioxide». En: *The Journal of Chemical Thermodynamics* 91 (dic. de 2015), págs. 378-383. DOI: 10.1016/J.JCT.2015.08.018.

brium cell, the stirring system was activated, the magnetic bar and the recirculation of the CO_2-rich phase, up to reaching the equilibrium conditions. Using the two sapphire windows, it was verified for the isotherms and for the entire pressure range the presence of two phases, fluid and solid. Samples of CO_2-rich phase were injected to the chromatograph (cf. subsection 2.2.2) for quantification (cf. subsection 2.3.2). The inherent error in estimates of y_2 were calculated using the procedure described by [116], in the Appendix A.

Pinocembrin solubility The solubility of Pn in multicomponent (CO_2 + Pn + int) systems was measured at 313 K and 323 K over a pressure range from (8.6 to 32.1 MPa). The cell was loaded with approximately $0.5\,\mathrm{g}$ of solid sc-extract and first temperature and pressure conditions were set. The operation of the cell to achieve equilibrium and quantify with the on-line HPLC was performed as mentioned in the previous paragraph. Typically five measurements were made for each system condition. After that, CO_2 was added to the cell using the syringe pump to increase system pressure as desired up to completing the isotherm at the last pressure measured.

Sorption equilibria

Preliminary experiments and uncertainty Initially, operation conditions were set in such a way that mass transport phenomena of the initial part of EIEC were governed by equilibrium [88]. The slope of the initial part of the curve represents the value of the apparent solubility for each compound in the complex mixture. If the solvent is saturated, it should be observed that the value of the slope will be the same for different flow rate-to-feed ratios and also show a linear shape [96]. Extractions were performed setting solvent flows, $20\,\mathrm{g/\,mín}$ for CO_2 and $2.8\,\mathrm{g/\,mín}$ for EtOH, and varying the amount of substrate loaded (0.04, 0.05 and $0.06\,\mathrm{kg_{subs}}$) in the 0.5 L vessel at 50 °C and 34 MPa. Uncertainty from experimental procedures was calculated based

on error propagation of algebraic operations doing triplicates for all measurements. This allowed to the estimate slope error associated with experimental work. Error values correspond to the t-student distribution parameter with $\alpha = 0.05$ and 2 freedom degrees multiplied by the average standard deviation of all experiments and divided by square root of 3.

Sorption equilibria experiments Dynamic extraction was used to study phase equilibrium and its characteristic parameters (*i.e.*, saturation concentration (y_s), partition or equilibrium coefficient (K) and transition concentration (x_t)) for Pn, Gn and cuticular waxes CW extractable from post-distillation phellandrene-rich chemotype of *L. origanoides*. To study thermodynamic parameters that affect equilibrium (P, T and E), experiments were performed at 18, 26 and 34 MPa values of P; 308, 323 and 338 K values of T and from 1.9 to 8.8 wt % of E range. CO_2 was separated from the extract during depressurization, but not EtOH. After depressurization, the EtOH-modified sc-extracts were collected and transferred to pre-weighed Petri dishes. Finally, they were dried in a forced convective hot air bath at 313 K during 3 h and then assessed gravimetrically. T and t of drying was determined by preliminary experiments.

2.5.3. Kinetics study Preliminary experiments were carried out with post-distillation substrate of carvacrol-rich chemotype to assess experimental reproducibility along the extraction curve (RSD<10 %). It was assumed that the variance found for this chemotype represents the variance of all the data. A 2^2 factorial design was developed using P and temperature T as variables and CW (e_{CW}) and Pn (e_{Pn}) yields as observables. The design consists of four experiments corresponding to interactions between low (200 bar - 40 °C) and high (460 bar - 60 °C) levels of extraction conditions and three measurements of central experimental conditions (340 bar – 50 °C) to calculate variance. Finally, d_p was studied separately carrying out extractions of the other two treatments of substrate (SP and LP) to the same conditions of temperature and

pressure that the central points of the design. The one-way Anova test and methods of multiple comparisons were applied to these data.

2.6. Mathematical modeling and simulation

2.6.1. Phase Equilibria

Thermodynamic solubility As discussed in chapter 1, [98], recently showed that the main components of the group of CW extracted from botanic material were the long-chain alkanes. The researchers also have shown that, if a mixture of such hydrocarbons should be represented by one component in a model for SFE, then the carbon chain of that component should be slightly longer than the average chain length in the mixture [94]. The present work did not have the methodological scope of identifying CW constituents of $scCO_2$ extracts from *L. origanoides* and *L. graveolens* or measuring their solubility in $scCO_2$. To achieve this, it would have been necessary to couple another detector type (not available) to the equilibrium cell described in subsection 2.4.2. To overcome the limitation, a widely studied long-chain hydrocarbon, *i.e.*, octacosane, was selected to represent the hydrocarbon mixture in model. Presumably, octacosane ($C_{28}H_{58}$) is in high concentrations present in $scCO_2$ extracts from *L. origanoides* and *L. graveolens* and has a slightly longer chain than the hydrocarbon that best predict SFE of cuticular waxes from oregano [98][124].

The dense gas approach [125] was applied as a thermodynamic model to correlate: solubility data from literature for octacosane in $scCO_2$ (binary system) and measured

---

[124] Filipe Gaspar. «Extraction of Essential Oils and Cuticular Waxes with Compressed CO2: Effect of Extraction Pressure and Temperature». En: *Industrial & Engineering Chemistry Research* 41.10 (abr. de 2002), págs. 2497-2503. DOI: 10.1021/ie010883i.

[125] John M Prausnitz, Rudiger N Lichtenthaler y Edmundo Gomes de Azevedo. *Molecular thermodynamics of fluid-phase equilibria*. Prentice Hall, 1999, págs. 671-749.

solubility data for pinocembrin in extract-scCO$_2$ (multiple solids system). The model treats the sc-fluid phase as a gas and uses a equation of state (EoS) directly in the solid-scCO$_2$ equilibrium calculations by introducing a solid phase fugacity f_2^{solid} function defined in terms of a phase reference state. Eq. 8 for binary system.

$$f_2^{solid} = f_2^{\mathrm{F}} \tag{7}$$

$$f_2^{solid} = P_2^{\mathrm{s}} \varphi_2^S \exp \int_{P_2^S}^{P} \frac{v_2^{solid} \, \mathrm{d}P}{RT} \tag{8}$$

$$f_2^{\mathrm{F}} = y_2 P \varphi_2^{\mathrm{F}} \tag{9}$$

Where f_2^{F} is fugacity of the solute in the supercritical phase, $P_2^{\mathrm{s}}(T)$ is the sublimation pressure of the pure solid, φ_2^S is the fugacity coefficient at sublimation pressure, v_2^{solid} is the molar volume of the solid, φ_2^{F} is the fugacity coefficient and y_2 the solubility (mole fraction) of the solute in the supercritical phase, all at P and T of the system. The model considers that the solubility of the gas in the solid is negligible and the v_2^{solid} remains constant. Therefore, the gas can be considered pure and all non-idealities of system behavior can be completely attributed to the sc-fluid phase. Then, the mole fraction of the solid component in the sc-phase, can be expressed as:

$$y_2 = \frac{P_2^{\mathrm{s}}}{P} \frac{\exp\left[\frac{v_2^{\mathrm{solid}}\left(P - P_2^s\right)}{RT}\right]}{\varphi_2^{\mathrm{F}}} \tag{10}$$

Therefore, the pure solute solubility is a function of its fusion properties and fugacity coefficient in the sc-phase, and the system T and P. The fugacity coefficient φ_2^{F} is calculated by a thermodynamic model and a mixing rule that for this work were the standard Peng-Robinson Equation of State with quadratic mixing rules respectively

[126].

For the more complex case of multicomponent solid-CO_2 equilibria, Sovová y Stateva (2015), following Prausnitz *et al* (1999), make the assumption known as Lewis fugacity rule that the fugacity of a component in a mixture is proportional to its mole fraction. Hence, the fugacity of the i^{th} solute in the solid phase can be calculated according to:

$$f_i^{\text{solid}} = s_i f_i^{\text{F}} \tag{11}$$

Where s_i is the mole fraction of the i^{th} solute in the system and f_i is the fugacity of the pure solute according to [94]. The mole fraction of the i^{th} solid component in the supercritical phase, *i.e.* its solubility in the SCF at the temperature and pressure of interest, is then:

$$y_2 = s_i \frac{P_i^{\text{s}}}{P} \frac{\exp\left[\frac{v_i^{\text{solid}}\left(P-P_i^s\right)}{RT}\right]}{\varphi_i^{\text{F}}} \tag{12}$$

Properties of pure CO_2 were taken from the *NIST* Standard Database v5.0 [117]. The pure component properties for octacosane and pinocembrin are shown in table 4. The binary interaction coefficients (K_{ij} and I_{ij}) for the systems at different T where used as optimization parameters fitted from experimental data. The binary interaction parameters for the octacosane-scCO_2 system were fitted from solubility data found in open literature for this binary system. On the other hand, the four binary interaction parameters to complete the multicomponent system, *i.e*, parameters for the pinocembrin-scCO_2 and pinocembrin-octacosane systems, were fitted from the pinocembrin solubility data measured in this work, using the best-fitted interaction

---

[126] Ding-Yu Peng y Donald B. Robinson. «A New Two-Constant Equation of State». En: *Industrial & Engineering Chemistry Fundamentals* 15.1 (feb. de 1976), págs. 59-64. DOI: 10.1021/i160057a011.

parameters for system octacosane-scCO$_2$ as input data of the multicomponent model of Eq. 12.

Table 4. Octacosane and pinocembrin pure component properties

Property	Octacosane	Pinocembrin
P_{c}, MPa	0.9694*	3.5600†
T_{c}, K	842.11*	878.12†
w, -	1.163*	1.67†
$v^{\mathrm{s}} \times 10^3$, m^3 mol^{-1}	0.4894*	0.1848‡
T_{f}, K	334.15‡	465.15‡
P^{s} at 313 K, MPa	7.213×10^{-13}*	4.982×10^{-11}§
P^{s} at 323 K, MPa	1.040×10^{-11}*	2.122×10^{-10}§
P^{s} at 333 K, MPa	1.278×10^{-10}*	8.210×10^{-10}§
P^{s} at 343 K, MPa	1.356×10^{-9}*	

* Data taken or calculated from [127]. Parameter P^{s} determined by $\ln P^{\mathrm{s}}[\mathrm{Pa}] = 72.09 - 27004.47/T[\mathrm{K}]$.
† Data calculated using group contribution method of [128] with the [129] correction for T_{b}.
‡ Data taken from NIST or ChemSpider Database.
§ Data calculated using Grain method from [130].

Sorption model Sorption models, have been proposed to describe the transition between dissolution of free solute and their desorption from substrate. These models describe how sc-extraction of botanic substrates is controlled first by solute-fluid interaction (solubility) and then by solute-solid interaction (adsorption) [131]. These models can be replaced by simpler semiempirical relationships like those proposed by [132], or **??**. The latter, has been considered as universal enough to interpret the data

[131] Motonobu Goto *y col.* «Modeling Supercritical Fluid Extraction Process Involving Solute-Solid Interaction». En: *JOURNAL OF CHEMICAL ENGINEERING OF JAPAN* 31.2 (1998), págs. 171-177. DOI: 10.1252/jcej.31.171.

[132] M Perrut *y col.* «Mathematical Modeling of Sunflower Seed Extraction by Supercritical CO2». En: *Industrial & Engineering Chemistry Research* 36.2 (feb. de 1997), págs. 430-435. DOI: 10.1021/ie960354s.

extraction of plant substrates [96]. [98] rewrote the sorption model proposed by del Valle y Urrego for multicomponent system with i components, Eq. 13.

$$e_i^* = K_i x_{\mathrm{i}} + \frac{x_{\mathrm{i}}^n}{x_{\mathrm{t}_i}^n + x_{\mathrm{i}}^n} \left(y_{\mathrm{s}_i} - K_i x_{\mathrm{i}}\right) \tag{13}$$

Where three equilibrium parameters characteristic for each component in the mixture were already described (*cf.* subsection 2.5.2). e_i^* (g_{sol}/kg_{subs}) is the gravimetrically measured yield of component (i) in the EIEC and x_{i} is initial concentration of the same component in substrate (solid phase) that was calculated from material balance considerations. Equilibrium parameters were adjusted by fitting to the model of each IEC.

2.6.2. Extraction kinetics using ethanol-modified scCO$_2$

Mathematical model The broken and intact cells (BIC) approach proposed by [107], for the mass transfer model of sc-extraction was applied to the extraction curves data of the kinetics study. This model considers substrate as particles that contain intact and broken cells. It is assumed that the extraction kinetics is fast or slow depending on whether the mass is transferred from the broken or intact cells respectively [74]. Sovová classified the extractions curves in four types from A to D, according to the regions of the discontinuous equilibrium function employed to describe the phase equilibrium stage. We selected type D ($Y_{\mathrm{s}} < 1, X_{\mathrm{t}} \geq 1, \overline{K} < 1$) as extraction type because, as will be seen later, the initial amount of free solute in the substrates was not sufficient to saturate the solvent at the beginning of the extraction and was not greater than x_t.

The dimensionless equations used to solve numerically the model were a set of

ordinary differential equations showed in Eq. 14:

$$\frac{\mathrm{d}Y_j}{\mathrm{d}\tau} + n\left(Y_j - Y_{j-1}\right) = J_{\mathrm{f}j} \tag{14a}$$

$$\frac{\mathrm{d}X_{1j}}{\mathrm{d}\tau} = \frac{1}{r} J_{\mathrm{s}j} - \Gamma J_{\mathrm{f}j} \tag{14b}$$

$$\frac{\mathrm{d}X_{2j}}{\mathrm{d}\tau} = -\frac{1}{1-r} J_{\mathrm{s}j} \quad \text{for} \quad j = 1, 2, \ldots, n. \tag{14c}$$

Where the dimensionless fluxes are:

$$J_{\mathrm{f}} = \frac{(Y^* - Y)}{\Theta_{\mathrm{e}}} \quad \text{for} \quad X_1 \neq X_{\mathrm{t}} \quad \text{or} \quad X_1 = X_{\mathrm{t}}, \quad Y < \overline{K} X_{\mathrm{t}}, \quad J_{\mathrm{f}} = 0;$$

$$\text{otherwise:} \quad J_{\mathrm{s}} = \left(X_2 - X_1\right)/\Theta_{\mathrm{i}} \tag{15}$$

and dimensionless equilibrium function:

$$\begin{aligned} Y^*\left(X_1\right) &= 1 \quad \text{for} \quad X_1 > X_{\mathrm{t}} \\ Y^*\left(X_1\right) &= \overline{K}\, X_1 \quad \text{for} \quad X_1 \leq X_{\mathrm{t}} \end{aligned} \tag{16}$$

With initial and boundary conditions:

$$\begin{aligned} Y_j =& X_{1j} = 1; \quad X_{2j} = 1 + \Gamma \quad \text{for} \quad \tau = 0 \quad \text{and} \quad j = 1, 2, \ldots, n; \\ Y_{j-1} =& 0 \quad \text{for} \quad j = 1 \end{aligned} \tag{17}$$

The dimensionless extraction curve is:

$$\Phi = \frac{\Gamma r}{1 + \Gamma} \int_0^{\tau} Y_{\mathrm{n}}\, \mathrm{d}\tau \tag{18}$$

To set F_{e} as an adjustable parameter, we modified the model by expressing the solid-phase mass transfer coefficient (k_{s}) in terms of the effective internal diffusivity D'_{e} as

proposed by del Valle y de la Fuente, 2006.

$$F_{\mathrm{e}} = \frac{D'_{\mathrm{e}}}{D_{12}} = \frac{k_{\mathrm{s}} d_{\mathrm{p}} K}{10 D_{12}}$$
$$k_{\mathrm{s}} = \frac{10 D_{12} F_{\mathrm{e}}}{d_{\mathrm{p}} K} \tag{19}$$

Eqs. 14-17 and parameters (K, r, F_{e}, k_{f} and, n) were integrated and fitted numerically using Runge-Kutta method and optimization toolbox in MATLAB *Math Works* (Natick, USA) respectively. The approximate solution of the Sovová model was employed to obtain initial values for the parameters fitting. Simulated extraction curves where expressed and plotted as $e = e(q)$, where e ($\mathrm{kg_{ext}}/\mathrm{kg_{subs}}$) is the extraction yield and q ($\mathrm{kg_{solv}}/\mathrm{kg_{subs}}$) is the relative amount of the passed solvent. The relationship of these variables with dimensionless ones are shown in Eq. 20.

$$e = x_u \Phi, \quad q = \gamma \tau \tag{20}$$

Where x_{u} ($\mathrm{kg_{ext}}/\mathrm{kg_{subs}}$) is the concentration in the untreated solid, Φ is dimensionless yield obtained from Eq. 18, γ ($\mathrm{kg_{solv}}/\mathrm{kg_{subs}}$) is the solvent-to-matrix ratio in the bed and τ is dimensionless time.

Substrate- and Physicochemical-parameters The model requires, among other parameters, the porosity of the extraction vessel (ϵ), calculated from particle density (ρ_{s}), estimated using gas pycnometer (*cf.* subsection 2.2.1), and bulk density (ρ_{b}) estimated using gravimetric procedure. The model also requires particle size (d_{p}) of the substrate; this value was calculated from the experimental particle size mass distribution (*cf.* subsection 2.2.1) which was discretized by means of a normal distribution function and its characteristic parameters were employed as input data to calculation

methodology of Sauter mean diameter (S_{md}) [133][134]. For the purpose of this work we reduce d_{p} value to the calculated S_{md} value as done by [135], for grape seeds. The x_{u}, measured by exhaustive extraction (*cf.* subsection 2.2.1) is also required.

The thermodynamic properties of CO_2 and EtOH pure substances were taken from the REFPROP program [117]. The physical properties of the binary CO_2-EtOH mixture (pseudo-component, $\mathtt{m}$) were estimated as follows. The density (ρ_{f}) was calculated applying the Predictive Soave-Redlich-Kwong (PSRK) equation of state EoS [136] implemented by [137], in their program developed to teach advanced EoS. MATLAB was the software to run the calculations. This EoS and mixing rule were chosen according to the good agreement between experimental and calculated data of the vapor-liquid equilibrium behavior of the CO_2-EtOH mixtures recently reported by [138]. This EoS was developed as EoS-gE type mixing rule combining the UNIFAC activity-coefficient model and the SRK EoS. This EoS approach has shown to be easily extended to mixtures containing sc-compounds. The three alpha function- and group decomposition-

---

[133] Terence. Allen. *Particle size measurement*. Chapman y Hall, 1981, pág. 678.

[134] Howard G. Barth. *Modern methods of particle size analysis*. Wiley, 1984, pág. 309.

[135] Helena Sovová. «Rate of the vegetable oil extraction with supercritical CO2 (I). Modelling of extraction curves». En: *Chemical Engineering Science* 49.3 (1994), págs. 409-414.

[136] T. Holderbaum y J. Gmehling. «PSRK: A Group Contribution Equation of State Based on UNIFAC». En: *Fluid Phase Equilibria* 70.2-3 (dic. de 1991), págs. 251-265. DOI: 10.1016/0378-3812(91)85038-V.

[137] Ángel Martín *y col.* «Teaching advanced equations of state in applied thermodynamics courses using open source programs». En: *Education for Chemical Engineers* 6.4 (dic. de 2011), e114-e121. DOI: 10.1016/J.ECE.2011.08.003.

[138] Renan Ravetti Duran *y col.* «Phase Equilibrium Study of the Ternary System CO2+H2O+Ethanol At Elevated Pressure: Thermodynamic Model Selection. Application to Supercritical Extraction of Polar Compounds». En: *The Journal of Supercritical Fluids* 138 (ago. de 2018), págs. 17-28. DOI: 10.1016/J.SUPFLU.2018.03.016.

parameters were taken from the supplementary data of [139]. The viscosity (μ_{m}) was estimated using ρ_{f} calculated and applying the Chung-Ajlan-Lee-Starling's mixing rules [140]. The hard-sphere diameters σ (3.261 92 Å for CO_2 and 4.237 38 Å for EtOH), taken from literature [141][142] that are based on Leonard-Jones's potential theory and the ratio between the minimum dual potential energy per Boltzmann constant (ϵ/k, 500.71 K for CO_2 and 1291.41 K for EtOH), taken from [141][142] were also required to estimate the self-diffusion coefficients of the $\mathtt{m}$ dense fluid and subsequently μ_{m}.
The "binary" diffusivity parameter (D_{12}), that to be precise is described as ($D_{1\mathrm{m}}$), was calculated for a representative solute present in the sc-extract (*i.e.*, octacosane $C_{28}H_{58}$, component 1) in the binary CO_2-EtOH mixture ($\mathtt{m}$) and its value was estimated applying the Stokes–Einstein theory using the [143], approach and [144], modification for epsilon parameter. μ_{m}, and the normal-boiling molar volumes of the solvent mix-

---

[139] Sven Horstmann *y col.* «PSRK group contribution equation of state: comprehensive revision and extension IV, including critical constants and α-function parameters for 1000 components». En: *Fluid Phase Equilibria* 227.2 (ene. de 2005), págs. 157-164. DOI: 10.1016/J.FLUID.2004.11.002.

[140] Bruce E Poling, John M Prausnitz y John P O'Connell. *The Properties of Gases & Liquids - Fifth Edition*. 2001, pág. 803. DOI: 10.1016/0894-1777(88)90021-0. arXiv: arXiv:1011.1669v3.

[141] J. Leite *y col.* «Measurement and modelling of tracer diffusivities of gallic acid in liquid ethanol and in supercritical CO2 modified with ethanol». En: *The Journal of Supercritical Fluids* 131 (ene. de 2018), págs. 130-139. DOI: 10.1016/J.SUPFLU.2017.09.004.

[142] Hongqin Liu, Carlos M. Silva y Eugénia A. Macedo. «Unified approach to the self-diffusion coefficients of dense fluids over wide ranges of temperature and pressureâ€"hard-sphere, square-well, Lennardâ€"Jones and real substances». En: *Chemical Engineering Science* 53.13 (jul. de 1998), págs. 2403-2422. DOI: 10.1016/S0009-2509(98)00036-0.

[143] W Hayduk y B S Minhas. «Correlations for prediction of molecular diffusivities in liquids». En: *The Canadian Journal of Chemical Engineering* 60.2 (abr. de 1982), págs. 295-299. DOI: 10.1002/cjce.5450600213.

[144] C. Mantell, M. Rodríguez y E.Martínez de la Ossa. «Measurement of the diffusion coefficient of a model food dye (malvidin 3,5-diglucoside) in a high pressure CO2+methanol system by the chromatographic peak-broadening technique». En: *The Journal of Supercritical Fluids* 25.1 (ene. de 2003), págs. 57-68. DOI: 10.1016/S0896-8446(02)00088-8.

ture (v_{bm}) and the solute (v_{b1}) are necessary for this calculation. v_{bm} was estimated using also Chung-Ajlan-Lee-Starling's mixing rules [140] employing the pure compound values of v_{b} ($33.32\,\mathrm{cm^3\,mol^{-1}}$ for CO_2, taken from [144], and $62.52\,\mathrm{cm^3\,mol^{-1}}$ taken from REFPROP [117]) of the mixture. The v_{b1} ($766\,\mathrm{cm^3\,mol^{-1}}$) was estimated using the additive volume method of [145], using the critical volume for octacosane v_{c1} ($1873\,\mathrm{cm^3\,mol^{-1}}$) obtained from Joback's group contribution method [146]. The average residence time of CO_2 in the extraction vessel (t_{r}), and the specific surface areas per unit volume of the packed bed (a_0) or the solid (a_{s}) were calculated as previously described by [107]. Finally, values of the external mass transfer k_{f} (Eq. 21), were estimated using the dimensionless correlation of [147], for the Sherwood number (Sh, Eq.22) as a function of the Schmidt number (Sc, Eq. 24) and the particle-size-dependent Reynolds number (Re, Eq. 23).

$$k_{\mathrm{f}} = \frac{ShD_{\mathrm{1m}}}{d_{\mathrm{p}}} \tag{21}$$

$$Sh = 0.38Re^{0.83}Sc^{1/3} \tag{22}$$

$$Re = \frac{\rho U d_{\mathrm{p}}}{\mu} \tag{23}$$

$$Sc = \frac{\mu D_{\mathrm{1m}}}{\rho} \tag{24}$$

---

[145] Gervaise Le Bas. *The Molecular Volumes of Liquid Chemical Compounds, from the Point of View of Kopp*. New York: Longmans, Green, 1915.

[146] Kevin G Joback y Robert C Reid. «Estimation of pure-component properties from group-contributions». En: *Chemical Engineering Communications* 57.1-6 (1987), págs. 233-243.

[147] Chung-Sung Tan, Shuen-Kwei Liang y Din-Chung Liou. «Fluidâ€"solid mass transfer in a supercritical fluid extractor». En: *The Chemical Engineering Journal* 38.1 (mayo de 1988), págs. 17-22. DOI: 10.1016/0300-9467(88)80049-2.

3. VALORIZATION OF SOLID RESIDUES FROM DISTILLATION OF *LIPPIA* spp. THROUGH THE EXTRACTION OF FLAVONOIDS

Steam distillation of essential oils from *Lippia origanoides* and *Lippia graveolens* leaves behind solid residues that can be valorized. Particularly, flavonoids in post-distillation substrates could be selectively extracted using ethanol-modified supercritical CO_2, as shown in this chapter. One chemotype was selected to conduct preliminary experiments to test extraction reproducibility. With the same chemotype a $2^{(6-2)}$ fractional factorial screening design was carried out to study the effect of pressure, temperature, time, CO_2 mass flow, particle size, and percent ethanol on the extraction yield of cuticular waxes and flavonoids. Once identified the variables having significance influence on yields (pressure, time, CO_2 mass flow, and percent ethanol) a deterministic optimization (simplex methodology) was applied to identify experimentally the values maximizing yield for the four substrates studied. A chemometric method for estimating flavonoid content by UV-Vis spectroscopy based on a multivariate calibration model was used to quantify samples during experimental development. UHPLC-ESI(+)-Orbitrap-MS was employed for the analytical identification and quantification of the higher-yield extracts from each substrate. It was found that it was possible to selectively extract post-distillation chemotypes, that differed among them in flavonoid initial content and make-up. Results of this section of the work will facilitate the implementation of $scCO_2$ extraction processes to valorize by-products of the essential oil industry.

3.1. Particle size characterization and drying test

Fig. 7 shows the particle size cumulative curve obtained by sieving the post-distillation chopped substrate of *L. origanoides* thymol-rich chemotype. The curves are clearly

different from each other, so it is reasonable to use these two aperture sizes as levels of the d_{p} variable in the experimental design. The S_{md} estimated for treatments with $0.5\,\mathrm{mm}$ and $2\,\mathrm{mm}$ openings in the mill were $0.308\,\mathrm{mm}$ and $0.253\,\mathrm{mm}$ respectively. The pre-extraction drying time was set at $120\,\mathrm{mín}$, obtained from a drying rate curve (Fig. 8) at $60\,℃$. Following two hours, the moisture content remained constant below $12\,\mathrm{wt}\,\%$. In most cases, the water present in the vegetable matrix competes with the solute to interact with the solvent, decreasing the yield of the extraction process. For this reason, drying the raw material is recommended [148]. The dry basis moisture for all plant material was ca. $13\,\mathrm{wt}\,\%$ (see Table 11). Generally, the botanical matrix should have a water content of around $4\,\mathrm{wt}\,\%$ to $14\,\mathrm{wt}\,\%$.

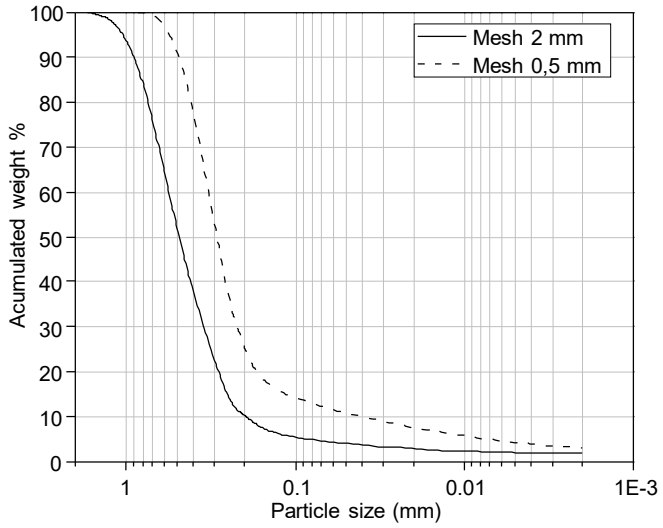

Figura 7. Cumulative curve of particle size distribution of *L. origanoides* thymol-rich chemotype milled with two different grid sizes.

[148] Camila G. Pereira y M. Angela A Meireles. «Supercritical fluid extraction of bioactive compounds: Fundamentals, applications and economic perspectives». En: *Food and Bioprocess Technology* 3.3 (2010), págs. 340-372. DOI: 10.1007/s11947-009-0263-2.

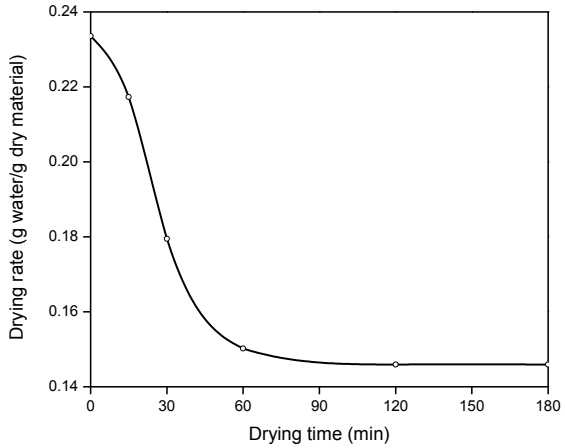

Figura 8. Drying curve of post-distillation chopped *L. origanoides* thymol-rich chemotype.

3.2. Preliminary extractions

Two different preliminary extraction conditions, i.e., $7.2\,\mathrm{kg_{CO_2}/kg_{subs}}$ at 40 ℃ and $200\,\mathrm{bar}$ and $9.6\,\mathrm{kg_{CO_2}/kg_{subs}}$ at 50 ℃ and $300\,\mathrm{bar}$, were carried out with three replicates in random order on three separate days. The obtained reproducibility RSD values were $7.7\ \%$ and $1.9\ \%$, for oleoresin yield of each experimental condition, respectively. In general, values below $10\ \%$ are considered acceptable in extractive techniques of bio-active compounds.

3.3. Selection of variables that affect the extraction process

Sixteen experiments corresponding to the $2^{(6-2)}$ fractional factorial design were carried out in random order for *L. origanoides* thymol-rich chemotype. Table 5 shows the values for two different responses: the CW yield (e_{CW}) and the flavonoids extract yield (e_{flv}), which is represented as the sum of flavonoids extracted. The two responses have a high positive Pearson correlation coefficient between them ($r = 0.97$). The independent variables may have influenced them in the same way. The results

from screening design show that yield increases with pressure. The same result was observed by N. Leitao *y col.* «Anacardium occidentale L. leaves extraction via SFE: Global yields, extraction kinetics, mathematical modeling and economic evaluation». En: *Journal of Supercritical Fluids* 78.July 2016 (jun. de 2013), págs. 114-123. DOI: 10.1016/j.supflu.2013.03.024 for the *Anacardium occidentale* extraction, and Patricia Francisco de Oliveira *y col.* «Supercritical fluid extraction of hernandulcin from Lippia dulcis Trev.» En: *Journal of Supercritical Fluids* 63.December 2008 (2012), págs. 161-168. DOI: 10.1016/j.supflu.2011.12.003 for *Lippia dulcis* extraction. It was observed that the highest yield values corresponded to high pressure and flow domains. The effects of all variables and possible binary combinations were estimated using the dot product method between the variable levels and results [149]. Fig. 9 shows the normal probability plots for the confused effects of first- and second-order for the two different responses, e_{CW} and e_{flv}. The aligned points correspond to effects indistinguishable from the experimental error, while those out of alignment are significant effects. According to the normal probability distribution test, P, F, and E had effect over both responses, e_{CW} and e_{flv}. The extraction time t influenced only the extraction yield of CW.Fig 10 complements this analysis with Pareto charts, in which the individual variances are plotted in descending order. For both responses, the results show that the changes of F, P and E largely explain the variability. However, with the inclusion of the confused effect (Ft and PT) and the effect of t, it is possible to explain more than 80 % of the total variability of the responses.

The analysis of variance (Table 6) confirms the importance of F, P and E variables on the extraction yields. Although T and d_{p} are important variables in the supercritical extraction process because they relate directly to the solubility and mechanisms of mass transfer, their effects were not significant in the experimental space studied.

---

[149] D. Montgomery. *Design and Analysis of Experiments*. 6.ª ed. New York: Sons, John Wiley y Sons, 2008.

Table 5. Yield results for $2^{(6-2)}$ fractional factorial design for sc-extraction of *L. origanoides* thymol-rich chemotype.

Exp.	*P*	*T*	*F*	d_{p}	*t*	*E*	e_{CW},*,%	e_{flav},†,%
1	-1	-1	-1	-1	-1	-1	6.0×10^{-2}	1.0×10^{-2}
2‡	1	-1	1	1	-1	-1	6.8×10^{-1}	9.8×10^{-2}
3	-1	1	-1	-1	1	1	4.2×10^{-2}	6.4×10^{-5}
4‡	-1	-1	1	-1	1	1	7.0×10^{-1}	1.0×10^{-1}
5	1	1	-1	1	-1	-1	3.0×10^{-1}	5.0×10^{-2}
6	-1	1	1	-1	-1	-1	8.0×10^{-2}	1.4×10^{-2}
7	1	-1	-1	-1	1	-1	1.8×10^{-1}	3.1×10^{-2}
8	1	-1	-1	1	1	1	4.2×10^{-1}	7.7×10^{-2}
9‡	1	1	1	-1	1	-1	9.8×10^{-1}	1.4×10^{-1}
10	-1	-1	1	1	1	-1	3.6×10^{-1}	6.3×10^{-2}
11‡	1	-1	1	-1	-1	1	8.4×10^{-1}	1.5×10^{-1}
12	-1	1	1	1	-1	1	4.6×10^{-1}	7.9×10^{-2}
13	-1	1	-1	1	1	-1	4.0×10^{-2}	2.7×10^{-5}
14	1	1	-1	-1	-1	1	3.8×10^{-1}	6.2×10^{-2}
15‡	1	1	1	1	1	1	1.7	2.8×10^{-1}
16	-1	-1	-1	1	-1	1	4.0×10^{-2}	6.8×10^{-3}

* Cuticular waxes yield corresponding to the sum of the extract obtained from Sep 1 and 2.
† Flavonoids yield corresponding to the sum of the extract obtained from Sep 1 and 2.
‡ Experiments selected to start simplex optimization.

The reason for the exclusion of d_{p} can be explained by how close the S_{md} values are to each other, i.e., the $0.5\,\mathrm{mm}$ and $2\,\mathrm{mm}$ openings in exit grids represent a very narrow range of particle size distribution. Therefore, there is no clear difference in the effect when one or the other mesh is used during milling. Based on this result, the optimization extractions should use the $2\,\mathrm{mm}$ exit grid opening because with this size the time that the solids are retained in the mill is shorter, which directly reduces operating time and thermal degradation of molecules.

In the case of temperature, which is considered one of the most important variables of the extraction process, experiments were performed in a domain to warrant

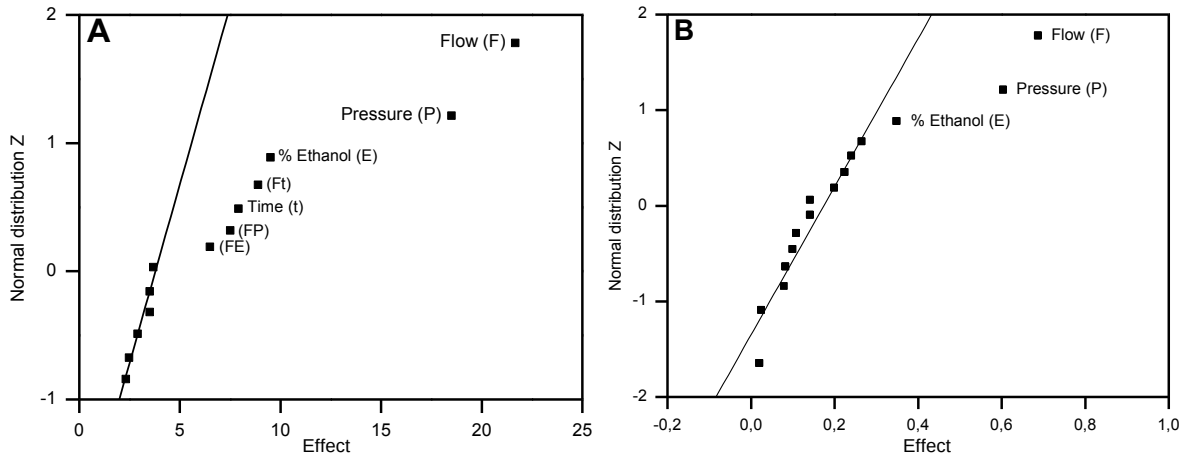

Figura 9. Normal probability plot to identify variablles with effect on (A) cuticular waxes extraction yield larger than experimental error and (B) flavonoid extraction yield higher than experimental error.

that the EtOH-modified $scCO_2$ mixture is in a single sc-phase [150]. Therefore, there were no phase discontinuities of the extractive medium. T is directly related to the solubility and the crossover pressure. There is always a crossover pressure, but this depends on the solute. It is a common feature of the pure solutes dissolved in supercritical fluids [151]. Crossover pressure is a near-critical pressure in the case of essential oils, and considerably larger in the case of triglycerides, but in the two cases it is between 80 bar and 400 bar. For sc-extracts from botanical materials that contain cuticular waxes (major compounds), in addition to the minor compounds (e.g., flavonoids), the crossover pressure is possibly between 100 bar and 300 bar. The shape of the solubility curves for extract in EtOH-modified $scCO_2$ are unknown, and along

[150] Kazuhiko Suzuki *y col.* «Isothermal vapor-liquid equilibrium data for binary systems at high pressures: carbon dioxide-methanol, carbon dioxide-ethanol, carbon dioxide-1-propanol, methane-ethanol, methane-1-propanol, ethane-ethanol, and ethane-1-propanol systems». En: *Journal of Chemical Engineering Data* 35.1 (1990), págs. 63-66. DOI: 10.1021/je00059a020.

[151] E. H. Chimowitz y R. J. Pennisi. «Process Synthesis Concepts for Supercritical Gas Extraction in the Crossover Region». En: *AIChE journal* 32.10 (1986), págs. 1665-1676. DOI: 10.1002/aic.690321010.

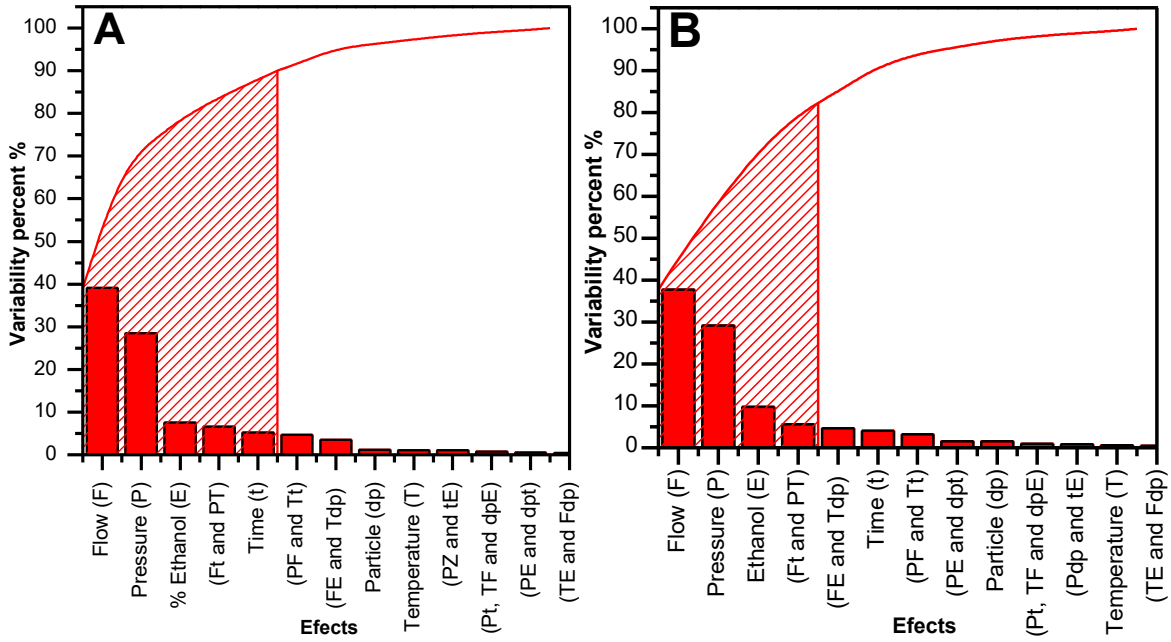

Figura 10. Pareto chart for (A) cuticular waxes extraction yield response, (B) flavonoids extraction yield response.

with it the crossing pressure. However, the behavior of the extraction of flavonoids in equilibrium may be similar to what was reported for naringenin [152], and quercetin [153], both flavonoids constituents of the extracts. The experience showed that solubility increased with increasing pressure and temperature. No crossing pressure trend was observed in the experimental region studied by both research groups. It has been observed that the solubility of the pure minor component is not directly related to the equilibrium of the extraction of the mixed substances [96], but presumably the extrac-

[152] Gonzalo A Núñez, José M del Valle y Juan C de la Fuente. «Solubilities in Supercritical Carbon Dioxide of (2E,6E)-3,7,11-Trimethyldodeca-2,6,10-trien-1-ol (Farnesol) and (2S)-5,7-Dihydroxy-2-(4-hydroxyphenyl)chroman-4-one (Naringenin)». En: *Journal of Chemical & Engineering Data* 55.9 (sep. de 2010), págs. 3863-3868. DOI: 10.1021/je900957v.

[153] Amparo Chafer *y col.* «Solubility of quercetin in supercritical CO2 + ethanol as a modifier: Measurements and thermodynamic modelling». En: *Journal of Supercritical Fluids* 32.1-3 (2004), págs. 89-96. DOI: 10.1016/j.supflu.2004.02.005.

Table 6. Analysis of variance for two monitored responses

Source	Cuticular waxes yield, (e_{CW})					Flavonoids yield, (e_{CW})				
	SS	df	MS	$F-\mathrm{test}$	p-value	SS	df	MS	F-test	p-value
F	1.18	1	1.18	256.5	0.004	0.03	1	0.03	964.4 *	0.001
P	0.86	1	0.86	186.8 *	0.005	0.02	1	0.02	744.9 *	0.001
E	0.23	1	0.23	49.3 *	0.020	0.01	1	0.01	248.5 *	0.004
Ft and PT	0.20	1	0.20	43.0 *	0.023	4.4×10^{-3}	1	4.4×10^{-3}	143.7 *	0.007
t	0.16	1	0.16	34.2 *	0.028	3.1×10^{-3}	1	3.1×10^{-3}	*102.6	0.01
PF and Tt	0.14	1	0.14	30.7 *	0.031	2.5×10^{-3}	1	2.5×10^{-3}	81.1 *	0.01
FE and Td_{p}	0.11	1	0.11	23.1 *	0.041	3.6×10^{-3}	1	3.6×10^{-3}	117.5 *	0.008
d_{p}	0.03	1	0.03	7.4	0.113	1.2×10^{-3}	1	1.2×10^{-3}	40.5 *	0.02
T	0.03	1	0.03	6.7	0.123	4.2×10^{-4}	1	4.2×10^{-4}	13.8	0.06
Pd_{p} and tE	0.03	1	0.03	6.7	0.123	6.2×10^{-4}	1	6.2×10^{-4}	20.3 *	0.04
Pt and TF and $d_{\mathrm{p}}E$	0.02	1	0.02	4.6	0.165	7.3×10^{-4}	1	7.3×10^{-4}	23.8 *	0.04
PE and $d_{\mathrm{p}}t$	0.02	1	0.02	3.4	0.208	1.2×10^{-3}	1	1.2×10^{-3}	40.9	0.02 *
TE and Fd_{p}	0.01	1	0.01	2.9	0.229	3.9×10^{-4}	1	3.9×10^{-4}	12.6	0.07
Error	0.01	2	0.00			6.1×10^{-5}	2	3.1×10^{-5}		
Total	3.01	15				0.078	15			

* The F value for the effect is greater than the critical value $\mathrm{F}_{\mathrm{critical}} = 18.5$.

tion of flavonoids in the equilibrium increases directly proportional to T and P, at least above the crossing pressure region for two of the target components in our extracts. Marleny D.A. Saldaña *y col.* «Apparent solubility of lycopene and β-carotene in supercritical CO2, CO2Â +Â ethanol and CO2Â +Â canola oil using dynamic extraction of tomatoes». En: *Journal of Food Engineering* 99.1 (jul. de 2010), págs. 1-8. DOI: 10.1016/J.JFOODENG.2010.01.017, observed a similar behavior in their study about the extraction of β-carotene and lycopene from the skin and pulp of tomato. It is possible that the explanation of the lack of significance of the temperature may be due to the fact that the pressure range was wide and, on the contrary, the temperature interval was narrow for the experiments, restricting the possibility of significance of temperature. As the influence of T was not significant, the temperature remained at 50 ℃ for subsequent experiments.

3.4. Empirical search for optimal extraction conditions

Based on the analysis of variance (Table 6), the experimental space comprising the variables F, P, E and t was selected to find the extraction conditions favoring the response increases through the simplex method [122]. The five experiments that had higher yields in the fractional factorial design (i.e., vertices 1-5 in tables 7-10) were used to construct the first simplex (S1). Tables 7-10 show the consecutive experiments for the optimization, using extraction e_{flv} as observable, from thymol-rich (LOT), carvacrol-rich (LOC) and phellandrene-rich chemotypes (LOP) of *L. origanoides* and *L. graveolens* (LG) post-distillation material. After these experiments were repeated, the lowest observable datum was discarded, and the coordinates of the new vertex were calculated according to Eq. 25. Where $\mathbf{V}_c$ is the centroid, which is the average of the responses of the vertices not rejected, b is a factor that determines whether the next vertex corresponds to a reflection ($b = 1$), an expansion ($b > 1$), a contraction ($0 < b < 1$), or a contraction with change of direction ($-1 < b < 0$).

$$\mathbf{V}_{(i+n+j)} = \mathbf{V}_{\mathrm{c}} + b\,(\mathbf{V}_{\mathrm{c}} - \mathbf{V}_p) \tag{25}$$

To illustrate the methodology of deterministic optimization used in the work, the experimental sequence applied to the thymol-rich chemotype is described as follows (Table 7). The first rejected vertex was 5, because its yield was the lowest of the five points that made up the S1. Using $b = 1$ a reflection was calculated to obtain the conditions of vertex 6. Vertex 6 slightly increased the response; so, another vertex of S1 was rejected, i.e., vertex 4. Reflections continued until vertex 9, where the yield was high, so a contraction ($b = 0.6$) was applied. In vertex 10 the extract yield decreased, and an expansion ($b = 1.3$) was applied to calculate vertex 11. In vertex 14 a reflection of vertex 13 was carried out from the S9 to produce vertex 14, one of

Table 7. Optimization conditions and results using the simplex method for *L. origanoides* thymol-rich chemotype.

Vertex	P, bar	F, g/ mín	t, mín	E, wt %	e_{CW}, %	e_{flv} %	Simplex	Vertex rejected
1	400	50	120	10	1.2	0.22		
2	400	50	120	0	0.92	0.13		
3	400	50	60	10	0.88	0.16		
4	80	50	120	10	0.76	0.13		
5	400	50	60	0	0.74	0.12	S1	
6	134	31	106	11	0.78	0.12	S2	5
7	417	24	46	3	0.48	0.042	S3	4
8	132	47	113	9	0.80	0.14	S4	7
9	359	45	66	2	0.84	0.13	S5	6
10	438	33	46	1	0.56	0.09	S6	8
11	160	46	106	9	1.0	0.14	S7	10
12	220	45	90	8	1.0	0.17	S8	9
13	154	32	101	3	0.76	0.11	S9	3
14	449	54	52	11	1.2	0.17	S10	13
15	307	43	92	5	1.2	0.15	S11	2
16	112	62	130	11	0.5	0.08	S12	12
17	334	53	139	13	0.98	0.18	S13	16
18	420	60	144	12	0.68	0.13	S14	17
19	380	40	96	8	1.1	0.19	S15	18
20	307	60	120	5	1.2	0.19	S16 *	11

* Vertex of S16 are 1, 14,15,19 and 20.

Table 8. Optimization conditions and results using the simplex method for *L. origanoides* carvacrol-rich chemotype.

Vertex	P, bar	F, g/ mín	t, mín	E, wt %	e_{CW}, %	e_{flv} %	Simplex	Vertex retained
1	323	50	90	8	1.01	0.04		
2	323	50	90	8	0.85	0.04		
3	350	27	90	11	1.39	0.06		
4	400	45	120	10	1.46	0.11		
5	300	50	60	5	0.85	0.03		
6	398	36	135	14	1.09	0.10	S1	1,2,3,4
7	412	29	128	13	1.01	0.06	S2	2,3,4,6
8	323	50	90	8	0.75	0.03	S3	2,3,4,6
9	372	64	128	9	1.14	0.08	S4	2,4,6,8
10	423	47	146	12	1.21	0.11	S5	2,4,6,9
11	400	25	118	13	0.63	0.07	S6	2,4,6,10
12	379	54	126	10	1.24	0.15	S7	2,4,6,10
13	438	43	152	13	1.48	0.15	S8	4,6,10,12
14	416	53	137	10	1.29	0.12	S9	4,10,12,13
15	393	50	121	9	0.91	0.12	S10	4,12,13,14

Table 9. Optimization conditions and results using the simplex method for *L. origanoides* phellandrene-rich chemotype.

Vertex	P, bar	F, g/ mín	t, mín	E, wt %	e_{CW}, %	e_{flv} %	Simplex	Vertex retained
1	100	50	60	10	0.25	0.18		
2	200	40	120	8	0.42	0.32		
3	300	60	60	5	0.14	0.10		
4	400	45	90	10	0.69	0.50		
5	220	65	60	12	0.68	0.35		
6	460	55	105	8	1.03	0.49	S1	2,3,4,5
7	340	43	128	14	1.44	0.72	S2	2,4,5,6
8	432	58	75	12	0.99	0.33	S3	4,5,6,7
9	455	46	109	11	0.91	0.48	S4	4,6,7,8
10	444	56	118	12	0.88	0.47	S5	6,7,8,9
11	411	48	97	11	0.65	0.47	S6	6,7,8,9
12	427	52	108	11	0.69	0.53	S7	6,7,8,9

Table 10. Optimization conditions and results using the simplex method for *L. graveolens*.

Vertex	P, bar	F, g/ mín	t, mín	E, wt %	e_{CW}, %	e_{flv} %	Simplex	Vertex retained
1	250	40	120	10	0.23	0.006		
2	250	60	90	8	0.32	0.009		
3	420	60	90	8	0.30	0.008		
4	350	50	90	9	0.27	0.008		
5	420	40	120	10	0.30	0.010		
6	415	58	86	5	0.33	0.012	S1	1,2,3,4
7	369	54	98	9	0.23	0.006	S2	1,2,4,5
8	247	56	89	8	0.25	0.008	S3	1,2,4,5
9	243	54	104	9	0.26	0.007	S4	1,2,4,7
10	209	50	102	9	0.35	0.011	S5	1,6,7,8
11	329	53	98	9	0.29	0.009	S6	1,6,8,9
12	269	52	137	9	0.38	0.011	S7	1,6,8,9
13	373	48	115	9	0.22	0.005	S8	1,6,8,9
14	406	43	140	10	0.34	0.009	S9	1,6,8,12
15	424	56	119	8	0.34	0.013	S10	1,6,12,13
16	438	52	110	9	0.56	0.027	S11	6,12,13,14
17	444	54	116	9	0.19	0.008	S12	6,13,14,15
18	442	61	92	8	0.30	0.012	S13	6,14,15,16

the high-yield experiments that remained until the end of optimization, as well as the subsequent vertex 15. For vertices 16, 17 and 18 the calculated reflections modified the variables, but the response was always lower than the last vertex in S11. This result showed that the new conditions calculated with the last simplex were moving away from the high yield space. Finally, vertices 19 and 20 were calculated and experimented, their responses were very similar with high yields. In consequence, it was decided to stop the optimization at S16. The vertices 1, 14, 15, 19 and 20 (S16) had the higher yields in the explored experimental space for post-distillation substrate of thymol-rich *L. origanoides*. The values of the responses of these experiments were not significantly different. Any of these conditions affords relatively high flavonoid amounts from the substrate. However, practical considerations make some conditions more favorable than others. Vertex 1 conditions, for example, use high values of P, t and E to get the best results, but vertex 14 conditions are operationally more favorable because using the same CO_2 and EtOH consumption, two extractions are possible in the same time. Accordingly, we found that the higher-yield extraction conditions for this substrate corresponded to vertex 15 with the lowest values of P (307 bar) and E (5 $\%$), moderate values of t (96 $\mathrm{mín}$) and F (43 $\mathrm{g/\,mín}$). The same treatment of the extraction conditions was done for the optimization of the rest of *L. origanoides* chemotypes and for *L. graveolens*. Fig. 11 is a graphical representation of the results of the simplex optimization for all substrates. The 3D scattering plot of bubbles mapped with colors presents the results of optimization of substrates A-D, locating the bubbles according to the extraction conditions of the experiment where $q = Ftsubs^{-1}$. Bubble sizes are proportional to e_{CW} that varies from 0.2 $\%$ to 1.5 $\%$. The gray scale changes according to e_{flv}, which varies from 0.005 $\%$ to 0.72 $\%$.

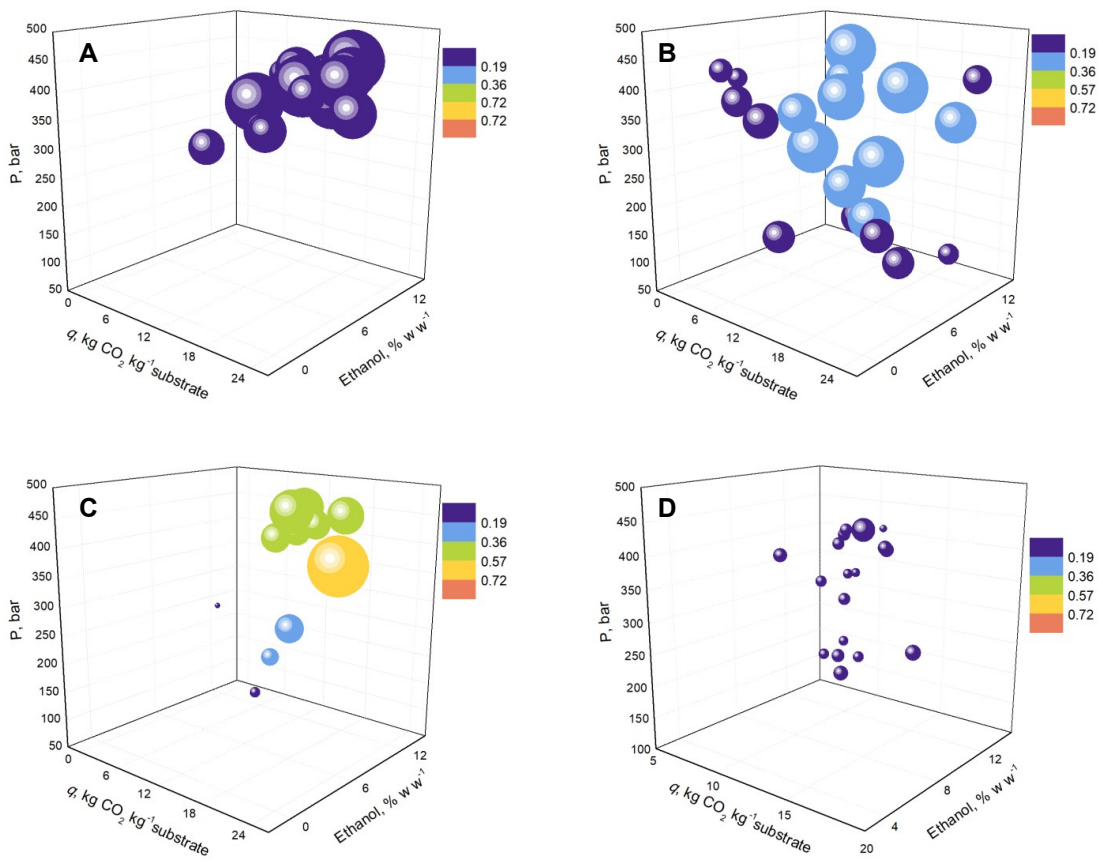

Figura 11. 3D Scattering plot of bubbles mapped with colors that shows results of the simplex optimization for extraction of *L. origanoides* chemotypes and *L. graveolens*. The bubble sizes are proportional to the extraction yield of cuticular waxes that varies from 0.2 % to 1.5 %. The colors varies according to the extraction yield of flavonoids between 0.05 % to 0.72 %. **A**. *L. origanoides* carvacrol-rich chemotype; **B**. *L. origanoides* thymol-rich chemotype; **C**. *L. origanoides* phellandrene-rich chemotype and **D**. *L. graveolens*.

3.5. Fitting multiple linear regression models

It is common in experimental screening and optimization designs that the response surface methodology be used to graphically interpret the effects of the variables that affect the response. Using experimental data from the screening design and optimization for *L. origanoides* thymol-rich chemotype, given that it is the chemotype that has both sets of experiments, different linear models with multiple combinations of the variables were tested. The best regression model found for the extraction yield of cuticular waxes is:

$$e_{\mathrm{CW}} = -1.89 + 3.6 \times 10^{-3} P + 2.75 \times 10^{-2} F + 3.16 \times 10^{-2} t + 1.96 \times 10^{-2} E + 2.07 \times 10^{-5} PF - 6.06 \times 10^{-6} P^2 - 3.23 \times 10^{-4} F^2 - 1.68 \times 10^{-5} t^2$$

and its statistical adjustment parameters are: $R^2 = 0.91$, $R^2_{adj} = 0.87$ and $RMSE = 0.13$. In the same way, the best regression model found for the extraction yield of flavonoids is:

$$e_{\mathrm{flav}} = -0.43 + 1.07 \times 10^{-2} t + 4.23 \times 10^{-6} PF + 2.44 \times 10^{-5} Ft + 1.25 \times 10^{-4} FE + 2.61 \times 10^{-7} P^2 - 3.1 \times 10^{-5} F^2 + 6.19 \times 10^{-5} t^2$$

and its statistical adjustment parameters are: $R^2 = 0.91$, $R^2_{adj} = 0.89$ and $RMSE = 0.02$.

To obtain these models, first a selection was carried out using statistical software *Statgraphics* Centurion XV. More than 10.000 possible combinations of variables were tested to determine the best models for each response. Fig. 12 shows the response surface for the best models found. Fig. 12 (A) corresponds to the model that explains $91\ \%$ of variability of CW extraction yield. The slope indicates a strong influence of pressure and CO_2 flow on the extraction yield. These two variables are directly

connected to mass transfer mechanisms occurring in the extraction. At higher pressures the (CO_2 + EtOH) mixture increases its density and solvent power. However, the extraction of waxes is enhanced, and the increase in extract mass does not necessarily represent an increase in the extracted flavonoids. There is a narrow region in the graph defined by the flow between $40\,\mathrm{g/\,mín}$ and $60\,\mathrm{g/\,mín}$ where the extraction yield is high. These values correspond to the experimental flow region where the residence time of the CO_2 in the extraction tank was adequate to promote the mass transfer mechanisms (diffusion and convection) and disfavor the phenomenon of axial dispersion. Fig. 12B shows the response surface for the model that represents $89\ \%$ of the variability of the yield of extraction of flavonoids. The yield increased with the increment of these variables, this time in a linear manner for the pressure and a slightly quadratic effect for the flow.

3.6. Spectroscopic characterization

Fig. 13 exemplifies the predicted concentrations of the flavonoids by decomposing the spectral signal of the extract obtained with the conditions of vertex 20 for the thymol-rich chemotype of *L. origanoides* i.e., pinocembrin $75.4\,\mathrm{mg/g_{ext}}$, naringenin $28.1\,\mathrm{mg/g_{ext}}$, and luteolin-apigenin $67\,\mathrm{mg/g_{ext}}$. The concentrations of luteolin and apigenin could not be determined individually due to the great similarity of their UV-Vis spectra at the 44 wavelengths selected to perform the multivariate calibration. This is a difficulty that the CLS method cannot overcome; it will not be able to establish differences between the molecules from the input information. A variation of CLS, i.e., the inverse method ILS, instead of using the spectral signals as input information, predicts the individual spectra of the molecules from known concentrations of the analytes in mixture, including signal overlapping. Despite this disadvantage of CLS, the method is convenient for the purposes of this section of the work, since the objective is to monitor the sum of the flavonoids in the extract, i.e., to quantify

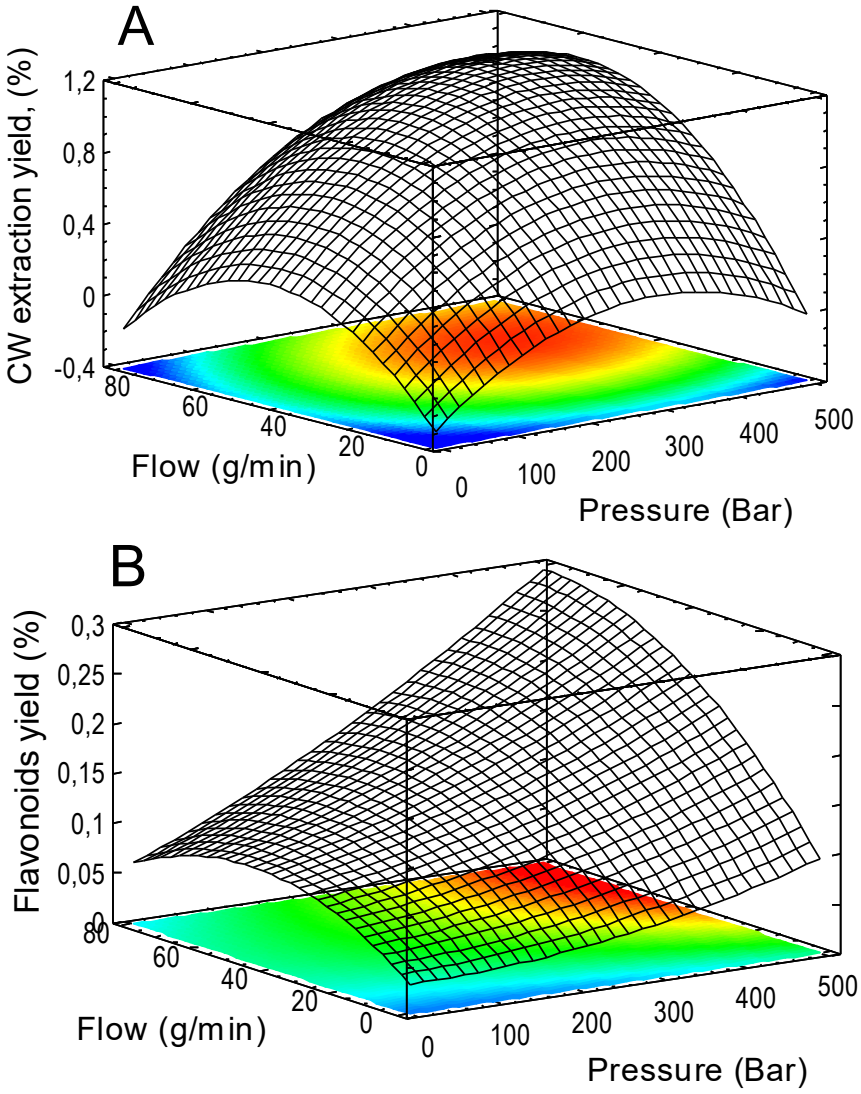

Figura 12. Surface response for: **A**. cuticular waxes extraction yield; 92 mín extraction time and 5 wt % ethanol, **B**. flavonoids extraction yield; 92 mín extraction time, 5 wt % ethanol.

the spectral signal according to the flavonoids that are likely to be found in the extracts. There are other methods, in addition to the multivariate approaches, such as the zero-crossing method or the classic univariate method, but also because of the high spectral superposition in extracts of botanical material, they are not suitable for the simultaneous determination of the flavonoids. Other graphical methods such as those used by RD Bautista *y col.* «Multicomponent analysis : Comparison of various graphical and numerical methods». En: *Talanta* 40.11 (1993), págs. 1687-1694. DOI: 10.1016/0039-9140(93)80085-6 and Bautista *y col.*, «Simultaneous determination of diazepam and pyridoxine in synthetic mixtures and pharmaceutical formulations using graphical and multivariate calibration-prediction methods.», to predict flavonoid concentrations, require regions in the spectrum where the derivatives of most of the signals are zero, but for the target compound the derivative is greater than zero in the required zone, which is clearly a limitation for complex mixtures.

3.7. Content of CW and flavonoids in the post-distillation substrates

The results of the Soxhlet and sc-extraction (Table 11) showed that the post-distillation substrates contained considerable amounts of cuticular waxes, flavonoids and pinocembrin. These are high levels compared to other residues in the essential oil industry [14][15] and even with plants identified as potential for commercial sources of pinocembrin such as seeds of *Alpinia katsumadai* Hayata with $2.5\,g_{Pn}/kg_{subs}$ [21] and two sub-species of *Eucalyptus preissiana* trees with $15\,g_{Pn}/kg_{subs}$ and $18\,g_{Pn}/kg_{subs}$ [23]. According to the experiments, *L. origanoides* phellandrene-rich chemotype showed the higher-yield results compared with all substrates studied cf. **C** in Fig. 11. Results of table 11 are common yields values for the $scCO_2$ extraction of botanical materials [14][8]. Although the post-distillation substrate of the *L. origanoides* phellandrene-rich chemotype is the residue with the highest recovery potential for EtOH-modified $scCO_2$ extraction, its yield of essential oil extraction ($1\ \%$ to $1.5\ \%$) is the lowest with

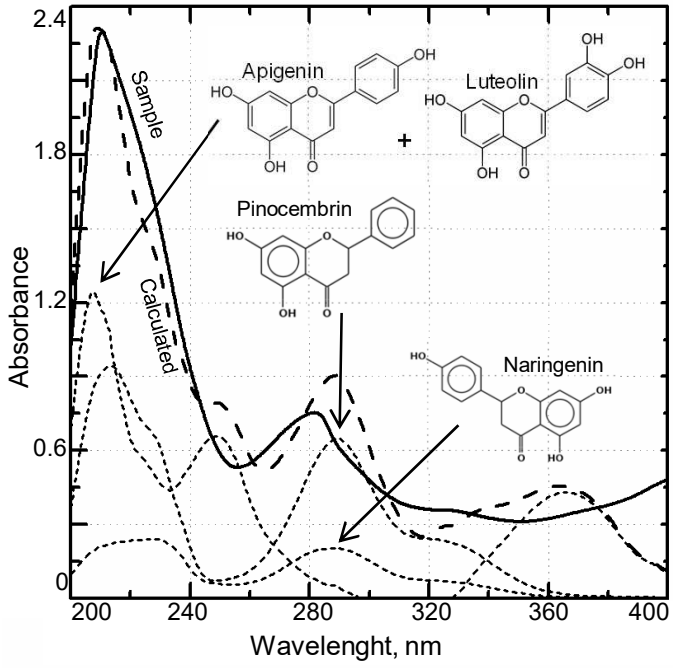

Figura 13. Absorption electronic spectra of sample vertex 20 (-) and its corresponding prediction (- -). Predicted flavonoid content: $170.5\,\mathrm{mg\,g^{-1}}$. Pinocembrin $75.4\,\mathrm{mg/g_{ext}}$ extract. naringenin $28.1\,\mathrm{mg/g_{ext}}$extract. and luteolin + apigenin $67\,\mathrm{mg/g_{ext}}$

Table 11. Constituents of extracts from Soxhlet and sc-extraction

Substrate	Soxhlet extraction			Sc-extraction			Dry Basis Moisture
	e_{CW}, $\mathrm{g_{CW}/kg_{subs}}$	e_{flv}, $\mathrm{g_{flv}/kg_{subs}}$	e_{Pn}, $\mathrm{g_{Pn}/kg_{subs}}$	e_{CW}, $\mathrm{g_{CW}/kg_{subs}}$	e_{flv}, $\mathrm{g_{flv}/kg_{subs}}$	e_{Pn}, $\mathrm{g_{Pn}/kg_{subs}}$	M_{d}, %
LOP	192	55	31	14	7	4	12
LOT	174	20	15	12	2	1	14
LOC	195	29	23	15	2	1	13
LG	69	6	5	6	0.3	0.2	14

very low content of phenylpropanoids as compared to *L. graveolens* (1 % to 3 %), carvacrol-rich (3.6 % to 4.4 %) and thymol-rich (2.4 % to 3.1 %) *L. origanoides* chemotypes [85].

These results show that the sc-extraction with the conditions studied, leaves behind a considerable amount of extract that is still retained in the matrix. However, the EtOH-modified $csCO_2$ extraction turned out to be considerably more selective for some chemotypes in the extraction of the target compounds (i.e., aglycones) when compared with the Soxhlet extraction. Flavonoid extraction selectivity using supercritical extraction (50 %) was almost twice higher than the Soxhlet counterpart (28 %). The same behavior has been observed for other botanical materials when comparing $scCO_2$ with solid-liquid extractive techniques using hydro-alcoholic mixtures, or when water is included as a polarity modifier of CO_2 [293031]. Experiments on phase equilibrium could help to understand the phenomenon of mass transfer and lead to increase extraction yields of $scCO_2$ extraction considering the potential of the substrates with respect to the content of flavonoids available in the substrate and the advantageous selectivity offered by this extractive technique.

3.8. Identification and quantification of obtained in higher yield extracts

Phenolic composition of the higher-yield extracts of *L. graveolens* and *L. origanoides* chemotypes (UHPLC-ESI(+)-Orbitrap-MS with positive ionization mode) were summarized in Table 12, including molecular formula, calculated and experimental m/z values and error (δ ppm). A total of 15 phenolic compounds, including flavones, flavanones, flavonols and flavanonol identified by comparison of MS spectra and retention times with those of available standards, were found as constituents of the extracts. Whereas, the investigated substrates contain mainly the same types of phenolics, differences in amounts of individual substances of the $scCO_2$ extracts were detected. A group of unidentified compounds with molecular weight around 600 Da, with

the longest retention times among the extract constituents, were also detected. They are probably related to chlorophyll pigments and cuticular waxes present in the extract. The phenolic compounds found in this work are similar to those reported by Leitão *y col.*, «Counter-current chromatography with off-line detection by ultra high performance liquid chromatography/high resolution mass spectrometry in the study of the phenolic profile of *Lippia origanoides*», in their study of ethanolic extracts of a *L. origanoides* thymol-carvacrol chemotype.

Table 12. Composition of EtOH-modified $scCO_2$ extracts from post-distillation residues (UHPLC-ESI(+)-Orbitrap-MS analysis). **A**. *L. origanoides* carvacrol-rich chemotype; **B**. *L. origanoides* thymol-rich chemotype; **C**. *L. origanoides* phellandrene-rich chemotype and **D**. *L. graveolens*.

Compound	Formula	[M+H]+		δ ppm	$\mu g/mg_{ext} \pm s\ (n=3)$			
		Experimental	Calculated		A	B	C	D
Taxifolin †	$C_{15}H_{12}O_7$	305.06557	305.06548	0.3	0.19 ± 0.02	0.20 ± 0.02	0.06 ± 0.01	<LOD §
Eriodictyol †	$C_{15}H_{12}O_6$	289.07121	289.07105	0.57	4.9 ± 0.2	3.6 ± 0.3	0.44 ± 0.10	0.08 ± 0.01
Quercetin *‡	$C_{15}H_{10}O_7$	303.05047	303.05044	0.12	1.00 ± 0.07	<LOD	0.16 ± 0.01	<LOD
Luteolin *‡	$C_{15}H_{10}O_6$	287.05556	287.05529	0.92	0.46 ± 0.07	0.43 ± 0.07	0.06 ± 0.01	0.072 ± 0.003
Naringenin *‡	$C_{15}H_{12}O_5$	273.07629	273.07621	0.28	4.6 ± 0.2	5.5 ± 0.6	1.06 ± 0.05	0.27 ± 0.04
Hesperetin †	$C_{16}H_{14}O_6$	303.08631	303.0862	0.35	0.77 ± 0.01	1.72 ± 0.08	0.06 ± 0.01	0.056 ± 0.004
Apigenin *‡	$C_{15}H_{10}O_5$	271.06064	271.06042	0.82	0.14 ± 0.01	0.44 ± 0.02	<LOD	0.046 ± 0.004
Chrysoeriol †	$C_{16}H_{12}O_6$	301.07066	301.07036	0.99	1.3 ± 0.1	2.3 ± 0.1	0.04 ± 0.01	0.063 ± 0.002
Dimethylated flavone †	$C_{17}H_{14}O_7$	331.08123	331.08106	0.5	0.23 ± 0.01	0.75 ± 0.02	0.01 ± 0.01	<LOD
Pinocembrin *‡	$C_{15}H_{12}O_4$	257.08138	257.08132	0.2	0.67 ± 0.04	2.0 ± 0.2	48.3 ± 1.0	7.9 ± 0.3
Cirsimaritin †	$C_{17}H_{14}O_6$	315.08631	315.08605	0.83	2.34 ± 0.04	3.5 ± 0.1	0.05 ± 0.01	0.50 ± 0.02
Sakuranetin †	$C_{16}H_{14}O_5$	287.0914	287.09132	0.28	3.10 ± 0.29	4.8 ± 0.1	1.42 ± 0.08	4.8 ± 0.3
Galangin †	$C_{15}H_{10}O_5$	271.06064	271.06051	0.49	<LOD	<LOD	7.2 ± 0.2	0.44 ± 0.03
Methylated galangin †	$C_{16}H_{12}O_5$	285.07575	285.07563	0.42	<LOD	<LOD	4.1 ± 0.2	<LOD
Methylated apigenin †	$C_{16}H_{12}O_5$	285.07575	285.07687	0.37	0.15 ± 0.02	0.66 ± 0.05	<LOD	<LOD

* quantified with calibration curve.
† tentative identification based on mass spectrum and fragmentation pattern
‡ confirmatory identification with certified standard substances
§ Limit of detection

3.9. Conclusions

The results of this work are conclusive in respect to the potential of each distillation residue studied to afford valuable byproducts that permit increasing the profitability of the extraction process of essential oils from *Lippia origanoides* and *Lippia graveolens*. The residue of *L. origanoides* phellandrene-rich chemotype is the byproduct

with the highest industrial recovery potential followed by the thymol-rich, carvacrol-rich chemotypes and finally, *L graveolens*. Flow, pressure, time, and percent ethanol have a significant effect on the global extraction yield and flavonoid extraction yield of *L. origanoides* and *L. graveolens* using supercritical CO_2. The interval of temperatures chosen in this work did not significantly affect both extraction responses. The d_{p}-range that was obtained from two grids ($0.5\,\mathrm{mm}$ and $2\,\mathrm{mm}$ opening) used in the chopper is not significant in the extraction yield responses. The best experimental conditions found for the $scCO_2$ extraction are $307\,\mathrm{bar}$, $5\ \%$ ethanol, $96\,\mathrm{mín}$ and $43\,\mathrm{g_{CO_2}/\,mín}$ under the specifications of the extraction system used.

4. PHASE EQUILIBRIA OF scCO$_2$ EXTRACTION OF *L. ORIGANOIDES* POST-DISTILLATION RESIDUES

The distillation residue of *L. origanoides* phellandrene-rich chemotype (LOP) is a by-product with high industrial recovery potential. The EtOH-modified scCO$_2$ extract from LOP contains valuable flavonoids such as pinocembrin and galangin. To optimize their selective sc-extraction, multi-component phase equilibria of CO$_2$, extract constituents and support matrix are necessary. This chapter provides data and modeling through a study with two fundamentally experimental approaches *i.e.*, phase equilibria between extract constituents and scCO$_2$ (thermodynamic approach), and phase equilibria between extract constituents, scCO$_2$ and support matrix, which takes into account the solutes-matrix interactions (operational approach). Analytical tools such as HPLC-DAD coupled to a high-pressure equilibrium cell and multivariate calibration (ILS) based on UV spectroscopy were employed and developed to quantify off- and on-line the phase equilibria data. ILS avoided the need to use chromatography to separate the flavonoids to estimate their concentration from extracts obtained experimentally. Measurements were at different P, T and E. Phase equilibria parameters were generated by fitting data to semi-empirical or thermodynamic models. Influence of sc-extraction conditions on phase equilibria was discussed. Lower temperatures decrease solubility of cuticular waxes without significantly affecting flavonoid solubility.The total oleoresin content readily available in chopped post-distillation *L. origanoides* is not enough to saturate the scCO$_2$ stream in the operational approach. E and P significantly affected operational solubility when sc-extraction was controlled by equilibrium. The phase equilibria data were useful to delimit mass transfer phenomena in the subsequent study of extraction kinetics.

4.1. Constituents of the EtOH-modified $scCO_2$ extract of the LOP

Chapter 3 showed that the distillation residues of LOP turned out to have the greatest potential for flavonoids recovery. Fig. 14 shows a truncated chromatographic profile of EtOH-modified $scCO_2$ extract from LOP that focuses on their major and valuable flavonoids *i.e.*, pinocembrin (Pn, peak 1) and galangin (Gn, peak 2). The chromatogram also shows peaks of smaller height corresponding to other phenolic compounds reported in Table 12. Those unnumbered peaks in the chromatogram are the called "interferences" (Intf) that absorb in the UV-region, (*cf.* subsection 2.3.1). Fig. 14 also shows, in a reflection plane, the chromatogram of Pn and Gn standards in mixture at $50\,\mu g\,mL^{-1}$, to confirm their presence in the extract through retention times comparison.

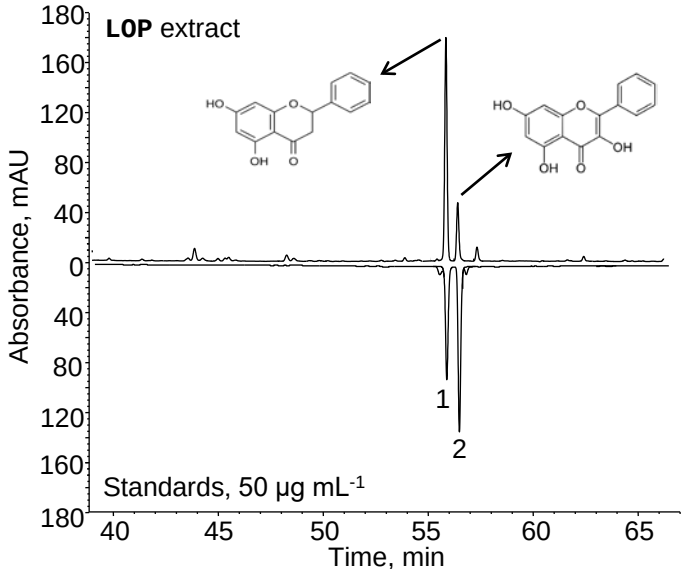

Figura 14. Chromatographic profile obtained by HPLC-DAD of EtOH-modified $scCO_2$ extract from post-distillation residues of *L. origanoides* phellandrene-rich chemotype. (1) pinocembrin $t_R = 55.7\,\mathrm{min}$ and (2) galangin $t_R = 56.2\,\mathrm{min}$ standards at $50\,\mu g\,mL^{-1}$ in reflection plane.

Despite the significant amount of flavonoids found in the LOP sc-extract, they are minority compared to co-extracted compounds such as fatty acids, waxes, pigments,

and resinoids among others [62]. Figure 15 shows the distribution of some of those compounds (wt %) according to the fatty acids analysis mentioned in subsection 2.2.2. Although the present work did not have the scope to quantify using GC-FID beyond fatty acids, apparently the n-hexane saponified fraction contained mainly long-chain n-alkanes (n-C_{25} to n-C_{35}, *ca.* 60 wt %), since it is widely known that the main co-extracted molecules belong to that family [64][65]. Researches that applied discriminant analysis to the composition of long-chain alkanes extracted from leaves of the Verbenaceae[154] plant family showed, in average for a sample of seven plants, that the main cuticular waxes (CW) present in the extracts are: hentriacontane ($C_{31}H_{64}$, 17.9 wt %), tritriacontane ($C_{33}H_{68}$, 30.9 wt %) and pentatriacontane ($C_{35}H_{72}$, 16.1 wt %) [67].

Multicomponent phase equilibria of complex solutes, such as sc-extracts, are generally assessed by simplifying the study system. Therefore, similar constituent substances of the extract usually are grouped and represented by a single molecule (pseudo-component) that presumably describes the thermodynamic behavior of its family in the system. The object of our study was valuable flavonoids due to their biological properties, but the main components of sc-extracts are CW. Therefore, the system was simplified to three components, *i.e.*, $scCO_2$, a representative molecule of the CW (majority compounds), and the flavonoid family (minority and valuable compounds).The purpose of simplifying a family into a molecule to represent the extract constituents, is to know the solubility limits of molecules in the hypothetical case that the whole extract is a mixture of two pseudo-components, the matrix effect does not interfere and the $scCO_2$ is saturated (thermodynamic solubility).

In sc-extraction of a mixture of long-chain alkanes, the solubility in $scCO_2$ decreases with increasing length of the carbon chain. Sovova *et al.* have shown that, if a mixture

---

[154] *Lippia* genus belong to Verbenaceae family

of such hydrocarbons should be represented by one component in a model for SFE, then the carbon chain of that component should be slightly longer than the average chain length in the mixture [94][98]. On the other hand, an experimental oregano sc-extraction conducted in equilibrium indicated that the exit wax concentration was similar to the solubility of pure n-heptacosane ($C_{27}H_{56}$) in $scCO_2$ [98][124]. For the present study, the octacosane (`Oct`, $C_{28}H_{58}$) was conveniently chosen to represent the `CW` family. This is because `Oct` solubility in $scCO_2$ has been widely reported and has a slightly longer chain than the best alkane predictor of sc`CW` extraction of oregano. The molecule selected to represent the flavonoids family was `Pn` as it is the main flavonoid in the sc-extract.

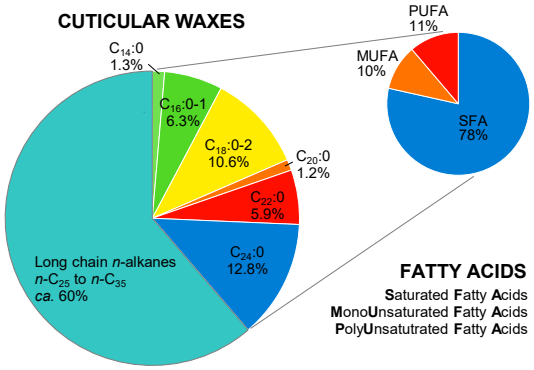

Figura 15. Distribution of cuticular waxes (wt %) constituent of sc-extract from post-distillation *L. origanoides* phellandre-rich chemotype.

4.2. Thermodynamic solubility of sc-extract constituents in $scCO_2$

4.2.1. Solubility of `CW` in $scCO_2$

Solubility of the binary system `Oct`-$scCO_2$ The `Oct` solubility data were taken from the experimental work of Mark A. McHugh, Andrew J. Seckner y Thomas J. Yogan. «High-pressure phase behavior of binary mixtures of octacosane and carbon dioxide». En: *Industrial & Engineering Chemistry Fundamentals* 23.4 (mayo de

1984), págs. 493-499. DOI: 10.1021/i100016a020; I. Swaid, D. Nickel y G.M. Schneider. «NIRâ€"spectroscopic investigations on phase behaviour of lowâ€"volatile organic substances in supercritical carbon dioxide». En: *Fluid Phase Equilibria* 21.1-2 (ene. de 1985), págs. 95-112. DOI: 10.1016/0378-3812(85)90062-7; Reverchon, Russo y Stassi, «Solubilities of solid octacosane and triacontane in supercritical carbon dioxide» and Thierry Chartier *y col.* «Solubility, in Supercritical Carbon Dioxide, of Paraffin Waxes Used as Binders for Low-Pressure Injection Molding». En: *Industrial & Engineering Chemistry Research* 38.5 (mar. de 1999), págs. 1904-1910. DOI: 10.1021/ie980552e. Table 13 shows experimental data used in this work. The Oct solubility in $scCO_2$ is from 1.9×10^{-5} to 440.5×10^{-5} mol_{Oct}/mol_{CO_2} for conditions between 313 to 343 K and 9 to 45 MPa.

Solubility modeling for Oct Since the pure solid solutes solubility in $scCO_2$ is directly related to the pure solvent density, in addition to thermodynamic modeling, the experimental data were assessed according to the Mendez-Santiago and Teja equation (MS-T, Janette Méndez-Santiago y Amyn S Teja. «The solubility of solids in supercritical fluids». En: *Fluid Phase Equilibria* 158-160 (1999), págs. 501-510. DOI: 10.1016/s0378-3812(99)00154-5):

$$\ln\left(y_{\text{sol}}P\right) = A + \frac{B + C\rho_1}{T} \tag{26}$$

where T, y_{sol}, ρ_1 and P are temperature, mole fraction of solute in the $scCO_2$ phase, pure CO_2 density ($g\,L^{-1}$) and pressure (MPa), respectively. In Eq. 26, the CO_2 density was from the *NIST* Standard Database v5.0 [117]. Parameters A, B and C were determined by correlating experimental data with a least squares method. The calculated values were 29.74, $-13\,664.51$ and 3.26 for A, B and C respectively. Table 14 shows deviation between experimental data and correlation results. Calculated solubility values are shown in Fig 16.

For the thermodynamical approach, the solubility of binary system `Oct` (3) in $scCO_2$ (1) was determined from the thermodynamic relationship for solid-liquid equilibrium at constant temperature and pressure as was discussed in subsection 2.6.1. The fugacity coefficient φ_3^{F} was calculated using standard Peng-Robinson Equation of State with quadratic mixing rules. The method employs two binary interaction coefficients, *i.e.* ($K_{13} = K_{31}$ and $I_{13} = I_{31}$), as adjustable parameters from experimental data of Table 13. The rest of the solute parameters, necessary for the calculation, were calculated or taken from literature. Their values are shown in Table 4. Estimated parameters for the cubic equation of state model are shown in Table 14 and calculated values are shown in Fig 16.

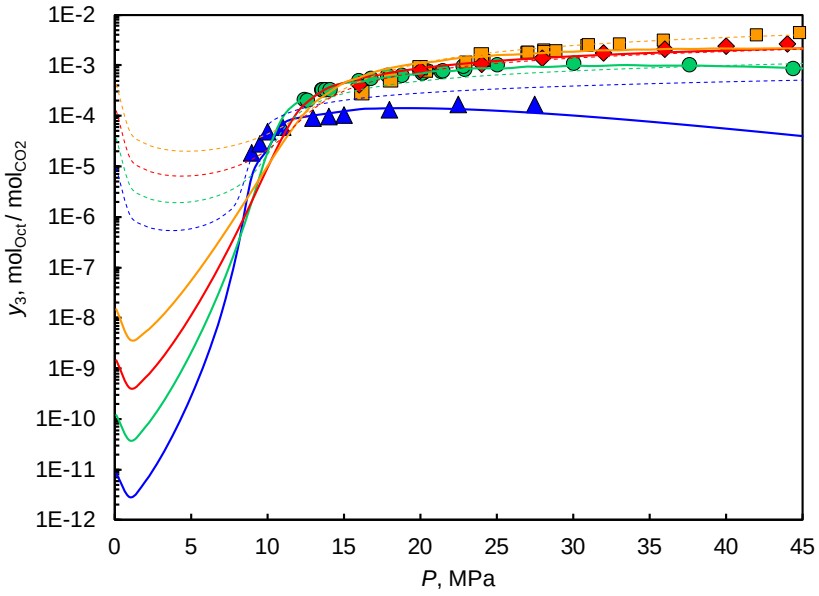

Figura 16. Solubility of octacosane-$scCO_2$ binary system as function of pressure and temperature. (▲), (●), (◆) and (■) are experimental data for 313, 323, 333 and 343 K respectively. The dashed lines, with the same color code for temperatures, are the solubility values calculated by MS-T correlation. Continuous lines are the correlation results calculated by the Peng-Robinson EoS.

The deviations between experimental data and correlation results were calculated

with Eq. 27:

$$AARD\% = \frac{100}{N}\sum_{i}^{N}\left|\frac{y_{\mathrm{sol,i}}^{\mathrm{exp}} - y_{\mathrm{sol,i}}^{\mathrm{calc}}}{y_{\mathrm{sol,i}}^{\mathrm{exp}}}\right| \tag{27}$$

where N is the data number per isotherm. Eq 27 is the absolute average relative deviation of the difference between experimental and calculated values.

In general, the thermodynamic model using PR-EoS fitted better the experimental data than MS-T correlation. Comparatively, PR-EoS was better for the 313 and 323 K isotherms, while the MS-T correlation was better for the 333 and 343 K isotherms. The lack of fit of the thermodynamic model at high temperatures is possibly due to the phase change, since the melting point of Oct is 334 ± 1 K. Thus, the solubility predictions for 343 K are outside the scope of the model, which is derived from equilibrium assumptions in solid-scCO_2 systems. For our purpose, it is not possible to use the models separately, since two or more solutes cannot be correlated with density-based models because these were derived for binary systems solute-scCO_2 [94]. Therefore, the thermodynamic model with the temperature restriction to the melting point was used in the subsequent analysis.

4.2.2. Solubility of the multi-component system LOP extract and scCO_2

Preliminary experiments to validate methodology Before measurement of the complex extract-scCO_2 system, preliminary tests were carried out with a molecule already reported in literature. Subsection 2.4.2 shows the details of the measurement system and the methodology used. Because the entire measurement system was first assembled to carry out this work, a solute with known solubility was used to compare reported data with those obtained for new system. The selected solute was nobiletin, a flavonoid whose solubility was measured using the same in-line configuration of an equilibrium cell coupled to HPLC-DAD [123]. Both, the solubility

measurement system reported by Cabrera *y col.* and the new system, belong to the LTP research group of Technical University Federico Santa María of Valparaíso, Chile. Fig. 17 shows the reported and measured values with the uncertainty for the solubility of nobiletin in $scCO_2$ for selected conditions of 18, 22 and 28 MPa and 313 and 333 K.

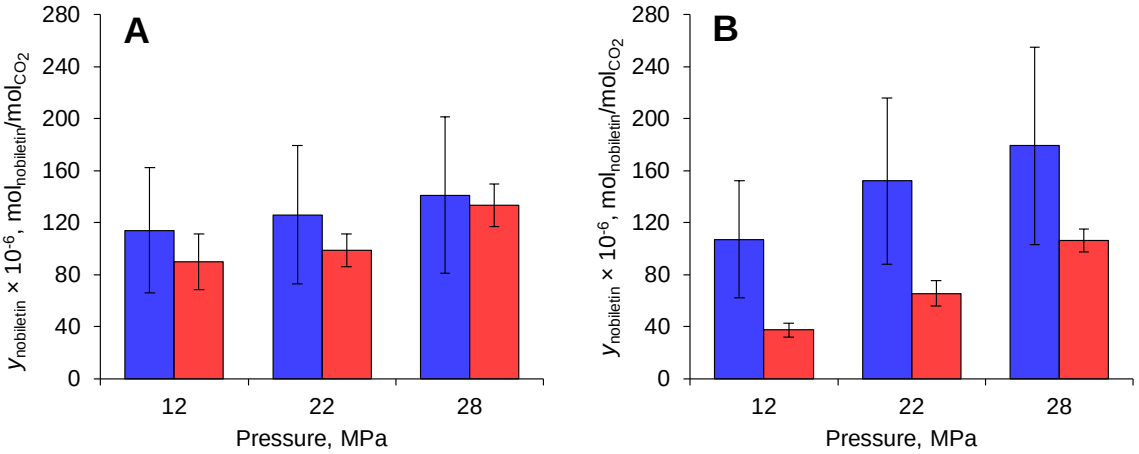

Figura 17. Comparison of nobiletin-$scCO_2$ solubility reported in literature and measured in this work. Blue bars are values reported by Adolfo L. Cabrera *y col.* «Measuring and validation for isothermal solubility data of solid 2-(3,4-Dimethoxyphenyl)-5,6,7,8-tetramethoxychromen-4-one (nobiletin) in supercritical carbon dioxide». En: *The Journal of Chemical Thermodynamics* 91 (dic. de 2015), págs. 378-383. DOI: 10.1016/J.JCT.2015.08.018, the red ones are values measured in this work. (A) Data for 313 K, (B) Data for 333 K.

In Figure 17, the average solubilities measured with the new system are lower than those reported by [123], as well as their uncertainties. Possibly due to the effect of the new sampling valve circuit and the improved chromatographic reproducibility of the new chromatograph. Four of the six measured data had no statistically significant difference with the reported data of Cabrera *y col.*, «Measuring and validation for isothermal solubility data of solid 2-(3,4-Dimethoxyphenyl)-5,6,7,8-tetramethoxychromen-4-one (nobiletin) in supercritical carbon dioxide». The trend of increasing solubility with pressure was maintained proportionally for both temperatures in the new mea-

surements. Preliminary measurements showed results consistent with those reported, so the new system was cleaned of nobiletin and loaded with the object study extract.

Solubility of extracted Pn in scCO$_2$ To the best of our knowledge, the solubility of the Pn-scCO$_2$ binary system has not yet been measured. The scope of our work was not to measure the solubility of this binary system, rather it was limited to measuring the solubility of Pn in mixture with coextracted substances and scCO$_2$, *i.e.* in the extract-scCO$_2$ system. Instead of pure Pn, the equilibrium cell was loaded with LOP sc-extract containing *ca.* 200 $\mathrm{mg_{Pn}/g_{ext}}$. We assumed that such amount of extract contained enough Pn to saturate the scCO$_2$ in the hypothetical case that only Pn was solubilized. Solubility values in scCO$_2$ for three flavanones and four flavones, available in literature, were used to calculate the minimum amount of extract to be loaded. Table 15 shows experimental data measured in this work. The solubility values found for Pn were between 4.5×10^{-6} to 33.5×10^{-6} $\mathrm{mol_{Pn}/mol_{CO_2}}$ for conditions between 313 to 323 K and 9 to 32 MPa.

Fig. 18 shows the results of the solubility measurement for Pn in the context of the reported values for other flavonoids derived from the flavone and flavanone skeleton. Judging by visual inspection, the increase of hydroxyl groups and their position in the structure affect scCO$_2$ solvation capacity. Thus, for anthoxanthins measured all but one by the same research group (*cf.* Fig. 18B), the molecules with two hydroxyl groups (7,8 dihydroxyflavone and chrysin) in their structure are less soluble than those with a single group (3-hydroxyflavone). Flavone and flavanone, molecules without hydroxyl groups, have the highest solubility in their families. The non polar character of CO$_2$ favors solubility of molecules with fewer surface areas formed by hydroxyl groups. In the flavanone group (*cf.* Fig. 18A), however, the reported solubility for 6-hydroxyflavanone, a molecule with a single hydroxyl group, is smaller than the Pn and naringenin values. This leads us to think that

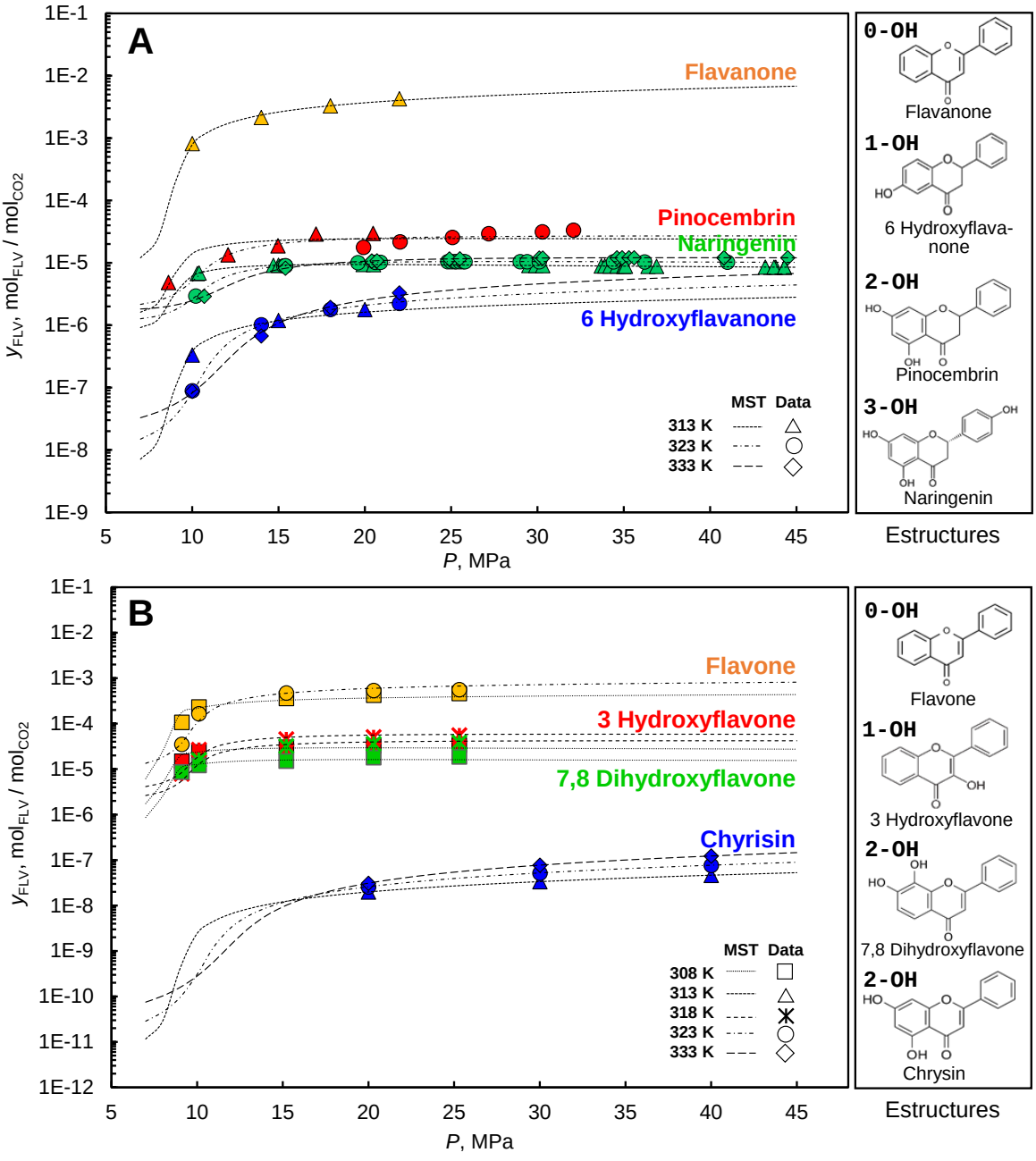

Figura 18. Data (symbols) and MS-T correlation (lines) of: (A) three flavanones (flavanone [155], 6-hydroxyflavanone[156], Naringenin[157]) and (B) four anthoxanthins (flavone[158], 3-hydroxyflavone[159], 7,8 dihydroxyflavone[160] and chyrisin[161]) solubilities in $scCO_2$ binary system. Pinocembrin data measured in extract-$scCO_2$ system mix.

there is a difference between measured and real magnitudes, possibly due to the measurement methods used by the two research groups. Although both methods are dynamic, the methodology used by Núñez, del Valle y de la Fuente, «Solubilities in Supercritical Carbon Dioxide of (2E,6E)-3,7,11-Trimethyldodeca-2,6,10-trien-1-ol (Farnesol) and (2S)-5,7-Dihydroxy-2-(4-hydroxyphenyl)chroman-4-one (Naringenin)», and followed in this work, does not introduce a constant CO_2 flow into the system and has the analytical measurement coupled online, while methodology used by Masaki Ota *y col.* «Measurement and correlation of flavanone, tangeritin, nobiletin, 6-hydroxyflavanone and 7-hydroxyflavone solubilities in supercritical CO2». En: *Journal of Supercritical Fluids* 128 (oct. de 2017), págs. 166-172. DOI: 10.1016/j.supflu.2017.05.024, introduces small amounts of CO_2 into the system and the solute must accumulate in a trap to be analyzed separately. The magnitude difference is probably because a methodology is better at achieving equilibrium conditions than its counterpart.

The range of solubility values found for Pn were slightly higher than those reported by Núñez, del Valle y de la Fuente, «Solubilities in Supercritical Carbon Dioxide of (2E,6E)-3,7,11-Trimethyldodeca-2,6,10-trien-1-ol (Farnesol) and (2S)-5,7-Dihydroxy-2-(4-hydroxyphenyl)chroman-4-one (Naringenin)» for naringenin, a flavanone with one more hydroxyl group than Pn. This fact, although probable, was not necessarily expected, since Pn was measured in mixture with CW. To have found a lower Pn solubility than that reported for naringenin would have been justified by the presence of waxes that reduce the occupation potential of clusters of sc-fluid molecules solvating Pn. Therefore, our remarks might be a manifestation of entrainer effects of the co-extracted substances, as was observed in extraction of theobromine and

theophylline from mate tea leaves and capsaicinoids from jalapeno pepper [96162163]. To be sure, it is still necessary to know the solubility of the Pn-scCO$_2$ binary system, which will probably be very close to the naringenin solubility, as Professor Mishima's group found for the solubilities of 3-hydroxyflavone and 7,8 dihydroxyflavone [164165].

Solubility modeling of the ternary system: sc$\mathrm{CO}_2^{(1)}$, Pn$^{(2)}$ and Oct$^{(3)}$ As mentioned above, the multicomponent phase equilibria of complex solute, such as LOP extract in scCO$_2$, are assessed by simplifying the system. To model the LOP extract-scCO$_2$ system, CWs were represented by a single component (Oct) and flavonoids by Pn. The pseudo-component mole fractions, 0.79 and 0.21 for Oct and Pn respectively, were calculated by the composition results from chromatography to calculate the mass of Pn and subtracting the amount of extract used in the analysis for the mass of Oct.

The solubility model of the scCO$_2^{(1)}$, Pn$^{(2)}$ and Oct$^{(3)}$ ternary system was calculated from the thermodynamic framework of subsection 2.6.1. The fugacity coefficients were calculated using standard Peng-Robinson Equation of State with quadratic mixing rules. The method used the two binary interaction parameters (K_{13} and I_{13}) fitted for the Oct-scCO$_2$ binary system, *cf.* table 14. The four binary interaction coefficients

---

[162] Marleny D A Saldaña *y col.* «Extraction of Purine Alkaloids from Maté (*Ilex paraguariensis*) using supercritical CO2». En: *J. Agric. Food Chem.* 47 (1999), págs. 3804-3808.

[163] J. M. Del Valle, M. Jiménez y J. C. De la Fuente. «Extraction kinetics of pre-pelletized jalapeño peppers with supercritical CO2». En: *Journal of Supercritical Fluids* 25.1 (2003), págs. 33-44. DOI: 10.1016/S0896-8446(02)00090-6.

[164] Hiroki Uchiyama *y col.* «Solubilities of Flavone and 3-Hydroxyflavone in Supercritical Carbon Dioxide». En: *Journal of Chemical & Engineering Data* 42.3 (mayo de 1997), págs. 570-573. DOI: 10.1021/je9603990.

[165] Kiyoshi Matsuyama *y col.* «Solubilities of 7,8-Dihydroxyflavone and 3,3â€˜,4â€˜,5,7-Pentahydroxyflavone in Supercritical Carbon Dioxide». En: *Journal of Chemical & Engineering Data* 48.4 (jun. de 2003), págs. 1040-1043. DOI: 10.1021/je030129z.

between Pn-scCO$_2$ (K_{12} and I_{12}) and Pn-Oct (K_{23} and I_{23}) were used as adjustable parameters from experimental data of Table 15. The solute parameters were calculated or taken from literature, and their values are shown in Table 4. Estimated parameters for the solubility modeling of ternary system are shown in Table 16. The data predicted by the model are shown with lines in Fig 19.

The model predicted a considerably higher solubility of Oct at 323 K than at 313 K, while the change in temperature did not significantly affect the solubility value of Pn. Given that the solubility of Pn in the ternary system is less sensitive to the increase of temperature than of Oct, the extract obtained from LOP extraction processes at temperatures close to the critical point would contain fewer CWs, which enhances the product. This solubility results have a direct impact on the rate, yield, design, and economy of the extraction process of LOP. If, on the other hand, the sc-extract fractionation was the study case to concentrate the flavonoid-rich fraction, the best option is to carry out the anti-solvent precipitation process at higher temperatures, favoring the wax solubility over that of the flavonoids [166][167][168].

4.3. Phase equilibria of multi-component EtOH-modified scCO$_2$ extraction

As discussed in Chapter 3, pressure (P) and percentage of ethanol (E), among other variables, have a significant effect on flavonoids extraction yield from LOP. These va-

---

[166] David Villanueva Bermejo *y col.* «High catechins/low caffeine powder from green tea leaves by pressurized liquid extraction and supercritical antisolvent precipitation». En: *Separation and Purification Technology* 148 (2015), págs. 49-56. DOI: 10.1016/j.seppur.2015.04.037.

[167] Abel Torres *y col.* «Perspectives on the Application of Supercritical Antisolvent Fractionation Process for the Purification of Plant Extracts: Effects of Operating Parameters and Patent Survey». En: *Recent Patents on Engineering* 10.2 (2016), págs. 88-97.

[168] Arturo Bejarano, Pedro C Simões y José M Del Valle. «Fractionation technologies for liquid mixtures using dense carbon dioxide». En: *Journal of Supercritical Fluids* 107 (2016), págs. 321-348. DOI: 10.1016/j.supflu.2015.09.021.

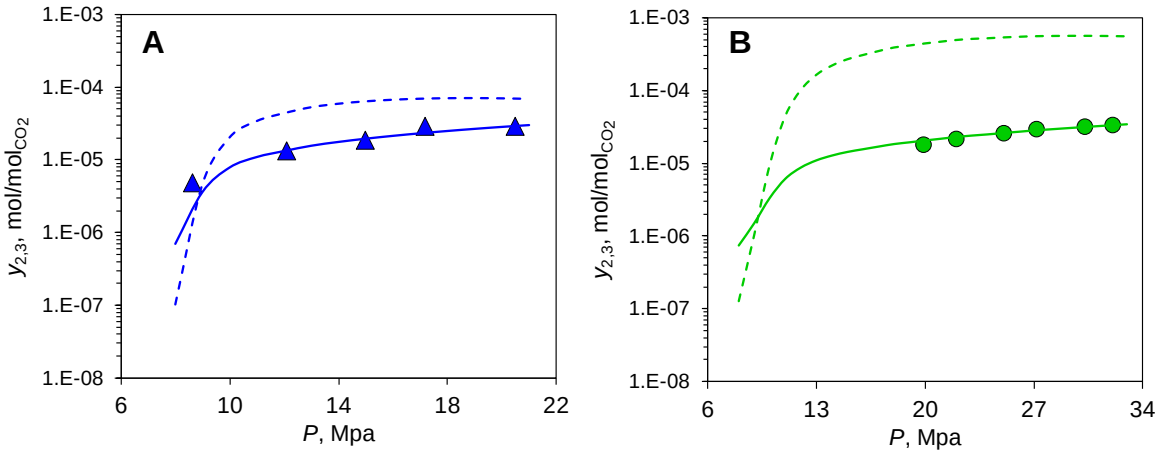

Figura 19. Solubilities of pinocembrin, octacosane and CO_2 in model ternary systems for LOP samples at different pressures and temperatures. (A) System at 313 K, (▲) are the measured solubilities for Pn; (B) System at 323 K, (●) are the measured solubilities for Pn. The dashed and continuous lines, are the solubilities values calculated applying Peng-Robinson equation of state for Oct and Pn respectively.

riables, together with the matrix-solute interaction, govern equilibrium and must be taken into account when studying the system with an operational approach, closer to the real extractive process. In the previous section, the thermodynamic limitations of the solute extracted from LOP were determined. In this section, we set out to find limitations of the extraction process, using a dynamic equilibrium extraction approach that included solute-matrix interaction and co-solvent effect. The first step was to establish a reliable methodology to quantify the flavonoids in the extract. With a validated analytic methodology and results of the previous section, characteristic parameters that describe the sorption equilibria of the solute from the matrix to the EtOH-modified scCO_2 in the extraction process were calculated.

4.3.1. Multivariate calibration and its validation Dynamic equilibrium extraction curves were constructed by quantifying the extract composition at the output of the process and plotting it as a time function. Processing such amount of data requires

a quick and effective analytical method that allows quantifying a large number of experimental samples. Avoiding chromatographic separation saves test expenses and time. Spectroscopy-based methods that employ multivariate calibration to decompose the spectral signal have worked well to solve the problem *cf.* subsection 2.3.1. Using well-trained models, these methods can estimate individual concentrations for multi-component mixtures, with certain analytical limitations, as expected when technologies are simplified. These methods are convenient to generate thermodynamic data, insofar as it is possible to validate the data predicted by the model with the data obtained by a reliable technique such as HPLC.

Samples calibration and quantification To validate the quantification methodology, different data sets were used to calibrate the method in order to study its influence on prediction. The sc-extract samples were represented for our purposes as mixtures of three constituents, *i.e.*, `Pn`, `Gn` and `Intf`. `Intf` was defined as the mixture of flavonoids that remain in a lesser proportion in the extract and the cuticular waxes that, although do not absorb in the UV region, they contribute to the matrix effect, *cf.* subsection 2.3.1. The first data set (`DS1`) were nine different mixtures of `Pn` and `Gn` standards. `DS1` does not consider `Intf` since the samples only contain flavonoids. Second data set (`DS2`) was prepared mixing a fixed concentration of extract ($2.55\,\mathrm{mg\,g^{-1}}$) with five different mixtures of `Pn` and `Gn` standards. In `DS2`, the moles of `Intf` remained constants due to the fixed amount of extract that was mixed with the flavonoid standards. Finally, the third data set (`DS3`) was prepared at three concentrations (*i.e.* 2.6, 7.7 and $12.8\,\mathrm{mg_{extract}/g_{sln}}$ of extract in MeOH). Calibration samples were prepared in triplicate and measured on both an HPLC-DAD (*cf.* subsection 2.2.2) and a miniature UV-Vis spectrophotometer (*cf.* subsection 2.2.2). The external calibration methodology was employed for quantification in HPLC-DAD by means of calibration curves of `Pn` and `Gn` standard substances, *cf.* subsection 2.3.2. Table 17 shows the statistical estimators of the calibration curve for HPLC-DAD.

Effect of the sample calibration data sets on prediction using ILS The approach to finding the ILS model parameters, that best predict Pn and Gn concentration, was to remove model training data sets and compare ILS prediction with HPLC-DAD results. The HPLC analysis results, and concentration estimated through the calibration curves in table 17, were taken as reliable estimated concentrations for comparison of methodologies. Fig. 20 shows the prediction comparison between the two quantification methodologies when DS1, DS2, and DS3 are used to calibrate the ILS model. The symbols deviation from the solid lines, on the ordinate axis, shows the discrepancy between the data predicted by the ILS model and those estimated by HPLC analysis. The lack of fit of the multivariate calibration model is remarkable for the prediction of Pn concentration. The *RMSE* statistics, 0.22 and 0.06 $\mu g\, g^{-1}$ for Pn and Gn respectively, are considerably larger than those obtained for HPLC (*cf.* table 17), especially for Pn.

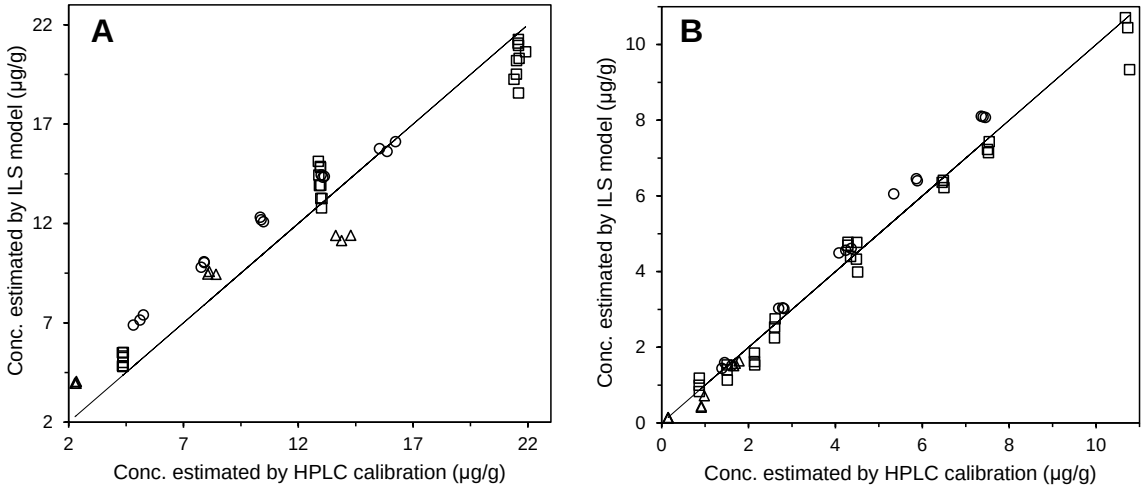

Figura 20. Comparison between estimated concentration using DS1, DS2, and DS3 for ILS model training and HPLC results. (A) Pinocembrin, (B) Galangin, (□) data set for flavonoids standard mixture (○) data set of extract enriched with flavonoids standards, (△) data set of extract diluted at different concentration. Solid lines are a projection of the concentration prepared for the calibration samples.

Analysis of the *RMSE* separately for each data sets showed that the model thus

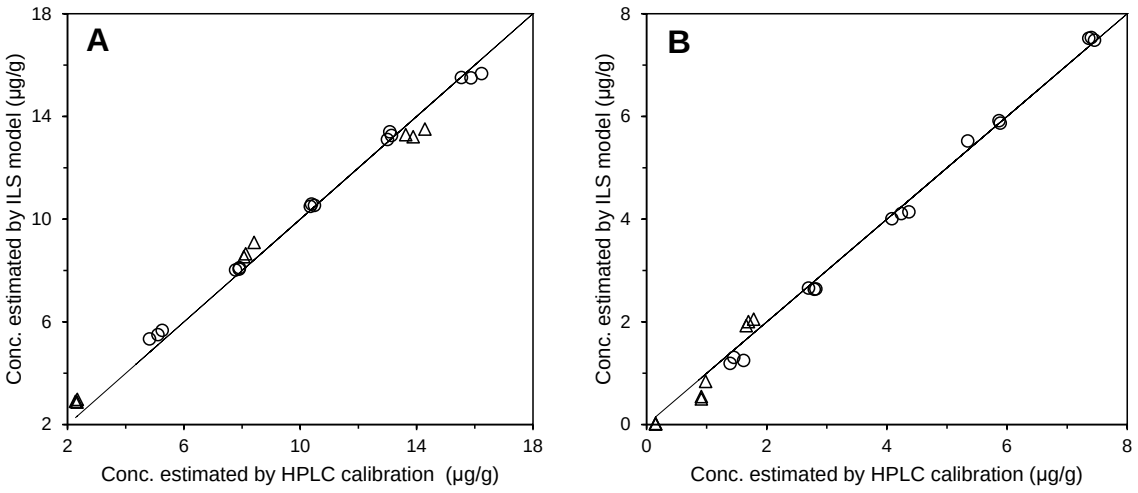

Figura 21. Comparison between estimated concentration using DS2, and DS3 for ILS model training and HPLC results. (A) Pinocembrin, (B) Galangin, (○) data set of extract enriched with flavonoids standards, (△) data set of extract diluted at different concentration. Solid lines are a projection of the concentration prepared for the calibration samples.

calculated, had a better estimate of DS1 (0.25 and 0.08 $\mu g\,g^{-1}$ for Pn and Gn respectively) compared to DS2 (0.43 and 0.12 $\mu g\,g^{-1}$ for Pn and Gn respectively) and DS3 (0.65 and 0.09 $\mu g\,g^{-1}$ for Pn and Gn respectively). This is not entirely convenient for calculating the concentration of flavonoids in sc-extracts since the presence of intf increases the prediction error. LOP sc-extracts are mainly composed of molecules that, although they do not absorb in the UV region, interfere with the sample spectral response. Consequently, a new model was fitted by excluding DS1 from the training data. Fig. 21 shows the prediction comparison between the two quantification methodologies when DS2, and DS3 were used to calibrate the ILS model. This time the calculated data was aligned with the real concentrations of the calibration samples obtained by HPLC and *RMSE* values (0.09 and 0.04 $\mu g\,g^{-1}$ for Pn and Gn respectively) improved considerably. These values are already in the same order of magnitude of error using HPLC, which comparatively makes them better than those obtained with the calibration that included DS1.

Therefore, it was observed that the absence of Intf in the calibration data sets negatively affects model accuracy. DS1 was considered as sample calibration to have selective information about UV spectra interaction between Pn and Gn. This information was thought to help the model distinguish between the two flavonoids whose spectra are relatively similar. However, when DS1 was included as training data, the model did not achieve good results for samples containing Intf. The presence of Intf strongly affects UV spectra of samples. For our practical purposes, Intf was calculated by material balance and was the difference between the extract mass and the Pn and Gn mass. Estimating the mass of Intf in this way means that the waxes co-extracted with flavonoids, which do not absorb in the UV region, are the major constituents. However, we assumed that the spectral responses of Intf minority constituents that absorb in the UV were proportional to their mass calculated from the material balance. Considering Intf in the model we improved the estimation of Pn and Gn concentration but nothing is known about the Intf concentration due to the difficulty of measuring all the molecules that compose it. The precision obtained with the model thus arranged was considered acceptable to measure apparent or operative solubility in $scCO_2$.

Leave one out (LOO) cross-validation methodology was applied in order to determine the capability to predict concentration without the information of a point in triplicate for models. Consequently, prediction coefficient, *i.e.*, Q^2 was calculated as a measure of goodness of prediction achieved with the sets of calibration data. Q^2 for Pn and Gn were 0.943 and 0.953 respectively, sufficiently satisfactory values. The determination coefficient for Pn and Gn in Fig. 21 were $R^2 = 0.994$ and $R^2 = 0.994$, respectively. Figures of merit to multivariate calibration were calculated based on Karl S. Booksh y Ziyi Wang. «Extension and application of univariate figures of merit to multivariate calibration». En: *Handbook of Environmental Chemistry* 2 (1995), págs. 209-227. DOI: 10.1007/978-3-540-49148-4-7: Selectivity $= 0.478$ and 0.225, LOD $= 0.877$

and 1.470 µg g^{-1}, sensitivity $= 0.788$ and 0.470 g au µg^{-1}, $\%AARD = 4.9$ and 17.1 for Pn and Gn respectively.

4.3.2. Sorption equilibria of LOP in the EtOH-modified scCO$_2$ extraction

Solvent saturation experiments The experimental errors found for preliminary equilibrium integral extraction curves (EIEC) were 6 % and 11 % for Pn and Gn respectively. Fig. 22 shows three EIEC, at the same extraction conditions, for different flow rate-to-feed ratios (*i.e.*, 0.6, 0.5 and 0.4 $\mathrm{kg_{solv}/kg_{subs}\,mín}$). The flow rate-to-feed ratio was modified by varying the amount of substrate loaded keeping the solvent flow constant (*cf.* subsection 2.5.2). Fig. 22 shows that the uncertainty lines and the slope of the curves tend to overlap for the values of 50 and 60 g of substrate. For subsequent experiments, 50 $\mathrm{g_{subs}}$ was added to the extraction vessel, since adding more substrate did not cause the solvent to dissolve more extract in the process.

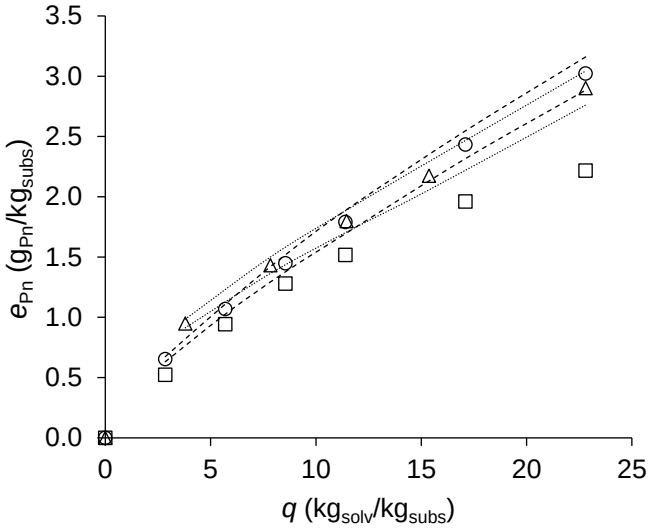

Figura 22. Experimental curves, at the same extraction conditions, for different amounts of the loaded substrate. (□) 0.04 $\mathrm{kg_{subs}}$, (○) 0.05 $\mathrm{kg_{subs}}$ and (△) 0.06 $\mathrm{kg_{subs}}$ (*ie.*, 0.6, 0.5 and 0.4 $\mathrm{kg_{solv}kg_{subs}^{-1}\,mín^{-1}}$ flow rate-to-feed ratio). Extractions at 50 ℃ and 34 MPa

Sorption equilibria measurements Table 18 shows the process conditions and extraction yields at 120 kg_{solv}/kg_{subs} (*i.e.*, e_{CW}, e_{Pn} and e_{Gn}) from the measured EIEC in the present work. Fig 23 shows the effects of T, P and E in the shape of some EIEC of table 18.

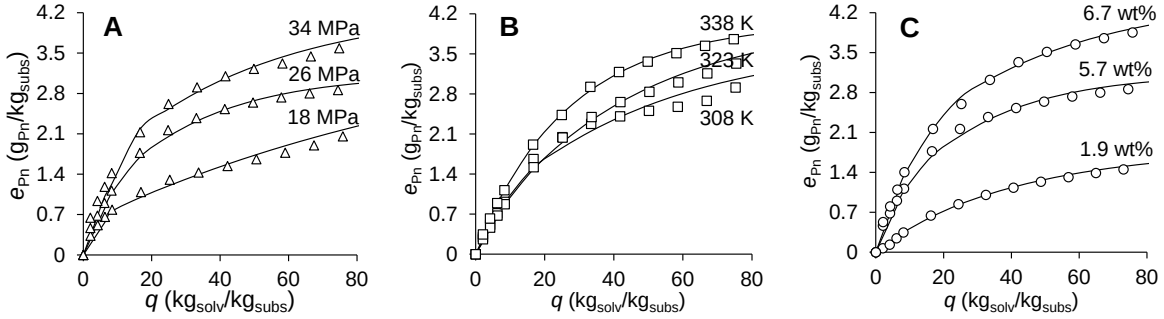

Figura 23. EIEC of pinocembrin versus specific solvent (EtOH-modified $scCO_2$) consumption. (A) Pressure variation at 338.2 K and *ca.* 5.6 wt % EtOH, (B) Temperature variation at 340 bar and *ca.* 4.5 wt % EtOH and (C) Cosolvent variation at 260 bar and 338.2 K

Judging by a visual inspection of the EIEC of Fig. 23, the change of E had a greater effect on e_{Pn}, compared to the effect of P and T on the same dependent variables. It is well known that addition of cosolvent to $scCO_2$ increases interactions between solutes and the solvent mixture, such as hydrogen bonding, clustering or complex formation that enhance the extraction yields of molecules with chemically active groups [169][170]. The polar character of Pn, whose chemical structure includes two hydroxyl groups, favors its molecular interactions with the EtOH-modified $scCO_2$. The effect of E was even greater for Gn, whose structure includes three hydroxyl groups, and was smaller for the whole extract, which is mainly made up of non-polar long-chain

[169] Simon S. T. Ting *y col.* «Solubility of naproxen in supercritical carbon dioxide with and without cosolvents». En: *Industrial & Engineering Chemistry Research* 32.7 (2005), págs. 1471-1481. DOI: 10.1021/ie00019a022.

[170] John M Walsh, George D Ikonomou y Marc D Donohue. «Supercritical phase behaivior: the entrainer effect». En: *Fluid Phase Equilibria* 33 (1987), págs. 295-314.

hydrocarbons [62], when the same curves were analyzed for those solutes (curves not shown). The selectivity of equilibrium sc-extraction towards Pn ($e_{\mathrm{Pn}}/e_{\mathrm{CW}}$) and Gn ($e_{\mathrm{Gn}}/e_{\mathrm{CW}}$) also increased with E especially at higher pressures and lower temperatures because those conditions decreased the e_{CW}. This is consistent with the thermodynamic solubility behavior for the Pn, Oct and scCO$_2$ ternary system, as the Oct solubility decreased with temperature, while Pn solubility remained almost the same, *cf.* Fig. 19. In addition to the molecular interactions between cosolvent and solute, interactions between cosolvent and matrix help improve diffusion by reducing the matrix's ability to retain the solute (swelling effect, Saldaña *y col.*, «Apparent solubility of lycopene and β-carotene in supercritical CO2, CO2Â +Â ethanol and CO2Â +Â canola oil using dynamic extraction of tomatoes»).

The ANOVA for yields of Table 18 showed that effects of E and P were the significant factors on extraction yiels, when data were analyzed as a response surface design without interactions between factors. P had a greater effect than T for all yields as it has a greater influence on the solvent mixture density. Increasing T decreases density, causing solubility to decrease. However, density is not the only thermodynamic determinant of solubility. Increasing T can also increase the solute sublimation pressure wich improves mass transfer from the available solid to the solvent. Depending on P, T can have a direct or inverse relationship with solubility. According to the ternary system's simulation results (our reference frame *cf.* Fig. 19), the crossover pressure would be between 10 and 15 MPa, an interval below our current experimental space. The increase in sublimation pressure due to the increase in temperature did not have a significant influence on yields.

One of the required properties to transform EIEC data in sorption isotherms/isobars is the solute initial concentration ($x_{\mathrm{i}|i}$). This value is usually taken from the horizontal asymptote at the end of the IECs. Since the partitioning of the solute between the substrate and the sc-solvent affects the extraction yields, it is important to decide

which asymptote from all possible experiments should be taken as $x_{\mathrm{i|CW}}, x_{\mathrm{i|Pn}}$, and $x_{\mathrm{i|Gn}}$. This occurs in cases where there is a fraction of strongly bound solutes that are not released from a solid matrix in the final stages of a sc-process **??**. The choice is not considered trivial since, on the one hand, the fit of the extraction kinetic models depends on the value of $x_{\mathrm{i}|i}$, and on the other hand, the initial concentration of solute depends only on the plant substrate. So $x_{\mathrm{i}|i}$ should be the same to model all experiments with the same substrate. Abrahamsson, Jumaah y Turner have addressed the problem by correlating the $x_{\mathrm{i}|i}$ values with their maximum experimental value and the co-solvent fraction used during extraction. That approach works for their practical purposes, but it causes the phase equilibrium effects to be confused between the proposed correlation and the Langmuir's isotherm used to describe partitioning. To stay close to physical reality, the $x_{\mathrm{i}|i}$ values in this work remained constant between sorption curves (*i.e.*, $x_{\mathrm{i|CW}} = 126\,\mathrm{g_{CW}/kg_{subs}}$, $x_{\mathrm{i|Pn}} = 22.5\,\mathrm{g_{Pn}/kg_{subs}}$ and $x_{\mathrm{i|Gn}} = 4.9\,\mathrm{g_{Gn}/kg_{subs}}$). In this sense, the sorption model used must be able to describe solvent saturation if this occurs, as well as the amount of solute tightly bound to the substrate that distributes between the solvent and the solid phase until full extraction of the post-distillation botanical substrate. The known sorption model that best overcomes these limitations was proposed by del Valle y Urrego, «Free solute content and solute-matrix interactions affect apparent solubility and apparent solute content in supercritical CO2 extractions. A hypothesis paper» (dVU, *cf.* Ec. 13), which is based on the idea of Perrut *y col.*, «Mathematical Modeling of Sunflower Seed Extraction by Supercritical CO2» sharp transition model and fits in a continuous line to the shapes of the experimentally observed smooth sorption curves. $x_{\mathrm{i}|i}$ Values were obtained by averaging the yields of the Soxhlet exhaustive extraction (*cf.* Table 11) and the preliminary exhaustive sc-extractions, carried out under high extraction conditions.

Something evident from visual inspection of Fig. 22 the succeeding EIEC and sor-

ption curves was the non-linearity in the section of the curves dominated by solubility, *i.e.*, the first part of the EIEC or the horizontal line with constant solvent concentration value in isotherms/isobars curves (*cf.* Fig. 3). This is an indication that the solvent has the ability to dissolve more solute before reaching its saturation concentration, but the amount of extract available in the matrix and the matrix-solute interaction prevent it. In general terms, it was observed that most of the experiments did not reach saturation concentration of the solvent, which are values greater than any measured operational solubility. Based on the above, to fit the dVU smooth equilibrium function to the `CW` data, thermodynamic solubility of `Oct` in scCO$_2$ binary system at T and P experimental conditions were fixed as $y_{\mathrm{s|CW}}$-value. For all experiments, $y_{\mathrm{Oct}}^{\mathrm{calc}}$ is greater than $y_{\mathrm{s|CW}}$ (*cf.* Table 18 and *cp.* columns 9 and 10).

Due to the differences between the $y_{\mathrm{Oct}}^{\mathrm{calc}}$ and the slope measurements of the first data with the origin in EIECs, it is reasonable to suppose that the `CW` concentration in the matrix ($x_{\mathrm{i|CW}}$) is less than the transition concentration ($x_{\mathrm{t|CW}}$). However, by adding the second data to calculate slopes, some values were very close to those previously calculated, which is a characteristic of solvent saturation. For this reason, fixing a $x_{\mathrm{t|CW}}$-value arbitrarily greater than $x_{\mathrm{i|CW}}$ was discarded as a strategy to reduce the number of fitting parameters. However, the dVU equation was rewritten to calculate $x_{\mathrm{t|CW}}$ as a relative parameter of $x_{\mathrm{i|CW}}$. In this way, if the best-fitted result is a value less than unity, there would be indications of solvent saturation, even if it were only in the initial extraction stage (*cf.* § in Table 18 notes). In addition to the $x_{\mathrm{t|CW}}$ term, two other properties were used as fitting parameters: the partition coefficient (K_{CW}) and the n-value (n_{CW}). Table 18 shows the best-fitted sorption parameters for `CW` which for this study describe equilibrium of the whole `LOP` sc-extract. The table also shows the *RMSE*-values whose order of magnitude can be compared with the $y_{\mathrm{s|CW}}$-values to size the fitting error. In experiments where evidence of solvent saturation was found (*i.e.*, $x_{\mathrm{t|CW}} < x_{\mathrm{i|CW}}$), the fit parameters were recalculated using the $y_{\mathrm{s|CW}}$-

value measured from the EIEC slope and not the $y_{\mathrm{Oct}}^{\mathrm{calc}}$-value. This, while reducing the goodness of fit, describes better the reality. Recalculation did not show a significant change in the other equilibrium descriptors, *i.e.*, K_{CW} and $x_{\mathrm{t|CW}}$.

The apparent solubility data measured from the EIECs comparable to those obtained by the thermodynamic framework in section 4.2 were those that reached solvent saturation. According to the results, there is a discrepancy to consider between these values in Table 18. Beyond the differences due to the use of co-solvent, it seems that `Oct` is not the long-chain hydrocarbon that best represents `LOP-CW`, since it exceeds solubility predicted from the thermodynamic framework compared to the measured value. Possibly a longer hydrocarbon chain, which has a lower solubility in $scCO_2$, will better represent this magnitude for the study case. The present work did not have the scope to measure the `CW` distribution in the `LOP` sc-extract since other analytic techniques than UV-Vis spectroscopy were not used. Therefore, the selection of long-chain hydrocarbon was carried out considering previous works with similar botanical substrates and the availability of experimental data found in the open literature. A better selection would be possible if the `CW` distribution and some saturation concentration values were known. For this, the most convenient would be to make preliminary measurements at different pressure points of at least one isotherm, either of the substrate or the extracted solute. Preliminary experiments with the substrate should preferably be at a condition close to the critical point, where solvent saturation is favored because the extract is less soluble, and less interaction with the matrix occurs. To predict reliable solubility values with the simplifying approach of grouping by families of molecules, it is still necessary to deepen in the thermodynamic parameterization of distributions that would represent the composition of the extracts in the model. If research on modeling the multicomponent extraction of botanical substrates continues, advances in the state of the art regarding parameterization and selection of molecule distributions may soon be published.

The CW equilibrium parameters in the Table 18 are of paramount importance in process optimization *via* mathematical simulations. Calculating these parameters from the extraction conditions is mathematically desirable and can be achieved through correlating experimental data. A regression model selection was applied to find the best correlation between the extraction variables and the equilibrium parameters. The independent variables used in the regression model selection were individual, transformed, and algebraically-combined extraction conditions, intuitively proposed based on the model's structures that correlate solubility of pure solids in scCO_2. CO_2 density, a thermodynamic property derived from the extraction conditions, was also included due to its linear relationship with the logarithm of solubility. Table 19 shows the best-correlated models with their statistical and fit descriptors. For all cases except K_{CW}, the best correlations were achieved by transforming the dependent variable into the product logarithm of the equilibrium parameter, and one of the extraction conditions, *i.e.*, E for $y_{\mathrm{s|CW}}$, T for $x_{\mathrm{t|CW}}$, and P for a proposed constant related to the partition of minority compounds in the extract. This last parameter will be discussed later. The determination coefficients (R^2) for $y_{\mathrm{s|CW}}$ understood as the slope of the line between the first EIEC data with the origin whether saturation has been reached or not, and $x_{\mathrm{t|CW}}$ explain more than 93 % of data variability. The Mallows Cp statistic, a measure of model bias, shows low values close to the number of model coefficients, indicating that the models are relatively accurate estimating true regression coefficients, and predicting future responses. With $Cp = 14.5$, the $x_{\mathrm{t|CW}}$ correlation is the model with the highest statistical bias. K_{CW} was the equilibrium parameter that showed the worst correlation results. The best independent variables for this model managed to explain only 57 % of the variability. There is still a percentage of variability that cannot be explained from the extraction conditions that is possibly related to the strong intermolecular forces of matrix, solute, and solvent interactions in sc-extraction or the mass transfer effects, difficult to discriminate from the EIEC **??**. With

this result, it would be difficult to estimate a K_{CW} value from correlations to simulate the IEC. Intermediate values within the limits of data in Table 18 require additional supporting evidence.

Up to this point, only the CWs equilibrium has been studied, which for this study represents the equilibrium of the whole LOP sc-extract, but the molecules of interest are the minority flavonoids. Depending on the approach, modeling sorption equilibrium for minority compounds in a multi-component extraction also requires the fitting of one or more parameters associated with the individual compounds. Given the convenience of keeping a small number of fitting-parameters in the models, we employed a constant dependent on the extraction conditions to represent the flavonoids partition in the extract to describe Pn and Gn sorption curves. The idea was to use a single partitioning constant for the sorption curves of minority compounds in multicomponent extraction ($K_{\mathrm{s}|i}$) that when multiplied by the CW concentration (e^*_{CW}, modeled from the dVU equilibrium equation) predicted the flavonoids concentration. The equilibrium parameters of minority compounds in this approach could be rewritten from the equilibrium parameters of CW and $K_{\mathrm{s}|i}$ (not to be confused with K_i, the partitioning constant between the substrate and the extracting solvent) as follows:

$$y_{\mathrm{s}|i} = K_{\mathrm{s}|i} y_{\mathrm{s}|\mathrm{CW}} \tag{28}$$

$$K_i = K_{\mathrm{s}|i} K_{\mathrm{CW}} \tag{29}$$

$$x_{\mathrm{t}|i} = \frac{x_{\mathrm{t}|\mathrm{CW}} x_{\mathrm{i}|i}}{x_{\mathrm{i}|\mathrm{CW}}} \tag{30}$$

Where i is the counter of minority compounds of the multi-component extraction (Pn, and Gn for this study case), and $x_{\mathrm{i}|i}$ is the initial concentration of i in the substrate. The fitting of $K_{\mathrm{s}|i}$-value was made by minimizing the RSD between the experimental and calculated data of e^*_i. Results are shown in Table 18. Fig. 24 shows the sorption

curves for CW and the two minor compounds, *i.e.*, Pn and Gn of the LOP sc-extract obtained at 308.2 K, 18 MPa and 4.2 wt % of EtOH. The line close to the experimental data shows how well this approach represents the equilibrium behavior of minority compounds in the extraction. The experimental errors ($RMSE_i$) are also shown in Table 18 and can be compared with the $K_{\mathrm{s}|i}y_{\mathrm{s}|\mathrm{CW}}$ product to dimension the error magnitude. Table 19 show the independent variables that best correlate $K_{\mathrm{s}|i}$ with the extraction conditions. The best correlation explains more than 80 % of the data variability for $K_{\mathrm{s}|i}$. This is a considerably good result considering the indirect way of measuring it.

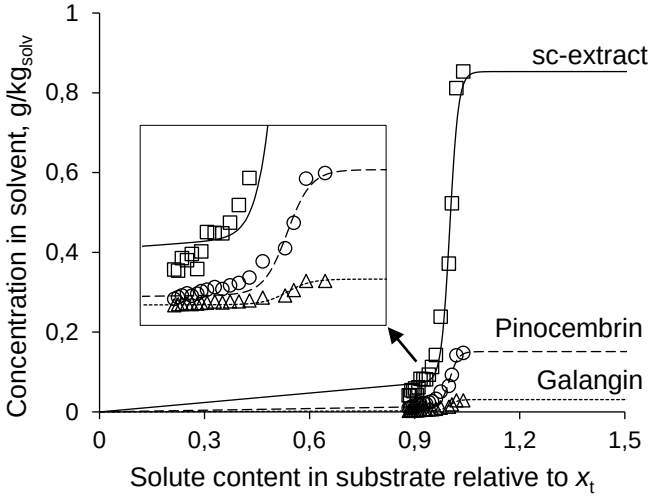

Figura 24. Sorption isotherms/isobars curve for sc-extract of LOP at 308.2 K, 18 MPa, 4.2 wt % of EtOH and 300 mín. (□) are data of sc-extract or CW, (○) are data for Pn and (△) are data for Gn

In the state of the art, it has been conveniently sought to reduce the number of fitting parameters from experimental data of simpler binary systems. However, parameters such as solubility of pure compounds do not provide sufficient information about the multicomponent extraction from botanical substrates **??**. This is due to the mixture complexity and the main role of the substrate in extraction. Binary solubility provides more information about the equilibrium of more soluble solutes and higher initial

concentration substrates, such as sc-extraction of seeds. If the apparent solubility is compared with the thermodynamic one for a specific compound, its composition in the extracted mixture must be considered. To do this, the authors have multiplied the apparent solubility, calculated from the first slope of the IEC, by the initial concentratio fraction between CW and the substance of interest ($x_{\mathrm{i}|\mathrm{CW}}/x_{\mathrm{i}|i}$) before comparing it with thermodynamic solubility measured for the pure substance [96]. This "corrected" solubility as a product of the apparent solubility and the reciprocal partition coefficient of minority compounds ($y_{\mathrm{sK}|i}$) is shown for Pn and Gn in Table 18. Values for $y_{\mathrm{sK}|\mathrm{Pn}}$, higher by *ca.* an order of magnitude than $y_{\mathrm{Pn}}^{\mathrm{calc}}$, show the entrainer effects of the co-solvent. On the other hand, $y_{\mathrm{sK}|\mathrm{Gn}}$ values *ca.* two orders of magnitude higher than $y_{\mathrm{Pn}}^{\mathrm{calc}}$, also show entrainer effects of co-extracted substances.

Some more suitable data to compare solubility values are those shown in Table 20. It compare experimental solubility results obtained from the thermodynamic framework with the measured sorption curves at 323 K. The Oct predicted solubility for the quaternary system was greater than the apparent solubility for the whole CW at points where solvent saturation presumably occurs. A value closer to reality observed from sorption curves would have been *ca.* $1\ \mathrm{g_{Hydrocarbon}/kg_{solv}}$, which could be achieved using a longer chain length hydrocarbon, as already mentioned. However, from this work, it was not possible to generate evidence that a single long-chain hydrocarbon can represent a distribution of CW at all extraction conditions. The state of the art is still in its first steps on this topic, and it will be some time before agreeing on the methodology for selecting the family representative substance or the thermodynamic parameters associated with CW distributions. Contrary to the solubility values obtained from the thermodynamic framework, the apparent solubility $y_{\mathrm{s}|\mathrm{CW}}$ (that would be better called "operational solubility" in Table 20) does not increase with pressure. This is due to its dependence on the other equilibrium parameters, mainly on $x_{\mathrm{t}|\mathrm{CW}}$, which dictates the amount of free solute available to saturate solvent when matrix interac-

tion is irrelevant and the extraction is entirely governed by solubility. The $y_{\mathrm{s|CW}}$-values in Table 20 would also increase with pressure if it had been worked with a substrate with higher extract availability. The high interaction of solid matrix which do not allow to reach saturation also promotes less CW solvation in the sc-solvent, making extraction more selective towards flavonoids, which, in contrast, increased *ca.* 2x due to the co-solvent entrainer effect. Under certain conditions the optimal extraction process does not depend on "thermodynamic" solubility as intuitively thought; instead, it is the interaction of all actors what influences the extraction of the target substance.

4.4. Conclusions

The mathematical approach and the parameters necessary to describe the phase equilibria of the post-distillation residues of LOP multi-component EtOH-modified sc-extraction were performed and calculated in this work for the following extraction conditions range: 308 to 338 K, 18 to 34 MPa and 2 to 9 wt % EtOH. Pinocembrin solubility of the multi-component LOP extract-scCO$_2$ system was measured and modeled through a thermodynamic framework that group cuticular waxes in a pseudo-component represented by the thermodynamic properties of octacosane. Sorption isotherm/isobar curves were measured and modeled using the thermodynamic solubility of octacosane as saturation concentration parameter of the dVU equilibrium model. The prediction of solubility for octacosane in the thermodynamic framework oversizes the solubility measured from the sorption curves that managed to saturate the solvent in the extraction stage governed by the solubility, so a longer chain linear hydrocarbon would be more convenient for the modeling thus proposed. It is possible to describe the sorption equilibria of minority compounds from the equilibrium parameters of cuticular waxes and the partition coefficients of minority compounds in the extract ($K_{\mathrm{s}|i}$). The strong interaction of the solute with the matrix, in addition to avoiding saturation of the solvent at the early stages of sc-extraction, is also responsible

for the increase in selectivity towards flavonoids with pressure.

Table 13. Octacosane ($C_{28}H_{58}$) solubility data in $scCO_2$. $y_3^{exp} \times 10^5$ mol_{Oct}/mol_{CO_2}

313 K*						333 K‡					
P, MPa	y_3^{exp}, -	P, MPa	y_3^{exp}, -	P, MPa	y_3^{exp},-	P, MPa	y_3^{exp}, -	P, MPa	y_3^{exp}, -	P, MPa	y_3^{exp}, -
9.0	1.9	13.0	9.1	22.5	16.7	16.0	41.2	28.0	139.8	40.0	237.1
9.5	2.8	14.0	9.6	27.5	17.1	20.0	78.7	32.0	174.5	44.0	262.3
10.0	4.8	15.0	10.3			24.0	103.5	36.0	211.6		
11.0	6.0	18.0	13.0								
323 K†						343 K§					
P, MPa	y_3^{exp}, -	P, MPa	y_3^{exp}, -	P, MPa	y_3^{exp}, -	P, MPa	y_3^{exp}, -	P, MPa	y_3^{exp}, -	P, MPa	y_3^{exp}, -
12.5	21.0	18.8	63.3	20.5	77.4	16.2	27.9	27.0	174.2	31.0	254.9
12.6	20.3	20.2	70.2	22.9	94.5	18.1	50.3	27.0	180.3	33.0	270.6
13.6	32.5	20.2	69.8	25.1	103.2	20.0	87.1	27.1	180.7	35.9	319.5
13.6	32.5	21.4	75.0	30.1	109.0	24.0	158.6	28.1	200.1	42.0	407.1
13.8	32.6	21.5	76.1	37.6	102.2	20.4	77.7	28.1	191.3	44.8	440.5
14.1	32.7	22.9	81.6	44.4	84.1	23.0	116.1	28.9	194.6		
16.0	49.3	24.5	83.8	48.9	79.1	24.2	123.2	30.9	249.0		
16.8	54.5	25.4	85.0	48.9	79.8						
17.9	61.7	26.2	85.5								

* Data taken from Ernesto Reverchon, Pietro Russo y Alberto Stassi. «Solubilities of solid octacosane and triacontane in supercritical carbon dioxide». En: *Journal of Chemical & Engineering Data* 38.3 (jul. de 1993), págs. 458-460. DOI: 10.1021/je00011a034.

† Data taken from Mark A. McHugh, Andrew J. Seckner y Thomas J. Yogan. «High-pressure phase behavior of binary mixtures of octacosane and carbon dioxide». En: *Industrial & Engineering Chemistry Fundamentals* 23.4 (mayo de 1984), págs. 493-499. DOI: 10.1021/i100016a020 and I. Swaid, D. Nickel y G.M. Schneider. «NIRâ€"spectroscopic investigations on phase behaviour of lowâ€"volatile organic substances in supercritical carbon dioxide». En: *Fluid Phase Equilibria* 21.1-2 (ene. de 1985), págs. 95-112. DOI: 10.1016/0378-3812(85)90062-7.

‡ Interpolated data from I. Swaid, D. Nickel y G.M. Schneider. «NIRâ€"spectroscopic investigations on phase behaviour of lowâ€"volatile organic substances in supercritical carbon dioxide». En: *Fluid Phase Equilibria* 21.1-2 (ene. de 1985), págs. 95-112. DOI: 10.1016/0378-3812(85)90062-7, Thierry Chartier *y col.* «Solubility, in Supercritical Carbon Dioxide, of Paraffin Waxes Used as Binders for Low-Pressure Injection Molding». En: *Industrial & Engineering Chemistry Research* 38.5 (mar. de 1999), págs. 1904-1910. DOI: 10.1021/ie980552e and Mark A. McHugh, Andrew J. Seckner y Thomas J. Yogan. «High-pressure phase behavior of binary mixtures of octacosane and carbon dioxide». En: *Industrial & Engineering Chemistry Fundamentals* 23.4 (mayo de 1984), págs. 493-499. DOI: 10.1021/i100016a020.

§ Data taken from Thierry Chartier *y col.* «Solubility, in Supercritical Carbon Dioxide, of Paraffin Waxes Used as Binders for Low-Pressure Injection Molding». En: *Industrial & Engineering Chemistry Research* 38.5 (mar. de 1999), págs. 1904-1910. DOI: 10.1021/ie980552e and I. Swaid, D. Nickel y G.M. Schneider. «NIRâ€"spectroscopic investigations on phase behaviour of lowâ€"volatile organic substances in supercritical carbon dioxide». En: *Fluid Phase Equilibria* 21.1-2 (ene. de 1985), págs. 95-112. DOI: 10.1016/0378-3812(85)90062-7.

Table 14. Fitted adjustable parameters for correlating octacosane solubility in $scCO_2$ with the Peng-Robinson Equation of State (PR-EoS) and quadratic mixing rules. Comparison of the goodness of fit between the thermodynamic model and the semi-empirical correlation of MS-T.

Temperature, K	Pressure range, MPa	K_{12}, –	I_{12}, –	N^o. Data	PR-EoS correlation, $AARD\%$	MS-T correlation, $AARD\,\%$
313	9–27.5	0.061	-18.24	10	22.7	74.8
323	12.5–48.9	0.042	-7.01	26	5.7	31.5
333	16–44	0.055	-5.81	8	17.1	10.5
343	16.2–44.8	0.079	-4.85	19	28.5	22.4

Table 15. Pinocembrin solubility in $scCO_2$ measured in mixture with the co-extracted compounds from the sc-extraction of post-distillation residues of LOP

Temperature, K	Pressure, MPa	$y_2^{\exp} \times 10^{-6} \mathrm{mol}_{\mathrm{Pn}}/\mathrm{mol}_{\mathrm{CO_2}}$
313	8.6	4.8
	12.1	13.4
	15.0	18.8
	17.2	29.0
	20.5	29.5
323	19.9	17.7
	22.0	21.7
	25.1	25.5
	27.2	29.3
	30.3	31.5
	32.1	33.3

Table 16. Fitted adjustable parameters for correlating solubility of the ternary system using PR-EoS and quadratic mixing rules.

Parameters	Temperature	
	313 K	323 K
Best-fitted parameters		
K-parameter for CO_2-Pn interaction (K_{12}, $-$)	0.348	0.378
I-parameter for CO_2-Pn interaction (I_{12}, $-$)	-0.010	-0.008
K-parameter for Pn-Oct interaction (K_{23}, $-$)	-0.004	0.006
I-parameter for Pn-Oct interaction (I_{23}, $-$)	-0.006	-0.001
Sublimation pressure ($P^{\text{sub}} \times 10^6$, MPa)	0.518	2.147
Application range and goodness of fit		
Pressure range (MPa)	8.5-20.5	19-32
Number of data	5	6
Average absolute relative deviation ($AARD$, %)	16.3	3.7

Table 17. Statistical estimators of the Pn and Gn calibration curves using HPLC-DAD.

Estimator	Pinocembrin	Galangin
Determination coefficient (R^2, -)	0.9997	0.999
Limit of Detection (LOD, µg g^{-1})	0.15	0.32
Response factor (Slope, µg g^{-1} au^{-1})	12.2	30.9
Intercept (µg g^{-1})	46	143
Root Mean Squared Error ($RMSE$, -)	0.01	0.02

Table 18. Sorption isotherms/isobars parameters for sc-extract of post-distillation residues of *Lippia origanoides* phellandrene-rich chemotype.

Extraction conditions			Yields			Selectivities		Sorption parameters for CW						Sorption parameters for Pn				Sorption parameters for Gn			
T, K	P, MPa	E, wt%	e_{CW}^{*}, g_{CW}/kg_{subs}	e_{Pn}^{*}, g_{Pn}/kg_{subs}	e_{Gn}^{*}, g_{Gn}/kg_{subs}	S_{Pn}, -	S_{Gn}, -	$y_{\mathrm{Oct}}^{\mathrm{calc}\dagger}$, g_{Oct}/kg_{CO_2}	$y_{\mathrm{s\|CW}}$, g_{CW}/kg_{solv}	$K_{\mathrm{CW}} \times 10^4$, -	$x_{\mathrm{t\|CW}}$, g_{CW}/kg_{subs}	n_{CW}	$RMSE_{\mathrm{CW}}$, g_{CW}/kg_{solv}	$K_{\mathrm{s\|Pn}}$, -	$y_{\mathrm{Pn}}^{\mathrm{calc}\ddagger}$, g_{Pn}/kg_{CO_2}	$y_{\mathrm{sK\|Pn}}$, -	$RMSE_{\mathrm{Pn}}$ g_{Pn}/kg_{solv}	$K_{\mathrm{s\|Gn}}$, -	$y_{\mathrm{Nn}}^{\mathrm{calc}\dagger}$, g_{Nn}/kg_{CO_2}	$y_{\mathrm{sK\|Gn}}$, -	$RMSE_{\mathrm{Gn}}$ g_{Gn}/kg_{solv}
308.15	18	4.2	15.7	3.3	0.8	0.21	0.05	1.8	0.85§	6.632	118.9	82	0.045	0.18	0.14	0.85	0.009	0.04	0.055	0.79	0.003
	18	5.1	16.0	2.8	0.4	0.18	0.02	1.8	1.33§	4.992	116.2	92	0.048	0.14	0.14	1.02	0.020	0.03	0.055	0.91	0.005
	18	5.6	14.5	3.3	0.7	0.22	0.05	1.8	1.02§	2.616	123.2	36	0.021	0.23	0.14	1.29	0.009	0.05	0.055	1.42	0.002
	34	3.4	16.0	3.4	0.9	0.21	0.06	2.7	0.75§	0.668	125.5	24	0.019	0.16	0.13	0.66	0.023	0.05	0.050	0.96	0.004
	34	4.3	14.4	3.7	1.0	0.26	0.07	2.7	0.74	0.152	129.5	22	0.021	0.20	0.13	0.84	0.015	0.05	0.050	0.92	0.004
323.15	18	8.1	21.4	3.2	0.3	0.15	0.01	3.6	1.31§	4.148	114.3	30	0.080	0.17	0.14	1.27	0.018	0.03	0.060	1.06	0.013
	18	8.9	22.6	3.8	0.6	0.17	0.03	3.6	1.22§	5.993	124.5	46	0.014	0.21	0.14	1.42	0.016	0.03	0.060	0.79	0.004
	26	4.3	17.6	3.3	0.6	0.19	0.03	5.9	1.22	0.006	133.3	19	0.005	0.20	0.15	1.37	0.012	0.05	0.064	1.65	0.003
	26	5.4	21.4	3.4	0.6	0.16	0.03	5.9	1.53	0.946	131.4	18	0.004	0.20	0.15	1.70	0.010	0.03	0.064	1.31	0.002
	34	2.6	16.3	3.3	0.8	0.20	0.05	7.6	0.86	0.409	144.6	16	0.001	0.18	0.16	0.89	0.009	0.04	0.064	0.90	0.003
	34	4.9	17.8	4.1	1.3	0.23	0.07	7.6	0.99	0.854	141.5	16	0.005	0.19	0.16	1.04	0.013	0.05	0.064	1.15	0.005
338.15	18	5.1	16.3	3.0	0.2	0.18	0.01	6.1	1.30	4.331	129.9	32	0.005	0.18	0.12	1.26	0.008	0.03	0.060	0.91	0.001
	18	8.3	21.0	3.7	0.3	0.17	0.02	6.1	1.42	0.006	129.6	18	0.006	0.15	0.12	1.19	0.011	0.03	0.060	1.01	0.002
	18	8.6	19.8	4.3	0.9	0.22	0.04	6.1	1.51	0.899	126.7	22	0.007	0.17	0.12	1.41	0.015	0.04	0.060	1.51	0.003
	26	1.9	11.3	1.8	0.3	0.16	0.03	13.6	0.82	0.181	132.6	36	0.001	0.06	0.16	0.28	0.016	0.01	0.075	0.21	0.003
	26	5.7	19.5	3.1	0.5	0.16	0.02	13.6	1.47	0.032	144.1	15	0.005	0.19	0.16	1.53	0.017	0.04	0.075	1.54	0.004
	26	6.7	22.4	4.5	0.9	0.20	0.04	13.6	1.59	1.737	140.7	15	0.005	0.18	0.16	1.56	0.019	0.04	0.075	1.70	0.005
	34	4.2	20.0	4.1	0.9	0.20	0.05	19.6	1.04	0.007	151.2	14	0.003	0.18	0.18	1.04	0.016	0.05	0.079	1.28	0.004
	34	5.9	19.9	4.3	1.4	0.22	0.07	19.6	1.64	0.686	142.8	17	0.003	0.23	0.18	2.07	0.020	0.05	0.079	2.17	0.014

* Extraction yields at equilibrium conditions and 120 kg_{solv}/kg_{subs}.
† Pure component solubility in $scCO_2$, binary system.
‡ Mixture solubility in $scCO_2$, LOC sc-extract and $scCO_2$ system. Conditions for which K_{ij}-values were not known, solubilities were interpolated from the calculable ones.
§ Preasumible solvent saturation: $x_{\mathrm{i}} > x_{\mathrm{t}}$.

Table 19. Correlation between equilibrium parameters and extraction conditions of EtOH-modified $scCO_2$ extraction of LOP.

Equilibrium parameters	Correlation	Coefficient-value				Statistical and fit descriptors		
		A	B	C	D	Cp Mallows	R^2	$AARD\,\%$
CW solubility*	$\ln\left(y_{\mathrm{s\|CW}}E\right) = A + B\ln E + C/T$	2.53	1.42	-999	-	3.7	94.6	11
CW transition concentration	$\ln\left(x_{\mathrm{t\|CW}}T\right) = A + BP + C\ln E + D(\rho/T)$	12.2	1.01×10^{-2}	1.22	-611	14.5	93.6	2.1
CW partitioning	$K_{\mathrm{CW}} = A + BP + C(\rho/T)$	1.12×10^{-4}	-2.6×10^{-5}	0.285	-	1.2	57.7	75
K_s partition for Pn	$\ln\left(K_{\mathrm{s\|Pn}}P\right) = A + B(\rho/T) + Cy_{\mathrm{s\|CW}} + D\ln x_{\mathrm{t\|CW}}$	-21.8	1147	0.537	4.04	6.6	81.1	14
K_s partition for Gn	$\ln\left(K_{\mathrm{s\|Gn}}P\right) = A + B(\rho/T + Cy_{\mathrm{s\|CW}} + D\ln x_{\mathrm{t\|CW}}$	-31.5	1597	0.609	5.44	-2.1	81.4	19

* It is understood as the value of the slope between the origin and the first data of the IEEC, whether saturation has been reached or not.

Table 20. Solubilities of cuticular waxes, octacosane and pinocembrin in $scCO_2$ and EtOH-modified $scCO_2$ obtained from the thermodynamic framework and the sorption curves at 323 K

Extraction conditions		Cuticular Waxes	Octacosane		Pinocembrin	
P, MPa	E, wt %	$y_{\mathrm{s\|CW}}$*, g_{CW}/kg_{solv}	y_{Oct}†, g_{Oct}/kg_{CO_2}	$y_{\mathrm{s\|Oct}}$*, g_{Oct}/kg_{solv}	y_{Pn}†, g_{Pn}/kg_{CO_2}	$y_{\mathrm{s\|Pn}}$*, g_{Pn}/kg_{solv}
18	8.1	1.31‡	2.79	1.04	0.14	0.23
18	8.9	1.22‡	2.79	0.94	0.14	0.25
26	4.3	1.22	5.66	0.91	0.15	0.24
26	5.4	1.53	5.66	1.18	0.15	0.30
34	2.6	0.86	8.32	0.66	0.16	0.16
34	4.9	0.99	8.32	0.76	0.16	0.19

* Solubility in EtOH-modified $scCO_2$ from sorption data.
† Solubility in $scCO_2$ from thermodynamic framework for ternary system.
‡ Preasumible solvent saturation: $x_{\mathrm{i}} > x_{\mathrm{t}}$

5. KINETICS OF $scCO_2$ EXTRACTION OF POST-DISTILLATION *LIPPIA* spp. RESIDUES

In chapter 3, the potential of post-distillation residues of *L. origanoides* as on industrial source of pinocembrin and the advantage in selectivity of EtOH-modified $scCO_2$ extraction were studied. In this chapter we focus on the oleoresin extraction kinetics, continuing with the idea of taking advantage of sc-extraction selectivity to obtain an extract enriched in pinocembrin. The proper description of the process extraction stage is essential for the scale-up of laboratory data for industrial design purposes. The extraction kinetics of the different post-distillation chemotypes of *L. origanoides* were studied. With the post-distillation residue of LOP, changes in kinetic parameters due to the P and T were measured. The effect of pelletization on the phenomena of mass transfer in extraction was also studied. This study of the variables that affect the phenomena of equilibrium and mass transfer in the sc-extraction, aimed to establishing the limits of the extractive technique. Extractions were simulated with the BIC model proposed and modified by Sovová, «Mathematical model for supercritical fluid extraction of natural products and extraction curve evaluation». The physicochemical and kinetic parameters were estimated and fitted to the experimental data. The results confirmed the selectivity of EtOH-modified $scCO_2$ extraction towards pinocembrin. The substrates interact differently in extraction at the same extraction conditions. Pelletization improved parameters of the model related to mass transfer, but compaction made it difficult to transfer mass from the pellet core. Inhomogenity in the extraction flow limited information on the flow pattern that control the extraction. The sc-extraction selectivity has great usability potential in fractionation stages after hydro-alcoholic extractions that are projected to have higher extractive yields. The results of this work contribute to the AEs industry by improving profit by extracting valuable by-products that remain in the matrix after the distillation process.

5.1. Physical properties and model parameters

5.1.1. Substrate properties Table 21 presents properties of substrates used for this section. The porosities of the extruded substrates, *i.e.*, SP and LP, are close to each other, although for LP the porosity is slightly higher because ρ_{s} is greater and ρ_{b} is lower than corresponding values for SP. As expected, the porosities of the extruded substrates were lower and the values of ρ_{s} and ρ_{b} were higher than those found for chopped substrates. Dry-based moisture (M_{d}) values were considerably lower for SP and LP because the extrusion process reduces the water content in the substrate by evaporation. The initial concentrations of cuticular waxes (x_{uCW}) and pinocembrin (x_{uPn}) in the substrates also decrease when the extrusion process is applied to the chopped substrate.

Table 21. Substrate properties of post-distillation residues of *L. origanoides* chemotypes and *L. graveolens*

Property	LOC *	LOT *	LG *	LOP *	SP †	LP ‡
Porosity (ϵ, -)	0.75	0.70	0.77	0.68	0.43	0.47
Solid density (ρ_{s}, kg m^{-3})	1068	1024	1053	1051	1359	1401
Bulk density (ρ_{b}, kg m^{-3})	264	305	238	338	773	739
Particle size (d_{p}, mm)	0.31	0.31	0.31	0.31	2.5	4
Dry basis moisture (M_{d}, %)	13.3	14.0	14.4	12.3	5.6	4.8
CW initial concentration (x_{u}, g_{CW}/kg_{subs})	128	114	45	126	92	110

* Chopped substrate
† *L. origanoides* phellandrene-rich chemotype small pellets, 2.5 mm
‡ *L. origanoides* phellandrene-rich chemotype large pellets, 4 mm

5.1.2. EtOH-modified scCO$_2$ mixture properties The physical properties of the EtOH-modified scCO$_2$ mixture were calculated as described in subsection 2.6.2. Their estimated values for the extraction conditions of 340 bar, 50 °C, 11 wt % E and 3.3×10^{-4} kg_{solv}/s, were: $U = 1.2$ mm s^{-1}, $\rho_{\mathrm{m}} = 843$ g cm^{-3} and $\mu_{\mathrm{m}} = 1.03 \times 10^{-4}$ Pa s. The physical parameters of binary diffusion (D_{m2})were 1.64×10^{-9} m^2 s^{-1} for $C_{28}H_{58}$

and $3.18 \times 10^{-9}\,\mathrm{m^2\,s^{-1}}$ for Pn. These values were used to model the IEC of: chopped material from post-distillation *Lippia* spp., central points of the 2^2 design of *L. origanoides* phellandrene-rich chemotype and the pelletized substrates of *L. origanoides* phellandrene-rich chemotype. Values at extraction conditions with different P and T, for the experimental factorial design, are shown in Table 23.

5.2. Experimental integral extraction curves

5.2.1. Uncertainty and preliminary extractions Preliminary experiments for *L. origanoides* carvacrol-rich chemotype carried out at the extraction conditions of 340 bar, 50 °C, 11 wt % E and $3.3 \times 10^{-4}\,\mathrm{kg_{solv}/s}$, showed an average-RSD to e_{CW} of 12 % and to e_{Pn} of 7.6 % for IEC points. These values were considered acceptable for the extraction of botanical material. The experiments were carried out with the same methodology for the rest of the curves of the study. Fig. 25 shows the preliminary IEC with the error bars corresponding to the standard deviation for each point of the curve. The highest confidence intervals found with the t-student test were $\pm 5.9\,\mathrm{g_{CW}/kg_{subs}}$ and $\pm 0.7\,\mathrm{g_{Pn}/kg_{subs}}$ for e_{CW} and e_{Pn} respectively, the lowest interval values were $\pm 3.8\,\mathrm{g_{CW}/kg_{subs}}$ and $\pm 0.2\,\mathrm{g_{Pn}/kg_{subs}}$ for e_{CW} and e_{Pn} respectively.

5.2.2. Experiments with post-distillation substrates of *L. origanoides* chemotypes and *L. graveolens* *L. origanoides* carvacrol-rich (LOC) and phellandrene-rich (LOP) chemotypes were the substrates with the highest yield in the extraction of CW at $q = 260\,\mathrm{kg_{solv}/kg_{subs}}$ (*cf.* Table 22), followed by the thymol-rich chemotype (LOT) and, *L. graveolens* (LG). The decreasing order of substrates yields found in this section is the same found for exhaustive Soxhlet extraction and the simplex optimization results used in the previous study of the substrates valorization, *cf.* subsection 3.7. LOC and LOP contained the highest amount of CW available in the matrix (*i.e.*, 195 and $192\,\mathrm{g\,kg^{-1}}$ respectively), and the sc-extraction recovered more CW from them. The yields were

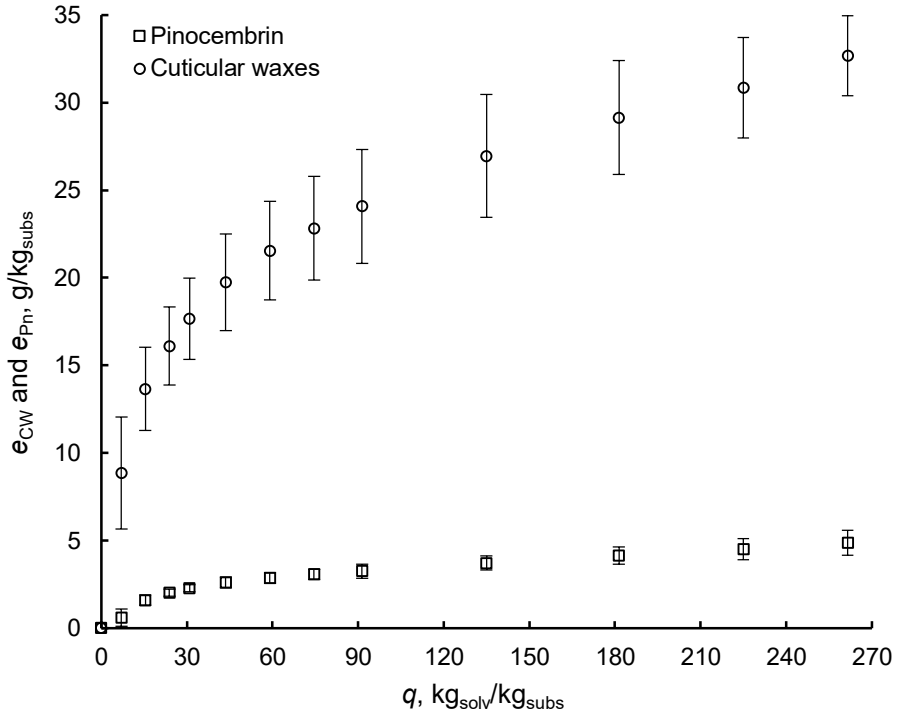

Figura 25. Preliminary integral extraction curve with standard deviation intervals for EtOH-modified scCO$_2$ extraction of *L. origanoides* carvacrol-rich chemotype

as high as those found at $q = 20\,\text{kg}_{\text{solv}}/\text{kg}_{\text{subs}}$ in the study of the substrates valorization of Chapter 3, because the values for flow and surface velocity of the solvent were increased in this section. Therefore, the residence time (t_r) of the solvent in the extractor decreased, and the external mass transfer resistance (Θ_e) increased because t_r is indirectly proportional to Θ_e [107].

LOP was the substrate with highest yield in the extraction of Pn. The extraction yields for LOC and LOT were very similar to each other and slightly lower than that for LOP. LG was the substrate with the lowest yield for pinocembrin extraction, with a considerably lower recovery than that achieved for *L. origanoides* chemotypes. There is no apparent methodological reason that explains the discrepancy in the yields for LO and LG. In fact, similar values were expected between substrates since *L. graveolens* is considered a synonym for *L. origanoides* according to phylogenetic studies

[171]. The variation in the composition of the extraction products obtained at the same extraction conditions from the same plants has also been observed in the extraction of essential oils, where the variation in their compositions is explained by the cycle of the vegetative harvest, the conditions of agricultural growth and the post-harvest treatment, among other causes [68][69]. LOP and LOT are the substrates for which greater selectivity was obtained in sc-extraction towards Pn. On the other hand, LG and LOT are the substrates for which the sc-extraction achieved greater selectivity towards Pn compared to the Soxhlet extraction. These facts led us to assert that, despite being the same plant, each substrate interacts differently with the same extractive solvent, possibly because the composition and concentration of the constituents of the extract in the matrix are different as shown in the identification and quantification of flavonoids present in the substrates (*cf.* Table 12). If solutes interact differently with each substrate, it would also be convenient to study in detail the phase equilibria and seasonal variations in the composition of the constituents of the LOC, LOT and LG extract before delving into the planning of the industrial operation.

Table 22. Yields and selectivity of Soxhlet and sc-extraction from post-distillation substrates of *L. graveolens* and chemotypes of *L. origanoides*

Substrate	e_{Pn}, g_{Pn}/kg_{subs}	e_{CW}, g_{CW}/kg_{subs}	Selectivity to Pn, $(e_{\mathrm{Pn}}/e_{\mathrm{CW}})$	
			Sc-extraction	Soxhleth extraction
LOC	5.3	35.0	0.15	0.12
LOP	6.6	33.7	0.20	0.16
LOT	5.1	26.3	0.19	0.09
LG	1.8	11.8	0.15	0.07

[171] Nataly O'Leary *y col.* «Species delimitation in *Lippia* section *Goniostachyum* (Verbenaceae) using the phylogenetic species concept». En: *Botanical Journal of the Linnean Society* 170.2 (sep. de 2012), págs. 197-219. DOI: 10.1111/j.1095-8339.2012.01291.x.

5.2.3. Experimental design Table 23 shows experimental design results. Yields reported were those reached at $240\,\mathrm{kg_{solv}/kg_{subs}}$ in the extraction curves. ANOVA for e_{CW} showed that effects of P (-4.43, *p*-value $= 0.22$), T (10.61, *p*-value $= 0.053$) and PT (-1.42, *p*-value $= 0.63$) were not significant (*p*-value ≤ 0.05) in the sc-extraction of *L. origanoides* phellandrene-rich chemotype. ANOVA for e_{Pn}, on the contrary, showed significant effect for T (2.46, *p*-value$= 0.03$) but not for P (-0.014, *p*-value$= 0.98$) and PT (-0.89, *p*-value$= 0.16$) in the sc-extraction of pinocembrin from *L. origanoides* phellandrene-rich chemotype. Contrary to the results of the ANOVA for *L. origanoides* thymol-rich chemotype (*cf.* Table 6), the temperature in this case was the only variable that had significance in the extraction yield, although only for e_{Pn} as response variable. This confirms the hypothesis exposed in subsection 3.3 where the lack of temperature significance was explained because the pressure range chosen in the fractional factorial design in Table 3 was wide. The recovery of pinocembrin increased by $5\ \%$ when the extraction was performed at 460 bar and by $11\ \%$ when the extraction was performed at 220 bar, as a result of an increase of 20 ℃ in the temperature. That behavior is typical of processes that take place above the crossover pressure and are controlled by solubility. The crossover pressures for natural compounds are above the critical pressure (73 bar) of CO_2 but usually below 200 bar, particularly in the case of some flavonoids such as naringenin **??**, quercetin [153], ca-

techin [172], epicatechin [173], ascorbic acid [174] and pigments like beta carotene [104175], among others. Initially in the IEC (for short extraction times) the process depends on the solubility of the constituents in the sc-solvent and the external mass transfer from substrate to the sc-solvent. In the end (at higher extraction times) the recovery no longer depends on the solubility but on the internal mass transfer in the substrate and the partition of the pinocembrin between the sc-solvent and the post-distillation substrate. The mass transfer parameters improve by decreasing the diameter of the particles, increasing the surface velocity of the sc-solvent, increasing the temperature or decreasing the pressure, which is consistent with our observations.

Depending on extraction conditions pinocembrin yield varied from 3.5 to $7.0\,g_{Pn}/kg_{subs}$ (recoveries from 11 to $23\,\%$ based on the $\mathtt{Pn}$ content obtained by Soxhlet extraction, *cf.* Table 11). This is a lower range of values than that obtained with hydroalcoholic extraction for the same plant according to the results of Long-Ze *y col.*, «Identification and quantification of flavonoids of Mexican oregano (*Lippia graveolens*) by LC-DAD-ESI/MS analysis», for *L. graveolens* (0.5 to $9.16\,g_{Pn}/kg_{subs}$) and of Stashenko *y col.*, «Chromatographic and mass spectrometric characterization of essential oils and extracts from *Lippia* (Verbenaceae) aromatic plants», for *L. origanoides* (0.05 to

---

[172] Felycia Edi Soetaredjo *y col.* «Catechin sublimation pressure and solubility in supercritical carbon dioxide». En: *Fluid Phase Equilibria* 358 (nov. de 2013), págs. 220-225. DOI: 10.1016/J.FLUID.2013.08.012.

[173] Felycia Edi Soetaredjo, Suryadi Ismadji y Yi-Hsu Ju. «Measurement and modeling of epicatechin solubility in supercritical carbon dioxide fluid». En: *Fluid Phase Equilibria* 340 (feb. de 2013), págs. 7-10. DOI: 10.1016/J.FLUID.2012.12.005.

[174] Tzu-Chi Wang y Po-Chao Chang. «Measurement and Correlation for the Solid Solubility of Antioxidants Sodium l-Ascorbate and Sodium Erythorbate Monohydrate in Supercritical Carbon Dioxide». En: *Journal of Chemical & Engineering Data* 60.3 (mar. de 2015), págs. 790-794. DOI: 10.1021/je5009153.

[175] A.J. Jay, D.C. Steytler y M. Knights. «Spectrophotometric studies of food colors in near-critical carbon dioxide». En: *The Journal of Supercritical Fluids* 4.2 (jun. de 1991), págs. 131-141. DOI: 10.1016/0896-8446(91)90042-5.

Table 23. Experimental results of EtOH-modified $scCO_2$ extraction of post-distillation *L. origanoides* phellandrene-rich chemotype ($U = 1\,\mathrm{mm\,s^{-1}}$, $E = 3\,\mathrm{wt}\,\%$ EtOH, $q = 240\,\mathrm{kg_{solv}/kg_{subs}}$).

Exp	P, bar	T, ℃	ρ_{m}, $\mathrm{g\,cm^{-3}}$	$\mu_{\mathrm{m}} \times 10^5$, Pa s	$k_{\mathrm{f}} \times 10^5$, $\mathrm{m\,s^{-1}}$	$D_{\mathrm{m2}} \times 10^9$ for $C_{28}H_{58}$, $\mathrm{m^2\,s^{-1}}$	e_{CW}, $\mathrm{g_{CW}/kg_{subs}}$	e_{Pn}, $\mathrm{g_{Pn}/kg_{subs}}$	Selectivity to Pn, $(e_{\mathrm{Pn}}/e_{\mathrm{CW}})$
1	220	40	819	9.98	2.23	1.59	21.2	3.5	0.17
2	220	60	737	8.05	3.06	1.92	33.2	6.9	0.21
3	460	40	914	11.9	1.96	1.58	18.2	4.4	0.24
4	460	60	861	10.2	2.51	1.86	27.3	6.0	0.22
5	340	50	843	10.3	2.24	1.64	35.5	6.2	0.17
6	340	50	843	10.3	2.24	1.64	33.2	6.5	0.20
7	340	50	843	10.3	2.24	1.64	30.9	7.0	0.23

$30\,\mathrm{g_{Pn}/kg_{subs}}$). Increasing the flow rate in the sc-extraction can still improve the percentages of pinocembrin recovery; however, it is not technically feasible to achieve the yield values of the hydro-alcoholic extraction given the nature of the CO_2-EtOH mixture purchased with the mixture of H_2O-EtOH. The results of the extraction showed a considerable amount of pinocembrin that the sc-extraction leaves retained in the substrates. Therefore, in the planning of the extraction process, solid-liquid extraction should be considered as more convenient than sc-extraction, since the recovery rates of the substances of interest are higher. The process selectivity, which cannot be exploited during extraction, can be exploited by adding a fractional separation stage to the process, where the different solubility values and concentration levels of molecules in the sc-solution are used to concentrate the fractions in families of compounds [62].

5.2.4. Particle size experiments The sc-extractions yields reached $110\,\mathrm{kg_{solv}/kg_{subs}}$ assuming a constant standard deviation ($s = 0.4$ for e_{Pn} and $s = 2.4$ for e_{CW}) for particle size treatments as shown in Table 24. One-way ANOVA showed that there is a significant differences between treatments of particle sizes for e_{Pn} (p-value $= 0.0006$) and e_{CW} ($p - \mathrm{value} = 0.007$). Two methods of multiple comparisons were applied to identify difference between treatments: Fisher's Least Significant Difference (LSD)

method and Tukey's Honest Significant Difference (HSD) test with a confidence level of 95 %. Intervals calculated by LSD and Tukey HDS for sc-extraction yields showed that all treatments were different from each other when e_{Pn} was the response. When e_{CW} was the response, both methods showed differences between CM and the other two treatments, *i.e.*, SP and LP. Fig. 26 shows the means and LSD intervals for 95 % confidence of flavonoids and cuticular waxes extraction yields with the different substrate treatments.

Table 24. Experimental results for Soxhlet and sc-extraction of chopped and pelletized *L. origanoides* phellandrene-rich chemotype ($U = 1\,\mathrm{mm\,s^{-1}}$, $E = 3\,\mathrm{wt\,\%}$ EtOH, $q = 110\,\mathrm{kg_{solv}/kg_{subs}}$).

Substrate	Sc-extraction, $\bar{x} \pm t_{(0.05,2)} s/\sqrt{n}$		Soxhlet extraction	
	e_{Pn}, $\mathrm{g_{Pn}/kg_{subs}}$	e_{CW}, $\mathrm{g_{CW}/kg_{subs}}$	e_{Pn}, $\mathrm{g_{Pn}/kg_{subs}}$	e_{CW}, $\mathrm{g_{CW}/kg_{subs}}$
CM of LOP	5.4 ± 1.1	27 ± 6	31	192
SP	2.5 ± 1.1	18 ± 6	17	140
LP	3.7 ± 1.1	19 ± 6	22	169

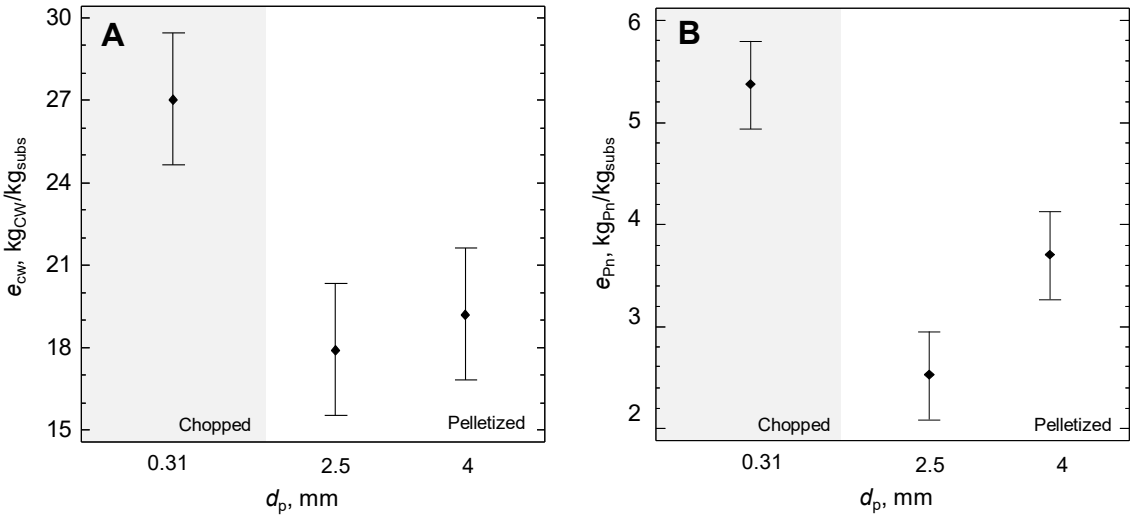

Figura 26. Confidence intervals of the LSD method for substrate treatments. (A) cuticular waxes extraction yield, (B) flavonoids extraction.

Apparently, pelletizing decreases the extraction yield of flavonoids and cuticular waxes. However, despite the lower extraction rates and yields of pellets compared to CM, it is possible that an optimized pelletizing treatment has the potential to improve the extraction. This was commented by Sielfeld, del Valle y Sastre, 2019, in their study of antioxidant extraction from pelletized rosemary in which the same results were obtained. We also consider that the pretreatment applied to the LOP did not develop optimally, since there are indications that the operating temperature when the pellets were forming exceeded the heat resistance of oleoresin components. This was visually observed during the pellet formation process and was subsequently confirmed with the values found for the Soxhlet extraction yield and the M_{d} of the substrates, which were considerably lower compared to the values found for the control substrate, *i.e.*, CM of LOP. (*cf.* Table 24 and 21). For SP, the substrate subjected to the greatest shear and compaction stresses, the yields were even lower than those found for LP.

The internal structure determining mass transfer within the pellet is the result of the destruction induced by shear stresses to cell walls and other barriers in plant tissues for mass transfer [176], and substrate compaction [177]. The destruction of internal mass transfer barriers affects extraction rates positively because solutes are released from cells, but compaction affects them negatively by decreasing the internal porosity of the solid substrate [177][178]. The extraction yield worsening with pellets compared to

---

[176] José M. del Valle *y col.* «Microstructural effects on internal mass transfer of lipids in prepressed and flaked vegetable substrates». En: *The Journal of Supercritical Fluids* 37.2 (abr. de 2006), págs. 178-190. DOI: 10.1016/J.SUPFLU.2005.09.002.

[177] Jose M. del Valle y Jose M. Aguilera. «Effects of Substrate Densification and CO2 Conditions on Supercritical Extraction of Mushroom Oleoresins». En: *Journal of Food Science* 54.1 (ene. de 1989), págs. 135-141. DOI: 10.1111/j.1365-2621.1989.tb08586.x.

[178] Edgar Uquiche, José M. del Valle y Mónica Ihl. «Microstructure-Extractability Relationships in the Extraction of Prepelletized Jalapeño Peppers with Supercritical Carbon Dioxide». En: *Journal of Food Science* 70.6 (mayo de 2006), e379-e386. DOI: 10.1111/j.1365-2621.2005.tb11442.x.

the chopped control material can be attributed almost exclusively to the increase in particle size. When the particle size increases, the specific surface area decreases, which negatively affects the exchange of mass between the solid and fluid phases; $scCO_2$ has to "travel a longer way"to reach and dissolve solute within the particle, and return to the surface of the particle [179]. In contrast of mass yield results, pelletizing the substrate increased the volumetric yield of cuticular waxes, from $9.2\,\mathrm{kg_{CW}/m^3_{subs}}$ for CM of `LOP` to $13.8\,\mathrm{kg_{CW}/m^3_{subs}}$ for `SP` and $14.2\,\mathrm{kg_{CW}/m^3_{subs}}$ for `LP`. That represents *ca.* $52\,\%$ increase in yield, which is especially convenient when the volume of the extractor vessel is a limitation of the productive capacity.

5.3. Mathematical modeling and simulation of EtOH-modified $scCO_2$ extractions

5.3.1. Extraction of chopped post-distillation *Lippia* spp. residues Fig. 27 shows experimental data and modeled curves for post-distillation *Lippia* spp. The four curves were fitted simultaneously to the BIC model of Sovová, «Mathematical model for supercritical fluid extraction of natural products and extraction curve evaluation» (*cf.* Eqs. 14). The shape of these extraction curves suggested a type-D equilibrium partition as expected for low initial solute contents. As was shown in the previous chapter (*cf.* Chapter 4), the post-distillation substrate does not have enough solute to saturate the solvent in the initial stage of extraction. Before fitting the structural and equilibrium parameters of the Sovová complete model, we estimated the values of the parameters using the approximate model proposed by the same author to obtain values close to the real ones and used them as seeds of the numerical method to solve the system of differential equations. We fixed x_{u} at values of Table 21 and k_{f}

[179] Caroline Sielfeld, José M. del Valle y Federico Sastre. «Effect of pelletization on supercritical CO2 extraction of rosemary antioxidants». En: *The Journal of Supercritical Fluids* 147 (mayo de 2019), págs. 162-171. DOI: 10.1016/J.SUPFLU.2016.04.010.

at estimated values of Table 25 to obtain seeds for K, r, F_{e}. The seed for number of mixers (n, flow pattern) was calculated according to the degree of axial dispersion in the extraction bed. We estimated the axial dispersion coefficient (D_{ax}) using Eq. 31 described by José M. del Valle *y col.* «Mass Transfer and Equilibrium Parameters on High-Pressure CO2 Extraction of Plant Essential Oils». En: *Food Engineering Series*. Springer, 2011, págs. 393-470. DOI: 10.1007/978-1-4419-7475-4_17, depending on the dimensionless number of Peclet for the particle (Pe_{P}, Eq 32) and for the packed bed (Pe_{L}, Eq 33) to decide between the plug flow and the ideal mixture flow pattern.

$$\frac{D_{\mathrm{ax}}}{D_{1\mathrm{m}}} = \frac{0.53 Pe_{\mathrm{P}}^2}{1 + 42.8 \frac{Pe_{\mathrm{P}}}{(L/d_{\mathrm{p}})}} \tag{31}$$

$$Pe_{\mathrm{P}} = ReSc = \frac{U d_{\mathrm{p}}}{D_{12}} \tag{32}$$

$$Pe_{\mathrm{L}} = \frac{UL}{D_{\mathrm{ax}} \epsilon} \tag{33}$$

Where L is the height of the extraction vessel, U is the superficial velocity of the solvent, and d_{p} is the diameter of a sphere with the same surface-to-volume ratio of the particle. The axial dispersion in the extraction vessel can be neglected if the Pe_{L} is above 100 [180]. This was the case in our experiments (Pe_{L} ranged from 109 to 125). Consequently, we fixed the scCO$_2$ extraction curves with high n-value considering that $n = 10$ is enough to simulate plug flow (when there is no axial dispersion) for type-D curves [181][107].

---

[180] Motonobu Goto, Bhupesh C. Roy y Tsutomu Hirose. «Shrinking-core leaching model for supercritical-fluid extraction». En: *The Journal of Supercritical Fluids* 9.2 (1996), págs. 128 -133. DOI: https://doi.org/10.1016/S0896-8446(96)90009-1.

[181] E. Reverchon. «Mathematical Modeling of Supercritical Extraction of Sage Oil». En: *AIChE Journal* 42.6 (1996), págs. 1765-1771. DOI: 10.1002/aic.690420627.

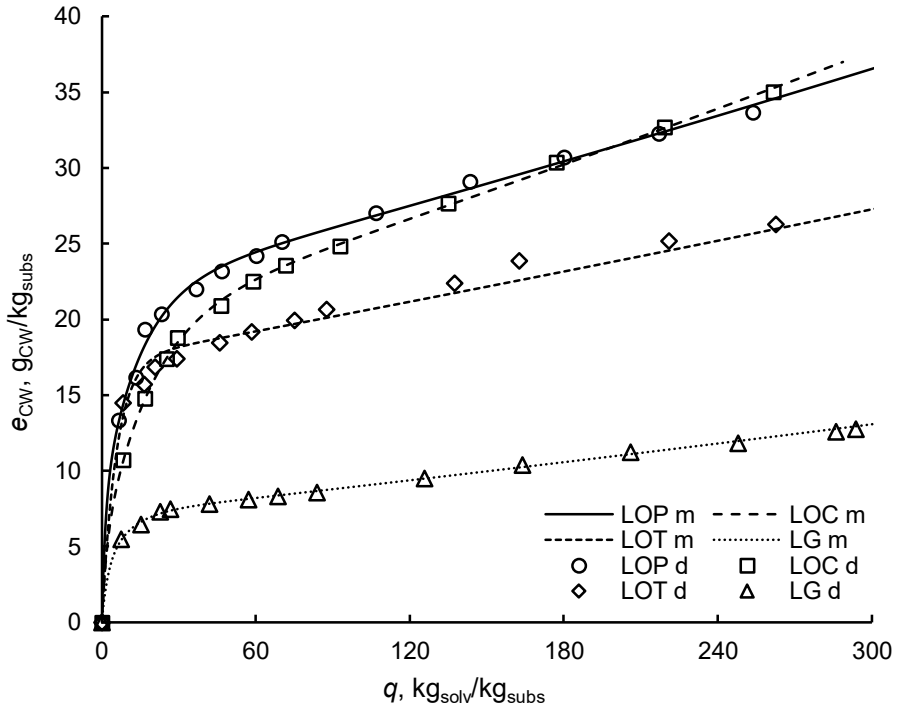

Figura 27. Integral extraction curves for post-distillation *Lippia* spp. d, experimental data; m, model prediction.

The next step was the simultaneous simulation of extraction curves using the complete model equations. First, setting n to a high value and k_{f} at the estimated value of Table 25, and subsequently including k_{f} and n as fit parameters. Table 25 summarizes values of model parameters, including best-fitting values of K, r and F_{e} and the goodness of fit for each extraction curve. Our extraction curves corresponded to the so-called equilibrium extraction curves whose value for the dimensionless external mass resistance coefficient (Θ_{e}) is less than 0.2 ($\Theta_{\mathrm{e}} = 0.015$). For this reason, we believe that the best-fitted parameters associated with equilibrium (*i.e.*, K and r) are very close to reality.

When k_{f} and n were included as fit parameters, the goodness of fit of the model improved considerably. k_{f} and n are parameters directly related to the solvent flow and its fit to unreal values (*cf.* estimated and best-fitted k_{f} parameter in Table 25)

shows a physical meaning different from that described by the Sovová model and which is compensated by affecting the terms related to the flow pattern. This led us to think that our simulation incorrectly describes the flow pattern possibly because in the experiments there was inhomogeneity of the flow due to channeling of the solvent in the bed or to the damage of the sintered frit that distributes the solvent in the cross section of the extractor. A consequence of these results is that from our work it is not possible to extract information concerning the flow pattern in the sc-extraction of *L. origanoides* studied. To obtain better estimates of these parameters, more experimental curves should be made by increasing the scale together with Θ_{e} and Γ values.

Table 25. BIC model parameters for extraction curves of post-distillation chemotypes of *Lippia* spp.

Parameter	LOC	LOT	LOP	LOG
Estimated parameters				
External mass transfer coefficient ($k_{\mathrm{f}} \times 10^5$, m s^{-1})	2.2	2.1	2.2	2.2
Axial dispersion coefficient ($D_{\mathrm{ax}} \times 10^6$, m^2 s^{-1})	2.2	2.1	2.2	2.2
Specific surface area per unit volume of extraction bed (a_0, m^{-1})	4807	5807	6274	4392
Best-fitted parameters				
Partition coefficient (K, $-$)	0.043	0.043	0.097	0.137
Grinding efficiency (r, $-$)	0.17	0.15	0.18	0.16
Microstructural factor, ($F_{\mathrm{e}} \times 10^7$, $-$)	5.9	3.4	9.1	16
External mass transfer coefficient, ($k_f \times 10^5$, s^{-1})	0.048	5.0	0.022	0.025
Goodness of fit				
Average absolute deviation (AAD, $\%$)	0.6	2.5	1.5	1.0
Determination coefficient (R^2, $-$)	0.9996	0.988	0.997	0.999

5.3.2. Experimental design with *L. origanoides* phellandrene-rich chemotype

Fig. 28 shows experimental data and modeled curves for post-distillation *L. origanoides* phellandrene rich chemotype at the pressures and temperatures of the experimental design. The five curves were fitted simultaneously to the BIC model of Sovová [107], Eqs. 14, keeping constant structural parameters r and F_{e} for all curves. Table 26 summarizes values of model parameters, including best-fitting values of K

and k_f for each experiment.

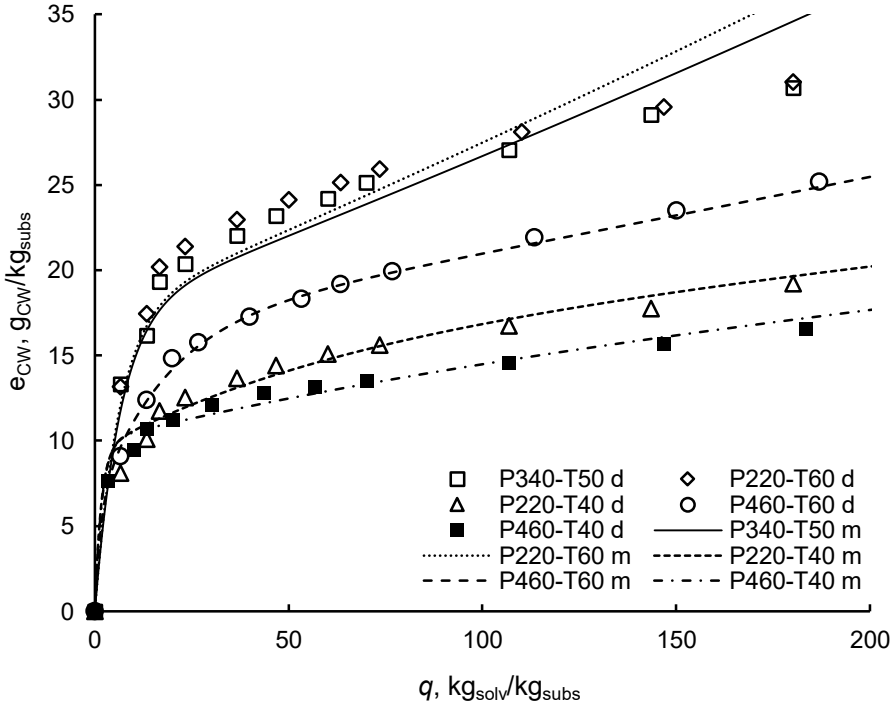

Figura 28. Integral extraction curves for post-distillation *L. origanoides* phellandrene rich chemotype. d, experimental data; m, model prediction.

The results of this simultaneous modeling show best-fitted values for structural parameters (*i.e.* r and F_{e}) different from those previously estimated and shown in the Table 25 (*cf.* `LOP` synonymous with `P340-T50` in Table 26). The difference between both estimations is that, for experimental design curves, the parameters were kept constant for all curves. The parameter r decreased four percent and F_{e}, despite maintaining the same order of magnitude, also decreased by almost half. This indicates that the effective diffusivity of extract in the plant matrix is even lower than estimated in the previous section and than binary diffusion coefficient in high-pressure EtOH-modified CO_2. The simultaneous adjustment of the experimental design curves also showed different values for K and k_{f} for the curve comparable with `LOP` in Table 25. K decreased but k_{f} increased at the same order of magnitude of estimated values in

Table 26. BIC model parameters for experimental design extraction curves of post-distillation *L. origanoides* phellandrene-rich chemotype. P, pressure (bar); T, temperature (°C). Best-fitted $r = 0.14$. Best-fitted $F_{\mathrm{e}} = 5.3 \times 10^{-7}$

Parameter	P340-T50	P220-T60	P220-T40	P460-T60	P460-T40
Estimated parameters					
External mass transfer coefficient ($k_{\mathrm{f}} \times 10^5$, m s^{-1})	2.2	3.1	2.2	2.5	2.0
Axial dispersion coefficient ($D_{\mathrm{ax}} \times 10^6$, m^2 s^{-1})	2.2	2.7	2.3	2.2	2.0
Best-fitted parameters					
Partition coefficient (K, $-$)	0.030	0.031	0.105	0.067	0.102
External mass transfer coefficient, ($k_f \times 10^5$, s^{-1})	5.0	6.3	0.003	0.02	0.0013
Goodness of fit					
Average absolute deviation (AAD, %)	5.9	7.2	5.1	2.1	3.7
Determination coefficient (R^2, $-$)	0.93	0.92	0.98	0.997	0.99

Table 26, which we assume are closer to reality. For the P220-T60 curve, it was also found that the fit led to a k_{f}-value closer to the estimated one, however, as for the P340-T50 curve, the simulation had a lower goodness of fit. The shape of these two curves suggests that the model is not representing well the stage controlled by the internal mass transfer, which it does well for the rest of the curves, but moving the k_{f}-values away from reality. As in the previous section, it is not possible to conclude about the flow pattern of the experiments, since when the fitted k_{f}-values are close to those estimated, the prediction of the stage controlled by k_{s} decreases considerably. Besides, low capacity of the models to fit data in the last zone of the extraction curve is possibly due to swelling of agglomerates in the bed depending on the extraction conditions in cases where there is some dissolved ethanol in the sc-phase [182].

5.3.3. Extraction of chopped and extruded material Fig. 29 shows experimental data and modeled curves for pellets of post-distillation *L. origanoides* phellandrene-rich chemotype at 340 bar, 50 °C and 11 wt %. The three curves were fitted simulta-

[182] Tarek Fahmy *y col.* «Modifier effects in the supercritical fluid extraction of solutes from clay, soil, and plant materials». En: *Analytical Chemistry* 65.10 (mayo de 2002), págs. 1462-1469. DOI: 10.1021/ac00058a026.

neously to the BIC model of Sovová [107], Eqs. 14, keeping constant r for SP and LP. Table 27 summarizes values of model parameters, including best-fitting values of K, F_{e} and k_{f} for pellets of *L. origanoides* phellandrene-rich chemotype.

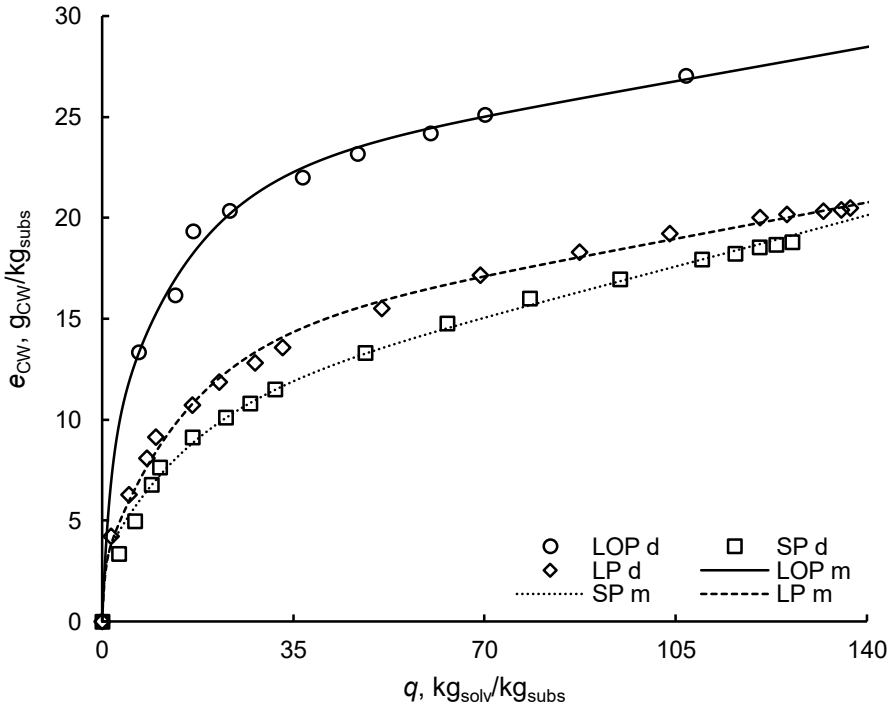

Figura 29. Integral extraction curves for pellets of post-distillation *L. origanoides* phellandrene-rich chemotype. d, experimental data; m, model prediction.

Parameter K had similar values for all extractions curves (*cf.* Table 27). The resulting F_{e} value indicates that the inner microstructure of *L. origanoides* pellets resulted in an effective diffusivity about 3 orders of magnitude higher than the binary diffusion coefficient. On the other hand, the resulting F_{e} value for LOP is two orders of magnitude lower than for pellets (*cf.* Table 27), thus suggesting that pelletization improves the inner mass transfer coefficients. Finally, the values of r were approximately the same for LOP and pellets considering results of previous section. Since the microstructural factor increased due to pelletization, then, we can assume that the effect of cell disruption exceeded that of compaction as found by Sielfeld, del Valle y Sastre,

«Effect of pelletization on supercritical CO2 extraction of rosemary antioxidants», in their study already commented above.

Table 27. BIC model parameters for extraction curves of pellets of post-distillation *L. origanoides* phellandrene-rich chemotype

Parameter	SP, 2.5 mm	LP, 4 mm	LOP
Estimated parameters			
External mass transfer coefficient, ($k_f \times 10^5$, s^{-1}	1.5	1.3	2.2
Axial dispersion coefficient ($D_{ax} \times 10^6$, $m^2\,s^{-1}$)	2.3	2.1	2.2
Specific surface area per unit volume of extraction bed (a_0, m^{-1})	1193	692	6274
Best-fitted parameters			
Partition coefficient (K, $-$)	0.11	0.08	0.10
Grinding efficiency, (r, $-$)	0.14	0.14	0.18
Microstructural factor, ($F_e \times 10^7$, $-$)	830	830	9.1
External mass transfer coefficient, ($k_f \times 10^5$, s^{-1})	0.058	0.16	0.022
Goodness of fit			
Average absolute deviation (AAD, $\%$)	3.7	2.5	1.5
Determination coefficient (R^2, $-$)	0.996	0.997	0.997

5.4. Conclusions

The kinetics of EtOH-modified $scCO_2$ extraction of oleoresin from residues of *L. origanoides* distillation were studied partially. Through the study of the kinetic extraction of *L. origanoides* chemotypes, it was observed that the solutes retained in the matrix after the distillation process interact differently with the matrix when the extraction is carried out. This is because the initial contents and the families of molecules that constitute oleoresin are different among chemotypes. The chemotypes with the greatest potential for the extraction of pinocembrin from residues of *L. origanoides* are LOC and LOP. By modifying the extraction conditions of the best chemotype (*i.e.*, LOP), the EtOH-modified $scCO_2$ extraction only managed to extract up to $23\,wt\,\%$ of extractable oleoresin, a value easily surpassed by other industrial extractive processes. The comparative advantage of selectivity of EtOH-modified $scCO_2$ extraction can be better exploited in post-extraction fractionation to enrich oleoresin in pinocembrin.

Pelletizing increases the volumetric yield of the extraction and also improves the internal mass transfer of the broken cells near the walls of the pellet. However, the effect of compaction made mass transfer difficult in the pellet inner part. The kinetic parameters of the extraction related to equilibrium were found for the Sovová, «Mathematical model for supercritical fluid extraction of natural products and extraction curve evaluation» model. However, due to inhomogeneity in the flow during the experiments, the parameters related to the flow regime should be re-estimated from new experiments that conveniently also could change scale.

6. CONCLUSIONS AND PERSPECTIVES

6.1. From the process engineering point of view

The industry of culinary seasonings and essential oils (EOs) of the *Lippia origanoides* and *Lippia graveolens* phenylpropanoid-producing plants, used as raw materials for food, cosmetics, and medicines, can increase their profits by taking advantage of their by-products and improving the quality of their products. Achieving this implies delving into different areas of knowledge within which Chemical Engineering acts as an integrator to determine the technical and economic feasibility of the processes and their modifications. Simulation, optimization, and analysis of processes are, among others, the areas of Chemical Engineering that lead the generation of designs with which implementation of new stages in the industrial extractive process would materialize coherently. Authors sought with this work to contribute to the advancement of this industry by achieving, with a holistic approach, the integrated extraction and rectification process that leads to the full use of the substrates and generate quality products. The patent in the Appendix 5 is tangible proof as it could be considered as the seed of the complete conceptual design of the process.

Continuing with the advancement of the next step basic design, the authors studied two process units, *i.e.*, fractional distillation and supercritical (sc)-extraction. These added to steam distillation have the potential to integrate and improve the industry profits. Details and mathematical descriptions are topics of discussion in the Appendix 4 and the Chapters of this manuscript, respectively. Despite being the minority of the process units proposed in the conceptual design, it is an advance that will contribute to consolidating a plant design described *via* mathematical simulation as close to reality as possible. The studies and mathematical descriptions of the other operating units are necessary to complete the information that provides relevant de-

cision data on the technical feasibility of the integral use of *L. origanoides* and *L. graveolens*. In our research group, some colleagues are currently carrying out studies aimed at complementing the process units of steam distillation, fractionation, and solid-liquid extraction, to name a few works.

Regarding the post-distillation residues of *L. origanoides* and *L. graveolens*, this work is conclusive about their valorization potential. Results of the Soxhlet- and sc-extraction showed that these substrates contained higher amounts of cuticular waxes, flavonoids, and pinocembrin (Pn) in comparison with other residues in the EOs industry and even with plants identified as potential commercial sources of Pn such as seeds of *Alpinia katsumadai* or leaves of *Eucalyptus preissiana*. The residue of *L. origanoides* phellandrene-rich chemotype is the byproduct with the highest industrial recovery potential followed by the thymol-rich, carvacrol-rich chemotypes and finally, *L graveolens*. The temperature of the steam distillation process did not significantly affect the availability of the compounds of interest in the substrate when comparing the extraction results with those published for the same substrates without distillation pretreatment. Therefore, it is convenient to add solid-fluid extraction stages after the steam distillation process since discarding the post-distillation residue loses the oleoresin benefits. Regarding sc-extraction, which was the unit extractive operation studied in-depth, in comparison with Soxhlet extraction it is more selective but leaves behind a considerable amount of solute retained in the substrate. This is a disadvantage compared to conventional solid-liquid extraction widely used for the same purposes. In the subsequent study of phase equilibria and kinetics extraction, it was explained and managed to increase selectivity towards flavonoids, but perhaps it was not enough to gain a place after substrate distillation. Probably the greatest benefit of sc-extraction is in a later stage fractionating the extract. We will have to wait for studies about solid-liquid extraction and fractionation of the extract to find out.

6.2. From the advances in extraction and quantification

Given the need to reduce the costs of sc-extraction and the opportunities for technological innovation that this technique allows, through interdisciplinary work, it was possible to reduce the experiment operating cost. The available extraction system *Thar Instruments* SFE-2000–2-FMC50 was modified to operate semi-batch and with CO_2 recirculation. Fractionation and recirculation stages (*cf.* Appendix 1) were added to the system. The extraction capacity was doubled in time and production cost was reduced from 26 to 11 USD/extraction.

A validated methodology with their figures of merit for instrumental multicomponent quantification of flavonoids in extracts was developed and applied to the measurement of sorption equilibria. This instrumental analysis methodology based on UV-Vis spectroscopy and chemometric methods (multivariate calibration using CLS and ILS models) avoided chromatographic separation and reduced solvent and time consumption in quantification of Pn and galangin (Gn) in extracts. RMSE of the higher accuracy ILS model (0.09 and 0.04 $\mu g\, g^{-1}$ for Pn and Gn respectively), built using training data sets and comparing results with those of HPLC-DAD, was of the same order of magnitude of error found for HPLC (0.01 and 0.02 $\mu g\, g^{-1}$ for Pn and Gn respectively) when the data that did not contain cuticular waxes (CW) from the extract was removed from the training data set. CW in sc-extracts are mainly composed of molecules that, although they do not absorb in the UV region, interfere with the sample spectral response. The precision obtained with the model thus arranged was considered acceptable to measure apparent or operative solubility in $scCO_2$. In addition to the quantification of flavonoids that absorb in the UV region, it is convenient to deepen the development of methodologies to quantify CW to obtain data that help to describe, as close to reality as possible, the complementary unit operations of the extractive process of EOs from botanical substrates. The same multivariate spectroscopic methodology developed in this work can be used to analyze Raman spectra or the

infrared region, with which there would already be a breakthrough.

6.3. From the supercritical-fluids state of the art

For the EtOH-modified scCO$_2$ extraction of *L. origanoides* and *L. graveolens* residues, the flow, pressure, time, and percent EtOH have a significant effect on the global- and flavonoid-extraction yield. The d_{p}-range that was obtained from two grids ($0.5\,\mathrm{mm}$ and $2\,\mathrm{mm}$ opening) used in the chopper is not significant in the extraction yield responses. Despite that the interval of temperatures chosen in the residues valorization study did not significantly affect the global- and flavonoid-extraction yields, in the study of phase equilibria, it was observed that the solubility of Pn in the ternary system scCO$_2$ + Pn + octacosane (Oct) is less sensitive to the increase in temperature than that of Oct. Therefore, the extract obtained from the extraction processes at temperatures close to the critical point contain less CWs, which improves the product. The best experimental conditions were found for each substrate under the specifications of the extraction system used. Best extraction conditions for *L. origanoides* pellandrene-rich chemotype residue (LOP), the substrate whose extract was the one with the highest yield, were $307\,\mathrm{bar}$, $5\ \%$ ethanol, $96\,\mathrm{mín}$ and $43\,\mathrm{g_{CO_2}/\,mín}$.
Pinocembrin solubility of the multi-component LOP extract-scCO$_2$ system was measured and modeled through a robust thermodynamic framework that group CWs in a pseudo-component represented by the thermodynamic properties of Oct. Sorption isotherm/isobar curves were measured and modeled for global extract using the thermodynamic solubility of Oct as saturation concentration parameter of the del-Valle Urrego sorption model (dVU). The prediction of solubility for Oct oversizes the solubility measured from the sorption curves, so a longer chain linear hydrocarbon would be more convenient for the modeling thus proposed. We describe the sorption equilibria of minority compounds such Pn and Gn from the equilibrium parameters of the dVU for CWs through a new proposed parameter called partition coefficients

of minority compounds in the extract ($K_{s|i}$). The strong interaction of the solute with the matrix, in addition to avoiding saturation of the solvent at the early stages of sc-extraction, was responsible for the increase in selectivity towards flavonoids with pressure.

Through the study of the extraction kinetics of *L. origanoides* chemotypes residues, it was observed that the solutes retained in the matrix after the distillation process interact differently with the matrix when the extraction is carried out. By modifying the extraction conditions of the best chemotype (*i.e.*, `LOP`), the EtOH-modified $scCO_2$ extraction only managed to extract up to $23\,\mathrm{wt}\,\%$ of extractable oleoresin, a value easily surpassed by other industrial extractive processes. The comparative advantage of selectivity of EtOH-modified $scCO_2$ extraction can be better exploited in post-extraction fractionation to enrich oleoresin in `Pn`. Pelletizing increases the volumetric yield of the extraction and also improves the internal mass transfer of the broken cells near the walls of the pellet. However, the effect of compaction made mass transfer difficult in the pellet inner part. The kinetic parameters of the extraction related to equilibrium were found for the Sovová, «Mathematical model for supercritical fluid extraction of natural products and extraction curve evaluation» model. However, due to inhomogeneity in the flow during the experiments, the parameters related to the flow regime should be re-estimated from new experiments that conveniently also could change scale.

6.4. From the academic training

The author assumes that the doctoral training objective that he sought to achieve when developing this work was fulfilled and presents for consideration of the evaluators the following academic products as evidence:

International patents

- WO2018069778 entitled “System for recirculating supercritical carbon dioxide, which uses an integrated device for liquefying and storing the fluid”
- WO2018122654 entitled “Method for making full use of *Lippia origanoides*”

Scientific articles published

- Optimization of flavonoids extraction from *Lippia graveolens* and *Lippia origanoides* chemotypes with ethanol-modified supercritical CO_2 after steam distillation. (2020). in “Industrial Crops and Products”, 146, 112170.
- Dynamic modeling and experimental validation of essential oils fractionation: Application for the production of phenylpropanoids. (2020). in “Computers and Chemical Engineering”, 135, 106738.

Manuscripts under review by co-authors

- Multicomponent solubility and equilibrium partition of *Lippia origanoides* solid distillation residues and its supercritical extract in presence of CO_2 and EtOH. It will be submited to “Journal of Supercritical Fluids”.
- Supercritical fluid extraction of agroindustrial *Lippia origanoides* residues: effect of chemotypes, extraction conditions and pelletization in two approach for modeling multicomponent mass transfer kinetics. It will be submited to “Journal of Supercritical Fluids”.

Manuscript in preparation

- Metodología validada para la medición instrumental multicomponente de flavonoides en extractos de plantas con sus respectivas figuras de mérito.

BIBLIOGRAPHY

Abrahamsson, Victor, Firas Jumaah y Charlotta Turner. «Continuous multicomponent quantification during supercritical fluid extraction applied to microalgae using in-line UV/Vis absorption spectroscopy and on-line evaporative light scattering detection». En: *The Journal of Supercritical Fluids* 131 (ene. de 2018), págs. 157-165. DOI: 10.1016/J.SUPFLU.2017.09.014 (vid. págs. 49, 51, 76, 79, 134).

Acosta Arriola, Violeta. «Variación en la composición química del aceite esencial de *Lippia graveolens*, en poblaciones silvestres de Yucatán, y su relación con factores edafoclimáticos». Tesis doct. Centro de Investigación científica de Yucatán, 2013, pág. 77 (vid. pág. 26).

Alcalá-Orozco, Maria *y col.* «Actividad repelente de los aceites esenciales de *Elettaria cardamomum*, *Salvia officinalis* y *Lippia origanoides* Carvacrol contra dos insectos plagas de productos almacenados». En: *2017*. 2017 (vid. pág. 36).

Allen, Terence. *Particle size measurement*. Chapman y Hall, 1981, pág. 678 (vid. pág. 88).

Araus, Karina A. *y col.* «Solubility of β-carotene in ethanol- and triolein-modified CO2». En: *The Journal of Chemical Thermodynamics* 43.12 (dic. de 2011), págs. 1991-2001 DOI: 10.1016/J.JCT.2011.07.013 (vid. págs. 70, 74, 79).

Barth, Howard G. *Modern methods of particle size analysis*. Wiley, 1984, pág. 309 (vid. pág. 88).

Batlle, Ramón *y col.* «On-line coupling of supercritical fluid extraction with high-performance liquid chromatography for the determination of explosives in vapour phases». En: *Journal of Chromatography A* 963.1-2 (jul. de 2002), págs. 73-82. DOI: 10.1016/S0021-9673(02)00136-X (vid. pág. 75).

Bautista, R D *y col.* «Simultaneous determination of diazepam and pyridoxine in synthetic mixtures and pharmaceutical formulations using graphical and multivariate calibration-prediction methods.» En: *Journal of pharmaceutical and biomedical analysis* 15.2 (1996), págs. 183-92. DOI: 10.1016/0731-7085(96)01844-4 (vid. págs. 66, 108).

Bautista, RD *y col.* «Multicomponent analysis : Comparison of various graphical and numerical methods». En: *Talanta* 40.11 (1993), págs. 1687-1694. DOI: 10.1016/0039-9140(93)80085-6 (vid. pág. 108).

Bejarano, Arturo, Pedro C Simões y José M Del Valle. «Fractionation technologies for liquid mixtures using dense carbon dioxide». En: *Journal of Supercritical Fluids* 107 (2016), págs. 321-348. DOI: 10.1016/j.supflu.2015.09.021 (vid. pág. 125).

Bianchi, Federica y Maria Careri. «Experimental Design Techniques for Optimization of Analytical Methods. Part I: Separation and Sample Preparation Techniques». En: *Current Analytical Chemistry* 4.1 (2008), págs. 55-74. DOI: 10.2174/157341108783339070 (vid. pág. 46).

Boethling, Robert S. y Donald Mackay. *Handbook of property estimation methods for environmental chemicals : environmental and health sciences*. Lewis Publishers, 2000, pág. 481 (vid. pág. 84).

Booksh, Karl S. y Ziyi Wang. «Extension and application of univariate figures of merit to multivariate calibration». En: *Handbook of Environmental Chemistry* 2 (1995), págs. 209-227. DOI: 10.1007/978-3-540-49148-4-7 (vid. pág. 130).

Braeuer, Andreas. *In situ Spectroscopic Techniques at High Pressure*. Ed. por Erdogan Kiran. 1.ª ed. Vol. 7. Amsterdam: Elsevier, 2015, págs. 1-394 (vid. pág. 51).

Brennecke, Joan F. y Charles A. Eckert. *Phase equilibria for supercritical fluid process design*. 1989. DOI: 10.1002/aic.690350902 (vid. págs. 52, 55).

Brogle, H. «CO2 in solvent extraction». En: *Chemistry and Industry* 19 (1982), págs. 385-390 (vid. págs. 26, 40).

Cabrera, Adolfo L. *y col.* «Measuring and validation for isothermal solubility data of solid 2-(3,4-Dimethoxyphenyl)-5,6,7,8-tetramethoxychromen-4-one (nobiletin) in supercritical carbon dioxide». En: *The Journal of Chemical Thermodynamics* 91 (dic. de 2015), págs. 378-383. DOI: 10.1016/J.JCT.2015.08.018 (vid. págs. 78, 119, 120).

Caude, Marcel y Didier Thiebaut. *Practical supercritical fluid chromatography and extraction*. Harwood Academic Publishers, 1999, pág. 442 (vid. pág. 44).

Chafer, Amparo *y col.* «Solubility of quercetin in supercritical CO2 + ethanol as a modifier: Measurements and thermodynamic modelling». En: *Journal of Supercritical Fluids* 32.1-3 (2004), págs. 89-96. DOI: 10.1016/j.supflu.2004.02.005 (vid. págs. 97, 153).

Chang, Chia-Chi *y col.* «Estimation of Total Flavonoid Content in Propolis by Two Complementary Colorimetric Methods». En: *Journal of Food and Drug Analysis* 10.3 (2002), págs. 178-182 (vid. pág. 48).

Chartier, Thierry *y col.* «Solubility, in Supercritical Carbon Dioxide, of Paraffin Waxes Used as Binders for Low-Pressure Injection Molding». En: *Industrial & Engineering Chemistry Research* 38.5 (mar. de 1999), págs. 1904-1910. DOI: 10.1021/ie980552e (vid. págs. 117, 143).

Cheng, Yang *y col. Pinocembrin is in preparation for treating the application in pulmonary fibrosis disease drug*. 2019 (vid. págs. 27, 37).

Chimowitz, E. H. y R. J. Pennisi. «Process Synthesis Concepts for Supercritical Gas Extraction in the Crossover Region». En: *AIChE journal* 32.10 (1986), págs. 1665-1676. DOI: 10.1002/aic.690321010 (vid. pág. 96).

Cid-Pérez, Teresa Soledad *y col. Mexican Oregano (Lippia berlandieri and Poliomintha longiflora) Oils*. Elsevier Inc., 2016, págs. 551-560. DOI: 10.1016/B978-0-12-416641-7.00063-8 (vid. pág. 38).

Cuadros-Rodríguez, Luis *y col.* «Principles of analytical calibration/quantification for the separation sciences». En: *Journal of Chromatography A* 1158.1-2 (jul. de 2007), págs. 33-46. DOI: 10.1016/J.CHROMA.2007.03.030 (vid. pág. 70).

D'Antuono, L. «Variability of Essential Oil Content and Composition of *Origanum vulgare* L. Populations from a North Mediterranean Area (Liguria Region, Northern Italy)». En: *Annals of Botany* 86.3 (2000), págs. 471-478. DOI: 10.1006/anbo.2000.1205 (vid. págs. 25, 34).

de Oliveira, Patricia Francisco *y col.* «Supercritical fluid extraction of hernandulcin from Lippia dulcis Trev.» En: *Journal of Supercritical Fluids* 63.December 2008 (2012), págs. 161-168. DOI: 10.1016/j.supflu.2011.12.003 (vid. pág. 94).

Dejaegher, Bieke e Yvan Vander Heyden. «Experimental designs and their recent advances in set-up, data interpretation, and analytical applications». En: *Journal of Pharmaceutical and Biomedical Analysis* 56.2 (2011), págs. 141-158 (vid. pág. 45).

Del Valle, J. M., M. Jiménez y J. C. De la Fuente. «Extraction kinetics of pre-pelletized jalapeño peppers with supercritical CO2». En: *Journal of Supercritical Fluids* 25.1 (2003), págs. 33-44. DOI: 10.1016/S0896-8446(02)00090-6 (vid. pág. 124).

del Valle, Jose M. y Jose M. Aguilera. «Effects of Substrate Densification and CO2 Conditions on Supercritical Extraction of Mushroom Oleoresins». En: *Journal of Food Science* 54.1 (ene. de 1989), págs. 135-141. DOI: 10.1111/j.1365-2621.1989.tb08586.x (vid. pág. 157).

del Valle, José M. y Juan C. de la Fuente. «Supercritical CO2 Extraction of Oilseeds: Review of Kinetic and Equilibrium Models». En: *Critical Reviews in Food Science and Nutrition* 46.2 (mar. de 2006), págs. 131-160. DOI: 10.1080/10408390500526514 (vid. págs. 56, 87, 154).

del Valle, José M. y Freddy a. Urrego. «Free solute content and solute-matrix interactions affect apparent solubility and apparent solute content in supercritical CO2 extractions. A hypothesis paper». En: *Journal of Supercritical Fluids* 66 (2012), págs. 157-175. DOI: 10.1016/j.supflu.2011.10.006 (vid. págs. 55, 56, 84, 85, 134, 137).

del Valle, José M. *y col.* «Mass Transfer and Equilibrium Parameters on High-Pressure CO2 Extraction of Plant Essential Oils». En: *Food Engineering Series*. Springer, 2011, págs. 393-470. DOI: 10.1007/978-1-4419-7475-4_17 (vid. pág. 159).

del Valle, José M. *y col.* «Microstructural effects on internal mass transfer of lipids in prepressed and flaked vegetable substrates». En: *The Journal of Supercritical Fluids* 37.2 (abr. de 2006), págs. 178-190. DOI: 10.1016/J.SUPFLU.2005.09.002 (vid. pág. 157).

Delegación SADER San Luis Potosí. *Crea INIFAP nueva tecnología para la producción de orégano resistente a fenómenos climáticos*. 2013 (vid. págs. 26, 40).

Díaz-Reinoso, Beatriz *y col.* «Supercritical CO2 extraction and purification of compounds with antioxidant activity». En: *Journal of Agricultural and Food Chemistry* 54.7 (2006), págs. 2441-2469. DOI: 10.1021/jf052858j (vid. págs. 29, 42).

Du, Guanhua *y col. Applications of pinocembrin in preparing anti-cerebral hemorrhage medicament*. 2018 (vid. págs. 27, 37).

Erlund, Iris. «Review of the flavonoids quercetin, hesperetin, and naringenin. Dietary sources, bioactivities, bioavailability, and epidemiology». En: *Nutrition Research* 24.10 (2004), págs. 851-874. DOI: 10.1016/j.nutres.2004.07.005 (vid. pág. 36).

Fahmy, Tarek *y col.* «Modifier effects in the supercritical fluid extraction of solutes from clay, soil, and plant materials». En: *Analytical Chemistry* 65.10 (mayo de 2002), págs. 1462-1469. DOI: 10.1021/ac00058a026 (vid. pág. 163).

Fiori, Luca. «Supercritical extraction of grape seed oil at industrial-scale: Plant and process design, modeling, economic feasibility». En: *Chemical Engineering and Processing: Process Intensification* 49.8 (2010), págs. 866-872. DOI: 10.1016/J.CEP.2010.06.001 (vid. pág. 42).

Fuentes, J. L. *y col.* «The SOS Chromotest applied for screening plant antigenotoxic agents against ultraviolet radiation». En: *Photochem. Photobiol. Sci.* 16 (9 2017), págs. 1424-1434. DOI: 10.1039/C7PP00024C (vid. pág. 35).

Ganzera, Markus. «Supercritical fluid chromatography for the separation of isoflavones». En: *Journal of Pharmaceutical and Biomedical Analysis* 107 (mar. de 2015), págs. 364-369. DOI: 10.1016/J.JPBA.2015.01.013 (vid. págs. 29, 42, 110).

García-Bores, A.M. *y col.* « *Lippia graveolens* photochemopreventive effect against UVB radiation-induced skin carcinogenesis». En: *Journal of Photochemistry & Photobiology, B: Biology* 167 (2017), págs. 72-81. DOI: 10.1016/j.jphotobiol.2016.12.014 (vid. pág. 38).

Gaspar, Filipe. «Extraction of Essential Oils and Cuticular Waxes with Compressed CO2: Effect of Extraction Pressure and Temperature». En: *Industrial & Engineering Chemistry Research* 41.10 (abr. de 2002), págs. 2497-2503. DOI: 10.1021/ie010883i (vid. págs. 81, 116).

Goodger, Jason Q.D. *y col.* «*Eucalyptus* subgenus *Eucalyptus* (Myrtaceae) trees are abundant sources of medicinal pinocembrin and related methylated flavanones». En: *Industrial Crops and Products* 131 (mayo de 2019), págs. 166-172. DOI: 10.1016/J.INDCROP.2019.01.050 (vid. págs. 28, 36, 108).

Goto, Motonobu, Bhupesh C. Roy y Tsutomu Hirose. «Shrinking-core leaching model for supercritical-fluid extraction». En: *The Journal of Supercritical Fluids* 9.2 (1996), págs. 128 -133. DOI: https://doi.org/10.1016/S0896-8446(96)90009-1 (vid. pág. 159).

Goto, Motonobu *y col.* «Modeling Supercritical Fluid Extraction Process Involving Solute-Solid Interaction». En: *JOURNAL OF CHEMICAL ENGINEERING OF JAPAN* 31.2 (1998), págs. 171-177. DOI: 10.1252/jcej.31.171 (vid. pág. 84).

Havsteen, B. «Flavonoids, a class of natural products of high pharmacological potency». En: *Biochemical Pharmacology* 32.7 (1983), págs. 1141-1148 (vid. pág. 37).

Hayduk, W y B S Minhas. «Correlations for prediction of molecular diffusivities in liquids». En: *The Canadian Journal of Chemical Engineering* 60.2 (abr. de 1982), págs. 295-299. DOI: 10.1002/cjce.5450600213 (vid. pág. 89).

Heo, Moon Y., Su J. Sohn y William W. Au. «Anti-genotoxicity of galangin as a cancer chemopreventive agent candidate». En: *Mutation Research - Reviews in Mutation Research* 488.2 (2001), págs. 135-150. DOI: 10.1016/S1383-5742(01)00054-0 (vid. pág. 38).

Hernandes, C. *y col.* «*Lippia origanoides* essential oil: an efficient and safe alternative to preserve food, cosmetic and pharmaceutical products». En: *Journal of Applied Microbiology* 122.4 (2017), págs. 900-910. DOI: 10.1111/jam.13398 (vid. págs. 33, 35).

Herrero, Miguel *y col.* «Supercritical fluid extraction: Recent advances and applications». En: *Journal of Chromatography A* 1217.16 (2010), págs. 2495-2511. DOI: 10.1016/J.CHROMA.2009.12.019 (vid. págs. 46, 52).

Holderbaum, T. y J. Gmehling. «PSRK: A Group Contribution Equation of State Based on UNIFAC». En: *Fluid Phase Equilibria* 70.2-3 (dic. de 1991), págs. 251-265. DOI: 10.1016/0378-3812(91)85038-V (vid. pág. 88).

Horstmann, Sven *y col.* «PSRK group contribution equation of state: comprehensive revision and extension IV, including critical constants and α-function parameters for 1000 components». En: *Fluid Phase Equilibria* 227.2 (ene. de 2005), págs. 157-164. DOI: 10.1016/J.FLUID.2004.11.002 (vid. pág. 89).

Huang, Zhen. «Mass Transfer Models for Supercritical Fluid Extraction». En: *Food Engineering Series*. Springer, 2015, págs. 77-115. DOI: 10.1007/978-3-319-10611-3_3 (vid. pág. 57).

Huang, Zhen, Xiao han Shi y Wei juan Jiang. *Theoretical models for supercritical fluid extraction*. 2012. DOI: 10.1016/j.chroma.2012.04.032 (vid. pág. 56).

International Organization for Standardization. *ISO 19817:2017 - Essential oil of thyme Thymus vulgaris L. and Thymus zygis L.], thymol type*. 2017 (vid. págs. 25, 34).

Jang, Meishiang *y col.* «Cancer chemopreventive activity of resveratrol, a natural product derived from grapes». En: *Science* 275.5297 (1997), págs. 218-220 (vid. pág. 37).

Jay, A.J., D.C. Steytler y M. Knights. «Spectrophotometric studies of food colors in near-critical carbon dioxide». En: *The Journal of Supercritical Fluids* 4.2 (jun. de 1991), págs. 131-141. DOI: 10.1016/0896-8446(91)90042-5 (vid. pág. 154).

Joback, Kevin G y Robert C Reid. «Estimation of pure-component properties from group-contributions». En: *Chemical Engineering Communications* 57.1-6 (1987), págs. 233-243 (vid. págs. 84, 90).

Kawaii, S *y col.* «Quantitation of flavonoids constituents in Citrus fruits». En: *Journal of Agricultural and Food Chemistry* 47 (1999), págs. 3565-3571 (vid. pág. 36).

Kenig, Eugeny Y. *y col.* «Modeling of Distillation Processes». En: *Distillation*. Boston: Academic Press, 2014. Cap. 10, págs. 383 -436. DOI: 10.1016/B978-0-12-386547-2.00010-7 (vid. pág. 41).

Khani, Rouhollah, Reza Rahmanian y Naser Valipour Motlagh. «UVâ€“Visible Spectrometry and Multivariate Calibration as a Rapid and Reliable Tool for Simultaneous Quantification of Ternary Mixture of Phenolic Acids in Fruit Juice Samples». En: *Food Analytical Methods* 9.5 (2016), págs. 1112-1119. DOI: 10.1007/s12161-015-0287-3 (vid. pág. 50).

Kirsanov, Dmitry *y col.* «UV–Vis spectroscopy with chemometric data treatment: an option for on-line control in nuclear industry». En: *Journal of Radioanalytical and Nuclear Chemistry* 312.3 (2017), págs. 461-470. DOI: 10.1007/s10967-017-5252-8 (vid. pág. 49).

Klejdus, B. *y col.* «Hyphenated technique for the extraction and determination of isoflavones in algae: Ultrasound-assisted supercritical fluid extraction followed by fast chromatography with tandem mass spectrometry». En: *Journal of Chromatography A* 1217.51 (2010), págs. 7956-7965. DOI: 10.1016/J.CHROMA.2010.07.020 (vid. págs. 29, 42).

Knez, Željko, Darija Cör y Maša Knez-Hrnčič. «Solubility of Solids in Sub- and Supercritical Fluids: A Review 2010-2017». En: *Journal of Chemical and Engineering Data* 63.4 (2018), págs. 860-884. DOI: 10.1021/acs.jced.7b00778 (vid. pág. 54).

Lan, Xi *y col.* «Pinocembrin protects hemorrhagic brain primarily by inhibiting toll-like receptor 4 and reducing M1 phenotype microglia». En: *Brain, Behavior, and Immunity* 61 (2017), págs. 326-339. DOI: 10.1016/J.BBI.2016.12.012 (vid. págs. 27, 37).

Le Bas, Gervaise. *The Molecular Volumes of Liquid Chemical Compounds, from the Point of View of Kopp*. New York: Longmans, Green, 1915 (vid. pág. 90).

Leitao, N. *y col.* «Anacardium occidentale L. leaves extraction via SFE: Global yields, extraction kinetics, mathematical modeling and economic evaluation». En: *Journal of Supercritical Fluids* 78.July 2016 (jun. de 2013), págs. 114-123. DOI: 10.1016/j.supflu.2013.03.024 (vid. pág. 94).

Leitão, Suzana Guimaraes *y col.* «Counter-current chromatography with off-line detection by ultra high performance liquid chromatography/high resolution mass spectrometry in the study of the phenolic profile of *Lippia origanoides*». En: *Journal of Chromatography A* 1520 (oct. de 2017), págs. 83-90. DOI: 10.1016/J.CHROMA.2017.09.004 (vid. págs. 26, 36, 111).

Leite, J. *y col.* «Measurement and modelling of tracer diffusivities of gallic acid in liquid ethanol and in supercritical CO2 modified with ethanol». En: *The Journal of Supercritical Fluids* 131 (ene. de 2018), págs. 130-139. DOI: 10.1016/J.SUPFLU.2017.09.004 (vid. pág. 89).

Lemmon, E. W., M. L. Huber y M.O. McLinden. *NIST Standard Reference Database 23: Reference Fluid Thermodynamic and Transport Properties (REFPROP), version 9.1*. Gaithersburg, 2013 (vid. págs. 71, 83, 88, 90, 117).

Li, Aifeng, Ailing Sun y Renmin Liu. «Preparative isolation and purification of three flavonoids from the chinese medicinal plant *Alpinia katsumadai* hayata by high-speed counter-current chromatography». En: *Journal of Liquid Chromatography & Related Technologies* 35.20 (ene. de 2012), págs. 2900-2909. DOI: 10.1080/10826076.2011.643523 (vid. págs. 28, 36, 108).

Liu, Hongqin, Carlos M. Silva y Eugénia A. Macedo. «Unified approach to the self-diffusion coefficients of dense fluids over wide ranges of temperature and pressureâ€"hard-sphere, square-well, Lennardâ€"Jones and real substances». En: *Chemical Engineering Science* 53.13 (jul. de 1998), págs. 2403-2422. DOI: 10.1016/S0009-2509(98)00036-0 (vid. pág. 89).

Long-Ze, LIn *y col.* «Identification and quantification of flavonoids of Mexican oregano (*Lippia graveolens*) by LC-DAD-ESI/MS analysis». En: *Journal of Food Composition and Analysis* 20.5 (2007), págs. 361-369. DOI: 10.1016/j.jfca.2006.09.005 (vid. págs. 26, 36, 38, 154).

Lopes, Antonia *y col. Formulção farmaceutica derivada de óleo essencial de Lippia origanoides H.B.K.* 2013 (vid. pág. 33).

López-Sebastián, Sara *y col.* «Dearomatization of antioxidant rosemary extracts by treatment with supercritical carbon dioxide». En: *Journal of Agricultural and Food Chemistry* 46.1 (1998), págs. 13-19. DOI: 10.1021/jf970565n (vid. págs. 29, 42).

Madrid-Garcés, Tomas Antonio, Jaime Eduardo Parra-Suescún y Albeiro López-Herrera. «La inclusión de aceite esencial de orégano (*Lippia origanoides*) mejora parámetros inmunológicos en pollos de engorde». En: *Biotecnología en el Sector Agropecuario y Agroindustrial* 15 (dic. de 2017), págs. 75-83 (vid. pág. 35).

Maffei, M. «Discriminant analysis of leaf wax alkanes in the Lamiaceae and four other plant families». En: *Biochemical Systematics and Ecology* 22.7 (oct. de 1994), págs. 711-728. DOI: 10.1016/0305-1978(94)90057-4 (vid. págs. 39, 115).

Maio, Giovanni *y col.* «Supercritical Fluid Extraction of Some Chlorinated Benzenes and Cyclohexanes from Soil: Optimization with Fractional Factorial Design and Simplex». En: *Analytical Chemistry* 69.4 (1997), págs. 601-606. DOI: 10.1021/ac960349y (vid. pág. 47).

Maisch, J. «On some useful plants of the natural order of Verbenaceae.» En: *American Journal of Pharmacy* 57 (1885), págs. 189-199 (vid. pág. 33).

Manne, Rolf. «On the resolution problem in hyphenated chromatography». En: *Chemometrics and Intelligent Laboratory Systems* 27.1 (1995), págs. 89 -94. DOI: https://doi.org/10.1016/0169-7439(95)80009-X (vid. pág. 49).

Mantell, C., M. Rodríguez y E.Martínez de la Ossa. «Measurement of the diffusion coefficient of a model food dye (malvidin 3,5-diglucoside) in a high pressure CO2+methanol system by the chromatographic peak-broadening technique». En: *The Journal of Supercritical Fluids* 25.1 (ene. de 2003), págs. 57-68. DOI: 10.1016/S0896-8446(02)00088-8 (vid. págs. 89, 90).

Mar, Josiana M. *y col.* «*Lippia origanoides* essential oil: An efficient alternative to control *Aedes aegypti*, *Tetranychus urticae* and *Cerataphis lataniae*». En: *Industrial Crops and Products* 111 (2018), págs. 292 -297. DOI: https://doi.org/10.1016/j.indcrop.2017.10.033 (vid. pág. 36).

Martín, Ángel *y col.* «Teaching advanced equations of state in applied thermodynamics courses using open source programs». En: *Education for Chemical Engineers* 6.4 (dic. de 2011), e114-e121. DOI: 10.1016/J.ECE.2011.08.003 (vid. pág. 88).

Martínez, Jairo, Juliana Agudelo y Elena Stashenko. «Criterio de calidad para *Lippia alba* y *Lippia origanoides* en aceites esenciales». En: *Vitae*. Ed. por Gloria Holguín Martínez. Vol. 18. 2 (2). Medellín: Vitae., 2011, S295 (vid. pág. 25).

Martinez, Jose L. *Supercritical fluid extraction of nutraceuticals and bioactive compounds*. CRC Press, 2007 (vid. pág. 52).

Martínez-Natarén, Daniela A. *y col.* «Essential oil Yield Variation Within and Among Wild Populations of Mexican Oregano (*Lippia graveolens* H.B.K.-Verbenaceae), and its Relation to Climatic and Edaphic Conditions». En: *Journal of Essential Oil Bearing Plants* 15.4 (ene. de 2012), págs. 589-601. DOI: 10.1080/0972060X.2012.10644093 (vid. págs. 26, 110).

Matsuyama, Kiyoshi *y col.* «Solubilities of 7,8-Dihydroxyflavone and 3,3â€˜,4â€˜,5,7-Pentahydroxyflavone in Supercritical Carbon Dioxide». En: *Journal of Chemical & Engineering Data* 48.4 (jun. de 2003), págs. 1040-1043. DOI: 10.1021/je030129z (vid. págs. 122, 124).

McHugh, Mark A., Andrew J. Seckner y Thomas J. Yogan. «High-pressure phase behavior of binary mixtures of octacosane and carbon dioxide». En: *Industrial & Engineering Chemistry Fundamentals* 23.4 (mayo de 1984), págs. 493-499. DOI: 10.1021/i100016a020 (vid. págs. 116, 143).

Méndez-Santiago, Janette y Amyn S Teja. «The solubility of solids in supercritical fluids». En: *Fluid Phase Equilibria* 158-160 (1999), págs. 501-510. DOI: 10.1016/s0378-3812(99)00154-5 (vid. pág. 117).

Meyer, J.J.M. *y col.* «Antiviral activity of galangin isolated from the aerial parts of *Helichrysum aureonitens*». En: *Journal of Ethnopharmacology* 56.2 (1997), págs. 165-169. DOI: 10.1016/S0378-8741(97)01514-6 (vid. pág. 38).

Miller, James N y Jane Charlotte Miller. *Statistics and chemometrics for analytical chemistry*. Sixth. Pearson Education, 2010 (vid. pág. 69).

Ming, Dong Sheng y G H Neil Towers. «Antifungal Activity of Benzoic Acid Derivatives from *Piper lanceaefolium*». En: 604 (2002), págs. 62-64 (vid. pág. 37).

Mira, B. *y col.* «Supercritical CO2 extraction of essential oil from orange peel. Effect of operation conditions on the extract composition». En: *Journal of Supercritical Fluids* 14.2 (1999), págs. 95-104. DOI: 10.1016/S0896-8446(98)00111-9 (vid. pág. 39).

Mohammadi, Amir H., Ali Eslamimanesh y Dominique Richon. «Wax Solubility in Gaseous System: Thermodynamic Consistency Test of Experimental Data». En: *Industrial & Engineering Chemistry Research* 50.8 (abr. de 2011), págs. 4731-4740. DOI: 10.1021/ie1022145 (vid. pág. 84).

Montgomery, D. *Design and Analysis of Experiments*. 6.ª ed. New York: Sons, John Wiley y Sons, 2008 (vid. pág. 94).

Muhammad Ahmad, Hafiz, Mahmood-Ur Rahman y Qurban Ali. «Plant cuticular waxes: a review on functions, composition, biosyntheses mechanism and transportation». En: *Industrial & Engineering Chemistry Research* 12 (2015), págs. 4861-4870 (vid. pág. 39).

Navarrete, A. *y col.* «Valorization of solid wastes from essential oil industry». En: *Journal of Food Engineering* 104.2 (mayo de 2011), págs. 196-201. DOI: 10.1016/J.JFOODENG.2010.10.033 (vid. págs. 27, 34, 40, 108).

Neira, Laura *y col.* «Toxicidad, genotoxicidad y actividad anti-Leishmania de aceites esenciales obtenidos de cuatro (4) quimiotipos del género *Lippia*». En: *Boletín Latinoamericano y del Caribe de Plantas Medicinales y Aromáticas* 17.1 (2018), págs. 68-83 (vid. pág. 35).

Nelder, John A y Roger Mead. «A simplex method for function minimization». En: *The Computer Journal* 7.4 (1965), págs. 308-313. DOI: 10.1093/comjnl/7.4.308 (vid. págs. 77, 99).

Núñez, Gonzalo A, José M del Valle y Juan C de la Fuente. «Solubilities in Supercritical Carbon Dioxide of (2E,6E)-3,7,11-Trimethyldodeca-2,6,10-trien-1-ol (Farnesol) and (2S)-5,7-Dihydroxy-2-(4-hydroxyphenyl)chroman-4-one (Naringenin)». En: *Journal of Chemical & Engineering Data* 55.9 (sep. de 2010), págs. 3863-3868. DOI: 10.1021/je900957v (vid. págs. 97, 122, 123, 153).

O'Haver, Tom. *Curve fitting B: Multicomponent Spectroscopy*. http://terpconnect.umd.edu/~toh/spectrum/CurveFittingB.html. Accedido: 2020-02-03. 2014 (vid. pág. 50).

O'Leary, Nataly *y col.* «Species delimitation in *Lippia* section *Goniostachyum* (Verbenaceae) using the phylogenetic species concept». En: *Botanical Journal of the Linnean Society* 170.2 (sep. de 2012), págs. 197-219. DOI: 10.1111/j.1095-8339.2012.01291.x (vid. pág. 152).

Oliveira, Danilo R. *y col.* «Chemical and antimicrobial analyses of essential oil of *Lippia origanoides* H.B.K». En: *Food Chemistry* 101.1 (2007), págs. 236-240. DOI: 10.1016/J.FOODCHEM.2006.01.022 (vid. pág. 34).

Oliveira, Eduardo L.G., Armando J.D. Silvestre y Carlos M. Silva. «Review of kinetic models for supercritical fluid extraction». En: *Chemical Engineering Research and Design* 89.7 (jul. de 2011), págs. 1104-1117. DOI: 10.1016/J.CHERD.2010.10.025 (vid. págs. 44, 56, 57, 85).

Olivieri, Alejandro C. *y col.* «Uncertainty estimation and figures of merit for multivariate calibration (IUPAC Technical Report)». En: *Pure and Applied Chemistry* 78.3 (ene. de 2006), págs. 633-661. DOI: 10.1351/pac200678030633 (vid. págs. 49, 65, 68).

Ortiz, R E *y col.* «Efecto del aceite esencial de orégano sobre el desempeño productivo de ponedoras y la estabilidad oxidativa de huevos enriquecidos con ácidos grasos poliinsaturados». Español. En: *Revista de la Facultad de Medicina Veterinaria y de Zootecnia* 64.1 (2017), págs. 61-70 (vid. págs. 33, 35).

Ota, Masaki *y col.* «Measurement and correlation of flavanone, tangeritin, nobiletin, 6-hydroxyflavanone and 7-hydroxyflavone solubilities in supercritical CO2». En: *Journal of Supercritical Fluids* 128 (oct. de 2017), págs. 166-172. DOI: 10.1016/j.supflu.2017.05.024 (vid. págs. 122, 123).

Pace-Asciak, Cecil R *y col.* «The red wine phenolic trans - resveratrol and quercetin block human platelet aggregation and eicosanoid synthesis: Implications for protection against coronary heart disease». En: *Clinica Chimica Acta* 235.2 (1995), págs. 207-219 (vid. pág. 37).

Paes, Juliana *y col.* «Extraction of phenolic compounds and anthocyanins from blueberry (*Vaccinium myrtillus* L.) residues using supercritical CO2 and pressurized liquids». En: *The Journal of Supercritical Fluids* 95 (nov. de 2014), págs. 8-16. DOI: 10.1016/J.SUPFLU.2014.07.025 (vid. págs. 29, 42, 110).

Pardo-Castaño, Camilo y Gustavo Bolaños. «Solubility of chitosan in aqueous acetic acid and pressurized carbon dioxide-water: Experimental equilibrium and solubilization kinetics». En: *Journal of Supercritical Fluids* 151 (2019), págs. 63-74. DOI: 10.1016/j.supflu.2019.05.007 (vid. pág. 62).

Pardo-Castaño, Camilo, Manuel Velásquez y Gustavo Bolaños. «Simple models for supercritical extraction of natural matter». En: *Journal of Supercritical Fluids* 97 (2015), págs. 165-173. DOI: 10.1016/j.supflu.2014.09.044 (vid. pág. 55).

Pardo-Castaño, Camilo *y col.* «Solubility of collinin and isocollinin in pressurized carbon dioxide: Synthesis, solubility parameters, and equilibrium measurements». En: *Journal of Chemical and Engineering Data* 64.9 (2019), págs. 3799-3810. DOI: 10.1021/acs.jced.9b00234 (vid. pág. 62).

Park, Yong K *y col.* «Antimicrobial Activity of Propolis on Oral Microorganisms». En: 36 (1998), págs. 24-28 (vid. pág. 37).

Passey, C A. «Commercial feasibility of a supercritical extraction plant for making reduced-calorie peanuts». En: *Supercritical Fluid Processing of Food and Biomaterials*. Ed. por S.S.H. Rizvi. 1.ª ed. London, UK: Blakie Academic & Professional, 1994, págs. 223-243 (vid. pág. 42).

Patel, D K *y col.* «Pharmacological and bioanalytical aspects of galangin-a concise report». En: *Asian Pacific Journal of Tropical Biomedicine* 2.1 (2012), S449-S455. DOI: 10.1016/S2221-1691(12)60205-6 (vid. pág. 38).

Paula, Julia T. *y col.* «Solubility of protocatechuic acid, sinapic acid and chrysin in supercritical carbon dioxide». En: *The Journal of Supercritical Fluids* 112 (jun. de 2016), págs. 89-94. DOI: 10.1016/J.SUPFLU.2016.02.014 (vid. pág. 122).

Peng, Ding-Yu y Donald B. Robinson. «A New Two-Constant Equation of State». En: *Industrial & Engineering Chemistry Fundamentals* 15.1 (feb. de 1976), págs. 59-64. DOI: 10.1021/i160057a011 (vid. pág. 83).

Pereira, Camila G. y M. Angela A Meireles. «Supercritical fluid extraction of bioactive compounds: Fundamentals, applications and economic perspectives». En: *Food and Bioprocess Technology* 3.3 (2010), págs. 340-372. DOI: 10.1007/s11947-009-0263-2 (vid. págs. 92, 108).

Peres, William. «Radicais Livres em nïveis biológicos». En: *Pelotas: Ed. Universidade Cat{ó}lica de Pelotas* (1994), págs. 49-81 (vid. pág. 37).

Pérez Zamora, Cristina M., Carola A. Torres y María B. Nuñez. «Antimicrobial Activity and Chemical Composition of Essential Oils from Verbenaceae Species Growing in South America». En: *Molecules* 23.3 (2018). DOI: 10.3390/molecules23030544 (vid. págs. 33, 35).

Perrut, M *y col.* «Mathematical Modeling of Sunflower Seed Extraction by Supercritical CO2». En: *Industrial & Engineering Chemistry Research* 36.2 (feb. de 1997), págs. 430-435. DOI: 10.1021/ie960354s (vid. págs. 84, 134).

Poling, Bruce E, John M Prausnitz y John P O'Connell. *The Properties of Gases & Liquids - Fifth Edition*. 2001, pág. 803. DOI: 10.1016/0894-1777(88)90021-0. arXiv: arXiv:1011.1669v3 (vid. págs. 89, 90).

Prausnitz, John M, Rudiger N Lichtenthaler y Edmundo Gomes de Azevedo. *Molecular thermodynamics of fluid-phase equilibria*. Prentice Hall, 1999, págs. 671-749 (vid. págs. 81, 83).

Preksha, Verma. *Allied Market Research. Essential Oil Market Size, Share, Essential Oil Industry Trends*. 2016 (vid. págs. 25, 39).

Ramsey, Edward D. *y col.* «Interfacing supercritical fluid reaction apparatus with online liquid chromatography: Monitoring the progress of a synthetic organic reaction performed in supercritical fluid solution». En: *Journal of Chromatography A* 1388 (abr. de 2015), págs. 141-150. DOI: 10.1016/J.CHROMA.2015.02.037 (vid. pág. 75).

Rasul, Azhar *y col.* «Pinocembrin: A novel natural compound with versatile pharmacological and biological activities». En: *BioMed Research International* 2013.2013 (2013), págs. 1-9. DOI: 10.1155/2013/379850 (vid. págs. 27, 37).

Ravetti Duran, Renan *y col.* «Phase Equilibrium Study of the Ternary System CO2+H2O+Ethanc At Elevated Pressure: Thermodynamic Model Selection. Application to Supercritical Extraction of Polar Compounds». En: *The Journal of Supercritical Fluids* 138 (ago. de 2018), págs. 17-28. DOI: 10.1016/J.SUPFLU.2018.03.016 (vid. pág. 88).

Reverchon, E. «Mathematical Modeling of Supercritical Extraction of Sage Oil». En: *AIChE Journal* 42.6 (1996), págs. 1765-1771. DOI: 10.1002/aic.690420627 (vid. pág. 159).

Reverchon, E y F Senatore. «Isolation of rosemary oil: Comparison between hydrodistillation and supercritical CO2 extraction». En: *Flavour and Fragrance Journal* 7.4 (1992), págs. 227-230. DOI: 10.1002/ffj.2730070411 (vid. pág. 72).

Reverchon, Ernesto. «Fractional Separation of SCF Extracts from *Marjoram* Leaves : Mass Transfer and Optimization». En: *Journal of Supercritical Fluids* 5 (1992), págs. 256-261 (vid. págs. 38, 115, 133, 155).

Reverchon, Ernesto, Pietro Russo y Alberto Stassi. «Solubilities of solid octacosane and triacontane in supercritical carbon dioxide». En: *Journal of Chemical & Engineering Data* 38.3 (jul. de 1993), págs. 458-460. DOI: 10.1021/je00011a034 (vid. págs. 39, 115, 117, 143).

Ribeiro, Alcy F. *y col.* «Circadian and seasonal study of the cinnamate chemotype from *Lippia origanoides* Kunth». En: *Biochemical Systematics and Ecology* 55 (2014), págs. 249-259. DOI: 10.1016/J.BSE.2014.03.014 (vid. pág. 33).

Ríos, Natalia, Elena E Stashenko y Jonny E Duque. «Evaluation of the insecticidal activity of essential oils and their mixtures against *Aedes aegypti* (Diptera: Culicidae)». En: *Revista Brasileira de Entomologia* 61.4 (2017), págs. 307-311 (vid. pág. 36).

Roy, Bhupesh C. *y col.* «Supercritical CO2 Extraction of Essential Oils and Cuticular Waxes from Peppermint Leaves». En: *Journal of Chemical Technology & Biotechnology* 67.1 (1996), págs. 21-26. DOI: 10.1002/(SICI)1097-4660(199609)67:1<21::AID-JCTB522>3.0.CO;2-0 (vid. pág. 53).

Russo, A, R Longo y A Vanella. «Antioxidant activity of propolis: role of caffeic acid phenethyl ester and galangin.» En: *Fitoterapia* 73 Suppl 1 (2002), S21-9 (vid. pág. 38).

Safaralie, Asghar, Shohreh Fatemi y Alireza Salimi. «Experimental design on supercritical extraction of essential oil from valerian roots and study of optimal conditions». En: *Food and Bioproducts Processing* 88.2-3 (jun. de 2010), págs. 312-318. DOI: 10.1016/J.FBP.2009.02.002 (vid. pág. 47).

Saldaña, Marleny D A *y col.* «Extraction of Purine Alkaloids from Maté (*Ilex paraguariensis*) using supercritical CO2». En: *J. Agric. Food Chem.* 47 (1999), págs. 3804-3808 (vid. pág. 124).

Saldaña, Marleny D.A. *y col.* «Apparent solubility of lycopene and β-carotene in supercritical CO2, CO2Â +Â ethanol and CO2Â +Â canola oil using dynamic extraction of tomatoes». En: *Journal of Food Engineering* 99.1 (jul. de 2010), págs. 1-8. DOI: 10.1016/J.JFOODENG.2010.01.017 (vid. págs. 98, 133, 139).

Sanchez, Eugenio y Bruce R. Kowalski. «Tensorial resolution: A direct trilinear decomposition». En: *Journal of Chemometrics* 4.1 (ene. de 1990), págs. 29-45. DOI: 10.1002/cem.1180040105 (vid. pág. 67).

Sánchez-Vioque, R. *y col.* «Polyphenol composition and antioxidant and metal chelating activities of the solid residues from the essential oil industry». En: *Industrial Crops and Products* 49 (ago. de 2013), págs. 150-159. DOI: 10.1016/J.INDCROP.2013.04.053 (vid. págs. 27, 34, 108).

Santos, Dayane Aparecida dos *y col.* «Multiproduct, Multicomponent and Multivariate Calibration: a Case Study by Using Vis-NIR Spectroscopy». En: *Food Analytical*

Methods 11.7 (2018), págs. 1915-1919. DOI: 10.1007/s12161-017-1099-4 (vid. pág. 51).

Santos-Gomes, Paula C. y Manuel Fernandes-Ferreira. «Organ- and Season-Dependent Variation in the Essential Oil Composition of Salvia officinalis L. Cultivated at Two Different Sites». En: *J. Agric. Food Chem.* 49 (2001), págs. 2908-2916. DOI: 10.1021/JF001102B (vid. págs. 41, 152).

Sarrazin, Sandra Layse F. *y col.* «Antimicrobial and Seasonal Evaluation of the Carvacrol-Chemotype Oil from *Lippia origanoides* Kunth.» En: *Molecules* 20.2 (2015), págs. 1860-1871. DOI: 10.3390/molecules20021860 (vid. pág. 35).

Schwarz, Karin, Waldemar Ternes y Eberhard Schmauderer. «Antioxidative constituents of *Rosmarinus officinalis* and *Salvia officinalis*». En: *Zeitschrift fur Lebensmittel-Untersuchung und -Forschung* 195.2 (ago. de 1992), págs. 104-107. DOI: 10.1007/BF01201767 (vid. págs. 29, 42).

Sematech, NIST. *e-Handbook of Statistical Methods*. 2006 (vid. pág. 77).

Sharif, K.M. *y col.* «Experimental design of supercritical fluid extraction–A review». En: *Journal of Food Engineering* 124 (2014), págs. 105-116. DOI: 10.1016/J.JFOODENG.2013.10.003 (vid. págs. 44-46).

Sielfeld, Caroline, José M. del Valle y Federico Sastre. «Effect of pelletization on supercritical CO2 extraction of rosemary antioxidants». En: *The Journal of Supercritical Fluids* 147 (mayo de 2019), págs. 162-171. DOI: 10.1016/J.SUPFLU.2016.04.010 (vid. págs. 157, 158, 164).

Silva, Alessandra P. da *y col.* «Tyrosinase inhibitory activity, molecular docking studies and antioxidant potential of chemotypes of *Lippia origanoides* (Verbenaceae)

essential oils». En: *PLOS ONE* 12.5 (2017). Ed. por Jamshidkhan Chamani, e0175598. DOI: 10.1371/journal.pone.0175598 (vid. págs. 33, 34).

Singleton, Vernon L., Rudolf Orthofer y Rosa M. Lamuela-Raventós. «Analysis of total phenols and other oxidation substrates and antioxidants by means of folin-ciocalteu reagent». En: *Methods in Enzymology* 299 (1998), págs. 152-178. DOI: 10.1016/S0076-6879(99)99017-1. arXiv: arXiv:1011.1669v3 (vid. pág. 48).

Skerget, M, Željko Knez y Maša Knez-Hrnčič. «Solubility of solids in sub-and supercritical fluids: a review». En: *Journal of Chemical & Engineering Data* 56 (2011), págs. 694-719. DOI: 10.1021/je1011373 (vid. pág. 54).

Smith, Robin M. «Optimization». En: *Chemical process: design and integration*. John Wiley & Sons, 2005. Cap. 3, págs. 35-56 (vid. pág. 47).

Soares, Bruna Viana *y col.* «Antiparasitic, physiological and histological effects of the essential oil of *Lippia origanoides* (Verbenaceae) in native freshwater fish Colossoma macropomum». En: *Aquaculture* 469 (2017), págs. 72 -78. DOI: https://doi.org/10.1016/j.aquaculture.2016.12.001 (vid. pág. 35).

Soetaredjo, Felycia Edi, Suryadi Ismadji y Yi-Hsu Ju. «Measurement and modeling of epicatechin solubility in supercritical carbon dioxide fluid». En: *Fluid Phase Equilibria* 340 (feb. de 2013), págs. 7-10. DOI: 10.1016/J.FLUID.2012.12.005 (vid. pág. 154).

Soetaredjo, Felycia Edi *y col.* «Catechin sublimation pressure and solubility in supercritical carbon dioxide». En: *Fluid Phase Equilibria* 358 (nov. de 2013), págs. 220-225. DOI: 10.1016/J.FLUID.2013.08.012 (vid. pág. 154).

Solana, M. *y col.* «A comparison between supercritical fluid and pressurized liquid extraction methods for obtaining phenolic compounds from *Asparagus officinalis* L». En: *The Journal of Supercritical Fluids* 100 (mayo de 2015), págs. 201-208. DOI: 10.1016/J.SUPFLU.2015.02.014 (vid. págs. 29, 42, 110).

Sovová, Helena. «Apparent Solubility of Natural Products Extracted with Near-Critical Carbon Dioxide». En: *American Journal of Analytical Chemistry* 3 (2012), págs. 958-965 (vid. págs. 53, 55, 79, 85, 97, 124, 140).

— «Mathematical model for supercritical fluid extraction of natural products and extraction curve evaluation». En: *The Journal of Supercritical Fluids* 33.1 (2005), págs. 35-52. DOI: 10.1016/J.SUPFLU.2004.03.005 (vid. págs. 57, 85, 90, 148, 151, 158, 159, 161, 164, 166, 171).

— «Rate of the vegetable oil extraction with supercritical CO2 (I). Modelling of extraction curves». En: *Chemical Engineering Science* 49.3 (1994), págs. 409-414 (vid. pág. 88).

Sovová, Helena, Marie Sajfrtová y Roumiana P. Stateva. «A novel model for multicomponent supercritical fluid extraction and its application to *Ruta graveolens*». En: *The Journal of Supercritical Fluids* 120 (feb. de 2017), págs. 102-112. DOI: 10.1016/J.SUPFLU.2016.10.008 (vid. págs. 52, 54, 81, 83, 116, 119).

Sovová, Helena y Roumiana P. Stateva. «New approach to modeling supercritical CO2 extraction of cuticular waxes: Interplay between solubility and kinetics». En: *Industrial and Engineering Chemistry Research* 54.17 (mayo de 2015), págs. 4861-4870. DOI: 10.1021/acs.iecr.5b00741 (vid. págs. 54, 81, 83, 85, 116).

Stahl, Egon *y col.* «Anwendungen verdichteter Gase zur Extraktion und Raffination». En: *Verdichtete Gase zur Extraktion und Raffination*. Springer Berlin Heidelberg, 1987, págs. 82-241. DOI: 10.1007/978-3-662-10763-8_4 (vid. págs. 39, 115).

Stashenko, E E *y col.* «Chromatographic and mass spectrometric characterization of essential oils and extracts from *Lippia* (Verbenaceae) aromatic plants». En: *Journal of Separation Science* 36.1 (2013), págs. 192-202. DOI: 10.1002/jssc.201200877 (vid. págs. 26, 27, 36, 65, 154).

Stashenko, Elena E. *y col.* «*Lippia origanoides* chemotype differentiation based on essential oil GC-MS and principal component analysis». En: *Journal of Separation Science* 33.1 (2010), págs. 93-103. DOI: 10.1002/jssc.200900452 (vid. págs. 25, 33, 34, 110).

Stein, S. E. y R. L. Brown. «Estimation of normal boiling points from group contributions». En: *Journal of Chemical Information and Computer Sciences* 34.3 (mayo de 1994), págs. 581-587. DOI: 10.1021/ci00019a016 (vid. pág. 84).

Suzuki, Kazuhiko *y col.* «Isothermal vapor-liquid equilibrium data for binary systems at high pressures: carbon dioxide-methanol, carbon dioxide-ethanol, carbon dioxide-1-propanol, methane-ethanol, methane-1-propanol, ethane-ethanol, and ethane-1-propanol systems». En: *Journal of Chemical Engineering Data* 35.1 (1990), págs. 63-66. DOI: 10.1021/je00059a020 (vid. pág. 96).

Swaid, I., D. Nickel y G.M. Schneider. «NIRâ€"spectroscopic investigations on phase behaviour of lowâ€"volatile organic substances in supercritical carbon dioxide». En: *Fluid Phase Equilibria* 21.1-2 (ene. de 1985), págs. 95-112. DOI: 10.1016/0378-3812(85)90062-7 (vid. págs. 117, 143).

Tan, Chung-Sung, Shuen-Kwei Liang y Din-Chung Liou. «Fluidâ€"solid mass transfer in a supercritical fluid extractor». En: *The Chemical Engineering Journal* 38.1 (mayo de 1988), págs. 17-22. DOI: 10.1016/0300-9467(88)80049-2 (vid. pág. 90).

Telci, Isa, Ibrahim Demirtas y Ayse Sahin. «Variation in plant properties and essential oil composition of sweet fennel (<i>Foeniculum vulgare<i/> Mill.) fruits during stages of maturity». En: *Industrial Crops and Products* 30.1 (jul. de 2009), págs. 126-130. DOI: 10.1016/J.INDCROP.2009.02.010 (vid. págs. 41, 152).

Ting, Simon S. T. *y col.* «Solubility of naproxen in supercritical carbon dioxide with and without cosolvents». En: *Industrial & Engineering Chemistry Research* 32.7 (2005), págs. 1471-1481. DOI: 10.1021/ie00019a022 (vid. pág. 132).

Torralba, R. *y col.* «Speciation and simultaneous determination of arsenic(III), arsenic(V), monomethylarsonate and dimethylarsinate by atomic absorption using inverse least squares multivariate calibration». En: *Spectrochimica Acta Part B: Atomic Spectroscopy* 49.9 (ago. de 1994), págs. 893-899. DOI: 10.1016/0584-8547(94)80078-2 (vid. pág. 67).

Torres, Abel *y col.* «Perspectives on the Application of Supercritical Antisolvent Fractionation Process for the Purification of Plant Extracts: Effects of Operating Parameters and Patent Survey». En: *Recent Patents on Engineering* 10.2 (2016), págs. 88-97 (vid. pág. 125).

Uchiyama, Hiroki *y col.* «Solubilities of Flavone and 3-Hydroxyflavone in Supercritical Carbon Dioxide». En: *Journal of Chemical & Engineering Data* 42.3 (mayo de 1997), págs. 570-573. DOI: 10.1021/je9603990 (vid. págs. 122, 124).

Ultra International B.V. *Essential Oils Market Report - Summer 2019*. Inf. téc. Spijkenisse: Ultra International B.V., 2019, pág. 37 (vid. págs. 25, 39).

Uquiche, Edgar, José M. del Valle y Mónica Ihl. «Microstructure-Extractability Relationships in the Extraction of Prepelletized Jalapeño Peppers with Supercritical Carbon Dioxide». En: *Journal of Food Science* 70.6 (mayo de 2006), e379-e386. DOI: 10.1111/j.1365-2621.2005.tb11442.x (vid. pág. 157).

Valle, José M. del, Juan C. de la Fuente y Damian A. Cardarelli. «Contributions to supercritical extraction of vegetable substrates in Latin America». En: *Journal of Food Engineering* 67.1-2 (2005), págs. 35-57. DOI: 10.1016/J.JFOODENG.2004.05.051 (vid. pág. 42).

Vessman, Jörgen *y col.* «Selectivity in analytical chemistry (IUPAC Recommendations 2001)». En: *Pure and Applied Chemistry* 73.8 (ago. de 2001), págs. 1381-1386. DOI: 10.1351/pac200173081381 (vid. pág. 68).

Villanueva Bermejo, David *y col.* «High catechins/low caffeine powder from green tea leaves by pressurized liquid extraction and supercritical antisolvent precipitation». En: *Separation and Purification Technology* 148 (2015), págs. 49-56. DOI: 10.1016/j.seppur.2015.04.037 (vid. pág. 125).

Walsh, John M, George D Ikonomou y Marc D Donohue. «Supercritical phase behavior: the entrainer effect». En: *Fluid Phase Equilibria* 33 (1987), págs. 295-314 (vid. pág. 132).

Wang, Tzu-Chi y Po-Chao Chang. «Measurement and Correlation for the Solid Solubility of Antioxidants Sodium l-Ascorbate and Sodium Erythorbate Monohydrate

in Supercritical Carbon Dioxide». En: *Journal of Chemical & Engineering Data* 60.3 (mar. de 2015), págs. 790-794. DOI: 10.1021/je5009153 (vid. pág. 154).

Wang, Wenzhu *y col.* «Using functional and molecular MRI techniques to detect neuroinflammation and neuroprotection after traumatic brain injury». En: *Brain, Behavior, and Immunity* 64 (2017), págs. 344-353. DOI: 10.1016/J.BBI.2017.04.019 (vid. págs. 27, 37).

Yamamoto, Norio *y col.* «Cardamonin stimulates glucose ptake through translocation of glucose transporter-4 in L6 myotubes». En: *Phytotherapy Research* 25.8 (2011), págs. 1218-1224. DOI: 10.1002/ptr.3416 (vid. págs. 28, 36).

Yang, Xu *y col.* «Pinocembrinâ€“lecithin complex: Characterization, solubilization, and antioxidant activities». En: *Biomolecules* 8.2 (2018), pág. 41. DOI: 10.3390/biom8020041 (vid. págs. 28, 40).

APPENDICES

Appendix A. International Patent 1

(12) SOLICITUD INTERNACIONAL PUBLICADA EN VIRTUD DEL TRATADO DE COOPERACIÓN EN MATERIA DE PATENTES (PCT)

(19) Organización Mundial de la Propiedad Intelectual
Oficina internacional

(43) Fecha de publicación internacional
19 de abril de 2018 (19.04.2018)

WIPO IPCT

(10) Número de publicación internacional
WO 2018/069778 A1

(51) Clasificación internacional de patentes:
B01D 53/04 (2006.01) *B01D 53/62* (2006.01)

(21) Número de la solicitud internacional:
PCT/IB2017/055640

(22) Fecha de presentación internacional:
18 de septiembre de 2017 (18.09.2017)

(25) Idioma de presentación: español

(26) Idioma de publicación: español

(30) Datos relativos a la prioridad:
NC20 16/0002034
20 de septiembre de 2016 (20.09.2016) CO

(71) Solicitante: **UNIVERSIDAD INDUSTRIAL DE SANTANDER** [CO/CO] ; Carrera 27 - Calle 9, Bucaramanga, **N/A** (CO).

(72) Inventores: **STASHENKO, Elena;** Carrera 27 calle 9, Bucaramanga, **N-A** (CO). **MARTINEZ MORALES, Jairo Rene;** Carrera 27 calle 9, Bucaramanga, **N/A** (CO). **ARIAS VELANDIA, Anderson Julián;** Carrera 27 calle 9, Bucaramanga, **N/A** (CO). **BELTRAN MORENO, Sergio Andrés;** Carrera 27 calle 9, Bucaramanga, **N/A** (CO). **GELVEZ AROCHA, Ornar Armando;** Carrera 27 calle 9, Bucaramanga, **N/A** (CO). **RIVERO GEREDA, Sergio Armando;** Carrera 27 calle 9, Bucaramanga, **N/A** (CO).

(74) Mandatario: **GOMEZ VILLA, Johan Sebastian** et al; TM Tamayo, Cra **13-A** No. 28-38 Bufete 230, Parque Central Bavaria, Bogotá, 110311 (CO).

(54) Title: SYSTEM FOR RECIRCULATING SUPERCRITICAL CARBON DIOXIDE, WHICH USES AN INTEGRATED DEVICE FOR LIQUEFYING AND STORING THE FLUID

(54) Título: SISTEMA DE RECIRCULACIÓN DE DIÓXIDO DE CARBONO SUPERCRÍTICO QUE USA UN DISPOSITIVO INTEGRADO DE LICUADO Y ALMACENAMIENTO DEL FLUIDO

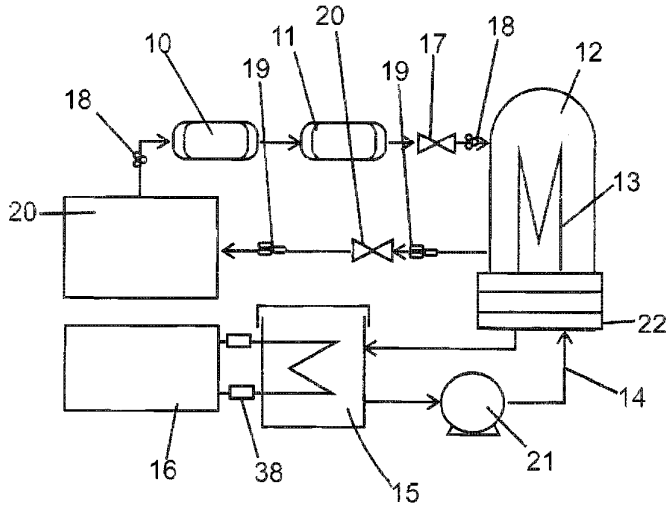

Fig. 1

(57) Abstract: The present invention relates to a recirculation device comprising a four-pass heat exchanger capable of liquefying carbón dioxide and storing same in the same device, a water-operated cooling subsystem being coupled to this exchanger, wherein the carbón dioxide from any process, at known pressure and temperature conditions, enters the specially designed exchanger, which exchanger removes heat so that the CO2, at a constant pressure, can be liquefied and stored in liquid state in the same device. In this way, it is possible to recover CO2 gas,

WO 2018/069778 A1

[Continúa en la página siguiente]

(81) Estados designados *(a menos que se indique otra cosa, para toda clase de protección nacional admisible)*: AE, AG, AL, AM, AO, AT, AU, AZ, BA, BB, BG, BH, BN, BR, BW, BY, BZ, CA, CH, CL, CN, CO, CR, CU, CZ, DE, DJ, DK, DM, DO, DZ, EC, EE, EG, ES, FI, GB, GD, GE, GH, GM, GT, HN, HR, HU, ID, IL, IN, IR, IS, JO, JP, KE, KG, KH, KN, KP, KR, KW, KZ, LA, LC, LK, LR, LS, LU, LY, MA, MD, ME, MG, MK, MN, MW, MX, MY, MZ, NA, NG, NI, NO, NZ, OM, PA, PE, PG, PH, PL, PT, QA, RO, RS, RU, RW, SA, SC, SD, SE, SG, SK, SL, SM, ST, SV, SY, TH, TJ, TM, TN, TR, TT, TZ, UA, UG, US, UZ, VC, VN, ZA, ZM, ZW.

(84) Estados designados *(a menos que se indique otra cosa, para toda clase de protección regional admisible):* ARIPO (BW, GH, GM, KE, LR, LS, MW, MZ, NA, RW, SD, SL, ST, SZ, TZ, UG, ZM, ZW), euro-asiática (AM, AZ, BY, KG, KZ, RU, TJ, TM), europea (AL, AT, BE, BG, CH, CY, CZ, DE, DK, EE, ES, FI, FR, GB, GR, HR, HU, IE, IS, IT, LT, LU, LV, MC, MK, MT, NL, NO, PL, PT, RO, RS, SE, SI, SK, SM, TR), OAPI (BF, BJ, CF, CG, CI, CM, GA, GN, GQ, GW, KM, ML, MR, NE, SN, TD, TG).

Publicada:

— *con informe de búsqueda internacional (Art. 21(3))*

— *antes de la expiración del plazo para modificar las reivindicaciones y para ser republicada si se reciben modificaciones (Regla 48.2(h))*

so that same can be re-pressurised and re-used in the application.

(57) Resumen: La presente invención consiste en un dispositivo de recirculación que consta de un intercambiador de calor de cuatro pasos que es capaz de licuar dióxido de carbono y almacenarlo en el mismo dispositivo; que tiene acoplado a este intercambiador un subsistema de refrigeración operado con agua; donde el dióxido de carbono proveniente de cualquier proceso a condiciones conocidas de temperatura y presión ingresa al intercambiador especialmente diseñado que se encarga de retirar el calor para que el CO_2 a una presión constante pueda ser licuado y almacenado en estado líquido dentro del mismo dispositivo. De esta manera es posible recuperar el $_{C02}$ gaseoso, para que este pueda volver a ser presurizado y usado nuevamente en la aplicación.

SISTEMA DE RECIRCULACIÓN DE DIÓXIDO DE CARBONO SUPERCRÍTICO QUE USA UN DISPOSITIVO INTEGRADO DE LICUADO Y ALMACENAMIENTO DEL FLUIDO

ESFERA TECNOLÓGICA

La presente invención consiste en un dispositivo de recirculación que consta de un intercambiador de calor de cuatro pasos que es capaz de licuar dióxido de carbono y almacenarlo en el mismo dispositivo; que tiene acoplado a este intercambiador un subsistema de refrigeración operado con agua; donde el dióxido de carbono proveniente de cualquier proceso a condiciones conocidas de temperatura y presión ingresa al intercambiador especialmente diseñado que se encarga de retirar el calor para que el C02 a una presión constante pueda ser licuado y almacenado en estado líquido dentro del mismo dispositivo. De esta manera es posible recuperar el C02 gaseoso, para que este pueda volver a ser presurizado y usado nuevamente en la aplicación.

ESTADO DE LA TÉCNICA

Se conoce de la invención, la solicitud de patente japonesa JP2004249175A con fecha de prioridad 2003-02-18 y fecha de Publicación 2004-09-09 titulada "IMPREGNATION TREATMENT METHOD FOR RECOVERING AND RECYCLING CARBON DIOXIDE AND PRODUCT WHICH IS SUBJECTED TO IMPREGNATION TREATMENT BYTHE METHOD" del inventor Keiichi Kikuchi Mitsuhiro Ohashi Itsuro. Esta invención describe la impregnación de sustancias en un material; a diferencia de la invención que nos ocupa como nueva que está diseñada para diferentes procesos fisicoquímicos que involucran al dióxido de carbono como materia prima y específicamente para un proceso extractivo que se lleve a cabo en condiciones supercríticas, pero puede ser aplicado a otros procesos que requieran recircular CO2. Este antecedente comprime el dióxido de carbono licuado o supercrítico y lo almacena en un tanque, el dióxido de carbono puede ser licuado o supercrítico derivado de un calentamiento de los tanques de almacenamiento. El antecedente no contempla el enfriamiento del gas; mientras que en la nueva invención el dióxido de carbono proveniente del proceso supercrítico a condiciones conocidas de temperatura y presión, ingresa al intercambiador que se encarga de retirar el calor para que el CO2

a una presión constante pueda ser licuado y almacenado en estado líquido dentro del mismo equipo.

Además, el antecedente utiliza un aparato de separación de gas para la eliminación de los componentes sólidos; mientras que la nueva invención cuenta con una etapa de limpieza que consiste en hacer pasar el fluido por filtro de material poroso y por lechos de carbón activado y zeolita funcionalizada para que los residuos queden capturados en la superficie del material absorbente.

La patente estadounidense US20030161780A1 con fecha de prioridad 2001-10-17 denominada "RECYCLE FOR SUPERCRITICAL CARBON DIOXIDE" del Inventor Henry Howard John Billingham es un antecedente que está diseñado para que la etapa de purificación y recirculación funcione de manera continua, utilizando un bypass que devuelve la corriente de CO2 limpia y líquida nuevamente a las etapas de limpieza y compresión, gastando recursos energéticos aún cuando la aplicación no esté en operación. La presente invención no opera de manera continua sino que el fluido es almacenado en un tanque integrado de licuado. El suministro de CO2 en la invención se provee por demanda, solamente mientras la aplicación esté funcionando, lo que también proporciona libertad para escoger el flujo de operación de la aplicación. Este antecedente US20030161780A1 utiliza un complejo sistema de columnas de destilación, lecho de absorción y oxidante catalítico para purificar el CO2 que fluye con contaminantes; mientras que la nueva invención emplea un solo sistema de lecho empacado para realizar la función específica de separación de partículas y retención de impurezas. Además, el antecedente contempla el uso de un compresor y al menos dos bombas para preparar el fluido para la aplicación, a diferencia de la invención, que no contempla el uso de compresor, sino que el CO2 es licuado a una temperatura constante para ser succionado posteriormente por la misma bomba de la aplicación. La presión recomendada para operar el antecedente está a la mitad de la presión que funcionaría con la invención.

Otro antecedente es la patente US6960242B2 con fecha de prioridad 2002-10-02 denominada "CO2 RECOVERY PROCESS FOR SUPERCRITICAL EXTRACTION" del inventor Kelly Leitch Gavin Hartigan Robert D'Orazio donde el dióxido de carbono recirculado no se almacena en estado líquido como en la nueva invención. La

refrigeración del antecedente no opera con agua y en el antecedente, el proceso de reciclo está compuesto por dos etapas: una de alta y otra de baja presión; a diferencia de la invención que integra en una etapa la licuefacción y almacenamiento del fluido.

REVELACIONES DE LA INVENCIÓN

Si bien existen en el estado de la técnica otros aparatos con una funcionalidad similar, no existe ninguna solución tecnológica que integre en un dispositivo los dos procesos de licuado y almacenamiento en una sola etapa de recirculación con las características de la presente invención. En el sistema están presentes todos los detalles de recirculación de CO_2 tales como limpieza del solvente, licuado y almacenamiento, pero de forma integrada. De esta manera se supera el prejuicio de separar las etapas de licuado y almacenamiento porque la invención es un dispositivo que permite realizar estas dos etapas en una sola. El resultado de aplicar este desarrollo no altera las características del producto de la aplicación, así que las ventajas de la técnica se mantienen.

Adicionalmente, la invención proporciona libertad para escoger el flujo de operación en la aplicación, pues, el suministro de CO_2 se provee por demanda solamente mientras la aplicación está funcionando.

El nuevo desarrollo soluciona el problema técnico de la recirculación del dióxido de carbono. Adicionalmente, no se han observado dispositivos que puedan enfriar y contener el fluido en el mismo equipo. Este desarrollo permite realizar en una etapa integrada lo que se llevaría a cabo convencionalmente en dos, licuefacción y almacenamiento. Esto reduce el número de partes de equipo que deben ser construidas lo cual influye en ahorros al momento de su fabricación y operación.

La solución provista a dicho problema técnico no podría ser obvia para un técnico versado en la materia ya que ninguno de los documentos relacionados en el estado de la técnica permiten derivar de su contenido la solución propuesta por la invención objeto de análisis, ni siquiera el antecedente más cercano a la invención, patente US6960242B2, permite inferir el nuevo procedimiento utilizado.

BREVE DESCRIPCION DE LAS FIGURAS

A continuación, se presenta una breve descripción de figuras y la manera de ejecutar la invención con la relación de cada uno de los componentes en la descripción asociados en cada figura:

La figura 1 muestra el esquema con los Componentes del sistema de recirculación de dióxido de carbono que usa un dispositivo integrado de licuado y almacenamiento del fluido.

La figura 2 muestra el condensador de CO2.

La figura 3 muestra el cabezal frontal tipo C de manera detallada.

La figura 4 muestra el casco del condensador.

MEJOR MANERA DE EJECUTAR LA INVENCIÓN

En este nuevo sistema de recirculación de dióxido de carbono que usa un dispositivo integrado de licuado y almacenamiento del fluido, el CO2 en estado gaseoso (18) proveniente de un proceso entre 45 bar - 55 bar y 20°C - 40°C pasa por dos filtros de limpieza, un primer filtro de limpieza (10) con carbón activado y un segundo filtro de limpieza (11) con zeolita funcionalizada ubicados en línea. Posteriormente el CO2 en estado gaseoso (18) pasa por una válvula de bola (17) que controla el paso a un condensador (12). El CO2 en estado gaseoso (18) tiene contacto con la superficie externa de los tubos (13) por los cuales circula en su interior agua refrigerada (14) a una temperatura de entre 9 °C - 11°C; lo que hace, a la presión de operación, que el CO2 se condense.

El CO2 líquido (19) para recirculación sale por la salida de CO2 líquido del condensador (12) y pasa por una válvula de bola (20) manteniendo el CO2 en estado líquido; mientras tanto el CO2 gaseoso es condensado, almacenado en el mismo intercambiador (12). Este tipo de disposición implica la fabricación de un sólo elemento condensador (12) que a su vez almacena fluido. El nuevo sistema de recirculación tiene una unidad condensadora (16) y tiene adaptada una bomba centrifuga (21) para circulación de agua (14) que pasa del reservorio de agua refrigerada (15) al condensador (12).

El Condensador de CO2 (12) es el componente donde se realiza la recuperación, condensación y almacenamiento del CO2, este condensador (12) está sometido a una

presión que varía entre 45 bar a 55 bar dependiendo del proceso, esto hace que la temperatura de su interior se deba mantener entre los 12°C y 18°C para que la condensación se realice de manera eficiente.

El condensador (12) tiene una capacidad de almacenamiento de 25 kilogramos de CO_2 líquido para garantizar el correcto funcionamiento. Consta de tubos (13), porta-tubos (23), brida ciega (24), pernos de brida ciega (25), pernos de base del porta-tubos (26), casco (27), y copa de casco (28). De esta manera el fluido es apto para ser succionado por bombas de desplazamiento positivo con una densidad mínima de 850 kg/m^3. El condensador (12) tiene acoplada una válvula de seguridad para evitar el incremento de la presión en caso de que se interrumpa el flujo eléctrico que mantiene el subsistema de enfriamiento de agua.

Este condensador (12) permite cumplir tanto con los requerimientos de transferencia de calor así como con los requerimientos de almacenamiento de CO_2. Este condensador (12) tiene un cabezal frontal tipo C (29), casco tipo E (30) y cabezal posterior tipo U (37); que corresponden a la descripción a continuación:

El cabezal frontal tipo C (29) tiene pernos (26), brida ciega (24) y placa porta-tubos (23), que permite realizar las labores de limpieza al casco (30) sin tener que desmontar el haz de tubos (13). Se compone de un tubo de acero de 10" (31) con una longitud de 0,2 metros soldado a una brida ciega (24) rating 300 que hace la función de la placa porta tubos; chapa de acero en forma de T (32), niple (33) y niple (34) con sus respectivas tuercas. En su extremo opuesto tiene una brida Slip-On rating 150 que permite el acceso al haz de tubos (13) como se muestra en la figura 3.

El casco tipo E (30) de la figura 4 se configura en el condensador (12) con una entrada superior y una salida inferior. Se compone de un tubo de acero de 10" (35) con una longitud de 1,1 metros soldado a un cabezal posterior tipo U (37) con copa de acero de 10" en la parte superior y una brida *Slip-On* (36) en la parte inferior. La figura 4 muestra el casco (30) junto con la brida ciega (24) que lo compone.

El cabezal posterior tipo U (37) del condensador (12) tiene una configuración permite realizar los cuatro pasos por los tubos (13) de manera independiente sin tener que

involucrar el casco (30), facilitando el retiro del mismo para las labores de mantenimiento. Se compone de los tubos (30) de circulación de agua (14) refrigerante doblados en forma de U de tal manera que le permita al agua refrigerante pasar cuatro veces por el casco (30) antes de abandonar el condensador (12)

El sistema de recirculación de dióxido de carbono que usa un dispositivo integrado de licuado y almacenamiento del fluido tiene los siguientes paramentos en su condensador (12): 124 tubos (13), paso transversal de 17 mm, paso longitudinal de 14,7 mm, diámetro de los tubos de 1/2", material de tubos cobre tipo m, longitud de tubos de 1 m, cuatro pasos por tubo, temperatura entre 9°C-1 1°C, presión en los tubos entre 1 bar - 2 bar y flujo másico de agua refrigerante de 80 g/min - 120 g/min, flujo de CO_2 con cuatro bafles, separación entre bafles de 20 cm, temperatura entrada de 20°C - 35°C, temperatura salida de 12°C - 13°C, densidad mínima de salida 850 kg/m^3, presión en el casco de 55 bar, flujo másico de CO_2 menor de 100 g/min y diámetro de casco 10".

El condensador (12) se caracteriza por un casco con espesor entre 3,45 mm - 9,27 mm, tubos con espesor entre 0,0396 mm - 0,635 mm, placa porta tubos con espesor entre 16,1 mm - 54 mm, 16 pernos con diámetro entre 3/4" - 1", torque de apriete requerido de 1670 Lbf-in, espesor requerido de la brida para el casco entre 53,6 mm - 54 mm.

El subsistema de refrigeración se compone de un reservorio de agua (15), una bomba (21) para desplazarla, un evaporador y una unidad condensadora (16) que emplea como líquido refrigerante R-22 (38) para enfriar el agua (14). Este subsistema se encarga de hacer circular el agua refrigerante por los tubos (13) de cobre que conforman el condensador (12) y almacenador de CO_2. La temperatura del refrigerante dentro de los tubos (13) de cobre deberá ser inferior a los 12°C de tal forma que la temperatura superficial de los mismos sea menor de 12,9°C para obtener CO_2 subenfriado con una densidad mínima de 850 kg/m^3. La cantidad de calor que se requiere extraer al CO_2 el cual se calcula que ingresa a un flujo de 100 g/min a una temperatura de 35°C y a unas condiciones de presión de 55 bar es de 360 Watts equivalentes a 1230 BTU/h ó 310 kcal/h, esto a una temperatura del agua refrigerante de 11°C ya que el proceso de condensación del CO_2 a 55 bar se inicia a los 18,27°C.

REIVINDICACIONES:

1. Sistema de recirculación de dióxido de carbono CARACTERIZADO por un intercambiador de calor de cuatro pasos que licúa el dióxido de carbono y lo almacena en el mismo dispositivo; que tiene acoplado a este intercambiador un subsistema de refrigeración operado con agua; donde el dióxido de carbono proveniente de una aplicación a condiciones conocidas de temperatura y presión ingresa al intercambiador que se encarga de retirar el calor para que el CO_2 a una presión constante pueda ser licuado y almacenado en estado líquido dentro del mismo dispositivo; con esto el CO_2 puede volver a ser presurizado y usado nuevamente ya que el sistema se compone por dos filtros de limpieza, un primer filtro de limpieza (10) con carbón activado y un segundo filtro de limpieza (11) con zeolita funcionalizada ubicados en línea por donde pasa el CO_2 en estado gaseoso (18) proveniente de la aplicación con presión entre 45 bar - 55 bar y 20°C - 40°C, una válvula de bola (17) que controla el paso de CO_2 en estado gaseoso a un condensador (12), en donde el CO_2 en estado gaseoso (18) tiene contacto con la superficie externa de los tubos (13) a la presión de operación a la que se condensa el CO_2, por los cuales circula en su interior agua refrigerada (14) a una temperatura de entre 9 °C - 11°C.
2. Sistema de recirculación de dióxido de carbono de acuerdo con la reivindicación 1 CARACTERIZADO por que el dispositivo integrado de licuado y almacenamiento del fluido se compone de un condensador (12) con una válvula de CO_2 (20) por la que pasa el CO_2 líquido (19) para recirculación; un condensador (12) que condensa CO_2 y que almacena el CO_2 en el mismo recipiente; una bomba centrifuga (21) para circulación de agua (14) que pasa de un reservorio de agua refrigerada (15) al condensador (12) y una unidad condensadora (16).
3. Sistema de recirculación de dióxido de carbono de acuerdo con la reivindicación 1 CARACTERIZADO por que el condensador (12) tiene una capacidad de almacenamiento de 25 kilogramos de CO_2 líquido para garantizar el correcto funcionamiento y consta de tubos (13), porta-tubos (23), brida ciega (24), pernos de brida ciega (25), pernos de base del porta-tubos (26), casco (27), y copa de casco (28).
4. Sistema de recirculación de dióxido de carbono de acuerdo con la reivindicación 1 CARACTERIZADO por que el fluido CO_2 líquido es succionado por bombas de

desplazamiento positivo con una densidad mínima de 850 kg/m^3.

5. Sistema de recirculación de dióxido de carbono de acuerdo con la reivindicación 1 CARACTERIZADO porque el condensador (12) tiene acoplada una válvula de seguridad para evitar el incremento de la presión en caso de que se interrumpa el flujo eléctrico que mantiene el subsistema de enfriamiento de agua.

6. Sistema de recirculación de dióxido de carbono de acuerdo con la reivindicación 1 CARACTERIZADO por que el condensador (12) tiene cabezal frontal tipo C (29), casco tipo E (30) y cabezal posterior tipo U (37); donde el cabezal frontal tipo C (29) tiene pernos (26), brida ciega (24) y placa porta-tubos (23), que permite realizar las labores de limpieza al casco (30) sin tener que desmontar el haz de tubos (13) y se compone de un tubo de acero de 10" (31) con una longitud de 0,2 metros soldado a una brida ciega (24) rating 300 que hace la función de la placa porta tubos; chapa de acero en forma de T (32), niple (33) y niple (34) con sus respectivas tuercas y en su extremo opuesto tiene una brida Slip-On rating 150 que permite el acceso al haz de tubos (13); el casco tipo E (30) se configura en el condensador (12) con una entrada superior y una salida inferior que tiene un tubo de acero de 10" (35) con una longitud de 1,1 metros soldado a un cabezal posterior tipo U (37) con copa de acero de 10" en la parte superior y una brida *Slip-On* (36) en la parte inferior; y donde el cabezal posterior tipo U del condensador (12) tiene una configuración que permite realizar los cuatro pasos por los tubos (13) de manera independiente sin tener que involucrar el casco (30), facilitando el retiro del mismo para las labores de mantenimiento y se compone de los tubos (13) de circulación de agua (14) refrigerante doblados en forma de U de tal manera que le permita al refrigerante pasar cuatro veces por el casco (30) antes de abandonar el condensador (12).

7. Sistema de recirculación de dióxido de carbono de acuerdo con la reivindicación 1 CARACTERIZADO por que el condensador (12) dispositivo integrado de licuado y almacenamiento del fluido tiene los siguientes parámetros en su condensador (12): 124 tubos (13), paso transversal de 17 mm, paso longitudinal de 14,7 mm, diámetro de los tubos de 1/2", material tubos cobre tipo m, longitud tubos de 1 m, cuatro pasos por tubo, temperatura entre 9°C-1 1°C, presión en los tubos entre 1 bar - 2 bar y flujo másico de agua refrigerante de 0,00185 kg/s, flujo de CO2 con cuatro bafles, separación entre bafles de 20 cm, temperatura entrada de 20°C - 35°C, temperatura salida de 12°C - 14°C, densidad mínima de salida 850 kg/m^3,

presión en el casco de 55 bar, flujo másico de CO_2 menor de 100 g/min y diámetro de casco 10".

8. Sistema de recirculación de dióxido de carbono supercrítico de acuerdo con la reivindicación 1 CARACTERIZADO por que el condensador (12) tiene un casco con espesor entre 3,45 mm - 9,27 mm, tubos con espesor entre 0,0396 mm - 0,635 mm, placa porta tubos con espesor entre 16,1 mm - 54 mm, 16 pernos con diámetro entre 3/4" - 1", Torque de Apriete requerido de1670 Lbf-in, espesor requerido de la brida para el casco entre 53,6 mm - 54 mm.

9. Sistema de recirculación de dióxido de carbono de acuerdo con la reivindicación 1 CARACTERIZADO por que el subsistema de Refrigeración se compone de un reservorio de agua (15), una bomba (21) para desplazarla, un evaporador y una unidad condensadora (16) que emplea como líquido refrigerante R-22 (38) para enfriar el agua (14), donde este subsistema se encargada de hacer circular el agua refrigerante por los tubos (13) de cobre que conforman el condensador (12) y almacenador de $C0_2$.(22), cuya temperatura del refrigerante dentro de los tubos (13) de cobre deberá ser inferior a los 12°C de tal forma que la temperatura superficial de los mismos sea menor de 12,9°C para obtener CO_2 subenfriado con una densidad mínima de 850 kg/m^3 y la cantidad de calor que se requiere extraer al CO_2 el cual se calcula que ingresa a una tasa de 100 g/min a una temperatura de 35°C y a unas condiciones de presión de 55 bar es de 360 Watts equivalentes a 1230 BTU/h ó 310 kcal/h a una temperatura del refrigerante de 11°C ya que el proceso de condensación del CO_2 a 55 bar se inicia a los 18,27°C.

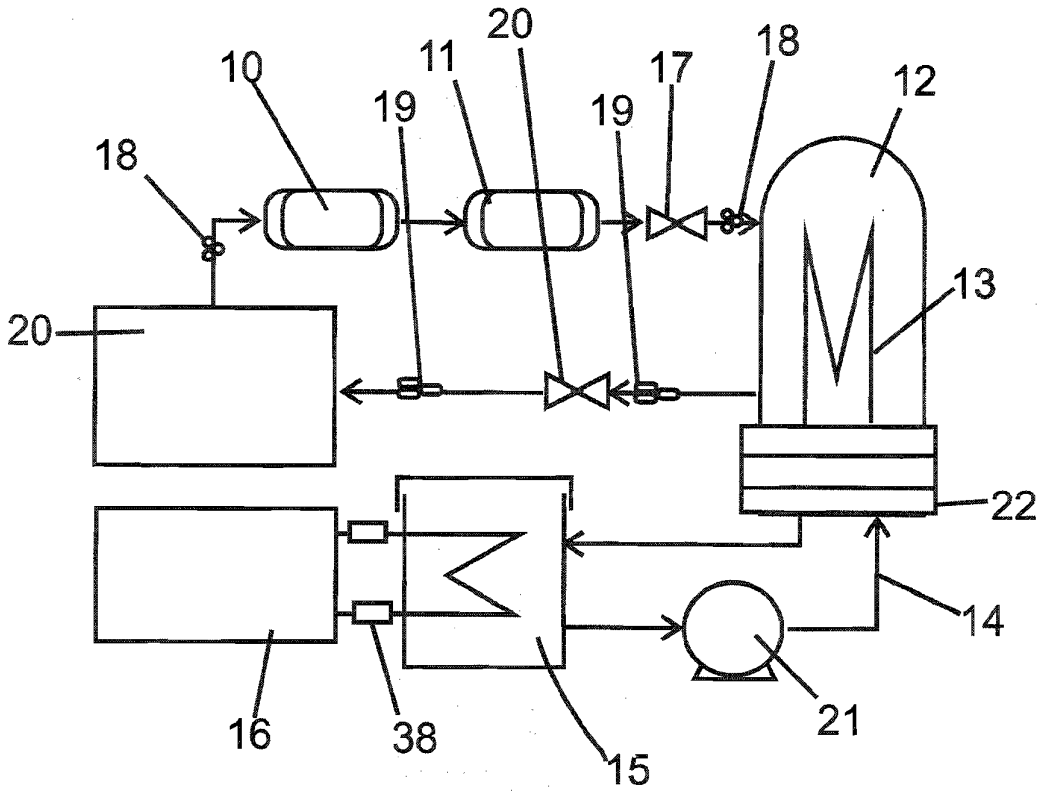

Fig. 1

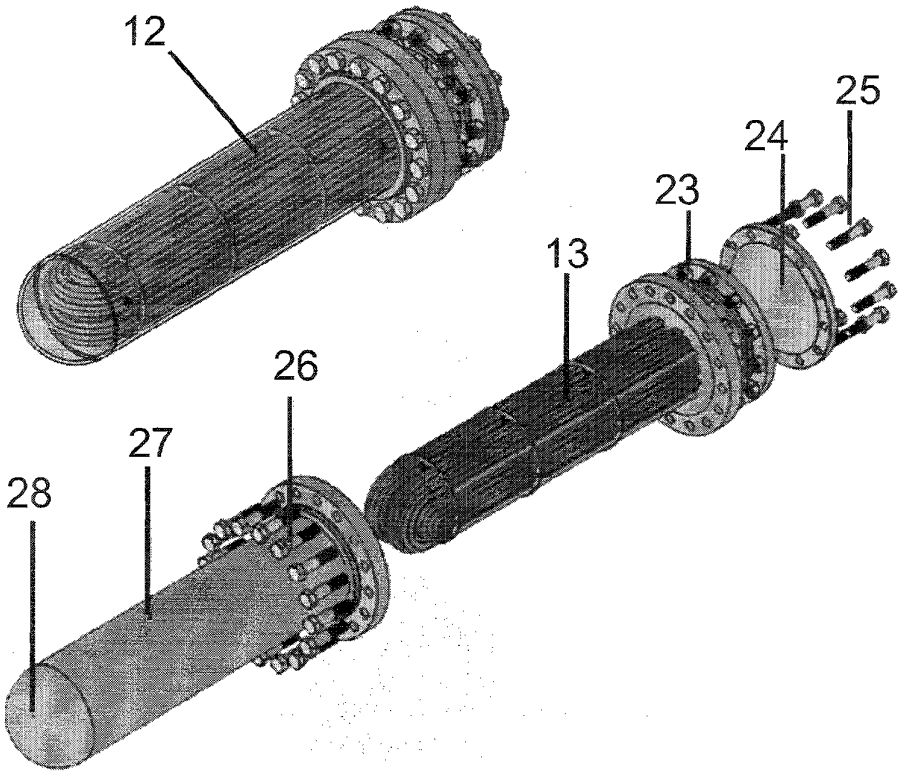

Fig. 2

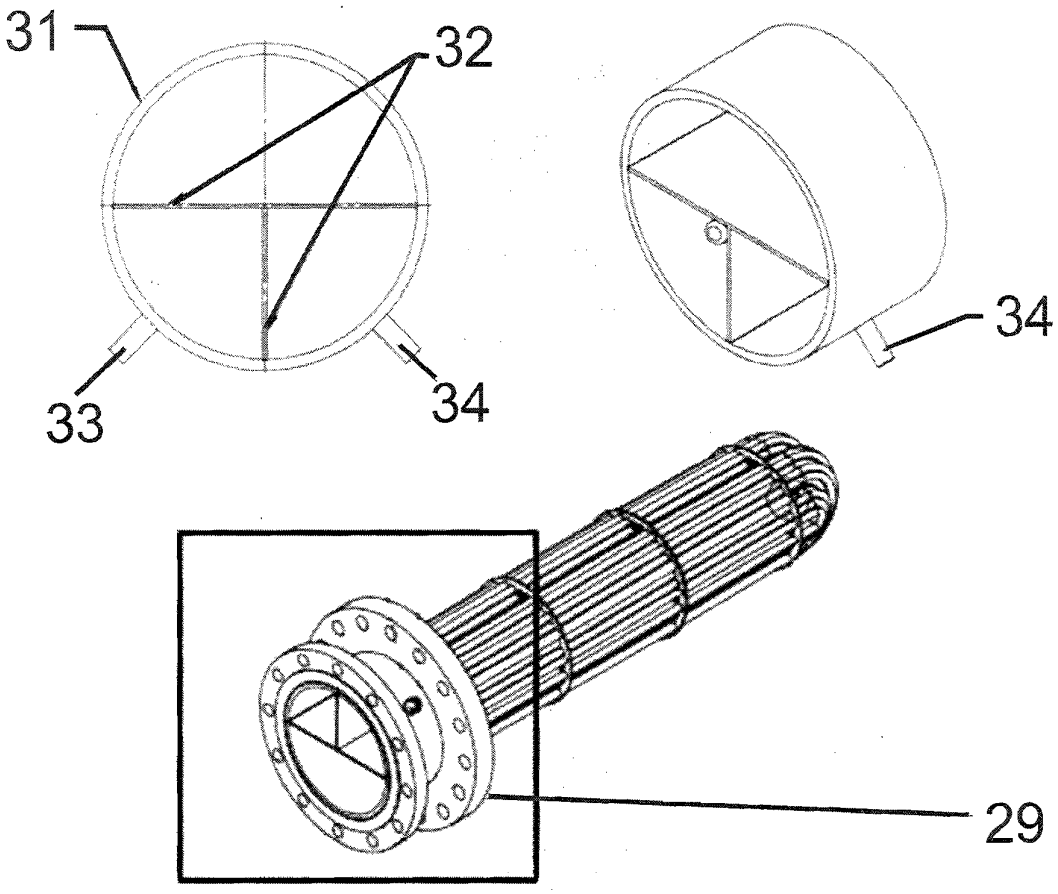

Fig. 3

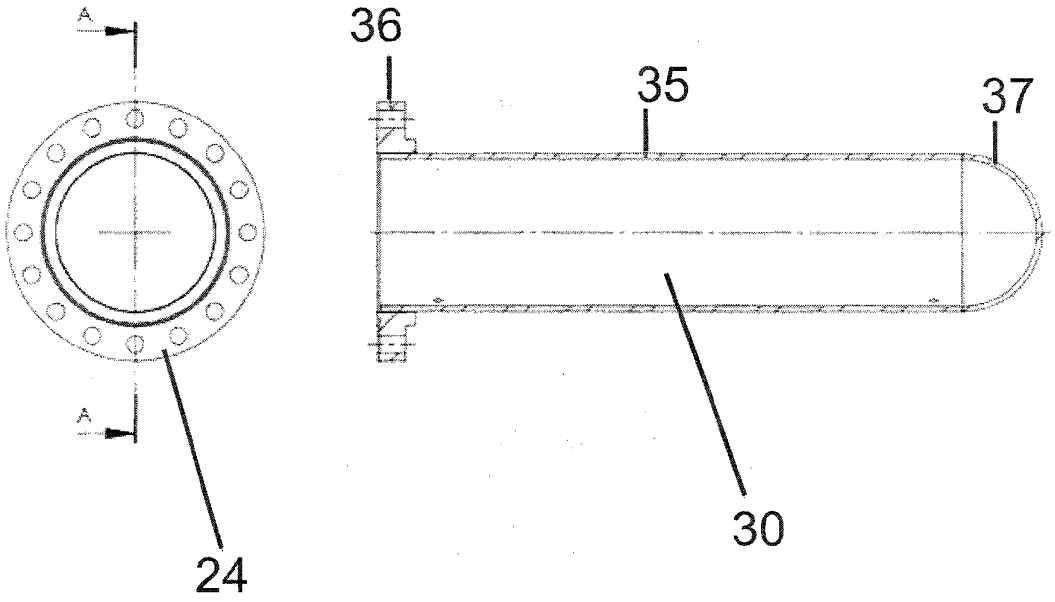

Fig. 4

INTERNATIONAL SEARCH REPORT

International application No.
PCT/IB2017/055640

A. CLASSIFICATION OF SUBJECT MATTER

B0W53/04 (2006.01)
B01D53/62 (2006.01)
According to International Patent Classification (IPC) or to both national classification and IPC

B. FIELDS SEARCHED

Mínimum documentation searched (classification system followed by classification symbols)
B01D

Documentation searched other than mimmum documentation to the extent fhat such documents are included in the fields searched

Electronic data base consulted during the international search (ñame of data base and, where practicable, search terms used)

EPODOC, INVENES

C. DOCUMENTS CONSIDERED TO BE RELEVANT

Category*	Citation of document, with indication, where appropriate, of the relevant passages	Relevant to claim No.
A	US 2015075636 A1 (SUGAWARA HIROSHI ET AL.) 19/03/2015, figures 1 - 2. Paragraphs [0001 -0054];	1-9
A	WO 2012000520 A2 (UNION ENGINEERING AS ET AL.) 05/01/2012, figure 2, paragraph [0019]; [0027- 0033]; [0035 - 0045];	1-9
A	US 2014075984 A1 (SUGAWARA HIROSHI ET AL.) 20/03/2014, figure 1, paragraphs [0015 - 0016]; [0030 - 0045];	1-9
A	US 5772783 A (STUCKER JOHN F) 30/06/1998, columns 5 - 12; figures 1 - 2.	1-9
A	US 4012194 A (MAFFEI RAYMOND L) 15/03/1977, columns 1 - 2; figure 1,	1-9

☒ Furfher documents are listed in the continuation of Box C. ☒ See patent family annex.

* Special categories of cited documents:
"A" document defining the general state of the art which is not considered to be of particular relevance.
"E" earlier document but published on or after the international filing date
"L" document which may throw doubts on priority claim(s) or which is cited to establish the publication date of another citation or other special reason (as specified)
"O" document referring to an oral disclosure use, exhibition, or other means.
"P" document published prior to the international filing date but later than the priority date claimed
"T" later document published after the international filing date or priority date and not in conflict wifh the application but cited to understand the principie or theory underlying the invention
"X" document of particular relevance; the claimed invention cannot be considered novel or cannot be considered to involve an inventive step when the document is taken alone
"Y" document of particular relevance; the claimed invention cannot be considered to involve an inventive step when the document is combined with one or more other documents , such combination being obvious to a person skilled in the art
"&" document member of the same patent family

Date of the actual completion of the international search	Date of mailing of the international search report
02/02/2018	**(05/02/2018)**
Ñame and mailing address of the ISA/ OFICINA ESPAÑOLA DE PATENTES Y MARCAS Paseo de la Castellana, 75 - 28071 Madrid (España) Facsímile No.: 91 349 53 04	Authorized officer C. Galdeano Villegas Telephone No. 91 3493099

Form PCT/ISA/210 (second sheet) (January 2015)

INTERNATIONAL SEARCH REPORT

International application No.
PCT/IB2017/055640

C (continuation). DOCUMENTS CONSIDERED TO BE RELEVANT

Category *	Citation of documents, with indication, where appropriate, of the relevant passages	Relevant to claim No.
A	US 5267455 A (DEWEES THOMAS G ET AL.) 07/12/1993, columns 2 - 4; figure 1,	1-9
A	EP 1405662 A2 (BOC GROUP INC) 07/04/2004, figure 1, paragraphs [0016 - 0039];	1-9

INTERNATIONAL SEARCH REPORT

Information on patent family members

International application No.
PCT/IB2017/055640

Patent document cited in the search report	Publication date	Patent family member(s)	Publication date
US2015075636 A1	19.03.2015	KR20140122259 A	17.10.2014
		KR101619007B B1	09.05.2016
		CN104105540 A	15.10.2014
		CN104105540B B	10.08.2016
		TW201345596 A	16.11.2013
		TWI558450B B	21.11.2016
		JP2013159501 A	19.08.2013
		JP5912596B B2	27.04.2016
		WO2013115156 A1	08.08.2013
WO2012000520 A2	05.01.2012	ZA201300171 B	26.03.2014
		ES2531570T T3	17.03.2015
		DK2588215T T3	09.03.2015
		CL2012003717 A1	12.07.2013
		NZ606552 A	29.08.2014
		JP2013536142 A	19.09.2013
		JP5886281B B2	16.03.2016
		EA201390052 A1	30.05.2013
		EA023639 B1	30.06.2016
		US2013133363 A1	30.05.2013
		US9851143 B2	26.12.2017
		KR20130032382 A	01.04.2013
		MX2012015031 A	29.01.2013
		CN102985160 A	20.03.2013
		CN102985160B B	09.03.2016
		AP3744 A	30.06.2013
		AP2013006691 A0	30.06.2013
		AU2011274008 A1	21.02.2013
		AU2011274008B B2	26.03.2015
		CA2802231 A1	05.01.2012
		EP2588215 A2	08.05.2013
		EP2588215 B1	03.12.2014
US2014075984 A1	20.03.2014	KR20160021305 A	24.02.2016
		JPWO2012157648 A1	31.07.2014
			30.04.2015
		JP5707491B B2	28.03.2017
		US9605895 B2	21.01.2014
		KR20140008454 A	29.01.2014
		CN103547531 A	23.09.2015
		CN103547531B B	16.03.2013
		TW201311335 A	21.05.2017
		TWI583435B B	22.11.2012
		WO2012157648 A1	
US5772783 A	30.06.1998		04.07.2000
		US6082150 A	23.05.1996
		WO9615304 A1	17.08.1999
		US5937675 A	27.08.1997
		EP0791093 A1	11.04.2001
		EP0791093 B1	23.08.2001
		DE69520687T T2	

INTERNATIONAL SEARCH REPORT

Information on patent family members

International application No.
PCT/IB2017/055640

Patent document cited in the search report	Publication date	Patent family member(s)	Publication date
		AU4106696 A	06.06.1996
US4012194 A	15.03.1977	NONE	
US5267455 A	07.12.1993	US5412958 A	09.05.1995
		WO9401613 A1	20.01.1994
		JPH07508904 A	05.10.1995
		ES2151513T T3	01.01.2001
		EP0651831 A1	10.05.1995
		EP0651831 A4	02.11.1995
		DE69329619T T2	08.03.2001
		CA2139950 A1	20.01.1994
		BR9306717 A	08.12.1998
		AU4672593 A	31.01.1994
		AU666037B B2	25.01.1996
EP1405662 A2	07.04.2004	TW200413079 A	01.08.2004
		US2004118281 A1	24.06.2004
		US6960242 B2	01.11.2005
		JP2004122127 A	22.04.2004

INFORME DE BÚSQUEDA INTERNACIONAL

Solicitud internacional n°
PCT/IB2017/055640

A. CLASIFICACIÓN DEL OBJETO DE LA SOLICITUD
B0W53/04 (2006.01)
B01D53/62 (2006.01)
De acuerdo con la Clasificación Internacional de Patentes (CIP) o según la clasificación nacional y CIP.

B. SECTORES COMPRENDIDOS POR LA BÚSQUEDA

Documentación mínima buscada (sistema de clasificación seguido de los símbolos de clasificación)
B01D

Otra documentación consultada, además de la documentación mínima, en la medida en que tales documentos formen parte de los sectores comprendidos por la búsqueda

Bases de datos electrónicas consultadas durante la búsqueda internacional (nombre de la base de datos y, si es posible, términos de búsqueda utilizados)
EPODOC, INVENES

C. DOCUMENTOS CONSIDERADOS RELEVANTES

Categoría*	Documentos citados, con indicación, si procede, de las partes relevantes	Relevante para las reivindicaciones n°
A	US 2015075636 A1 (SUGAWARA HIROSHI ET AL.) 19/03/2015, figuras 1 - 2. Párrafos [0001 -0054];	1-9
A	WO 2012000520 A2 (UNION ENGINEERING AS ET AL.) 05/01/2012, figura 2, párrafo [0019]; [0027 - 0033]; [0035 - 0045];	1-9
A	US 2014075984 A1 (SUGAWARA HIROSHI ET AL.) 20/03/2014, figura 1, párrafos[0015 - 0016];[0030 - 0045];	1-9
A	US 5772783 A (STUCKER JOHN F) 30/06/1998, columnas 5 - 12; figuras 1 - 2.	1-9
A	US 4012194 A (MAFFEI RAYMOND L) 15/03/1977, columnas 1 - 2; figura 1,	1-9

|X| En la continuación del recuadro C se relacionan otros documentos ☒ Los documentos de familias de patentes se indican en el anexo

* Categorías especiales de documentos citados:

"A" documento que define el estado general de la técnica no considerado como particularmente relevante.

"E" solicitud de patente o patente anterior pero publicada en la fecha de presentación internacional o en fecha posterior.

"L" documento que puede plantear dudas sobre una reivindicación de prioridad o que se cita para determinar la fecha de publicación de otra cita o por una razón especial (como la indicada).

"O" documento que se refiere a una divulgación oral, a una utilización, a una exposición o a cualquier otro medio.

"P" documento publicado antes de la fecha de presentación internacional pero con posterioridad a la fecha de prioridad reivindicada.

"T" documento ulterior publicado con posterioridad a la fecha de presentación internacional o de prioridad que no pertenece al estado de la técnica pertinente pero que se cita por permitir la comprensión del principio o teoría que constituye la base de la invención.

"X" documento particularmente relevante; la invención reivindicada no puede considerarse nueva o que implique una actividad inventiva por referencia al documento aisladamente considerado.

"Y" documento particularmente relevante; la invención reivindicada no puede considerarse que implique una actividad inventiva cuando el documento se asocia a otro u otros documentos de la misma naturaleza, cuya combinación resulta evidente para un experto en la materia.

"&" documento que forma parte de la misma familia de patentes.

Fecha en que se ha concluido efectivamente la búsqueda internacional.	Fecha de expedición del informe de búsqueda internacional.
02/02/2018	**05 de febrero de 2018 (05/02/2018)**
Nombre y dirección postal de la Administración encargada de la búsqueda internacional OFICINA ESPAÑOLA DE PATENTES Y MARCAS Paseo de la Castellana, 75 - 28071 Madrid (España) N° de fax: 91 349 53 04	Funcionario autorizado C. Galdeano Villegas N° de teléfono 91 3493099

INFORME DE BÚSQUEDA INTERNACIONAL

Solicitud internacional n°

PCT/IB2017/055640

C (Continuación). DOCUMENTOS CONSIDERADOS RELEVANTES

Categoría *	Documentos citados, con indicación, si procede, de las partes relevantes	Relevante para las reivindicaciones n°
A	US 5267455 A (DEWEES THOMAS G ET AL.) 07/12/1993, columnas 2 - 4; figura 1,	1-9
A	EP 1405662 A2 (BOC GROUP INC) 07/04/2004, figura 1, párrafos [0016 - 0039];	1-9

INFORME DE BÚSQUEDA INTERNACIONAL

Informaciones relativas a los miembros de familias de patentes

Solicitud internacional nº

PCT/IB2017/055640

Documento de patente citado en el informe de búsqueda	Fecha de Publicación	Miembro(s) de la familia de patentes	Fecha de Publicación
US2015075636 A1	19.03.2015	KR20140122259 A	17.10.2014
		KR101619007B B1	09.05.2016
		CN104105540 A	15.10.2014
		CN104105540B B	10.08.2016
		TW201345596 A	16.11.2013
		TWI558450B B	21.11.2016
		JP2013159501 A	19.08.2013
		JP5912596B B2	27.04.2016
		WO2013115156 A1	08.08.2013
WO2012000520 A2	05.01.2012	ZA201300171 B	26.03.2014
		ES2531570T T3	17.03.2015
		DK2588215T T3	09.03.2015
		CL2012003717 A1	12.07.2013
		NZ606552 A	29.08.2014
		JP2013536142 A	19.09.2013
		JP5886281B B2	16.03.2016
		EA201390052 A1	30.05.2013
		EA023639 B1	30.06.2016
		US2013133363 A1	30.05.2013
		US9851143 B2	26.12.2017
		KR20130032382 A	01.04.2013
		MX2012015031 A	29.01.2013
		CN102985160 A	20.03.2013
		CN102985160B B	09.03.2016
		AP3744 A	30.06.2013
		AP2013006691 A0	30.06.2013
		AU2011274008 A1	21.02.2013
		AU2011274008B B2	26.03.2015
		CA2802231 A1	05.01.2012
		EP2588215 A2	08.05.2013
		EP2588215 B1	03.12.2014
US2014075984 A1	20.03.2014	KR20160021305 A	24.02.2016
		JPWO2012157648 A1	31.07.2014
			30.04.2015
		JP5707491B B2	28.03.2017
		US9605895 B2	21.01.2014
		KR20140008454 A	29.01.2014
		CN103547531 A	23.09.2015
		CN103547531B B	16.03.2013
		TW201311335 A	21.05.2017
		TWI583435B B	22.11.2012
		WO2012157648 A1	
US5772783 A	30.06.1998		04.07.2000
		US6082150 A	23.05.1996
		WO9615304 A1	17.08.1999
		US5937675 A	27.08.1997
		EP0791093 A1	11.04.2001
		EP0791093 B1	23.08.2001
		DE69520687T T2	

INFORME DE BÚSQUEDA INTERNACIONAL

Informaciones relativas a los miembros de familias de patentes

Solicitud internacional nº

PCT/IB2017/055640

Documento de patente citado en el informe de búsqueda	Fecha de Publicación	Miembro(s) de la familia de patentes	Fecha de Publicación
		AU4 106696 A	06.06.1996
US4012194 A	15.03.1977	NINGUNO	
US5267455 A	07.12.1993	US5412958 A	09.05.1995
		WO9401613 A1	20.01.1994
		JPH07508904 A	05.10.1995
		ES2151513T T3	01.01.2001
		EP0651831 A1	10.05.1995
		EP0651831 A4	02.11.1995
		DE69329619T T2	08.03.2001
		CA2139950 A1	20.01.1994
		BR9306717 A	08.12.1998
		AU4672593 A	31.01.1994
		AU666037B B2	25.01.1996
EP1405662 A2	07.04.2004	TW200413079 A	01.08.2004
		US2004 118281 A1	24.06.2004
		US6960242 B2	01.11.2005
		JP2004122127 A	22.04.2004

Appendix B. Analytical methodology

Metodología validada para la medición instrumental multicomponente de flavonoides en extractos de plantas con sus respectivas figuras de mérito

Julián Arias y Andrés Cáceres

A continuación, se presenta una metodología que emplea el método de calibración multivariada *Inverse Least Square*, ILS por sus siglas en inglés para predecir la concentración de flavonoides a partir de una muestra de extracto. La calibración del método se lleva a cabo con mezclas previamente cuantificadas por HPLC-DAD, una metodología analítica ampliamente usada y aceptada por la comunidad científica para cuantificación. La metodología que se expone se ejemplifica con las moléculas de pinocembrina y galangina, las cuales están presentes en el extracto supercrítico de *Lippia origanoides*. El modelo multivariado que predice la concentración de los flavonoides a partir de los espectros en mezcla fue validado a partir de los datos de calibración empleando el método de validación cruzada *Leave One Out*, LOO por sus siglas en inglés. Los resultados de la aplicación de esta metodología cumplen satisfactoriamente el propósito de remplazar la metodología analítica de separación cromatográfica por la descomposición multivariable del espectro de UV de la mezcla de extracto. Ya que usar espectroscopía en lugar de cromatografía líquida para cuantificar muestras tiene algunas ventajas, e.g. el espectro UV puede ser medido de forma inmediata, *in situ* y relativamente rápido, permitiendo procesar un número mayor de muestras. Además, los costos de medición y demanda de espacio físico son mayores comparado con montajes de HPLC.

1. Metodología

1.1 Espectroscopía UV

Para determinar el contenido de los flavonoides (pinocembrina y galangina) en las muestras, fue empleado el espectrofotómetro miniatura UV-VIS (FLAME-S-UV-VIS-ES, 200-850 nm rango de longitud de onda, 25 µm de apertura, 1:5 nm de resolución focal (FWHM), lentes tipo L2 y un sensor de detección Sony ILX511b) con lentes colimadores (74-UV,5 mm de diámetro, 10 mm de longitud focal y 200-2000 nm rango de longitudes de onda), una fuente de luz halógena y de deuterio (DH-2000-DUV, rango de longitud de onda 190-2500 nm), sondas de fibra óptica QP455-025-XSR-BX, resistencia a solarización y rango de longitudes de onda de 180-900 nm). Estos equipos fueron obtenidos de Ocean Optics (Dunedin, EE. UU). Una cubeta de cuarzo SIGMA C-9292 (Steinheim, Alemania) fue utilizada para cargar las soluciones a medir y pasar a través de ella un haz de luz proveniente de la fuente. El espectro ultravioleta fue medido de 200 a 400 nm.

1.2 Cromatografía líquida

Para la identificación y cuantificación de los falvonoides (pinocembrina y galangina) se empleó un cromatógrafo líquido de alta eficiencia Agilent Technologies HPLC 1260 Infinity (Palo Alto, California, EE. UU.), acoplado a un detector de arreglo de diodos (DAD G1315D) y un detector de onda múltiple (G1365D). La separación de los analitos se realizó en una columna C18 Gemini (Phenomenex, Torrance, CA, EE. UU), 250 mm, L, x 4.6 mm, D.I., x 5 µm de tamaño de partícula, la detección de los compuestos se realizó a 290 nm. La fase móvil fue A: agua (0,5 % de ácido fórmico) y B: acetonitrilo. El flujo fue de 1 mL/min y el volumen de inyección de 10 µL. La programación del método fue 0 min: 98% B, 15 min: 88% B, 15-23 min: 88% B, 46 min: 60% B, 71 min: 10% B, 71-75 min: 10% B, 80 min: 98% B, 80-85 min: 98% B.

1.3 Calibración para cuantificación de muestras de entrenamiento

La metodología de calibración en HPLC utilizando patrón externo fue empleada. Este método utiliza curvas de calibración de sustancias de referencia para relacionarlas con el área cromatográfica de cada pico obtenido [1]. Las muestras seleccionadas como grupo de entrenamiento para la calibración multivariada fueron cuantificados por estas curvas. Cada punto de la curva fue preparado tres veces desde una solución madre que contiene una mezcla de patrones de los flavonoides, para el caso de nuestro ejemplo fueron pinocembrina y galangina a iguales concentraciones. Los valores de concentración fueron 12.8, 38.3, 63.8, 102, 127.5, 255.1 y 510 mg/g respectivamente. Las curvas de calibración fueron preparadas y analizadas a las mismas condiciones cromatográficas que las muestras a ser medidas.

Contextualización. *La calibración multivariada es comúnmente usada para determinar la concentración de sustancias presentes en una mezcla utilizando análisis espectral. Aquí, las concentraciones de los analitos son las variables para predecir y las absorbancias en un rango de longitudes de onda son la respuesta a estas variables. El análisis multivariado es apropiado cuando el espectro de las sustancias presentes en la mezcla se superpone, es decir que tienen una respuesta de absorbancia a las mismas longitudes de onda. Esto ocasiona que no pueda distinguirse la respuesta instrumental que corresponde a cada sustancia y por lo tanto utilizar calibración univariada no ofrece una buena estimación. Utilizando calibración multivariada e información suficiente sobre mezclas de concentración conocida es posible determinar qué parte de la respuesta instrumental corresponde a cada sustancia y así determinar de forma precisa su concentración. El método de mínimos cuadrados inverso (ILS), es uno de los métodos más comunes que pueden ser utilizados para este fin. Este método tiene también una ventaja comparado con el método de mínimos cuadrados directo, ya que minimiza el error durante la calibración [2]. Para realizar los cálculos de la concentración de los analitos se utilizan las ecuaciones descritas a continuación:*

$$Z = b \cdot R\,, \qquad (1a)$$

$$b = [S^T \cdot S]^{-1} \cdot S^T, \qquad (1b)$$

$$S = [c \cdot c^T]^{-1} \cdot c \cdot A, \qquad (1c)$$

Donde, $Z(i \times k)$ *es la matriz de concentraciones desconocidas de los analitos a estimar,* i *es el número de analitos que se considera están presentes en la muestra y* k *es el número de mezclas de concentración desconocida que se desean calcular.* $R\ (j \times k)$ *es la matriz de absorbancias medidas de las mezclas desconocidas, donde* j *es el número de longitudes de onda seleccionadas en el espectro, y* $b\ (i \times j)$ *es el factor de respuesta a cada longitud de onda (columnas) y a cada analito (filas) [3]. Este factor de respuesta puede ser estimado utilizando la Eq. 1b donde* $S\ (j \times i)$*, es la matriz de espectros puros de cada analito cuando están en mezcla.*

1.4 Muestras de entrenamiento del modelo de calibración

Para fines de calibración multivariada, se consideró que las muestras son una mezcla de pinocembrina, galangina y un pseudo-componente, el cual contiene información agrupada acerca de otros componentes presentes en el extracto supercrítico de *Lippia origanoides*. Este pseudo compuesto tienen en menor proporción absorbancia en la región ultravioleta. Este pseudo-componente es considerado como una interferencia dentro del modelo. De este modo, el factor de respuesta para esta sustancia es un vector-parámetro optimizable que permite mejorar la predicción de la concentración de pinocembrina y galangina en las soluciones. El espectro puro de cada analito (en mezcla) es calculado utilizando la Ec. 1c, donde $A(j \times n)$ es la matriz de absorbancias de las mezclas de calibración y n es el número de mezclas de calibración utilizadas. $c(i \times n)$ es la matriz de concentraciones conocidas de cada mezcla de calibración. Para estas mezclas, fueron preparados tres grupos de datos con el fin de proporcionar suficiente información de entrenamiento a ILS cuando ocurren interacciones entre las tres sustancias a diferentes concentraciones.

El primer grupo de datos fue (GD1) nueve mezclas de patrones de referencia de pinocembrina y galangina a las concentraciones: 21.6:10.7, 21.6:7.5, 21.6:4.3, 13:6.5, 13:4.5, 13:2.6, 4.4:2.1, 4.4:1.5, 4.4:0.9 µg/g, las cuales fueron medidas gravimétricamente. El segundo grupo de datos (GD2) fue preparado mezclando a una concentración constante de extracto (2.6 mg/g) con cinco mezclas de patrones a las concentraciones de pinocembrina:galangina 2.8:1.3, 5.6:2.6, 8.1:4.1, 10.8:5.5, 13.6:7.3 µg/g. Finalmente, el tercer grupo de datos (GD3) fue preparado a tres niveles de concentración del extracto: 2.6, 7.7 and 12.8 mg/g). Para medir el espectro ultravioleta de GD2 y GD3 fueron tomados 100 µL de la muestra preparada para HPLC, y luego aforados a 5 mL en MeOH, debido a que soluciones de alta concentración pueden causar desviaciones del comportamiento lineal de la absorbancia. Todas las mezclas fueron preparadas por triplicados. En resumen, fueron preparadas y medidas por triplicado 17 mezclas para calibración multivariada.

1.5 Validación del modelo

La metodología de validación cruzada *"Leave one out"* fue utilizada para determinar la capacidad del modelo para predecir una determinada concentración sin información de uno de los triplicados. Los valores de Q^2 fueron calculados para los modelos de pinocembrina y galangina como una medición de la calidad de predicción alcanzada con los grupos de datos de calibración. Sumado a esto los datos predichos con el modelo fueron comparados con los datos encontrados por HPLC para las muestras de calibración.

2. Resultados

Las curvas de calibración con estándares de pinocembrina y galangina para cromatografía líquida (HPLC) tuvieron las siguientes figuras de mérito: R^2 0.9997 and 0.9990, LOD (0.15 µg/g 0.32 ug/g), factor de respuesta 12.2 y 30.0 µg/g·cuentas, intercepto 46 y 143 µg/g, RMSE 0.01 y 0.02, respectivamente. Estas curvas de calibración fueron utilizadas para determinar la concentración de las muestras en GD2 y GD3. La Fig. 1 muestra el perfil cromatográfico típico de un extracto con CO2 y EtOH de LOF. Los compuestos mayoritarios que tienen una respuesta de absorbancia ultravioleta son galangina y pinocembrina los que corresponden los picos 1 y 2, respectivamente. Otros picos pueden ser observados en el cromatograma y en conjunto representan la interferencia.

Usar todas las mezclas para entrenar ILS no fue apropiado para la calibración multivariada. Utilizando solamente los GD2 y GD3, el modelo alcanzó valores de RMSE de 0.09 y 0.04 µg/g, para pinocembrina y galangina, respectivamente. Analizando por separado se obtuvo un RMSE para GD2 de 0.08 y 0.04 y para GD3 de 0.2 y 0.09. En cuanto al método "*Leave one out*" en la validación cruzada, se realizó la calibración del modelo sacando uno de los puntos por triplicado. Es decir, si GD2 y GD3 tienen en total 24 puntos, se sacó un triplicado. Con los 21 puntos restantes se calculó un vector de factores de respuesta nuevo "b" y luego se calculó el punto excluido. Esto se realizó con todos los triplicados (8), teniendo así la predicción de ocho puntos excluidos a partir de información ajena a ese punto. Al relacionar

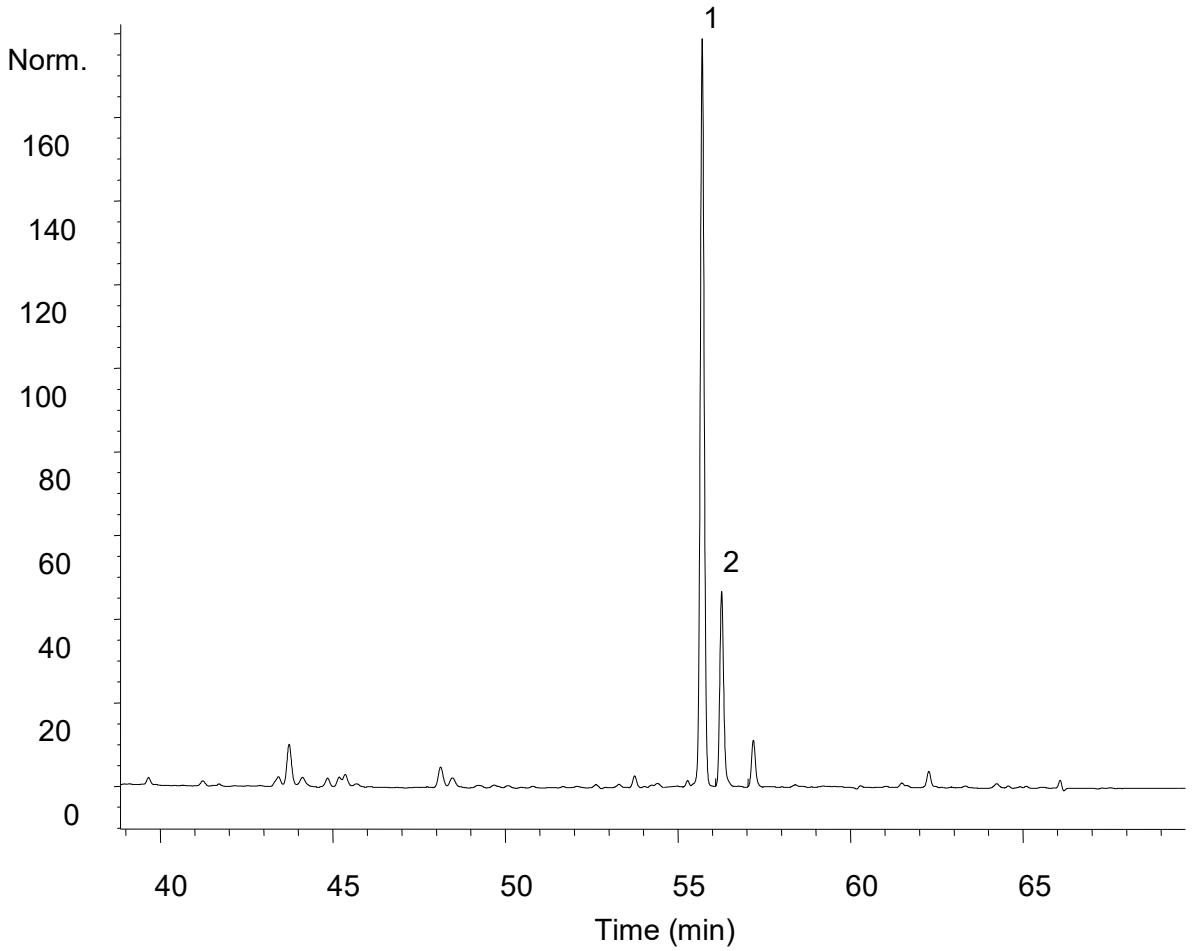

Figura 1. Perfil cromatográfico típico de un extracto con CO2-EtOH de *Lippia origanoides* quimiotipo felandreno.

todos los datos calculados y los experimentales que fueron excluidos se puede obtener el valor de Q^2 para los modelos de pinocembrina y galangina. Estos valores fueron de 0.943 y 0.953 para pinocembrina y galangina.

2.1 Composición del extracto y la interferencia

En la Figura 1 se observa el perfil cromatográfico típico de un extracto de material vegetal pos-destilado de *Lippia* origanoides quimiotipo Felandreno utilizando CO_2-EtOH supercrítico. Los picos no identificados, que fueron llamados previamente como componentes que también absorben en la región ultravioleta y juntos representan la interferencia (para propósitos de modelamiento). Varios autores han reportado la presencia

de más moléculas diferentes de pinocembrina y galangina en los extractos de *Lippia origanoides* utilizando técnicas analíticas como HPLC-DAD y UHPLC-MS. Stashenko encontró naringenina y luteolina [4], Lin *et al.* encontraron pentahydroxyfavanona-A-hexosido, naringenina y 6-hydroxyluteolin 7-O-hexosido [5] Leitão *et al.* reportó eriodictiol, naringenina y rhammnocitrina [6]. La mayoría de estas moléculas ha sido identificadas como parte de la biosíntesis de flavonoides [7,8]. Estos compuestos minoritarios son presumiblemente los picos no identificados en el cromatograma de la Figura 1. Considerando estas moléculas para calibración, podría no ser conveniente ya que las respuestas individuales de absorbancia son muy pequeñas para ser cuantificadas de forma precisa utilizando espectroscopía. Además, introducir más sustancias al modelo de calibración causa una reducción en la precisión de la estimación de pinocembrina y galangina. Esto debido a que cuando más moléculas son consideradas, el modelo tendrá menos grados de libertad para ajustar los factores de respuesta cuando minimice el error.

2.2 Modelo de calibración multivariada y su comparación HPLC-DAD

Cuando todos los grupos de datos son incluidos para la calibración multivariada utilizando (ILS), el RMSE[1] para pinocembrina y galangina fue de 0.22 y 0.06 μg/g, respectivamente. Cuando se analizó el RMSE de forma individual para cada grupo de datos se encontró que el modelo estimaba de una mejor forma el GD1 (0.25 y 0.08 μg/g), el cual no contiene ninguna interferencia, comparado con los GD2 (0.43 and 0.12 μg/g) y GD3 (0.65 and 0.09 μg/g). Puede observarse que la presencia o ausencia de los interferentes en los grupos de mezclas de calibración afecta negativamente la precisión del modelo. El GD1 fue preparado y alimentado al modelo con el fin de que aumentara la información disponible acerca del comportamiento del espectro UV a diferentes cantidades relativas de galangina y pinocembrina. Sin embargo, cuando este grupo de datos es incluido, el modelo no logró una buena estimación para las mezclas que contienen interferentes. Esto quiere decir que la

[1] *Root Mean Square Error* o error cuadrático medio

presencia de estas sustancias que también absorben en la región ultravioleta afecta fuertemente el comportamiento del espectro UV de pinocembrina y galangina en las mezclas. Todas las muestras que se quieren cuantificar contienen estos mismos interferentes. Por tal razón, el modelo fue recalibrado excluyendo el GD1. Los grupos de datos fueron preparados de tal forma que todos los casos de concentraciones relativas entre las tres sustancias fueran abarcadas, con el fin de representar las interacciones en muestras reales. Los GD2 y GD3 proporcionan información sobre el comportamiento del espectro UV, cuando la concentración de los interferentes es constante y diferente, respectivamente.

De esta forma, el modelo alcanzó valores de RMSE de 0.09 y 0.04 μg/g para todos los datos, 0.08 y 0.04 μg/g para GD2 y 0.2 y 0.09 μg/g para el GD3, para pinocembrina y galangina, respectivamente. Para propósitos de modelamiento la interferencia fue considerada como la masa de extracto diferente a pinocembrina y galangina, calculada a partir de un balance de masa. La mayoría de esta masa no absorbe en la región ultravioleta, sin embargo nosotros consideramos que la interferencia en la región UV es proporcional a esta masa. Esto permitió al modelo tomar en cuenta la influencia de la interferencia, lo cual mejoró la precisión en la estimación de las cantidades de pinocembrina y galangina. Sin embargo, esta consideración no permite (y no es su objetivo) predecir los valores de concentración de las interferencias debido a la imposibilidad de determinar su concentración real en las mezclas de entrenamiento.

La Fig. 2 muestra la comparación de las concentraciones calculadas para las mezclas de calibración utilizando ILS contra los valores de concentración obtenidos utilizando HPLC para lo datos de calibración GD2 y GD3. El coeficiente de determinación para pinocembrina y galangina fueron de R^2=0.994 and R^2=0.994, respectivamente. Las figuras de mérito para la calibración multivariada fueron calculadas basándose en las relaciones descritas por Booksh y Wang [9]: Selectividad = 0.478 and 0.225, LOD = 0.877 and 1.470 μg/g, sensibilidad = 0.788 and 0.470 g·A/μg, %AARD = 4.9 y 17.1 para pinocembrina y galangina, respectivamente. Cómo se observa los datos están fuertemente correlacionados linealmente

pero como era de esperarse, se obtiene una estimación más precisa de la concentración empleando la técnica HPLC, si se comparan los RMSE. Sin embargo, los valores de desviación obtenidos con ILS son aceptables para los propósitos de este trabajo. El anexo adjunto contiene el código implementado en Scilab para calcular los modelos de ILS a partir de datos de entrenamiento y sus respectivas figuras de mérito.

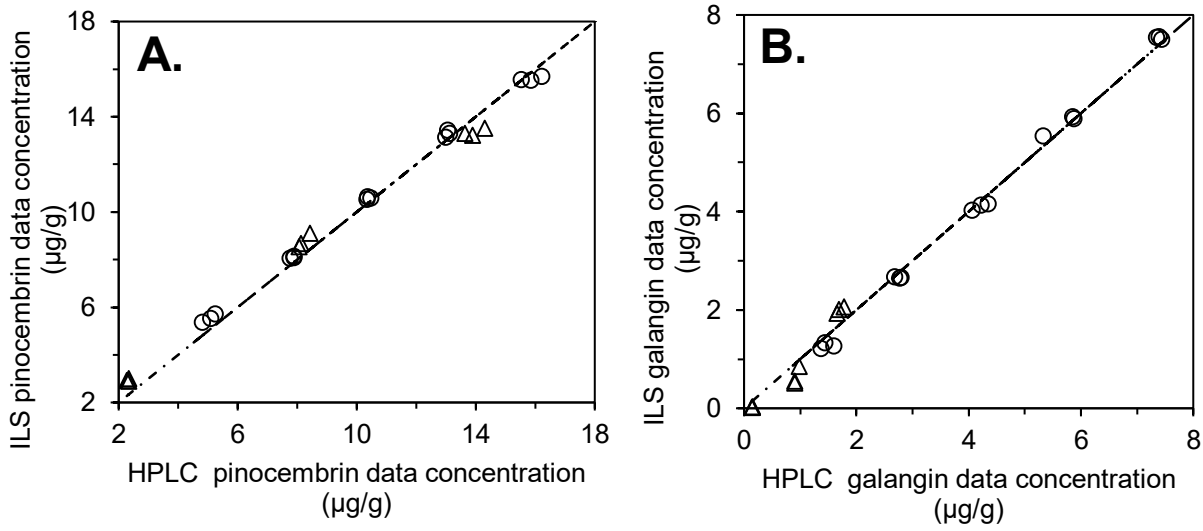

Figura 2. Valores de concentración predicha usando ILS versus valores de concentración encontrados con HPLC usando el método externo de calibración. (A) Pinocembrina, (B) Galangina. R^2=0.994 para ambas moléculas

3. Bibliografía

[1] J.N. Miller, J.C. Miller, Statistics and chemometrics for analytical chemistry, Sixth, Pearson Education, 2010.

[2] M. Bonilla, D.C. Bhicas, E.U.I.T.D.O. Rlblicas, A. Palacios, D.Q. Analltica, C. Universitaria, ANALYTICAL Speciation and simultaneous determination of arsenic (III), arsenic (V), monomethylarsonate and dimethylarsinate by atomic absorption using inverse least squares multivariate calibration, 498 (1994).

[3] A.C. Olivieri, N.K.M. Faber, J. Ferré, UNCERTAINTY ESTIMATION AND FIGURES OF MERIT FOR MULTIVARIATE CALIBRATION (IUPAC Technical Report) Uncertainty estimation and figures of merit, 78 (2006) 633–661. doi:10.1351/pac200678030633.

[4] E.E. Stashenko, J.R. Martínez, M.P. Cala, D.C. Durán, D. Caballero, Chromatographic and mass spectrometric characterization of essential oils and extracts from Lippia (Verbenaceae) aromatic plants, J. Sep. Sci. 36 (2013) 192–202. doi:10.1002/jssc.201200877.

[5] L.Z. Lin, S. Mukhopadhyay, R.J. Robbins, J.M. Harnly, Identification and quantification of flavonoids of Mexican oregano (Lippia graveolens) by LC-DAD-ESI/MS analysis, J. Food Compos. Anal. 20 (2007) 361–369. doi:10.1016/j.jfca.2006.09.005.

[6] S.G. Leitão, G.G. Leitão, D.K.T. Vicco, J.P.B. Pereira, G. de Morais Simão, D.R. Oliveira, R. Celano, L. Campone, A.L. Piccinelli, L. Rastrelli, Counter-current chromatography with off-line detection by ultra high performance liquid chromatography/high resolution mass spectrometry in the study of the phenolic profile of Lippia origanoides, J. Chromatogr. A. 1520 (2017) 83–90. doi:10.1016/J.CHROMA.2017.09.004.

[7] A. Berim, D.R. Gang, Methoxylated flavones: occurrence, importance, biosynthesis, Phytochem. Rev. 15 (2016) 363–390. doi:10.1007/s11101-015-9426-0.

[8] I. Miyahisa, N. Funa, Y. Ohnishi, S. Martens, T. Moriguchi, S. Horinouchi, Combinatorial biosynthesis of flavones and flavonols in Escherichia coli, Appl. Microbiol. Biotechnol. 71 (2006) 53–58. doi:10.1007/s00253-005-0116-5.

[9] K.S. Booksh, Z. Wang, Extension and Application of Univariate Figures of Merit to Multivariate Calibration, Handb. Environ. Chem. 2 (1995) 209–227. doi:10.1007/978-3-540-49148-4-7.

4. Anexos

1. Código Scilab para calcular ILS y figuras de mérito

```
clc
clear
nomvars=['Numero de Mezclas a cuantificar';'Número de sustancias a cuantificar';'Concentración
máxima en espectros de calibración ';'Número de puntos de calibración';'Volumen de alícuota
(mL)';'Volumen de aforo (mL)';'Ingrese longitudes de onda del espectrofotometro';'Ingrese número
de longitudes de onda a seleccionar';'Ingrese repeticiones en los puntos de calibración'];
txtvars=string(zeros(9,1));
txtvars=x_mdialog('Ingrese los siguientes datos',nomvars,txtvars);
valvars=evstr(txtvars);


//Mezclas a Cuantificar
M=valvars(1,1)+1;
//Sustancias a cuantificar
Ns=valvars(2,1);
//Concentración de la mayor concentración
Cmax=valvars(3,1);
//Número de mezclas de calibración
Mcal=valvars(4,1)+1;
//Volumen de la alícuota en mL
Al=valvars(5,1);
//Volumen de aforo en mL
Af=valvars(6,1);
//Número de longitudes de onda medidas por el espectrofotómetro
F=valvars(7,1);
//Número de longitudes de onda seleccionadas
NL=valvars(8,1);
//Repeticiones en los puntos de la curva de calibración
T=valvars(9,1);
//Matriz de datos de calibraciòn: "Cal"
Cal=[zeros(F,Mcal)];
titulos=['Ingrese absorbancia de las mezclas de calibración';'Longitudes de onda en la primera
columna'];
Cal=x_matrix(titulos,Cal);
//Matriz de datos de absorbancia de mezclas a cuantificar
X=[zeros(F,M)];
titulos=['Ingrese absorbancia de las mezclas a cuantificar';'Longitudes de onda en la primera
columna'];
X=x_matrix(titulos,X);
//Vector de longitudes de onda seleccionadas para calibración y cuantificación
Y=[zeros(NL,1)];
titulos=['Ingrese Longitudes de onda a seleccionar'];
Y=x_matrix(titulos,Y);
//Matriz de concentraciones conocidas de cada mezcla de calibración
Cc=[zeros(Ns,Mcal-1)];
titulos=['Ingrese las concentraciones de cada sustancia en cada mezcla de calibración (ug/g)';'Cada
fila es una sustancia y cada columna una mezcla diferente']
```

```
Cc=x_matrix(titulos,Cc)/Cmax;
//Matriz de las mezclas a cuantificar con valores de absorbancia seleccionados
Z=[zeros(NL,M)]
for i=1:NL
   for j=1:F
   if X(j,1)==Y(i)
      Z(i,:)=X(j,:)
   end
   end
  end
//Matriz de las mezclas de calibración con valores de absorbancia seleccionados
R=[zeros(NL,Mcal)]
for i=1:NL
   for j=1:F
   if Cal(j,1)==Y(i)
      R(i,:)=Cal(j,:)
   end
   end
  end
//Matriz de espectros de las sustancias en mezcla "S"
S=(inv(Cc*Cc')*Cc*R(1:NL,2:Mcal)')';
Sf=inv(S'*S)*S';
Cd=[zeros(M-1,Ns)];
for i=1:M-1
for j=1:Ns
   if j==1
Cd(i,j)=Sf(j,:)*Z(:,i+1)*Cmax*Af/Al;
      if Cd(i,j)<0
         Cd(i,j)=0
         end
else
   if j==2
   Cd(i,j)=Sf(j,:)*Z(:,i+1)*Cmax*Af/Al;
         if Cd(i,j)<0
         Cd(i,j)=0
      end
   else
         Cd(i,j)=Sf(j,:)*Z(:,i+1)*Cmax*Af/Al;
         if Cd(i,j)<0
         Cd(i,j)=0
      end
      end
end
end
end
i=1
j=1
editvar Cd
//CALCULO DE FIGURAS DE MÉRITO
for i=1:NL
k=2
```

```
for j=1:(Mcal-1)/T
      Desv(i,j)=stdev(R(i,k:k+2))
      Rp(i,j)=mean(R(i,k:k+2))
      k=k+T
end
end

for j=1:(Mcal-1)/T
   De(j)=norm(Desv(:,j))
   NRp(j)=norm(Rp(:,j))
   SN(j)= NRp(j)/De(j)
   end

i=1
j=1
for i=1:Ns
   //Cálculo de sensibilidad a ada sustancia (absorbancia/masa)
   SEN(i)=1/(norm(Sf(i,:))*Cmax);
   //Cálculo de la selectividad
   SEL(i)=SEN(i)*Cmax/(norm(S(:,i)));
   //Cálculo del límite de detecciòn
   LOD(i)=3*Af*mean(De)/(SEN(i)*Al);
end

disp('Selectividad, Sensibilidad, Relación Señal/Ruido, Límite de detección')
LOD
SEN
SEL
//I=Mcal
//J=NL
//K=Ns
//R=Z
//end
Rm=inv(R(1:NL,2:Mcal)'*R(1:NL,2:Mcal))*R(1:NL,2:Mcal)'; //(24x540); R (540x25)
b=Rm'*Cc';//(540x3)
I=eye(NL,Mcal-1)
varc=R'*(I-R(1:NL,2:Mcal)+R(1:NL,2:Mcal))*R/(NL-Ns)
varr=
for i=1:M
   h(i)=R(:,i)'*Rm'
end
```

Appendix C. Article 1

Industrial Crops & Products 146 (2020) 112170

Contents lists available at ScienceDirect

Industrial Crops & Products

journal homepage: www.elsevier.com/locate/indcrop

Optimization of flavonoids extraction from *Lippia graveolens* and *Lippia origanoides* chemotypes with ethanol-modified supercritical CO_2 after steam distillation

Julián Arias, Jesica Mejía, Yuri Córdoba, Jairo René Martínez*, Elena Stashenko, José Manuel del Valle

Department of Chemical and Bioprocess Engineering, Pontificia Universidad Católica de Chile, Avda. Vicuña Mackenna 4860, Macul, Santiago, Chile

ARTICLE INFO

Keywords:
Lippia origanoides
Lippia graveolens
Residues valorization
simplex optimization
Supercritical extraction
Essential oils

ABSTRACT

Steam distillation of essential oils from *Lippia origanoides* K. and *Lippia graveolens* K. leaves plant material residues that can be valorized. Flavonoids can be selectively extracted from these substrates using ethanol-modified supercritical CO_2, as attempted in this work. The thymol-rich *L. origanoides* chemotype was used to test extraction reproducibility. The effects of pressure, temperature, time, CO_2 mass flow, particle size, and percent ethanol on the extraction yield of oleoresin and flavonoids were examined with a $2^{(6-2)}$ fractional factorial screening design. The variables with a significant influence on yields (pressure, time, CO_2 mass flow, and percent ethanol) were used in a simplex optimization to determine the conditions for maximum extraction from *L. graveolens* and three *L. origanoides* chemotypes. The extracts' flavonoid content was estimated by UV–vis spectroscopy with a multivariate calibration model. UHPLC-ESI(+)-Orbitrap-MS was employed for extract identification and quantification. The extracts from the various plant material residues had qualitative and quantitative differences in flavonoid composition. Under the best extraction conditions found (307 bar, 5 % ethanol, 43 g CO_2/min), the steam-distilled plant material from the phellandrene-rich *L. origanoides* chemotype afforded 4.1 g of pinocembrin per kg of dry substrate. Results of this work facilitate the implementation of supercritical CO_2 extraction processes to valorize byproducts of the essential oil industry by obtaining extracts that contain flavonoids.

1. Introduction

Lippia origanoides K. and *L. graveolens* K. (Mexican oregano) are aromatic shrubs native to Central America and the northern region of South America. They are raw materials for the production of culinary seasonings and essential oils enriched in phenylpropanoids that are useful in the food, cosmetic, and pharmaceutical industries (Hernandes et al., 2017; Lopes et al., 2013; Ortiz et al., 2017; Stashenko et al., 2018). At least five chemotypes have been distinguished among these two (apparently the same) species (da Silva et al., 2017; Maisch, 1885; Ribeiro et al., 2014; Stashenko et al., 2010), which differ in essential oil composition. Essential oils are obtained by steam distillation, which leaves residual plant material that can be valorized. These plants, in addition to essential oils, also contain flavonoids (Leitão et al., 2017; Li et al., 2007; Stashenko et al., 2013) that could be extracted as demonstrated for other byproducts from the essential oil industry (Navarrete et al., 2011; Sánchez-Vioque et al., 2013). Pinocembrin (PC) is one of the flavonoids contained in *L. origanoides* and *L. graveolens* that, incidentally, appears in patent applications as medication for the treatment of acute intracerebral hemorrhage (Du et al., 2018) and pulmonary fibrosis (Cheng et al., 2019; Du et al., 2018), because of its effectiveness against these ailments (Lan et al., 2017, 2016; Rasul et al., 2013; Wang et al., 2017). The amount of pinocembrin in *L. origanoides* ($30 \pm 1\ mg\ g^{-1}$ dry weight, DW) (Stashenko et al., 2013) is remarkably higher than that found in commercial products (0.6–2.5 g k g_{DS}^{-1}; DS: dry substrate) (Li et al., 2012; Yamamoto et al., 2011) and in crops recently identified as promising sources of this medicinal flavanone (15 and 18 g k g_{DS}^{-1}) (Goodger et al., 2019). Therefore, discarding the plant material after distillation would waste a clear opportunity of improving profitability.

Pinocembrin and other flavonoids should remain stable during steam distillation because there is no variation in the thermogram line

* Corresponding author at: Research Center for Biomolecules, CENIVAM Research Center, Universidad Industrial de Santander, Carrera 27, Calle 9, Bucaramanga, Colombia.
E-mail address: jmartine@uis.edu.co (J.R. Martínez).

https://doi.org/10.1016/j.indcrop.2020.112170
Received 7 July 2019; Received in revised form 21 December 2019; Accepted 24 January 2020

of pinocembrin from 50 °C to the endothermic peak starting at ca. 204 °C for pinocembrin melting (Yang et al., 2018). Not only should pinocembrin and other thermoresistant flavonoids remain intact during steam distillation of the substrate, but modification of the plant material structure during steam distillation would favor subsequent mass transfer and improve extraction yield as compared with the control (undistilled) counterpart (Navarrete et al., 2011).

Supercritical (sc) CO_2 extraction can very efficiently recover phenolics from vegetable substrates (Díaz-Reinoso et al., 2006). The extraction yield and selectivity may depend on humidity, particle size (d_p), pressure (P), temperature (T), superficial velocity of the CO_2, the modifier type and percentage (E), and treatment time (t). Due to the large number of variables, experimental screening designs are applied first to help select relevant extraction conditions prior to studying and modeling extraction curves, scaling-up, and cost analysis (Oliveira et al., 2011; Sharif et al., 2014).

The main objective of this work was to select suitable extraction conditions to maximize the yields of oleoresin and flavonoids from steam distilled *L. origanoides* and *L. graveolens* plant material. To achieve this objective, the experimental work was organized by taking as reference previous work that, in addition to the screening of variables, also applied simplex optimization (Bermúdez et al., 2002; Maio et al., 1997; Safaralie et al., 2010). Steam distilled thymol-rich *L. origanoides* chemotype was used to perform preliminary experiments and evaluate the experimental error. A fractional factorial $2^{(6-2)}$ design was performed to determine the variables that affect the $scCO_2$ extraction of the same substrate. The deterministic simplex experimental method of Nelder and Mead (1965) was used then to optimize the extraction yield of oleoresins and flavonoids from the four studied substrates (namely, byproducts from the steam distillation of *L. graveolens*, and the thymol-, carvacrol-, and phellandrene-rich chemotypes of *L. origanoides*). The extract of each substrate obtained in highest yield was characterized and quantified by means of a robust chromatography technique, i.e., UHPLC-ESI(+)-Orbitrap-MS.

2. Materials and methods

2.1. Culture, harvest and plant material

Different experimental lots of *L. graveolens* and three *L. origanoides* chemotypes (i.e., thymol-, carvacrol- and phellandrene-rich chemotypes) were grown at the main campus (7° 8' 26.406'' N 73° 7' 10.45'' W, Bucaramanga, Colombia) and at the Barbosa campus (6° 27' N 75° 19' 59.988'' W, Barbosa, Colombia) of the Universidad Industrial de Santander during the 2014–2016 period. The harvest was collected every 3 months during these years and steam-distilled to remove essential oils, which were not the subject of this work. The residual biomass from the distillation processes was separated, dried in the shade, and stored under controlled conditions. All of the dried plant material was ground separately. The particle size was reduced in two steps, first with a chaff cutting machine (PE800 Penagos, Girón, Colombia) and then with a cutting mill (Retsch SM100, Haan, Germany). For the thymol-rich chemotype, exit grids with 0.5- or 2-mm openings were used in order to use particle size as a variable for the screening design that is discussed in a following subsection. For the remaining chemotypes, only the 2-mm opening exit grid was used. A portable sieve shaker RX-24 (Cleveland, OH, USA) was used to determine the particle size distribution of the chopped material. By discretizing these data into a normal distribution function, the Sauter mean diameter (S_{md}) was calculated (Allen, 1981; Barth, 1984). The chopped material was stored at 22 °C in separate containers for each chemotype and particle size.

Moistures of the post-distilled substrate (DS) were determined gravimetrically (105 °C, 24 h, WTC oven, Binder, Tutlingen, Germany). The initial oleoresin content in the substrates was also measured gravimetrically by extracting samples to exhaustion (24 h, ca. 2 cycles h^{-1}) in a 250 mL Soxhlet apparatus using an azeotropic ethanol/water mixture. The ethanol-water mixture was removed from the extract in an R-Style rotary evaporator (Büchi Labortechnik AG, Flawil, Switzerland). A 10 mg extract sample was devoted to flavonoid quantitation (Section 2.4).

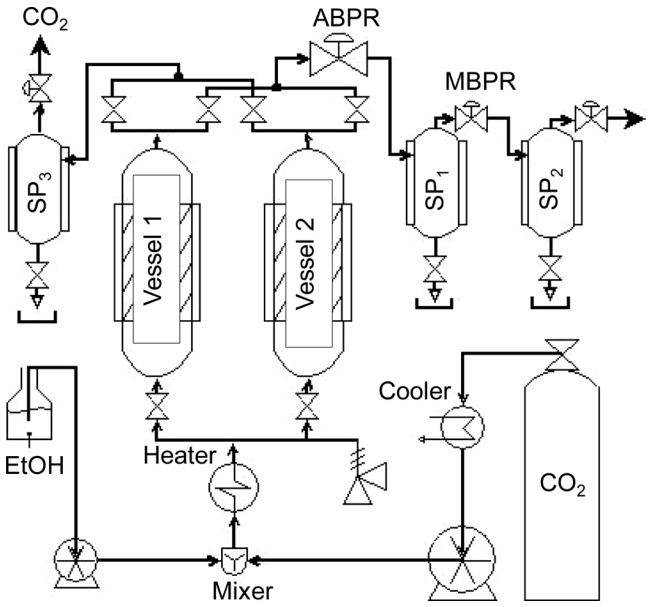

Fig. 1. Schematic diagram of supercritical fluid extraction process used in this work.

2.2. Supercritical fluid extraction

Before the extraction, the raw material was dried at 60 °C for 12 h in an oven (Indumegas, Bucaramanga Colombia). The drying time was determined with a drying rate plot. Plant material (500 g for each experiment) was extracted in one-pass pilot scale modified Thar SFE-2000-2-FMC50 equipment (Thar Instruments, Pittsburgh, PA, USA) at corresponding conditions. The modified equipment consists of two extraction vessels in parallel (2000 cm^3 capacity each one, D = 7.62 cm inner diameter, H = 43.86 cm height) equipped with heat transfer jackets; two piston pumps (P200 for CO_2 and P50 for ethanol) from Thar Technologies; three separators (500 cm^3 capacity) equipped with heat transfer jackets, two of them in series and one for CO_2 discharge; and one automated and two manual back-pressure regulator valves from Thar Technologies. Fig. 1 shows the process diagram for the extraction system.

The conditions used in the separators to obtain fractions were 80 bar and 35 °C in the first separator SP_1, atmospheric conditions and 20 °C in the second separator SP_2; these conditions are similar to those used in a rosemary extraction study (Reverchon and Senatore, 1992). Extractions were carried out using 99.8 % pure CO_2 from Praxair (Bucaramanga, Colombia) and industrial-quality ethanol from Suquin (Bucaramanga, Colombia). For these experiments, single samples were collected during the time of the extractions. The extracts from both separators were pooled, and most of the solvent was removed on the R-Style rotary evaporator. The extract was completely cleaned of solvent in a subsequent stage of convective drying using nitrogen flow. Dried extract samples were collected in pre-weighed glass vials and recovered extracts were assessed gravimetrically. After that, the samples were stored at 4 °C in amber vials.

2.3. Experimental design and optimization

Six preliminary experiments with the thymol-rich chemotype were used to assess reproducibility (RSD < 10 %). Triplicates with two different experimental conditions were performed and the variance

Table 1
Extraction variables values for fractional factorial design 2^{6-2}.

Factors	Symbol	Domain	
		1	−1
Pressure, bar	P	400	80
Temperature, ºC	T	60	40
Flow, g/min of CO_2	F	50	10
Particle size[a], mm	d_p	2	0.5
Extraction time, min	t	120	60
Percent ethanol, %	E	10	0

[a] Refers to the exit grids opening the mill, not the real size of the particles.

found for these experiments was assumed to be the experimental error of each experiment in the screening design. The thymol-rich chemotype was used in the screening design under the assumption that the independent variables of extraction affect all substrates studied in the same way, because, in general terms, it is considered that they come from the same plant. The effects of pressure (P), temperature (T), extraction time (t), CO_2 flow (F), particle size (d_p), and percent ethanol (E) were examined in the screening design. Since the experiments were conducted in the same extraction vessel, it was preferable to use flow (F) instead of the CO_2 superficial velocity. The variable d_p refers to the opening of the mill exit grids not to the actual particle size. A $2^{(6-2)}$ fractional factorial design of resolution 4 was employed (Sematech, 2006). Table 1 shows the selected levels used in accordance with the equipment constraints.

The values of the variables that showed significant influence in the screening design were changed according to the simplex optimization method proposed by Nelder and Mead (1965) in order to find the extraction conditions that produced the highest extraction yield of flavonoids in the selected experimental space. Although a few works on simplex optimization of supercritical fluid extraction are found in the literature, this may be a more convenient optimization approach, because the search for the optimum is more refined compared with the widely used response surface methodology, and because the effects of the variables are already known from the experimental design of the previous stage. The top five experimental conditions in the screening design were used as the initial point of the search. Three scalar parameters were specified to define a complete Nelder–Mead method (i.e., reflection-, expansion- and contraction- coefficient). These were used according to their convenience in improving the experimental results.

2.4. Flavonoids detection and quantification

2.4.1. UV–vis spectroscopy

A classical least squares (CLS) multivariate calibration method (Olivieri et al., 2006) was employed to determine the flavonoid contents of the extracts. The extract spectral signal was modeled as the sum of contributions from the analytes (flavonoids) in the supercritical extract of *L. origanoides* and *L. graveolens*. These are as follows: pinocembrin, naringenin, luteolin, and apigenin (Stashenko et al., 2013), which were purchased from Sigma-Aldrich (St. Louis, MO, USA) as high purity standards (> 98 %).

The quantification method assumed a linear additive signal for the constituents, as represented mathematically by matrix Eq. (1).

$$\boldsymbol{R} = \boldsymbol{SC} + \boldsymbol{e} \tag{1}$$

where $\boldsymbol{R}$ is the measured absorbance data matrix, $\boldsymbol{S}$ is the matrix from which proportionality constants are calculated on the basis of the selected standards of known concentrations, $\boldsymbol{C}$ is the concentration matrix, and $\boldsymbol{e}$ is the vector of noise. The following matrix equation (Bautista et al., 1996) was used to predict concentration $\boldsymbol{C}$:

$$\boldsymbol{C} = (\boldsymbol{S}'\boldsymbol{S})^{(-1)}\boldsymbol{S}'\boldsymbol{R} \tag{2}$$

The concentrations of all constituents were obtained by fitting the pure-component signal $\boldsymbol{S}$ to the spectrum of the prediction sample $\boldsymbol{R}$ with an ordinary least-squares (OLS) fit. A UV–vis *Perkin-Elmer* Lambda 10 (Waltham, USA) spectrophotometer was used to obtain all of the UV–vis spectra (Lecture speed 240 nm/min, smooth: 6). A group of 44 wavelengths, which represent the variations in the spectral signals of the molecules, was conveniently selected to perform the calculations. Methanol was used as the eluent of the samples, and it was supplied by Mallinckrodt Baker Inc. (Phillipsburg, PA, USA).

2.4.2. Liquid chromatography

A Thermo-Scientific Exactive Plus LC–MS (Palo Alto, CA) system equipped with a heated electrospray interface and orbitrap detection was employed for the determination and quantification of the extract obtained in highest yield from each chemotype. A Hypersil GOLD aQ (Thermo Scientific, Sunnyvale, CA; 100 × 2.1 mm i.d., 1.9 µm) column was used. The column temperature was maintained at 35 °C. A 0.2 cm^3/min mixture of H_2O (A), acetonitrile (B), each one with 0.5 % formic, was used as the mobile phase with the following gradient program: 100 % A changed linearly to 100 % B in 8 min, maintained constant for 4 min, returned to 100 % A in 1 min, and kept unchanged for the last 3 min. The mass spectra were obtained in positive mode; injection volume: 1 µL; gas temperature: 350 °C; drying gas: 7 L/min, N_2; nebulizer gas: 40 psi; capillary voltage: 3.5 kV; mass range 100 − 1100 *m/z*. Mass spectra were acquired in the all-ion fragmentation mode for energies of 10, 20, 30, and 40 eV at the high-energy collision dissociation chamber. Chromatographic and mass spectrometric data were processed with Xcalibur software, version 4.0. Compound identification was based on the extracted ion chromatogram (EIC), exact masses, comparison with standard compounds, and fragment pattern interpretation. The external calibration methodology was employed for quantification using the calibration curves of available standard substances (i.e., quercetin, luteolin, naringenin, apigenin, and pinocembrin) to relate concentration with chromatographic peak area (Miller and Miller, 2010). The quantification of the substances for which no standards were available was obtained from a surrogate (i.e., kaempferol) with the internal standard method (Cuadros-Rodríguez et al., 2007).

3. Results and discussion

3.1. Particle size characterization and drying test

Fig. 2 shows the particle size cumulative curve obtained by sieving

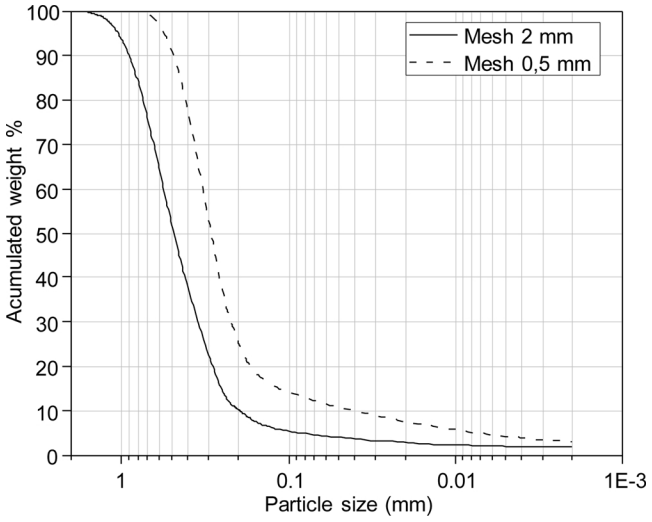

Fig. 2. Cumulative curve of particle size distribution of *L. origanoides* thymol-rich chemotype milled with two different grid sizes.

the chopped substrate. The curves are clearly different from each other, so it was reasonable to use these two aperture sizes as levels of the d_p variable in the experimental design. The S_{md} estimated for treatments with 2- and 0.5-mm openings in the mill were 0.308 and 0.253 mm, respectively. The pre-extraction drying time was set at 120 min, which was obtained from a drying rate curve made at 60 °C (Pereira and Meireles, 2010). Following this time, the moisture content remained constant below 12 %. The dry basis moisture for all plant material was ca. 13 %.

3.2. Preliminary extractions

Two different preliminary extraction conditions, 7.2 kg_{CO_2} kg_{DS}^{-1} at 40 °C and 200 bar and 9.6 kg_{CO_2} kg_{DS}^{-1} at 50 °C and 300 bar, were carried out with three replicates in random order in three separate days. The obtained reproducibility *RSD* values were 7.7 and 1.9 %, for the oleoresin yield of the two experimental conditions, respectively. Values below 10 % are considered acceptable.

3.3. Selection of variables that affect the extraction process

Sixteen experiments corresponding to the 2^{6-2} fractional factorial design were carried out in random order. Supplementary Table S1 shows the values for two different responses: the oleoresin yield (e_{ole}) and the flavonoids extract yield (e_{flv}), which is represented as the sum of flavonoids extracted. The two responses have a high positive Pearson correlation coefficient ($r = 0.97$); the independent variables could have influenced them in the same way.

The results for the screening design showed that the yield increased with pressure. The same result was observed by Leitao et al. (2013) for the *Anacardium occidentale* extraction and de Oliveira et al. (2012) for *Lippia dulcis* extraction. It was observed that the highest yields corresponded to high pressure and flow domains. The effects of all variables and possible binary combinations were estimated using the dot product method between the variable levels and results (Montgomery, 2008). According to the normal probability distribution test, *P*, *F*, and *E* had an effect over both responses, e_{ole} and e_{ext}. The extraction time *t* influenced only the oleoresin extraction yield. For both responses, the results showed that the changes of *F*, *P* and *E* largely explained the variability. However, with the inclusion of the confused effect (*F t – P T*) and the effect of *t*, it is possible to explain more than 80 % of the total variability of the responses. *F* and *E* directly affected the solvent density, a variable that in turn is determinant for solubility. The increase in *P* and *E* directly increased the mixture density, which gives the extraction solvent the ability to solubilize more of the extract constituents (enhancement of CO_2 solvation power). In addition to contributing to the density value, E also helps increase extraction yield via polarity modification, which benefits phenolic compounds solubilization. However, the solubility of a wide range of components present in the substrate also increases, which affects selectivity.

The analysis of variance (Table 2) confirmed the importance of *F*, *P* and *E* on the extraction yields. Although the temperature (*T*) and the particle size (d_p) were important variables in the extraction process, because they relate directly to the solubility and mechanisms of mass transfer, their effects were not significant in the experimental space studied. The reason for the exclusion of d_p can be explained by how close the S_{md} values are to each other, i.e., the 0.5- and 2- mm openings in exit grids convey a very narrow range of particle size distribution. Therefore, there was no clear difference in the effect when one or the other mesh was used. Based on this result, the optimization extractions used the 2 mm exit grid opening, because with this size, the time that the solids are retained in the mill is shorter. This directly minimizes operating time and the thermal degradation of substances.

The influence of *T* was not significant. This may be due to the fact that the pressure range was wide but the temperature interval was narrow for the experiments, restricting the possibility of noticing significant temperature effects. The temperature was maintained at 50 °C for subsequent experiments. The temperature domain employed was chosen to warrant that the ethanol-modified CO_2 mixture was in a single supercritical phase (Suzuki et al., 1990). Temperature was directly related to the solubility and the crossover pressure. There is always a crossover pressure, but this depends on the solute. It is a common feature of the pure solutes dissolved in supercritical fluids (Chimowitz and Pennisi, 1986). Crossover pressure is a near-critical pressure in the case of essential oils, and it is considerably larger in the case of triglycerides, but in the two cases it is between 80 and 400 bar. For extracts from botanical materials that contain cuticular waxes (major compounds) in addition to the minor compounds (e.g., flavonoids), the crossover pressure is possible between 100 and 300 bar. The shape of the solubility curves for extract in ethanol-modified supercritical CO_2 are unknown, as well as the crossing pressure. However, the behavior of the extraction of flavonoids in equilibrium may be similar to what was reported for naringenin (Núñez et al., 2010), and quercetin (Chafer et al., 2004), both flavonoids are constituents of the extracts under study. These works showed that solubility increased with increasing pressure and temperature. No crossing pressure trend was observed in the experimental region studied by both research groups. It has been observed that the solubility of the pure minor component is not directly related to the equilibrium of the extraction of the mixed substances (Sovová, 2012), but presumably the extraction of flavonoids in the equilibrium increases directly proportional to *T* and *P*, at least above the crossing pressure region for two of the target components in the extracts. Saldaña et al. (2010) observed a similar behavior in their study about the extraction of β-carotene and lycopene from tomato skin and pulp.

3.4. Empirical search for optimal extraction conditions

Based on the analysis of variance (Table 2), the extraction conditions for higher yields were sought in the experimental space comprising the variables *F*, *P*, *E* and *t* through the simplex method (Nelder and Mead, 1965). The five experiments that had the highest yields in the fractional factorial design (i.e., vertices 1–5 in Table 3) were used to construct the first simplex (S1) for thymol-rich chemotype. Table 3 shows the consecutive experiments for the optimization of flavonoids extraction yield from thymol-rich chemotype. The methodology was applied to the other chemotypes (results not shown). After these experiments were repeated, the lowest observable datum was discarded, and the coordinates of the new vertex were calculated according to Eq. (3)

$$\boldsymbol{V}_{(i+n+j)} = \boldsymbol{V}_c + b(\boldsymbol{V}_c - \boldsymbol{V}_p), \tag{3}$$

where $\boldsymbol{V}_c$ is the centroid, which is the average of the responses of the vertices not rejected, b is a factor that determines whether the next vertex corresponds to a reflection ($b = 1$), an expansion ($b > 1$), a contraction ($0 < b < 1$), or a contraction with change of direction ($-1 < b < 0$).

The results along with the conditions of all chemotype experiments are shown in Supplementary Tables S2–S4. Table 3 shows the sequence of experiments performed as follows. The first rejected vertex was 5, because its yield was the lowest of the five points that made up the S1. Using $b = 1$, a reflection was calculated to obtain the conditions of vertex 6. Vertex 6 slightly increased the response; so, another vertex of S1 was rejected, i.e., vertex 4. Reflections continued until vertex 9, where the yield was high, so a contraction ($b = 0.6$) was applied. In vertex 10 the extract yield decreased, and an expansion ($b = 1.3$) was applied to calculate vertex 11. In vertex 14 a reflection of vertex 13 was carried out from the S9 to produce vertex 14, one of the best experiments that remained until the end of optimization, as well as the subsequent vertex 15. For vertices 16, 17, and 18 the calculated reflections modified the variables, but the response was always lower than the last

Table 2
Analysis of variance for two monitored responses.

Source	Oleoresin yield, (e_{ole})					Flavonoids yield, (e_{flv})				
	SS	*df*	*MS*	*F*-test	*P*-value	*SS*	*df*	*MS*	*F*-test	*P*-value
F	1.18	1	1.18	[a]256.5	0.004	0.03	1	0.03	[a]964.4	0.001
P	0.86	1	0.86	[a]186.8	0.005	0.02	1	0.02	[a]744.9	0.001
E	0.23	1	0.23	[a]49.3	0.020	0.01	1	0.01	[a]248.5	0.004
F t – P T	0.20	1	0.20	[a]43.0	0.023	4.4×10^{-3}	1	4.4×10^{-3}	[a]143.7	0.007
t	0.16	1	0.16	[a]34.2	0.028	3.1×10^{-3}	1	3.1×10^{-3}	[a]102.6	0.01
P F – T t	0.14	1	0.14	[a]30.7	0.031	2.5×10^{-3}	1	2.5×10^{-3}	[a]81.1	0.01
F E – T d_p	0.11	1	0.11	[a]23.1	0.041	3.6×10^{-3}	1	3.6×10^{-3}	[a]117.5	0.008
d_p	0.03	1	0.03	7.4	0.113	1.2×10^{-3}	1	1.2×10^{-3}	[a]40.5	0.02
T	0.03	1	0.03	6.7	0.123	4.2×10^{-4}	1	4.2×10^{-4}	13.8	0.06
P d_p *– t E*	0.03	1	0.03	6.7	0.123	6.2×10^{-4}	1	6.2×10^{-4}	[a]20.3	0.04
P t – T F – d_p *E*	0.02	1	0.02	4.6	0.165	7.3×10^{-4}	1	7.3×10^{-4}	[a]23.8	0.04
P E - d_p *t*	0.02	1	0.02	3.4	0.208	1.2×10^{-3}	1	1.2×10^{-3}	[a]40.9	0.02
T E – F d_p	0.01	1	0.01	2.9	0.229	3.9×10^{-4}	1	3.9×10^{-4}	12.6	0.07
Error	0.01	2	0.00			6.1×10^{-5}	2	3.1×10^{-5}		
Total	3.01	15				0.078	15			

[a] The *F* value for the effect is greater than the critical value $F_{critical} = 18,5$.

vertex in S11. This result showed that the new conditions calculated with the last simplex were moving away from the high yield space. Finally, vertices 19 and 20 were calculated and experimented, their responses were very similar with high yields. In consequence, the optimization was stopped at S16.

The vertices 1, 14, 15, 19, and 20 (S16) had the higher yields in the explored experimental space for distilled substrate of thymol-rich *L. origanoides*. The values of the responses of these experiments were not significantly different. Any of these conditions afforded relatively high flavonoid amounts from the substrate. However, practical considerations make some conditions more favorable than others. Vertex 1 conditions, for example, use high values of *P*, *t* and *E* to get the best results, but vertex 14 conditions are operationally more favorable because using the same CO_2 and ethanol consumption, two extractions are possible in the same time. Accordingly, it was found that the best extraction conditions for this substrate corresponded to vertex 15 with the lowest values of *P* (307 bar) and *E* (5 %) and moderate values of *t* (96 min) and *F* (43 g/min). The same treatment of the extraction conditions was done for the optimization of the rest of *L. origanoides* chemotypes and for *L. graveolens*. Fig. 3 is a graphical representation of the results of the simplex optimization for all substrates. The 3D scattering plot of bubbles mapped with colors presents the results of the optimization of substrates A–D, locating the bubbles according to the extraction conditions of the experiment where $q = F{\cdot}t{\cdot}DS^{-1}$. Bubble sizes are proportional to e_{ole} that varied from 0.2 to 1.5 %. The colors change according to e_{flv}, which varied from 0.05 to 0.72 %.

3.5. Spectroscopic characterization

Fig. 4 exemplifies the predicted concentrations of the flavonoids by decomposing the spectral signal of the extract obtained with the conditions of vertex 20 for the thymol-rich chemotype of *L. origanoides* i.e., pinocembrin 75.4 mg g_{ext}^{-1}, naringenin 28,1 mg g_{ext}^{-1}, and luteolin-apigenin 67 mg g_{ext}^{-1}. The concentrations of luteolin and apigenin could not be determined individually due to the great similarity of their UV–vis spectra at the 44 wavelengths selected to perform the multivariate calibration. This is a difficulty that the CLS method cannot overcome; it will not be able to establish differences between the molecules from the input information. A variation of CLS, i.e., the inverse least squares method (ILS), instead of using the spectral signals as input information,

Table 3
Optimization conditions and results using the simplex method for *Lippia origanoides* thymol-rich chemotype.

Vertex	*P,* bar	*F,* g/min	*T,* min	*E,* %	e_{ole}[a].,%	e_{flav}[b]., %	CO_2 consumption, kg_{CO_2}/g_{ext}	Flavonoids, g_{flv}	Simplex	Vertex rejected
1	400	50	120	10	1.2	0.22	1.0	1.5		
2	400	50	120	0	0.92	0.13	1.3	1.1		
3	400	50	60	10	0.88	0.16	0.7	1.1		
4	80	50	120	10	0.76	0.13	1.6	0.9		
5	400	50	60	0	0.74	0.12	0.8	0.9	S1	
6	134	31	106	11	0.78	0.12	0.8	0.8	S2	5
7	417	24	46	3	0.48	0.042	0.5	0.3	S3	4
8	132	47	113	9	0.80	0.14	1.3	0.9	S4	7
9	359	45	66	2	0.84	0.13	0.7	0.9	S5	6
10	438	33	46	1	0.56	0.09	0.5	0.7	S6	8
11	160	46	106	9	1.0	0.14	1.0	1.0	S7	10
12	220	45	90	8	1.0	0.17	0.8	1.2	S8	9
13	154	32	101	3	0.76	0.11	0.9	0.9	S9	3
14	449	54	52	11	1.2	0.17	0.5	1.2	S10	13
15	307	43	92	5	1.2	0.15	0.7	1.3	S11	2
16	112	62	130	11	0.5	0.08	3.2	0.6	S12	12
17	334	53	139	13	0.98	0.18	1.5	1.1	S13	16
18	420	60	144	12	0.68	0.13	2.5	0.8	S14	17
19	380	40	96	8	1.1	0.19	0.7	1.3	S15	18
20	307	60	120	5	1.2	0.19	1.2	1.3	S16[c]	11

[a] Oleoresin yield.
[b] Flavonoids yield.
[c] Vertex of S16 are 1, 14, 15, 19 and 20.

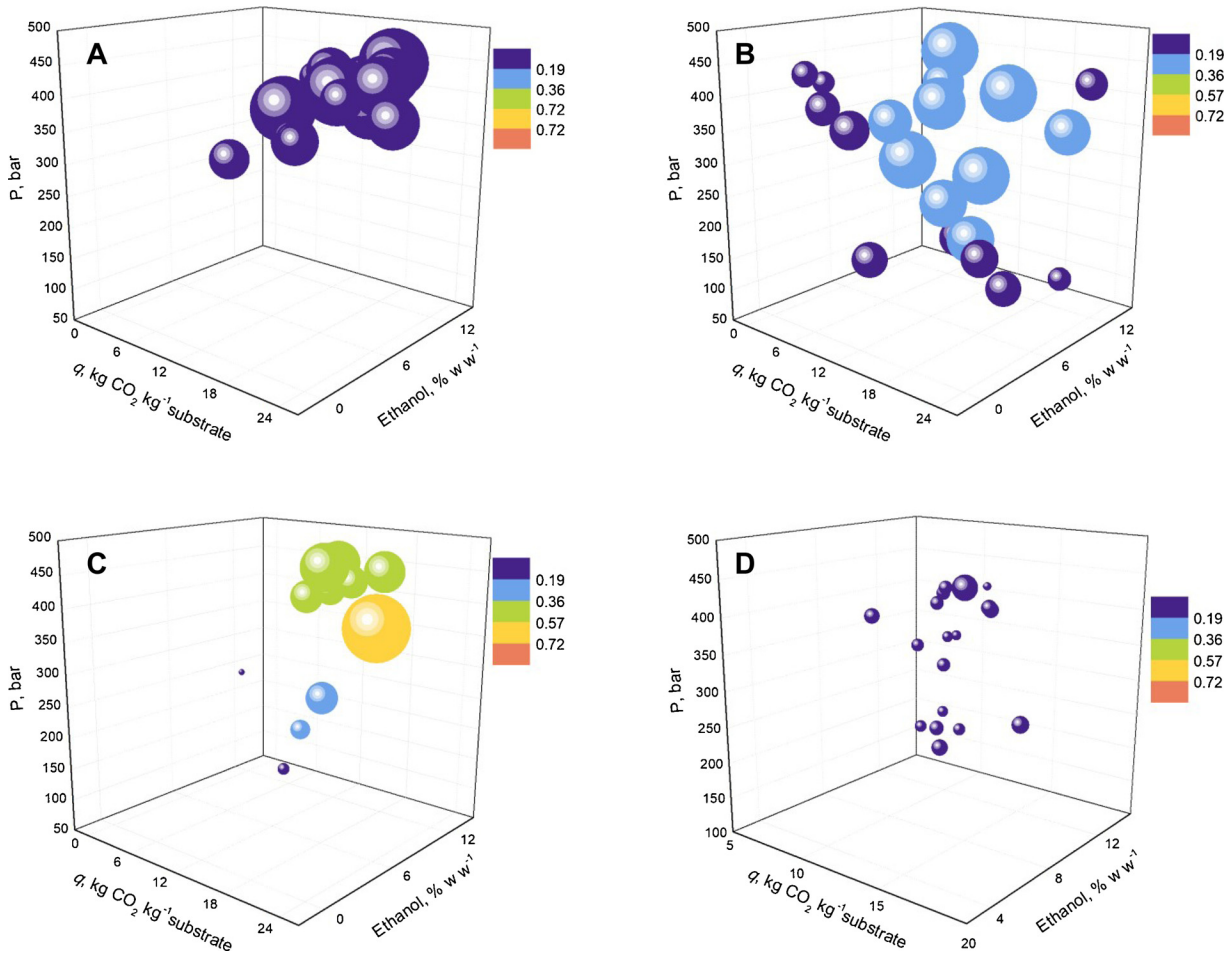

Fig. 3. 3D Scattering plot of bubbles mapped with color scale that shows results of the simplex optimization for extraction of *L. origanoides* chemotypes and *L. graveolens*. The bubbles sizes are proportional to the extraction yield of oleoresin that varies from 0.2 to 1.5 %. The color scale varies according to the extraction yield of flavonoids between 0.05 to 0.72 %. **A**. *L. origanoides* carvacrol-rich chemotype; **B**. *L. origanoides* thymol-rich chemotype; **C**. *L. origanoides* phellandrene-rich chemotype and **D**. *L. graveolens*.

predicts the individual spectra of the molecules from known concentrations of the analytes in a mixture, including signal overlapping. Despite this disadvantage of CLS, the method is convenient for the purposes of the present work, since the objective was to monitor the sum of the flavonoids in the extract, i.e., to quantify the spectral signal according to the flavonoids that are likely to be found in the extracts. There are other methods, in addition to the multivariate approaches, such as the zero-crossing method or the classic univariate method, but also because of the high spectral superposition in extracts of botanical material, they are not suitable for the simultaneous determination of the flavonoids. Other graphical methods, such as those used by Bautista et al. (1993, 1996) to predict flavonoid concentrations, require regions in the spectrum where the derivatives of most of the signals are zero, but for the target compound the derivative is greater than zero in the required zone, which is clearly a limitation for complex mixtures.

3.6. Content of flavonoids in the distilled substrates

The results of the Soxhlet extraction showed that the distilled substrates contained considerable amounts of oleoresin, flavonoids, and pinocembrin: 192 g_{ole} kg_{DS}^{-1}, 55 g_{flv} kg_{DS}^{-1}, and 31 g_{PC} kg_{DS}^{-1} (ole: oleoresin; flv:flavonoids; PC: pinocembrin; DS:dry substrate) for *L. origanoides* phellandrene-rich chemotype; 174 g_{ole} kg_{DS}^{-1}, 20 g_{flv} kg_{DS}^{-1}, 15 g_{PC} kg_{DS}^{-1} for *L. origanoides* thymol-rich chemotype; 195 g_{ole} kg_{DS}^{-1}, 29 g_{flv} kg_{DS}^{-1}, and 23 g_{PC} kg_{DS}^{-1} for *L. origanoides* carvacrol-rich chemotype; and 69 g_{ole} kg_{DS}^{-1}, 6.1 g_{flv} kg_{DS}^{-1}, and 5 g_{PC} kg_{DS}^{-1} for *L. graveolens* thymol-rich chemotype. These are high levels compared with other residues in the essential oil industry (Navarrete et al., 2011; Sánchez-Vioque et al., 2013) and even with plants identified as potential commercial sources of pinocembrin such as the seeds of *Alpinia katsumadai* Hayata with 2.5 g_{PC} kg_{DS}^{-1} (Li et al., 2012) and two sub-species of *Eucalyptus preissiana* trees with 15 and 18 g_{PC} kg_{DS}^{-1} (Goodger et al., 2019).

According to the experiments, 14.4 g_{ole} kg_{DS}^{-1}, 7.2 g_{flv} kg_{DS}^{-1}, and 4.1 g_{PC} kg_{DS}^{-1} were the best extraction yields for the phellandrene-rich *L. origanoides* chemotype. These were the best results for all substrates studied as shown for C in Fig. 3. 12.4 g_{ole} kg_{DS}^{-1}, 2.2 g_{flv} kg_{DS}^{-1}, and 1.3 g_{PC} kg_{DS}^{-1} were best yields for the thymol-rich chemotype, 14.8 g_{ole} kg_{DS}^{-1}, 1.5 g_{flv} kg_{DS}^{-1}, and 0.5 g_{PC} kg_{DS}^{-1} for carvacrol-rich chemotype, and 5.6 g_{ole} kg_{DS}^{-1}, 0.27 g_{flv} kg_{DS}^{-1}, and 0.16 g_{PC} kg_{DS}^{-1} for *L. graveolens*. These are common yield values for the $scCO_2$ extraction of botanical materials (Pereira and Meireles, 2010). Although the distilled substrate of the *L. origanoides* phellandrene-rich chemotype is the residue with the highest recovery potential for ethanol-modified $scCO_2$ extraction, its yield of essential oil extraction (1–1.5%) was the lowest with a very low content of phenylpropanoids as compared with *L. graveolens* (1–3%) and the carvacrol-rich (3.6–4.4%), thymol-rich (2.4–3.1%) *L. origanoides* chemotypes (Martínez-Natarén et al., 2012; Stashenko et al., 2010).

These results showed that supercritical extraction at the conditions studied leaves behind a considerable amount of extract that is still retained in the matrix. However, the ethanol-modified $scCO_2$ extraction turned out to be considerably more selective for some chemotypes in the extraction of the target compounds (i.e., aglycones) when compared

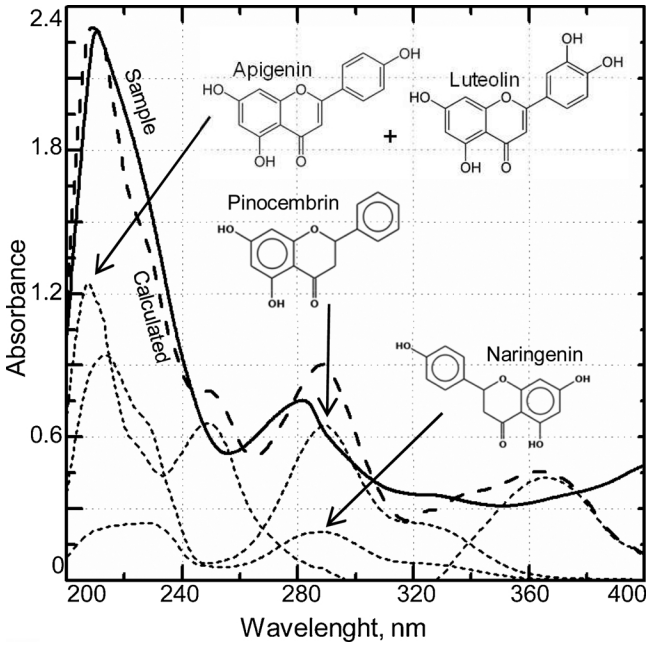

Fig. 4. Absorption electronic spectra of sample vertex 20 (-) and its corresponding prediction (- -). Predicted flavonoid content: 170.5 mg g^{-1}. Pinocembrin 75.4 mg $g^{-1}_{extract}$. naringenin 28.1 mg $g^{-1}_{extract}$. and luteolin + apigenin 67 mg $g^{-1}_{extract}$.

with the Soxhlet extraction. Flavonoid extraction selectivity using supercritical extraction (0.5 %) was almost twice that of the Soxhlet counterpart (2.8 %). The same behavior has been observed for other botanical materials when comparing $scCO_2$ with solid-liquid extractive techniques using hydro-alcoholic mixtures, or when water is included as a polarity modifier of CO_2 (Ganzera, 2015; Paes et al., 2014; Solana et al., 2015). Experiments on phase equilibrium could help to understand the phenomenon of mass transfer and lead to an increase in extraction yields of $scCO_2$ extraction considering the potential of the substrates with respect to the available flavonoids content and the advantageous selectivity offered by this technique.

3.7. Identification and quantification of best extracts

Phenolic composition results for the extracts according to UHPLC-ESI(+)-Orbitrap-MS with positive ionization mode are summarized in Table 4, including molecular formula, calculated and experimental *m/z* values, and error (δ mg/kg). A total of 15 phenolic compounds, including flavones, flavanones, flavonols, and flavanonol, identified by comparison of MS spectra and retention times with those of available standards, were found as constituents of the extract. Whereas, the investigated substrates contained mainly the same type of phenolics, differences in the amounts of individual substances in the $scCO_2$ extracts were detected. A group of unidentified compounds with molecular weights around 600 Da, with the longest retention times among the extract constituents, were also detected. They are probably related to chlorophyll pigments and cuticular waxes present in the extract. The phenolic compounds found in this work are similar to those reported by Leitão et al. (2017) in their study of ethanolic extracts of a *L. origanoides* thymol-carvacrol chemotype.

4. Conclusions

The results of this work were conclusive with respect to the potential of each distilled substrate studied to afford valuable byproducts that permit increasing the profitability of the extraction process of essential oils from *Lippia origanoides* and *Lippia graveolens*. The distilled substrate of *L. origanoides* phellandrene-rich chemotype is the byproduct with the highest industrial recovery potential (14.4 g_{ole} kg^{-1}_{DS}, 7.2 g_{flv} kg^{-1}_{DS} and 4.1 g_{PC} kg^{-1}_{DS}) using 0.8 kg_{CO_2}/g_{ole} followed by the thymol-rich (12.4 g_{ole} kg^{-1}_{DS}, 2.2 g_{flv} kg^{-1}_{DS} and 1.3 g_{PC} kg^{-1}_{DS}) using 1 kg_{CO_2}/g_{ole} and carvacrol-rich chemotypes (14.8 g_{ole} kg^{-1}_{DS}, 1.5 g_{flv} kg^{-1}_{DS} and 0.5 g_{PC} kg^{-1}_{DS}) using 0.9 kg_{CO_2}/g_{ole} and finally, *L graveolens* (5.6 g_{ole} kg^{-1}_{DS}, 0.27 g_{flv} kg^{-1}_{DS} and 0.16 g_{PC} kg^{-1}_{DS}) using 2 kg_{CO_2}/g_{ole}. Flow, pressure, time, and percent ethanol had a significant effect on the global extraction yield and flavonoid extraction yield of *L. origanoides* and *L. graveolens* using supercritical CO_2. The interval of temperatures chosen in this work did not significantly affect both extraction responses. The d_p-range that was obtained from two grids (0.5 and 2 mm opening) used in the chopper was not significant in the extraction yield responses. The best experimental conditions found for the supercritical CO_2 extraction of *L. origanoides* and *L. graveolens* were 307 bar, 5 % ethanol, 96 min,

Table 4
Composition of supercritical ethanol-modified CO_2 extracts from distillation byproducts of *Lippia origanoides* chemotypes and *Lippia graveolens* according to UHPLC-ESI(+)-Orbitrap-MS analysis. **A**. *Lippia origanoides* carvacrol-rich chemotype; **B**. *Lippia origanoides* thymol-rich chemotype; **C**. *Lippia origanoides* phellandrene-rich chemotype and **D**. *Lippia graveolens*.

Compound	Formula	[M+H]+		Δ, mg/kg	μg mg^{-1} extract ± *s* (*n* = 3)			
		Experimental	Calculated		A	B	C	D
Taxifolin[b]	$C_{15}H_{12}O_7$	305.06557	305.06548	0.3	0.19 ± 0.02	0.20 ± 0.02	0.06 ± 0.01	< LOD[d]
Eriodictyol[b]	$C_{15}H_{12}O_6$	289.07121	289.07105	0.57	4.9 ± 0.2	3.6 ± 0.3	0.44 ± 0.1	0.08 ± 0.01
Quercetin[a,c]	$C_{15}H_{10}O_7$	303.05047	303.05044	0.12	1.00 ± 0.07	< LOD	0.16 ± 0.01	< LOD
Luteolin[a,c]	$C_{15}H_{10}O_6$	287.05556	287.05529	0.92	0.46 ± 0.07	0.43 ± 0.07	0.06 ± 0.01	0.072 ± 0.003
Naringenin[a,c]	$C_{15}H_{12}O_5$	273.07629	273.07621	0.28	4.6 ± 0.2	5.5 ± 0.6	1.06 ± 0.05	0.27 ± 0.04
Hesperetin[b]	$C_{16}H_{14}O_6$	303.08631	303.0862	0.35	0.77 ± 0.01	1.72 ± 0.08	0.06 ± 0.01	0.056 ± 0.004
Apigenin[a,c]	$C_{15}H_{10}O_5$	271.06064	271.06042	0.82	0.14 ± 0.01	0.44 ± 0.02	< LOD	0.046 ± 0.004
Chrysoeriol[b]	$C_{16}H_{12}O_6$	301.07066	301.07036	0.99	1.3 ± 0.1	2.3 ± 0.1	0.04 ± 0.01	0.063 ± 0.002
Dimethylated flavone[a]	$C_{17}H_{14}O_7$	331.08123	331.08106	0.5	0.23 ± 0.01	0.75 ± 0.02	0.01 ± 0.01	< LOD
Pinocembrin[a,c]	$C_{15}H_{12}O_4$	257.08138	257.08132	0.2	0.67 ± 0.04	2.0 ± 0.2	48.3 ± 1.0	7.9 ± 0.3
Cirsimaritin[b]	$C_{17}H_{14}O_6$	315.08631	315.08605	0.83	2.34 ± 0.04	3.5 ± 0.1	0.05 ± 0.01	0.5 ± 0.02
Sakuranetin[b]	$C_{16}H_{14}O_5$	287.0914	287.09132	0.28	3.1 ± 0.29	4.8 ± 0.1	1.42 ± 0.08	4.8 ± 0.3
Galangin[b]	$C_{15}H_{10}O_5$	271.06064	271.06051	0.49	< LOD	< LOD	7.2 ± 0.2	0.44 ± 0.03
Methylated galangin[b]	$C_{16}H_{12}O_5$	285.07575	285.07563	0.42	< LOD	< LOD	4.1 ± 0.2	< LOD
Methylated apigenin[b]	$C_{16}H_{12}O_5$	285.07575	285.07687	0.37	0.15 ± 0.02	0.66 ± 0.05	< LOD	< LOD[d]

[a] Quantified with calibration curve.
[b] Tentative identification based on mass spectrum and fragmentation pattern.
[c] Confirmatory identification with certified standard substances.
[d] Limit of detection.

and 43 g CO_2/min under the specifications of the extraction system used.

CRediT authorship contribution statement

Julián Arias: Methodology, Software, Investigation. **Jesica Mejía:** Investigation. **Yuri Córdoba:** Investigation. **Jairo René Martínez:** Supervision, Writing - review & editing. **Elena Stashenko:** Supervision, Funding acquisition. **José Manuel del Valle:** Writing - review & editing.

Declaration of Competing Interests

The authors declare that they have no known competing financial interests or personal relationships that could have appeared to influence the work reported in this paper.

Acknowledgments

Financial support from Universidad Industrial de Santander [grant number 1872], and *Patrimonio Autónomo Fondo Nacional de Financiamiento para la Ciencia, la Tecnología y la Innovación, Francisco José de Caldas*, Contract RC 0572-2012, are acknowledged. JA acknowledges the economic support of Departamento Administrativo de Ciencia, Tecnología e Innovación de Colombia (COLCIENCIAS) through the PhD Scholarship, Call 567 of 2012. Diego Castiblanco, Andrea Gómez y Giocarlo Vásquez are gratefully acknowledged for their support in the experimental development of the work.

Appendix A. Supplementary data

Supplementary material related to this article can be found, in the online version, at doi:https://doi.org/10.1016/j.indcrop.2020.112170.

References

Allen, T., 1981. Particle Size Measurement. Chapman and Hall.

Barth, H.G., 1984. Modern Methods of Particle Size Analysis. Wiley.

Bautista, R., Jimenez, F., Jimenez, A.I., Arias, J.J., 1993. Multicomponent analysis: comparison of various graphical and numerical methods. Talanta 40, 1687–1694. https://doi.org/10.1016/0039-9140(93)80085-6.

Bautista, R.D., Jiménez, A.I., Jiménez, F., Arias, J.J., 1996. Simultaneous determination of diazepam and pyridoxine in synthetic mixtures and pharmaceutical formulations using graphical and multivariate calibration-prediction methods. J. Pharm. Biomed. Anal. 15, 183–192. https://doi.org/10.1016/0731-7085(96)01844-4.

Bermúdez, M.-D., Carrión-Vilches, F.-J., Martínez-Nicolás, G., Pagán, M., 2002. Supercritical carbon dioxide extraction of a liquid crystalline additive from polystyrene matrices. J. Supercrit. Fluids 23, 59–63. https://doi.org/10.1016/S0896-8446(01)00139-5.

Chafer, A., Fornari, T., Berna, A., Stateva, R.P., 2004. Solubility of quercetin in supercritical CO2 + ethanol as a modifier: measurements and thermodynamic modelling. J. Supercrit. Fluids 32, 89–96. https://doi.org/10.1016/j.supflu.2004.02.005.

Cheng, Y., Honggang, Z., Huiying, L., Lixin, L., Ruiqiu, S., Jingjing, G., Weihe, L., Min, Q., Shuai, S., Haiyan, B., Kai, H., Ruxia, D., Yiying, W., Yunyao, C., Jiakun, B., 2019. Pinocembrin is in Preparation for Treating the Application in Pulmonary Fibrosis Disease Drug. CN109806256A. .

Chimowitz, E.H., Pennisi, R.J., 1986. Process synthesis concepts for supercritical gas extraction in the crossover region. AIChE J. 32, 1665–1676. https://doi.org/10.1002/aic.690321010.

Cuadros-Rodríguez, L., Bagur-González, M.G., Sánchez-Viñas, M., González-Casado, A., Gómez-Sáez, A.M., 2007. Principles of analytical calibration/quantification for the separation sciences. J. Chromatogr. A 1158, 33–46. https://doi.org/10.1016/J.CHROMA.2007.03.030.

da Silva, A.P., Silva, N., de, F., Andrade, E.H.A., Gratieri, T., Setzer, W.N., Maia, J.G.S., da Silva, J.K.R., 2017. Tyrosinase inhibitory activity, molecular docking studies and antioxidant potential of chemotypes of *Lippia origanoides* (Verbenaceae) essential oils. PLoS One 12, e0175598. https://doi.org/10.1371/journal.pone.0175598.

De Oliveira, P.F., MacHado, R.A.F., Bolzan, A., Barth, D., 2012. Supercritical fluid extraction of hernandulcin from Lippia dulcis Trev. J. Supercrit. Fluids 63, 161–168. https://doi.org/10.1016/j.supflu.2011.12.003.

Díaz-Reinoso, B., Moure, A., Domínguez, H., Parajó, J.C., 2006. Supercritical CO2 extraction and purification of compounds with antioxidant activity. J. Agric. Food Chem. 54, 2441–2469. https://doi.org/10.1021/jf052858j.

Du, G., Ma, Y., Song, J., Li, L., Niu, Z., Wu, S., Lv, Y., 2018. Applications of Pinocembrin in Preparing Anti-Cerebral Hemorrhage Medicament. WO2018090358 (A1). .

Ganzera, M., 2015. Supercritical fluid chromatography for the separation of isoflavones. J. Pharm. Biomed. Anal. 107, 364–369. https://doi.org/10.1016/J.JPBA.2015.01.013.

Goodger, J.Q.D., Senaratne, S.L., van der Peet, P., Browning, R., Williams, S.J., Nicolle, D., Woodrow, I.E., 2019. *Eucalyptus* subgenus *Eucalyptus* (Myrtaceae) trees are abundant sources of medicinal pinocembrin and related methylated flavanones. Ind. Crops Prod. 131, 166–172. https://doi.org/10.1016/J.INDCROP.2019.01.050.

Hernandes, C., Pina, E.S., Taleb-Contini, S.H., Bertoni, B.W., Cestari, I.M., Espanha, L.G., Varanda, E.A., Camilo, K.F.B., Martinez, E.Z., França, S.C., Pereira, A.M.S., 2017. *Lippia origanoides* essential oil: an efficient and safe alternative to preserve food, cosmetic and pharmaceutical products. J. Appl. Microbiol. 122, 900–910. https://doi.org/10.1111/jam.13398.

Lan, X., Wang, W., Li, Q., Wang, J., 2016. The natural flavonoid pinocembrin: molecular targets and potential therapeutic applications. Mol. Neurobiol. 53, 1794–1801. https://doi.org/10.1007/s12035-015-9125-2.

Lan, X., Han, X., Li, Qian, Li, Qiang, Gao, Y., Cheng, T., Wan, J., Zhu, W., Wang, J., 2017. Pinocembrin protects hemorrhagic brain primarily by inhibiting toll-like receptor 4 and reducing M1 phenotype microglia. Brain Behav. Immun. 61, 326–339. https://doi.org/10.1016/J.BBI.2016.12.012.

Leitao, N., Prado, G.H.C., Veggi, P.C., Meireles, M.A., Pereira, C.G., 2013. Anacardium occidentale L. leaves extraction via SFE: global yields, extraction kinetics, mathematical modeling and economic evaluation. J. Supercrit. Fluids 78, 114–123. https://doi.org/10.1016/j.supflu.2013.03.024.

Leitão, S.G., Leitão, G.G., Vicco, D.K.T., Barreto-Pereira, J.P., de Morais-Simão, G., Oliveira, D.R., Celano, R., Campone, L., Piccinelli, A.L., Rastrelli, L., 2017. Countercurrent chromatography with off-line detection by ultra high performance liquid chromatography/high resolution mass spectrometry in the study of the phenolic profile of *Lippia origanoides*. J. Chromatogr. A 1520, 83–90. https://doi.org/10.1016/J.CHROMA.2017.09.004.

Li, Long-Ze, Mukhopadhyay, S., Robbins, R.J., Harnly, J.M., 2007. Identification and quantification of flavonoids of Mexican oregano (*Lippia graveolens*) by LC-DAD-ESI/MS analysis. J. Food Compos. Anal. 20, 361–369. https://doi.org/10.1016/j.jfca.2006.09.005.

Li, A., Sun, A., Liu, R., 2012. Preparative isolation and purification of three flavonoids from the Chinese medicinal plant *Alpinia katsumadai hayata* by high-speed countercurrent chromatography. J. Liq. Chromatogr. Relat. Technol. 35, 2900–2909. https://doi.org/10.1080/10826076.2011.643523.

Lopes, A., Dantas, J., Freire, M., Bressan, R., Accioly, T., 2013. Formulção farmaceutica derivada de óleo essencial de Lippia origanoides H.B.K. BRPI1105457-3 A2. .

Maio, G., von Holst, C., Wenclawiak, B.W., Darskus, R., 1997. Supercritical fluid extraction of some chlorinated benzenes and cyclohexanes from soil: optimization with fractional factorial design and simplex. Anal. Chem. 69, 601–606. https://doi.org/10.1021/ac960349y.

Maisch, J., 1885. On some useful plants of the natural order of Verbenaceae. Am. J. Pharm. 57, 189–199.

Martínez-Natarén, D.A., Parra-Tabla, V., Dzib, G., Acosta-Arriola, V., Canul-Puc, K.A., Calvo-Irabién, L.M., 2012. Essential oil yield variation within and among wild populations of Mexican Oregano (*Lippia graveolens* H.B.K.-Verbenaceae), and its relation to climatic and edaphic conditions. J. Essent. Oil Bear. Plants 15, 589–601. https://doi.org/10.1080/0972060X.2012.10644093.

Miller, J.N., Miller, J.C., 2010. Statistics and Chemometrics for Analytical Chemistry, sixth. ed. Pearson Education.

Montgomery, D., 2008. Design and Analysis of Experiments, 6a ed. John Wiley and Sons, New York.

Navarrete, A., Herrero, M., Martín, A., Cocero, M.J., Ibáñez, E., 2011. Valorization of solid wastes from essential oil industry. J. Food Eng. 104, 196–201. https://doi.org/10.1016/J.JFOODENG.2010.10.033.

Nelder, J.A., Mead, R., 1965. A simplex method for function minimization. Comput. J. 7, 308–313. https://doi.org/10.1093/comjnl/7.4.308.

Núñez, G.A., del Valle, J.M., de la Fuente, J.C., 2010. Solubilities in supercritical carbon dioxide of (2e,6e)-3,7,11-trimethyldodeca-2,6,10-trien-1-ol (farnesol) and (2s)-5,7-dihydroxy-2-(4-hydroxyphenyl)chroman-4-one (naringenin). J. Chem. Eng. Data 55, 3863–3868. https://doi.org/10.1021/je900957v.

Oliveira, E.L.G., Silvestre, A.J.D., Silva, C.M., 2011. Review of kinetic models for supercritical fluid extraction. Chem. Eng. Res. Des. 89, 1104–1117. https://doi.org/10.1016/J.CHERD.2010.10.025.

Olivieri, A.C., Faber, N.M., Ferré, J., Boqué, R., Kalivas, J.H., Mark, H., 2006. Uncertainty estimation and figures of merit for multivariate calibration (IUPAC Technical Report). Pure Appl. Chem. 78, 633–661. https://doi.org/10.1351/pac200678030633.

Ortiz, R.E., Afanador, G., Vásquez, D.R., Ariza-Nieto, C., 2017. Efecto del aceite esencial de orégano sobre el desempeño productivo de ponedoras y la estabilidad oxidativa de huevos enriquecidos con ácidos grasos poliinsaturados. Rev. la Fac. Med. Vet. y Zootec. 64, 61–70.

Paes, J., Dotta, R., Barbero, G.F., Martínez, J., 2014. Extraction of phenolic compounds and anthocyanins from blueberry (*Vaccinium myrtillus* L.) residues using supercritical CO2 and pressurized liquids. J. Supercrit. Fluids 95, 8–16. https://doi.org/10.1016/J.SUPFLU.2014.07.025.

Pereira, C.G., Meireles, M.A.A., 2010. Supercritical fluid extraction of bioactive compounds: fundamentals, applications and economic perspectives. Food Bioprocess Technol. 3, 340–372. https://doi.org/10.1007/s11947-009-0263-2.

Rasul, A., Millimouno, F.M., Ali Eltayb, W., Ali, M., Li, J., Li, X., 2013. Pinocembrin: a novel natural compound with versatile pharmacological and biological activities. Biomed Res. Int., 379850. https://doi.org/10.1155/2013/379850.

Reverchon, E., Senatore, F., 1992. Isolation of rosemary oil: comparison between hydrodistillation and supercritical CO2 extraction. Flavour Fragr. J. 7, 227–230.

https://doi.org/10.1002/ffj.2730070411.
Ribeiro, A.F., Andrade, E.H.A., Salimena, F.R.G., Maia, J.G.S., 2014. Circadian and seasonal study of the cinnamate chemotype from Lippia origanoides Kunth. Biochem. Syst. Ecol. 55, 249–259. https://doi.org/10.1016/J.BSE.2014.03.014.
Safaralie, A., Fatemi, S., Salimi, A., 2010. Experimental design on supercritical extraction of essential oil from valerian roots and study of optimal conditions. Food Bioprod. Process. 88, 312–318. https://doi.org/10.1016/J.FBP.2009.02.002.
Saldaña, M.D.A., Temelli, F., Guigard, S.E., Tomberli, B., Gray, C.G., 2010. Apparent solubility of lycopene and β-carotene in supercritical CO2, CO2 + ethanol and CO2 + canola oil using dynamic extraction of tomatoes. J. Food Eng. 99, 1–8. https://doi.org/10.1016/J.JFOODENG.2010.01.017.
Sánchez-Vioque, R., Polissiou, M., Astraka, K., de los Mozos-Pascual, M., Tarantilis, P., Herraiz-Peñalver, D., Santana-Méridas, O., 2013. Polyphenol composition and antioxidant and metal chelating activities of the solid residues from the essential oil industry. Ind. Crops Prod. 49, 150–159. https://doi.org/10.1016/J.INDCROP.2013.04.053.
Sematech, N., 2006. e-Handbook of Statistical Methods [WWW Document]. URL http://www.itl.nist.gov/div898/handbook/ (Accessed 5 November 2018). .
Sharif, K.M., Rahman, M.M., Azmir, J., Mohamed, A., Jahurul, M.H.A., Sahena, F., Zaidul, I.S.M., 2014. Experimental design of supercritical fluid extraction—a review. J. Food Eng. 124, 105–116. https://doi.org/10.1016/J.JFOODENG.2013.10.003.
Solana, M., Boschiero, I., Dall'Acqua, S., Bertucco, A., 2015. A comparison between supercritical fluid and pressurized liquid extraction methods for obtaining phenolic compounds from *Asparagus officinalis* L. J. Supercrit. Fluids 100, 201–208. https://doi.org/10.1016/J.SUPFLU.2015.02.014.
Sovová, H., 2012. Apparent solubility of natural products extracted with near-critical carbon dioxide. Am. J. Anal. Chem. 03, 958–965. https://doi.org/10.4236/ajac.2012.312a127.
Stashenko, E.E., Martínez, J.R., Ruíz, C.A., Arias, G., Durán, C., Salgar, W., Cala, M., 2010. *Lippia origanoides* chemotype differentiation based on essential oil GC-MS and principal component analysis. J. Sep. Sci. 33, 93–103. https://doi.org/10.1002/jssc.200900452.
Stashenko, E.E., Martínez, J.R., Cala, M., Durán, D.C., Caballero, D., 2013. Chromatographic and mass spectrometric characterization of essential oils and extracts from *Lippia* (Verbenaceae) aromatic plants. J. Sep. Sci. 36, 192–202. https://doi.org/10.1002/jssc.201200877.
Stashenko, E., Martínez, J., Arias, J., Córdoba, Y., Durán, D., Mejia, J., Tavera, C., 2018. Method for making full use of *Lippia origanoides*. WO2018122654A1. .
Suzuki, K., Sue, H., Itou, M., Smith, R.L., Inomata, H., Arai, K., Saito, S., 1990. Isothermal vapor-liquid equilibrium data for binary systems at high pressures: carbon dioxide-methanol, carbon dioxide-ethanol, carbon dioxide-1-propanol, methane-ethanol, methane-1-propanol, ethane-ethanol, and ethane-1-propanol systems. J. Chem. Eng. Data 35, 63–66. https://doi.org/10.1021/je00059a020.
Wang, W., Zhang, H., Lee, D.-H., Yu, J., Cheng, T., Hong, M., Jiang, S., Fan, H., Huang, X., Zhou, J., Wang, J., 2017. Using functional and molecular MRI techniques to detect neuroinflammation and neuroprotection after traumatic brain injury. Brain Behav. Immun. 64, 344–353. https://doi.org/10.1016/J.BBI.2017.04.019.
Yamamoto, N., Kawabata, K., Sawada, K., Ueda, M., Fukuda, I., Kawasaki, K., Murakami, A., Ashida, H., 2011. Cardamonin stimulates glucose uptake through translocation of glucose transporter-4 in L6 myotubes. Phyther. Res. 25, 1218–1224. https://doi.org/10.1002/ptr.3416.
Yang, X., Wang, X., Chen, X.Y., Ji, H.Y., Zhang, Y., Liu, A.J., 2018. Pinocembrin–lecithin complex: characterization, solubilization, and antioxidant activities. Biomolecules 8, 41. https://doi.org/10.3390/biom8020041.

Appendix D. Article 2

Computers and Chemical Engineering 135 (2020) 106738

Contents lists available at ScienceDirect

Computers and Chemical Engineering

journal homepage: www.elsevier.com/locate/compchemeng

Dynamic modeling and experimental validation of essential oils fractionation: Application for the production of phenylpropanoids

Julián Arias[a], Daniel Casas-Orozco[b], Andrés Cáceres-León[a], Jairo Martínez[a], Elena Stashenko[a], Aída-Luz Villa[b,*]

[a] Biomolecules Research Center, CIBIMOL, Universidad Industrial de Santander, UIS, Carrera 27 calle 9, Bucaramanga, Colombia
[b] Environmental Catalysis Research Group, Chemical Engineering Department, Engineering Faculty, Universidad de Antioquia UdeA, Calle 70 No. 52-51, Medellín, Colombia

ARTICLE INFO

Article history:
Received 9 October 2019
Revised 12 December 2019
Accepted 15 January 2020
Available online 23 January 2020

Keywords:
Oregano essential oil
Batch distillation
Dynamic modeling
Fractionation
Rectification
Data reconciliation

ABSTRACT

Batch distillation is useful in the essential oil (EO) industry to standardize and improve EO properties. Using the *Lippia origanoides* EO as a source of phenylpropanoids, a methodology was developed to solve and experimentally validate a batch distillation model, which described separation of EO major constituents over time. Nine EOs were distilled and their composition and distillation products were determined. Seven major constituents were used to represent the EOs and their distillation products in the mathematical analyses performed, namely, data reconciliation to modify the streams compositions in order to meet material balances, and a rigorous distillation model to describe the system dynamics. Statistical parameters ($r^2 = 0.95$, $MSE = 0.002$) were calculated to compare predicted and experimental data, showing that the model can accurately predict the composition of distillation cuts. This methodology can be extended to other EOs of industrial interest to support their fractionation processes.

1. Introduction

The useful bioactive properties of "oregano" EO are widely known. Its benefits are mainly attributed to the presence of two phenylpropanoids, namely, thymol and carvacrol. These molecules have aroused interest in commercial applications such as food additive, preservative, or pest control agent, among others (Madrid Garcs et al., 2017; Ortiz et al., 2017; Hernandes et al., 2017; Mar et al., 2018; Ríos et al., 2017). The most widely known natural sources of thymol and carvacrol are thyme (*Thymus vulgaris*) and mediterranean oregano (*Origanum vulgare*), both of Eurasian origin.

Thymol and carvacrol contents in the essential oil (EO) of thyme (ISO 19817:2017) are 37-55wt % and 0.5-5.5wt %, respectively, and approximately 22 wt % and 18wt %, respectively, for mediterranean oregano (dAntuono et al., 2000). *Lippia origanoides*, also called mountain oregano, is found in tropical America in various chemotypes. Thymol (52-78wt %) and carvacrol (36-72wt %) are the main components of the EO of three of these chemotypes (Oliveira et al., 2007; Stashenko et al., 2010; da Silva et al., 2017). The bioactivity of the EOs of these plants has been studied extensively in recent years, e.g., the antigenotoxic capacity against UV radiation (Fuentes et al., 2017), the antimicrobial capacity due to the presence of compounds that alter the permeability of the bacterial membrane (Sarrazin et al., 2015; Prez Zamora et al., 2018), the anti-*Leishmania* capacity with certain limitations of oral and cutaneous toxicity (Neira et al., 2018) and the *in vitro* antiparasitic capacity against *Colossoma macropomum*, with limitations of application in native freshwater fish (Soares et al., 2017).

The variation in the composition of the EOs obtained at the same extraction conditions from the same plants, is due to the vegetative harvest cycle, the agricultural conditions of the growth and the post-harvest treatment, among other causes (Santos-Gomes and Fernandes-Ferreira, 2001; Telci et al., 2009). To carry out the formulation of industrial products based on EOs, it is indispensable to standardize their composition. It may even be of interest to isolate single, high-purity compounds. This is carried out by separation operations, of which distillation is one of the oldest and most commonly used (Kenig et al., 2014). Fractionation of EOs by distillation processes, although few in the literature, has been applied in different ways. For instance, Castillo-Herrera et al. collected fractions of the streams coming from the hydrodistillation process of *Lippia graveolens* (one of the synonyms of *L. origanoides* (O'Leary et al., 2012)) to increase the concentration of phenyl-propanoids (i.e., thymol and carvacrol). Other works have focused on the fractional distillation of hydrodistillation products

* Corresponding author.
E-mail address: aida.villa@udea.edu.co (A.-L. Villa).

https://doi.org/10.1016/j.compchemeng.2020.106738
0098-1354/

(e.g., *Citrus* EOs (Silvestre et al., 2016; Habsari et al., 2018; Perini et al., 2017; Stuart et al., 2001; Fang et al., 2004; Lopes et al., 2003; Zamar et al., 2005) and EOs from other botanical substrates (Farah et al., 2006; Beneti et al., 2011; Shaw, 1951; Milojević et al., 2010; Almeida et al., 2018; Alighiri et al., 2018; Pires et al., 2019; Asadi, 2014)) at ambient or reduced pressure, improving the quality of products and/or the operation conditions in all cases. However, we agree with Almeida et al. that the reports on modeling and simulation of EOs fractionation are limited in the literature, since the numerical solution can be complex and, up to date, the EOs industry has been developed mainly on heuristic bases (Almeida et al., 2018).

Since the late 1960's, when the first models of the complete dynamics of a multi-component batch distillation were proposed (Distefano, 1968; Domenech and Enjalbert, 1974), simplifications to those rigorous models (shortcuts methods) have been proposed to simplify and accelerate the calculations (Bonsfills and Puigjaner, 2004). These approaches are based on the assumption that batch distillation can be regarded as a series of short-time, continuous distillation steps, for which the Fenske–Underwood–Gilliland method applies (Diwekar and Madhavan, 1991; Sundaram and Evans, 1993). By this means, algebraic equations with relatively straightforward solution schemes are obtained (Mujtaba, 2004; Diwekar, 2012). These methods usually neglect intermediate column holdup and assume constant volatility during the entire operation. Based on this approach, other authors have developed similar calculation methods (Salomone et al., 1997; Zamar et al., 1998; García et al., 2014) with preliminary design purposes, and to develop tools for optimal control and production planning of batch distillation processes (Sundaram and Evans, 1993; Bonsfills and Puigjaner, 2004; Farhat et al., 1990). Another set of simplified batch distillation models retain the original differential form of the set of governing equations (Distefano, 1968), but vary the way of calculating phase equilibria (constant relative volatility vs. rigorous VLE computations with activity and/or fugacity coefficients), whether internal molar flows are constant or time-dependent (no need for energy balances in the former case) or whether internal holdups are kept constant or time-dependent, leading to 1-index differential-algebraic equations (DAE) systems or 2-index DAE systems, respectively (Mujtaba, 2004).

From the literature of the last 50 years, it is clear that the approach and application of multi-component batch distillation models evolved along with the calculation and computational resources. Regarding the application of batch distillation to EOs, the literature dates back to 2005, when Zamar et al. applied a shortcut batch distillation model developed by the same authors (Zamar et al., 1998) to support the planning of separations in the orange EO industry (Zamar et al., 2005). Using *Aspen Plus®*, Milojević et al. (2010) modeled the batch fractionation of *Juniperus communis* with good fit of the experiments with the model predictions (Milojević et al., 2010), whereas Asadi studied the continuous distillation of spearmint EO at atmospheric pressure (a rather uncommon operation given the prevalence of batch distillation in EO rectification) considering non-idealities of the mixture in both liquid and vapor phases (Asadi, 2014). The most recent studies on the modeling of EOs fractionation by batch distillation are for EOs of *Eucalyptus* (Almeida et al., 2018) and *Achyrocline satureioides* (Pires et al., 2019). These works focus on the thermodynamic correlations used to obtain the properties required in phase-equilibria calculations, i.e., vapor pressures estimated through a Corresponding-States with Group Contribution (CSGC) method, and activity coefficients estimated through quantum calculations (COSMO-SAC method). Our observation, after reviewing the five works found in the open literature on the subject, is the same one made by Bonsfills and Puigjaner (Bonsfills and Puigjaner, 2004) more than a decade ago: only a few research works are experimentally validated in batch distillation, i.e., there is a lack of experimental studies in batch distillation. As a consequence, the way in which the predictive capacity of the model is affected when the feeding stream varies in its composition, as in the case of essential oils, is generally not studied or reported.

In this work, we aim to assert the predictive capacity of a rigorous batch distillation model applied to foresee *L. origanoides* EO distillation products. For this purpose, EOs with different initial compositions were fractionally distilled and the compositions of their cuts were determined. Prior to comparing the experimental results with simulated data, data reconciliation (Tamhane and Mah, 1985; Özyurt and Pike, 2004) was applied to the collected distillation composition data to enforce the fulfillment of material balances, a methodology not implemented in the literature of batch distillation of EOs to the best of our knowledge. A rigorous distillation model, which includes material and energy balances, along with phase equilibria relations, was described and solved. Finally, reconciled data were compared with predicted data to test model prediction capacity.

Our manuscript is organized as follows: Section 2 shows the experimental and computational resources used to develop this study. Section 3 presents the mathematical framework to solve the data reconciliation problem and the dynamic batch distillation model. Sections 4 and 5 show the results of the batch distillation experiments, and the comparison between reconciled and simulated data, including a statistical analysis on the observed deviations.

2. Materials and methods

2.1. Standard substances and essential oils

p-Cymene (99%), γ-terpinene ($\geq$ 97%), thymol ($\geq$ 99.5%), carvacrol ($\geq$ 98%) and *trans*-β-caryophyllene ($\geq$ 98.5%) were obtained from Sigma-Aldrich (St. Louis, MO, USA). Nine different essential oils isolated by steam distillation from different harvests of the same *L. origanoides* experimental plantation were employed in this work. The essential oils were obtained at the pilot agroindustrial complex of the National Center for Agroindustrialization of Aromatic and Medicinal Tropical Vegetal Species, CENIVAM, at Universidad Industrial de Santander, in Bucaramanga and Barbosa, Colombia.

2.2. Batch fractional distillation apparatus

The batch fractional distillation process was carried out on a B/R Micro fractional distillation apparatus (B/R Instruments 800. Easton, MD, USA). The batch distillation column was 0.34 m high and 7×10^{-3} m internal diameter. The column contains a Teflon-coated rotary screw (spinning band), which confers 30 theoretical stages. A feeding reboiler of 25 mL is connected at the bottom of the column. An electric blanket (800 W) heats the boiler. The steam flow passes through a glass condenser at the top of the column. The system has a fraction collector with four vials of 4 mL. The auxiliary equipments are: a rotatory vane vacuum pump (Edwards RV8, Burgess Hill, WS, UK) connected to the volatiles trap, a cooling circulating bath (Lauda Alpha RA8, Derlan, NJ, USA) connected to the condenser, a pressure transducer, and a digital thermometer with two (T1 and T2) K-type thermocouples that are used to measure the temperatures at the top and bottom of the column.

2.3. Batch fractional distillation of the essentials oils

A 25 mL reboiler was used to feed the EO. The reboiler was heated by a surrounding sand bath, with a maximum temperature of 473 K. The heating rate was selected in preliminary experiments

to reach column temperatures up to 413 K after 8 hours of distillation. The temperature of the cooling circulating bath was set at 275 K. The operation pressure was set at 7 torr according to the best results of preliminary experiments using different EO compositions of *L. origanoides*. From 9-13 g of EO were fed for each one of the nine experiments (L01–L09). 100 μL were removed from the reboiler for GC-FID analysis. Bottom and top column temperatures were read and recorded every 4 min. A reflux valve remained closed during the distillation process (total reflux), and was opened only to collect the cut when the last 5 temperatures registered at the column top reached a relative standard deviation (*RSD*) of less than 2.5%. Then, the reflux valve was closed, the vacuum valve was opened and the vacuum pump was turned off to momentarily stop the distillation when the *RSD* increased above 2.5%. The fraction collected in the reservoir, the EO remaining in the reboiler and the fraction retained in the trap were weighed and their compositions were determined by gas chromatography. Therefore, the experimental measurements were the compositions and masses of feed, top, and bottom fractions together with the top and bottom column temperatures. The experimental data are available in the supporting information, cf. Section 0.3. The reboiler, which contained the previous bottom fraction, was again connected to the column to continue with the next distillation step. One (for L02, L04–L09) or two (for L01 and L03) consecutive distillation steps were carried out for the experiments, depending on experimental performance. For L01 and L03, the mass of the intermediate bottom-feed fraction was not measured, but estimated by material balance. The experiment ended when the temperature in the reboiler was greater than 373 K.

2.4. Gas chromatography

A 6890N (Agilent Technologies Palo Alto, California, U.S.A.) gas chromatograph equipped with FID, split/splitless injector (1:30 split ratio), and a data system (ChemStation Rev.B.03.02) was used for analysis and quantification of essential oil components. The detector and the injector temperatures were set at 523 K. A DB-5 (J&W Scientific, Folsom, CA, U.S.A.) 25 m $\times$ 0.20 mm $\times$ 0.33 μm id capillary column coated with 5%-phenyl poly(methylsiloxane) was used for quantification and linear retention indices determination. The GC oven temperature was programmed from 318 K (5 min) to 423 K (2 min) at 4 K min, then to 523 K (5 min) at 5 K min^{-1}, and finally, to 573 K (60 min) at 10 K min^{-1}. The temperatures of the injection port, ionization chamber, and of the transfer line were set at list 523 K, 503 K 558 K, respectively. Helium (99.995%, Linde, Bucaramanga, Colombia) was used as carrier gas, with 117 kPa column head pressure and 26 cm s^{-1} linear velocity (1 mL min^{-1}, at constant flow).

2.5. Quantification

The external calibration methodology (EC) was employed for quantification. This method uses calibration curves of standard substances to relate concentration with chromatographic peak area (Miller and Miller, 2005). We avoided quantifying with the method of internal standard (IS), which is not properly considered as a calibration methodology (Cuadros-Rodrguez et al., 2007). Calibration curves, for *p*-cymene, γ-terpinene, thymol, carvacrol and *trans*-β-caryophyllene, were prepared and analyzed under the same chromatographic conditions used with the EO and their fractions. The quantification of the substances for which the standard was not available were calculated from a surrogate. Thus, the composition of β-myrcene and humulene employed the *p*-cymene and *trans*-β-caryophyllene calibrations curves, respectively. Each point of the curve was prepared two times from a stock solution containing the reference substances in mixture at the same mass concentration. The concentrations were 0.1, 0.5, 1, 5, 10, 15 and 20 mg mL^{-1}.

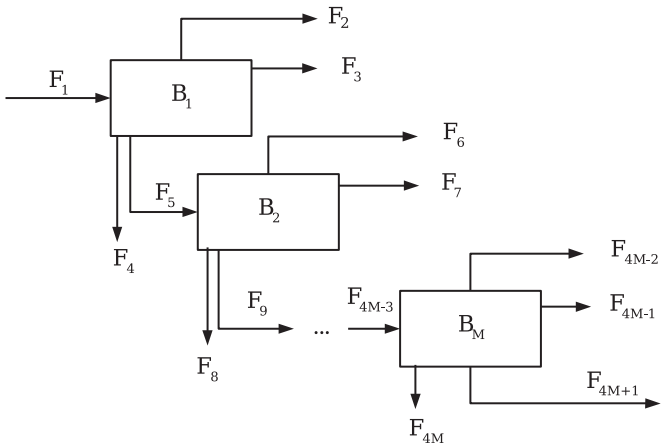

Fig. 1. Generalized block representation for the distillation tests. Odd streams: measured data, even streams: material losses, B: distillation stage.

2.6. Computational resources

All the computational tools used in this work were written in `Python 3.7`. The reconciliation problem was solved using IPOPT (Wächter and Biegler, 2006) through the `Python` interface `cyipopt`. Routines for the calculation of the gradient of the objective function and the (constant) jacobian of the set of constraints were provided, and properly checked with the `derivative_test` option of IPOPT.

The dynamic batch distillation model was solved using the Differential Algebraic Equation (DAE) integrator IDA (SUNDIALS (Hindmarsh et al., 2005)), through the `Python` interface `Assimulo` (Andersson et al., 2015). IDA internally implements Backward Differentiation Formulas (BDF (Hairer and Wanner, 1991)).

3. Theory and calculation

3.1. Reconciliation problem

The distillation process in this work can be schematized as shown in Fig. 1. In general, oils were rectified in a sequential manner, i.e. a fraction is collected as top product and the remaining bottom is fed to the next distillation. Since the column was operated at reduced pressure, material losses were observed at the top (vapor trap); additionally, some amount of oil is retained in the column (on its internal surface). Therefore, both top and bottom losses (even-numbered streams in Fig. 1) were included in the reconciliation problem.

Process streams F can be conveniently mapped using a matrix S with modeling and computational purposes, as shown in Eq. (1) (M distillation steps -blocks in Fig. 1- and $N = 4M + 1$ flows):

$$S = \begin{bmatrix} S_{11} & S_{12} & \cdots & S_{1N} \\ S_{21} & S_{22} & \cdots & S_{2N} \\ \vdots & \vdots & \ddots & \vdots \\ S_{M1} & S_{M2} & \cdots & S_{MN} \end{bmatrix} \tag{1}$$

S_{mn} terms ($m = \{1, 2, \cdots, M\}$, $n = \{1, 2, \cdots, N\}$) in Eq. (1) take the value $\pm F_n$ if stream F_n enters or exits block B_m. For instance, S_{11} takes the value F_1, because F_1 enters block B_1, whereas S_{13} corresponds to $-F_3$, because F_3 exits block B_1. Accordingly, $S_{21} = 0$, because F_1 does not enter nor exits block B_2.

Similarly, mass fraction data were organized in matrix form, for p ($p = 1, \ldots, P$) flows and q ($q = 1, \ldots, Q$) components:

$$X^{data} = \begin{bmatrix} x_{11} & x_{12} & \cdots & x_{1Q} \\ x_{21} & x_{22} & \cdots & x_{2Q} \\ \vdots & \vdots & \ddots & \vdots \\ x_{P1} & x_{P2} & \cdots & x_{PQ} \end{bmatrix} \tag{2}$$

With the above definitions, the reconciliation problem was posed as an equality-constrained optimization problem, Eqs. (3a). The purpose of this optimization problem is to make material balances consistent, by obtaining a new set X of *reconciled* mass fractions (decision variables in the optimization problem) that i) is as close as possible to the original (measured) mass fraction data X^{data}, ii) meets material balances for each component in each distillation stage (see Fig. 1) and iii) sum to one for each process stream (row-wise when $X^{reconciled}$ is arranged as shown in Eq. (2)).

$$\underset{X}{\text{minimize}} \sum_{p} \sum_{q} \left(x_{pq} - x_{pq}^{data}\right)^2 \tag{3a}$$

$$\text{subject to } \text{vec}[(S \cdot X)^T] = 0 \tag{3b}$$

$$1 - \sum_{q=1}^{Q} x_{pq} = 0 \quad p = 1, \ldots, P \tag{3c}$$

$$0 \le x_{pq} \le ub_{pq} \quad p = 1, \ldots, P \quad q = 1, \ldots, Q \tag{3d}$$

where:

- Eqs. (3b) represent the material balance constraints for all the component in all the process blocks (material input for component q in any block must equate the sum of all its outputs from that block). The operator vec concatenates the columns of the product $(S \cdot X)^T$ (a $q \times p$ matrix) into an $q \cdot p$ column vector of constraints (Macedo and Oliveira, 2013; Petersen and Pedersen, 2012).
- Eqs. (3c) enforce the sum of mass fractions to be 1 in for each process stream p.
- Eqs. (3d) constraint the decision variables between zero and an upper bound ub_{pq}. In general, $ub_{pq} = 1$. However, certain measured fractions were below their corresponding quantification limits, i.e. $x_{pq}^{data} < LQ_q$ (see Table 2). Therefore, the optimization variable x_{pq} associated with that measured composition was assigned with an upper bound equal to the quantification limit LQ_q of compound q.

Eqs. (3a) represent a quadratic programming problem, with the gradient of the objective function written as:

$$\frac{\partial SSE}{\partial x_{pq}} = 2(x_{pq} - x_{pq}^{exp}) \quad \text{for all } p \text{ and } q \tag{4}$$

The jacobian of the constraints, Eqs. (3b) and (3c), is constant because all constraints are linear. Thus, the constant jacobian was provided to the optimization package to avoid recomputations.

Finally, the compositions of the non-measured streams (even streams in Fig. 1), used to initialize the optimization problem were set as the compositions of the measured flows that were also at the top or at the bottom of the corresponding block. For instance, seed compositions of stream F_2 were set to the measured compositions of stream F_3, and stream F_4 was initialized with the measured compositions of stream F_5. In accordance with the literature (Özyurt and Pike, 2004; Knopf, 2012), non measured variables do not participate in the objective function, Eq. (3a), but do participate in the constraints, from which their reconciled values are retrieved.

3.2. Distillation model

The batch distillation model used in this work has the following assumptions (Diwekar, 2012; Mujtaba and Macchietto, 1998):

- No chemical reactions.
- Ideal gas phase (column operated at reduced pressure).
- Plates numbered from reflux tank ($j = 1$) to reboiler ($j = N_p$), Fig. 2.
- Constant molar hold-up for reflux tank (H_C) and internal plates (H_P).
- Total condenser without sub-cooling.
- Liquid and vapour phases in thermodynamic equilibrium.
- Essential oil is fed at its bubble point.
- No heat losses.
- Fast energy dynamics: changes in liquid molar enthalpies are negligible compared with molar flows.

3.2.1. Material balances

Top product tank:

$$\frac{dx_a^{(i)}}{dt} = \frac{L_D}{H_a}\left(x_1^{(i)} - x_a^{(i)}\right) \tag{5}$$

$$\frac{dH_a}{dt} = L_D \tag{6}$$

$$L_D = V_2(1 - r) \tag{7}$$

where L_D: liquid flow going to top product tank (mol h^{-1}), H: liquid hold-up (kmol), r: internal reflux ratio (L_1/V_2).

Reflux tank ($j = 1$):

$$\frac{dx_1^{(i)}}{dt} = \frac{V_2}{H_C}\left(y_2^{(i)} - x_1^{(i)}\right) \tag{8}$$

$$0 = rV_2 - L_1 \tag{9}$$

where x: molar composition in the liquid phase, y: molar composition in the vapour phase, V: vapour flow (mol h^{-1}).

Plates ($j = 2, \ldots, N_p - 1$):

$$\frac{dx_j^{(i)}}{dt} = \frac{1}{H_P}\left[x_{j-1}^{(i)}L_{j-1} + y_{j+1}^{(i)}V_{j+1} - x_j^{(i)}L_j - y_j^{(i)}V_j\right] \tag{10}$$

$$0 = L_{j-1} + V_{j+1} - L_j - V_j \tag{11}$$

Reboiler ($j = N_p$):

$$\frac{dx_{N_p}^{(i)}}{dt} = \frac{1}{H_{N_p}}\left[L_{N_p-1}\left(x_{N_p-1}^{(i)} - x_{N_p}^{(i)}\right) - V_{N_p}\left(y_{N_p}^{(i)} - x_{N_p-1}^{(i)}\right)\right] \tag{12}$$

$$\frac{dH_{N_p}}{dt} = L_{N_p-1} - V_{N_p} \tag{13}$$

The compositions of the bottom contents at the end of the operation ($x_{end}^{(i)}$, Eq. (14)) are calculated with a material balance that includes the holdups of the reboiler and plates ($j = 1, \ldots, N_p$) and that of the reflux tank. Contents of the reflux tank are also considered in this material balance, since the batch distillation apparatus used in this work does not have a separate condenser, i.e. it is embedded.

$$x_{end}^{(i)} = \frac{\left(H_{N_p}x_{N_p}^{(i)} + H_P\sum_{j=2}^{N_p-1}x_j^{(i)} + H_C x_a^{(i)}\right)}{M_{bot}} \tag{14}$$

$$M_{bot} = H_{N_p} + (N_P - 2)H_P + H_C \tag{15}$$

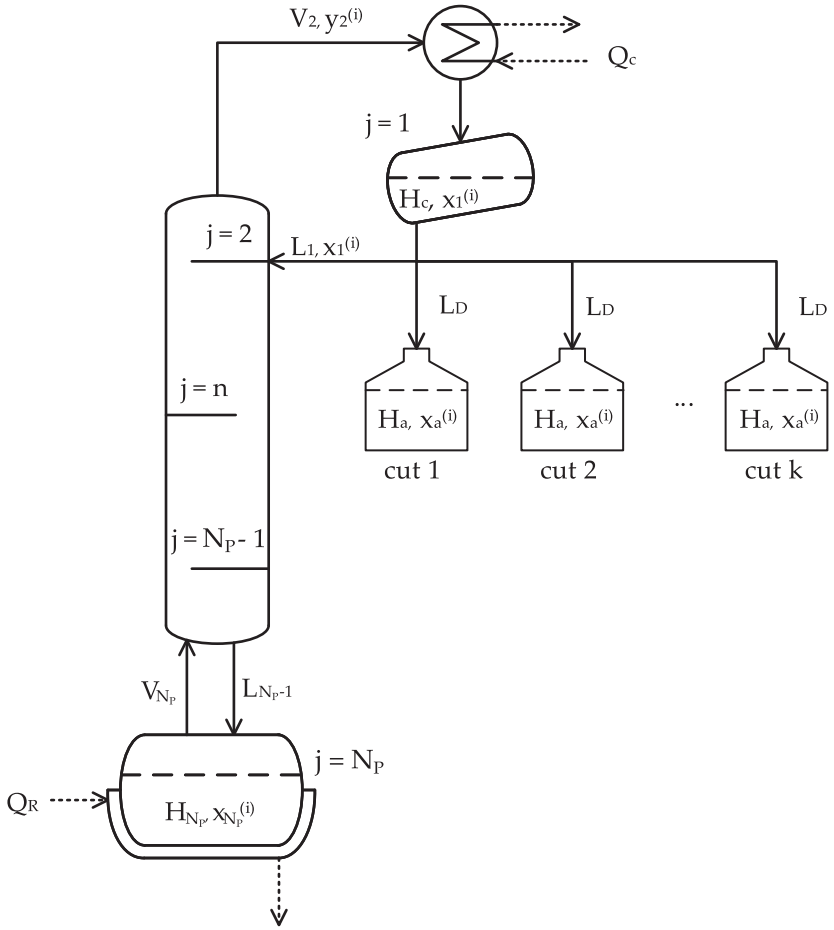

Fig. 2. Scheme of the batch distillation column.

3.2.2. Energy balances

As mentioned in the model assumptions, fast energy dynamics are considered, i.e., the derivatives of type $\frac{dh}{dt}$ either for the liquid or vapour phase, are neglected in the energy balances. Considering this, the energy balances are shown for each section of the column.

Condenser:

$$0 = V_2\left(h_2^V - h_1^L\right) - Q_C \tag{16}$$

Plates ($j = 2, \ldots, N_p - 1$):

$$0 = L_{j-1}h_{j-1}^L + V_{j+1}h_{j+1}^V - L_j h_j^L - V_j h_j^V \tag{17}$$

Reboiler:

$$0 = L_{N_p-1}h_{N_p-1}^L - V_{N_p}h_{N_p}^V - Q_R \tag{18}$$

Enthalpies of liquid and vapour phases were calculated with the following relations (Wankat, 2012):

$$h_j^L = \sum_i x_j^{(i)} C_{pl,j}^{(i)}\left(T_j - T_r\right) \tag{19}$$

$$h_j^V = \sum_i \left[y_j^{(i)}\lambda_j^{(i)} + C_{pv,j}^{(i)}\left(T_j - T_r\right)\right] \tag{20}$$

with λ: enthalpy of vaporization (kJ kmol^{-1}), C_{pl}, C_{pv}: heat capacities of the liquid and vapor phases, respectively (kJ kmol^{-1} K^{-1}). Superscripts: L liquid phase, V vapor phase.

3.2.3. Phase equilibria

Vapor liquid equilibria (VLE) were predicted using a modified Raoult's Law (Smith et al., 2000):

$$y_j^{(i)}P = x_j^{(i)}\gamma_j^{(i)}P_j^{s\,(i)} \tag{21}$$

with γ: Activity coefficient, P: Pressure (bar).

Vapor pressures for pure components $P_j^{s\,(i)}$ were calculated using the Antoine Equation, whereas activity coefficients $\gamma_j^{(i)}$ were estimated using the UNIQUAC model (Abrams and Prausnitz, 1975). Binary interaction parameters for UNIQUAC were estimated through a group-contribution method (UNIFAC-Dortmund), using the software *Aspen Plus®*.

An alternative form of Eq. (21) was used to obtain a bubble point expression, which is solved for temperature in each plate:

$$\sum_{i=1}^{N_c} x_j^{(i)}(K_j^{(i)} - 1) = 0 \quad j = 2, \cdots, N_P \tag{22}$$

with

$$K_j^{(i)}(T) = \frac{\gamma_j^{(i)}P_j^{s\,(i)}}{P} \quad j = 2, \cdots, N_P \tag{23}$$

and

$$\gamma_j^{(i)} = f(T, x_j^{(1)}, \cdots, x_j^{(k)}) \quad j = 2, \cdots, N_P \tag{24}$$

with $P^{s(i)}$ in bar.

3.2.4. Model solution

The resulting set of equations compose a DAE system, where the differential subset comprises Eqs. (6), (8), (10), (12) and (13), whereas the algebraic part includes Eqs. (9), (11), (16), (17), (18) and (22). A total of $[(N_P + 1)N_c + 2]$ variables ($x_j^{(i)}$, H_a and H_{N_P}) are involved in the differential section and $(3N_P - 1)$ variables (L_j, V_j, Q_C, Q_R and T_j) in the algebraic section.

In order to initialize the column, the algorithm was run at total reflux ($r = 1$) until the temperatures all along the distillation column attained the steady state, Eq. (25) (Diwekar, 2012), assuming that all the plate hold-ups were filled with liquid at its bubble point and feed composition (Sorensen, 1994; Mujtaba and Macchietto, 1998; Diwekar, 2012). An estimate of 1.5% of feed was assumed for H_a, and 0.25% for H_P after Low and Sorensen (Low and Sorensen, 2004).

$$\left\| \frac{d\mathbf{T}}{dt} \right\| < 1 \times 10^{-3} \tag{25}$$

with $\mathbf{T}$ being all the temperatures in the system (T_j for all j).

The distillation model was solved using as feed compositions the reconciled mass fractions of stream F_1 in Fig. 1. It is worth to mention that the developed `Python` code was written for a general number of equilibrium stages and number of components in the mixture, as long as the interaction parameters among all the possible pairs of compounds for the UNIQUAC model were provided.

Once the column attained the steady state, product removal was run by setting a low reflux ratio ($r = 0.1$), trying to approximate the real condition used in the experiments ($r = 0$). Lower reflux ratios were tested but they led to unstable numerical conditions, increasing the stiffness of the DAE system (Diwekar, 2012). The algorithm was allowed to run at $r = 0.1$ until a mass that matched a measured stream (e.g. F_2) was collected as top product. Next, the distillation routine was run again at total reflux, with a feed corresponding to the sum of the remaining liquid in the reboiler and the mass contained in the reflux tank, Eq. (14). This adjustment to the initial feed is made since the reboiler apparatus does not have a physical reflux tank, as mentioned above. This way of process operation causes discontinuities in the state variables profiles at the transitions between total reflux and product withdrawal periods, since the integrator has to recalculate consistent initial values to reinitialize the integration at those transitions.

4. Results

4.1. Calibration curves and EO composition

From reports of *L. origanoides* EO it is known that their main components are the phenylpropanoids thymol and carvacrol, along with their biogenetic precursors, β-myrcene, *p*-cymene and γ-terpinene. Adding two sesquiterpene hydrocarbons to this list, i.e. trans-β-caryophyllene and humulene, more than 90% of the total area obtained by GC-FID cromatograms is represented. Aiming to limit the study to a reasonable number of molecules that facilitate the solution of the distillation model, it was assumed that these seven substances represent in a significant and sufficient way the original EOs, and subsequently were employed to monitor the changes in the composition throughout the present work. Previous studies conducted by some of the authors have shown that the EO of wild *Lippia origanoides* chemotypes can be composed of up to 139 constituents (Stashenko et al., 2010). Fig. 3 shows GC-FID chromatogram of one essential oil of *L. origanoides* obtained by hydrodistillation employed in this study. The seven compounds listed correspond to the constituents selected to represent the EO and its distillation products in the modeling of batch distillation. In the figure it is observed that these compounds together represent the majority of the total chromatographic peak area.

Table 1 shows calibration equations used for quantification for each substance. Table 2 shows the mass fraction of the original EOs calculated from these calibration curves and the sums of the calculated mass fractions which were different from 1. This "inconsistency" is attributable to random errors inherent to data collection impossible to avoid when implementing the external calibration methodology and the EO representation as the mixture of only seven molecules. Data adjustment to achieve consistent material balances can be accomplished by changing the mass fraction data with values that are as close as possible to the measured data and whose sum is equal to 1. For that reason, data reconciliation was carried out as an optimization problem, as mentioned in Section 3.1, where limits of detection (LOD) and quantification (LOQ) were employed as constraints.

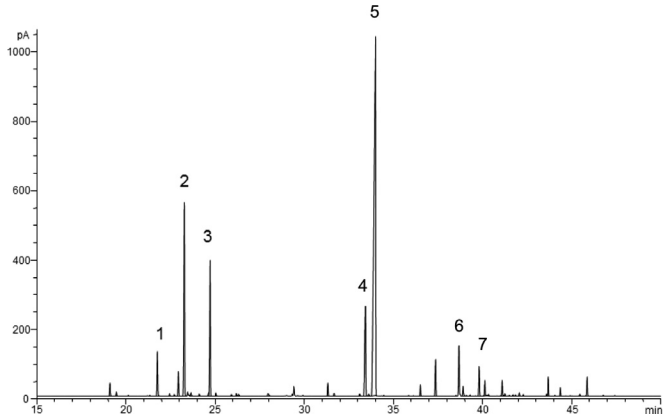

Fig. 3. GC-FID chromatogram of essential oil of *L. origanoides* obtained by hydrodistillation. Constituents numerated according to Table 2.

4.2. Distillation results

Table 3 shows the batch fractional distillation results in terms of mass and temperature. This table contains the initial amount of EO, fractions and losses of mass collected in each experiment as well as the average temperature at which the fractions were collected. The proportion in which the compounds are distributed in the EO of *L. origanoides* used in this work and the restrictions imposed to avoid overheating some thermolabile substances, allowed us to generate two cuts only for two EOs (`L01` and `L03`) (B2 in Fig. 1). However, the model notation and the methodology remained general, as the model is intended to be applied to other EO whose composition allows obtaining more than two cuts. The operation of the first three experiments (`L01`-`L03`) differed slightly from the others experiments in that the temperature in the reboiler reached up to ca. 413 K, for these experiments it was observed that the color of the bottom fraction darkened, indicating a thermal degradation of the compounds. The other experiments (`L04`-`L09`) were adjusted so that they did not exceed 388 K in the reboiler during the operation. The streams data composition are available in supplementary material.

4.3. Reconciliation problem

Results for data reconciliation are illustrated with experiment `L01` (Table 4). Both material balances for each component and the summation of mass fractions in each stream were satisfied (the maximum values of Eqs. (3b) and (3c) at the end of the optimization were 9.22×10^{-8} and 1.92×10^{-8}, respectively). Converged mass fractions X shown in Table 4 can be graphically compared with their corresponding measured values, Fig. 4. As explained at the end of Section 3, the compositions of losses were not measured, although their masses were available. For that reason, mass fractions of those streams can be seen as entirely *modeled* (determined from the constraint set, Eqs. (3b), (3c) and (3d)). For that reason, the reconciled set X was divided into measured (data) and modeled (losses), the first group being streams F_1, F_3, F_5 and F_7 (square marks), whereas the second group is formed by streams F_2,

Table 1
Linear calibration equations employed to quantify EO and their fractions obtained with batch distillation .

Compound	Calibration equation		LOD (mg mL^{-1})	LOQ (mg mL^{-1})	r^2
	Slope	Intercept			
(1) β-myrcene	$3.6 \pm 0.1 \times 10^{-4}$	0.2 ± 0.1	2.08	6.33	0.993
(2) *p*-cymene,	$3.59 \pm 0.09 \times 10^{-4}$	0.2 ± 0.1	2.08	6.33	0.993
(3) γ-terpinene	$2.52 \pm 0.07 \times 10^{-4}$	0.15 ± 0.07	2.07	6.89	0.993
(4) thymol	$3.7 \pm 0.1 \times 10^{-4}$	0.1 ± 0.1	2.16	7.00	0.992
(5) carvacrol	$3.74 \pm 0.09 \times 10^{-4}$	0.10 ± 0.08	1.65	5.23	0.995
(6) *trans*-β-caryophyllene	$7.7 \pm 0.2 \times 10^{-5}$	0.03 ± 0.02	1.96	6.14	0.993
(7) humulene	$7.7 \pm 0.2 \times 10^{-5}$	0.03 ± 0.02	1.96	6.14	0.993

* Limit of detection. † Limit of quantification, ($y_B + 10S_B$) where y_B is the blank signal and s_B standard deviation of the blank (Miller and Miller, 2005).

Table 2
Composition measured (mass fraction) of the main components of *L. origanoides* EO used in this work .

Compound	LO1	LO2	LO3	LO4	LO5	LO6	LO7	LO8	LO9
(1) β-myrcene	0.00	0.03	0.02	< LOQ	0.00	< LOQ	< LOQ	< LOQ	< LOQ
(2) *p*-cymene	0.02	0.17	0.07	0.00	0.00	0.08	0.15	0.07	0.12
(3) γ-terpinene	0.00	0.09	0.11	0.05	0.08	0.07	0.13	0.07	0.11
(4) thymol	0.07	0.07	0.30	0.20	0.19	0.07	0.06	0.08	0.07
(5) carvacrol	0.74	0.48	0.19	0.12	0.11	0.53	0.48	0.55	0.47
(6) *trans*-β-caryophyllene	0.03	0.04	0.11	0.34	0.29	0.18	0.17	0.20	0.17
(7) humulene	0.01	0.02	0.05	0.17	0.15	0.10	0.09	0.10	0.09
Total	0.87	0.90	0.86	0.88	0.82	1.02	1.08	1.08	1.04

Table 3
Results for batch fractional distillation of nine different *L.origanoides* EO.

EO	F_1 (g)	F_3 (g)	F_7 (g)	F_{4M+1} † (g)	Lost mass $\sum_{i=1}^{2M\dagger} F_{2\cdot i}$ (g)	Recovered mass (%)	T_{F_3} (K)	T_{F_5} (K)	T_{F_7} (K)	T_{F_9} (K)
LO1	9.00	0.55	4.43	1.80	2.23	75	321	386	389	408
LO2	13.00	8.09	-	2.76	2.15	83	389	412	-	-
LO3	13.00	1.91	4.12	5.10	1.87	86	328	379	382	405
LO4	11.76	0.51	-	9.10	2.15	82	320	374	-	-
LO5	12.09	0.15	-	9.35	2.59	79	312	384	-	-
LO6	9.15	0.49	-	7.50	1.16	87	328	373	-	-
LO7	9.15	0.89	-	6.79	1.47	84	333	380	-	-
LO8	9.15	0.91	-	6.70	1.54	83	329	378	-	-
LO9	9.15	0.34	-	7.94	0.87	90	331	385	-	-

* Streams measured experimentally, cf. Fig. 1. †$M = 2$ for experiments LO1 and LO3; $M = 1$ for the rest of the experiments. ‡ Distillation mass losses calculated by material balances, even streams in Fig. 1.

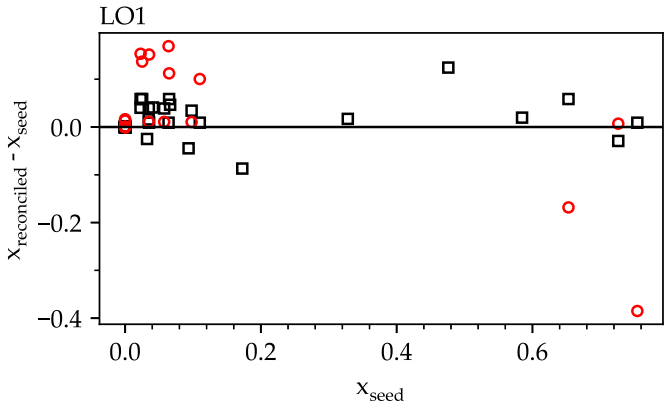

Fig. 4. Residuals vs. measured mass fraction after optimization for experiment LO1.

F_4, F_6 and F_8 (circle marks). It can be seen that the largest changes in mass fraction before and after reconciliation correspond to the modeled streams, whose seed (starting) values for the optimization problem, in the absence of measured data, were taken as those of the nearest stream (e.g. mass fractions of F_5 were used to initialize F_4). The reason is that those mass fractions x_{ij} do not participate in the objective function, and their mass fractions were allowed to take values within the entire interval $0 - 1$, allowing the optimizer to vary them as much as necessary in order to meet material balances for each component *j*, without affecting the objective function. The lack of information on the composition of mass losses is an important source of model uncertainty.

Some isolated significant changes did occur for measured values, e.g. $x_{seed} = 0.173$ in Fig. 4, which had a change of -0.1064 with respect to the measured value (reconciled mass fraction of 0.0666, Table 4, flow F_1, compound 2). This was generally caused by the sum of initial mass fractions for a given stream not being equal to 1, which is then enforced during the optimization. In the particular case of experiment LO1, the sum of the measured compositions for F_1 was 0.904. Conversely, the residuals were lower for a stream whose initial sum of mass fractions was closer to 1, e.g. F_7 (Table 4). In general, the mass fractions of the loss streams varied in a greater extent than those of the measured streams, as shown of Residuals vs. measured mass fraction in supplementary material. Reconciled data from all experimental fractions are also available in the supplementary material.

4.4. Batch distillation model

A total of 30 equilibrium states were simulated, the equivalent number of plates that the spinning band column can accommodate (Section 2). The model solved in this work was comprised by 219 differential equations and 89 algebraic equations ($N_p = 30$ and $N_c = 7$, see Section 3.2.4). The solution of each cut involved

Table 4
Initial and reconciled mass fractions for experiment LO1 (compound names in Table 2).

Measured/seed values							
Flow	Compound						
	1	2	3	4	5	6	7
F_1	0.032	0.173	0.094	0.066	0.476	0.041	0.023
F_2	0.035	0.585	0.328	0	0	0	0
F_3	0.035	0.585	0.328	0	0	0	0
F_4	0	0	0	0.098	0.726	0.058	0.035
F_5	0	0	0	0.098	0.726	0.058	0.035
F_6	0	0	0	0.110	0.755	0.064	0.035
F_7	0	0	0	0.110	0.755	0.064	0.035
F_8	0	0	0	0.065	0.653	0.023	0.025
F_9	0	0	0	0.065	0.653	0.023	0.025
Reconciled values							
Flow	Compound						
	1	2	3	4	5	6	7
F_1	0.006	0.067	0.038	0.118	0.618	0.086	0.067
F_2	0.044	0.598	0.339	0.006	0.002	0.006	0.006
F_3	0.050	0.605	0.345	0	0	0	0
F_4	0.015	0.021	0.017	0.107	0.728	0.067	0.045
F_5	0	0	0	0.134	0.689	0.099	0.077
F_6	0	0	0	0.193	0.478	0.182	0.147
F_7	0	0	0	0.119	0.763	0.073	0.044
F_8	0	0	0	0.225	0.284	0.261	0.230
F_9	0	0	0	0.123	0.712	0.081	0.084
Combined losses (mass fraction)	0.013	0.120	0.070	0.141	0.405	0.138	0.114
Total mass losses (%)	51.3	44.5	44.9	29.5	16.2	39.5	42.3

† Seed values for the losses streams were set as the measured nearest flow, as explained at the end of Section 3.1. ‡ Material losses

4 simulation periods, i.e. two top withdrawal periods (one for top losses and one for top product) with their accompanying stabilization runs at total reflux. This means that simulations for EOs LO1 and LO3 had 8 consecutive runs each, whereas the remaining EOs had 4 consecutive simulation runs. Computational time for one cut ranged from 5.1 to 9.3 min in an Intel® Core i7 Linux machine running at 2.4 GHz, with 8 GB of available RAM memory.

The dynamics of the composition profiles is shown with experiment LO1, which had four consecutive distillation steps. Fig. 5 shows the mass fraction as a function of time for all the seven compounds in the mixture. Shaded areas correspond to product-withdrawal periods, whereas non-shaded areas are periods of stabilization at total reflux, a common practice in batch distillation (Mujtaba and Macchietto, 1998).

Fig. 5 shows that most of the process corresponds to column stabilization, Eq. (25), due to the large number of process state variables that must attain constant values prior to product withdrawal (besides mass fraction, temperature and internal flows, as shown in Section 3.2) and the large amount of equivalent equilibrium stages ($N_p = 30$). The reported times are only for reference (about 6 h of total running time), since the model was intended to predict mass fractions rather than operation times. The purpose of calculating operation times was to compare the relative duration of stabilization and top product withdrawal times. A vapor flowrate $V_N = 120\ mol\ h^{-1}$ was set to obtain the reported times. Product withdrawal times are negligible compared with stabilization times, since small masses of top product withdrawal are simulated.

A first fraction of overhead losses (F_2 in Table 5) is collected in cut 1. It can be seen that *p*-cymene, the second most volatile oil constituent, appears in this fraction with an amount 8 times higher than that of the lighter β-myrcene (the latter is in a small amount in the feed oil). Similarly, the first recovered top fraction (cut 2 in Table 5) resulted in high contents of *p*-cymene (2) and γ-terpinene (3) at a temperature of 352 K, higher than the saturation temperature of the mentioned compounds (323 K and 329 K, respectively). This is caused by the significant amount of carvacrol in this stream (boiling point of 378 K), which is enriched up to 8.1% in the top product and is a major compound in the feed oil.

The third loss stream (F_6) consists mainly of thymol. This stream represents the major source of thymol losses (32.6% of thymol with respect to the inlet stream), which fairly agrees with the value found after reconciliation (Table 4, 29.5% thymol losses). Finally, the last top fraction was composed of heavy compounds, mainly carvacrol (76.6%), while the three lightest components were almost absent. Mass fraction and cuts temperatures calculated from simulation are available in the supplementary material.

4.5. Experimental, reconciled and calculated data

In Fig. 6 experimental (non reconciled) and reconciled distillation data were compared with calculated mass fractions from the batch distillation model. Each point in the figure represents a composition value for one compound in a given stream of some experiment. Filled circles and triangles represent reconciled and experimental data, respectively. Data away from the identity line denote lack of fit or erroneous experimental measurement. The residues of the reconciled data are also represented by a normal probability plot, Fig. 7. A Paired Sample *t*−Test was applied to these data. The *t*-Test evaluates the null hypothesis that the difference between reconciled and calculated data mean is equal to zero versus the alternate hypothesis that the difference between reconciled and calculated data mean is not equal to zero (Montgomery and Runger, 2010). Because the *p*-value for this test 0.99 is greater than 0.05, the null hypothesis cannot be rejected, with a confidence level of 95%. The determination coefficient and mean squared error were calculated: $r^2 = 0.85,\ MSE = 0.006$ for the reconciled data, and $r^2 = 0.81,\ MSE = 0.013$ for non-reconciled data.

When the experimental temperatures were compared with the steady-state values obtained by simulation, a good linear correlation was found but with lower accuracy ($r^2 = 0.73$ and $MSE = 16K$). Furthermore, greater dispersion in top than bottom temperatures was observed.

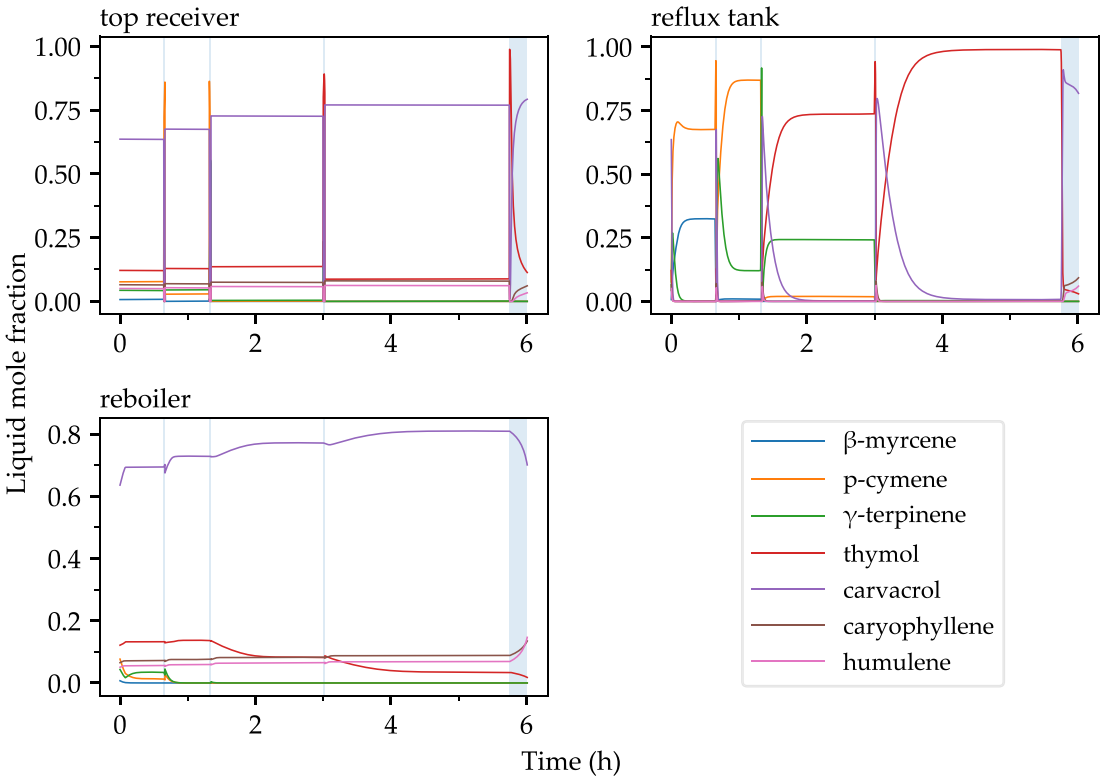

Fig. 5. Simulated time-dependent mole fraction profiles for experiment LO1. Components listed in order of decreasing volatility.

Table 5
Results of the batch distillation simulation for LO1 (w: mass fraction. For component order see Table 2).

Cut	Stream	Mass (g)	w_1	w_2	w_3	w_4	w_5	w_6	w_7	T (K)
1	feed (F_1)	8.62	0.007	0.086	0.049	0.113	0.600	0.082	0.063	358.3
	top (F_2)	0.72	0.087	0.757	0.156	0	0	0	0	327.0
	condenser	0.11	0.001	0.353	0.645	0.001	0	0	0	327.0
	bottom	7.78	0	0.020	0.030	0.125	0.665	0.091	0.070	370.6
2	feed	7.90	0	0.024	0.039	0.123	0.655	0.089	0.069	368.1
	top (F_3)	0.55	0	0.346	0.519	0.053	0.082	0	0	352.4
	condenser	0.11	0	0.017	0.212	0.212	0.557	0.003	0	352.4
	bottom (F_4)	7.23	0	0	0	0.127	0.700	0.098	0.075	379.1
3	feed (F_5)	6.95	0	0	0.003	0.128	0.698	0.096	0.074	378.3
	top (F_6)	0.72	0	0.003	0.031	0.591	0.372	0.003	0	378.0
	condenser	0.10	0	0	0	0.134	0.838	0.026	0.002	378.0
	bottom	6.13	0	0	0	0.074	0.734	0.108	0.084	379.5
4	feed	6.23	0	0	0	0.075	0.736	0.107	0.082	379.5
	top (F_7)	4.43	0	0	0	0.100	0.772	0.083	0.045	379.9
	condenser	0.09	0	0	0	0.023	0.775	0.123	0.079	379.9
	bottom ($F8$, F_9)	1.71	0	0	0	0.013	0.640	0.168	0.179	381.2

5. Discussion

5.1. Comparison of experimental, reconciled and calculated data

Reconciled mass fractions for the heavier EO compounds, e.g. humulene, are closer to the experimental data than those of more volatile compounds such as *p*-cymene. This trend was observed for all the calculated streams and could be related to material losses. As expected, these losses were large for volatile compounds since EOs are being distilled at reduced pressures, causing the lighter molecules to be dragged out of the process by the action of the vacuum pump. This adds uncertainty to the experimental measurement of the mass fractions and also explains why the model predicts small concentrations of light molecules in the heavy cuts, even when none of them could be detected by chromatography. These material losses are also related to the lack of fit of the model as will be discussed in the following subsection.

Although some data in Fig. 6 are away from the diagonal, there is no significant evidence that invalidates the predictions of the distillation model, according to a Paired Sample *t*-Test. A considerably good fit, as dictated by the determination coefficient $r^2 = 0.85$ and mean squared error $MSE = 0.006$ was reached comparing all available reconciled-calculated data compositions. For experimental-calculated data the same statistical descriptors are smaller but still considerably well correlated ($r^2 = 0.81$ and $MSE = 0.013$). Fig. 7 shows the normal probability plot for the 154 residues ($x_{reconciled} - x_{predicted}$) data. The figure shows a reasonably linear pattern at the center of the data and two tails departing from the fitted line. The non-aligned data with respect to the central straight line are presumably outliers. To identify the number of outliers, we analyzed the studentized values of standard deviation ($\sigma = 0.08$) with deletion, which indicate how many standard deviations each observation lies from the sample mean when that observation is not used in the calculations. 143 data are

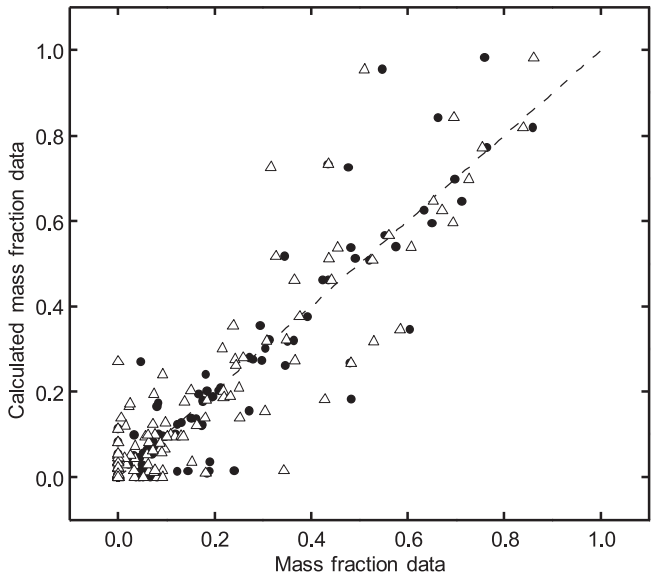

Fig. 6. Experimental and reconciled vs calculated mass fraction data. (•) Reconciled data, (△) Experimental data.

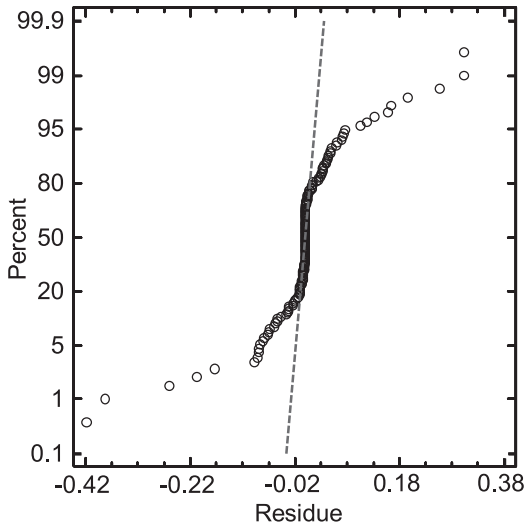

Fig. 7. Normal probability plot for residues between reconciled and calculated data.

distributed in the region $\pm\sigma$, whereas 8 and 3 data points were enclosed between the $\pm 2\sigma$ and $\pm 3\sigma$ regions, respectively. These 11 data were reviewed and considered as outliers, and their exclusion is explained in the next subsection from the experimental error of the distillation operation. Without those outliers, the model accuracy to predict reconciled data raises to $r^2 = 0.95$ and $MSE = 0.002$ which represents a reliable model fit. Removing the same outliers from the correlation between experimental and calculated data the model accuracy to predict experimental data is $r^2 = 0.94$ and $MSE = 0.003$.

5.2. Model lack of fit

Mass fraction values far away from the 45° line in Fig. 6 (or non-aligned in Fig. 7) can be explained as outliers due to factors affecting distillation column operation. For instance, momentary flooding caused by excessive vapor flowing up the column occurs for EOs containing large amounts of the most volatile compounds, for which the heating rate in the boiler turned out to be high (Kister, 2010).

Measuring mass losses (due to evaporation) and the mass of EO remaining in the column walls at the end of operation (Perry et al., 1999) is difficult, especially when the collected fraction is small. These two losses were considered as one stream for modeling purposes, and are generally assumed to correspond to non-condensable volatiles distilled off during the experiment. Therefore, the first obtained fraction does not correspond to real evaporated mass values, which is why the compositions predicted by the model are not accurate, with greater influence if the collected mass is small. These losses and the uncertainty in their mass and composition could also explain the lack of fit in the calculated temperatures since the simulation attained higher or lower steady-state temperatures depending on the mass loss of components calculated from data reconciliation. Nine of the eleven outliers, which deviate from the normal distribution of the residuals, can be explained by this limitation in the modeling of losses. Therefore, it is a source of considerable error that must be taken into account and even more if the distillation is carried out at reduced pressure.

The last cause for the observed lack of fit was the thermal decomposition of the molecules in the reboiler fractions for experiments that were heated above 388 K (L01–L03). Chromatographic signals not present in the original EO were found in the composition analysis of these bottom fractions. The amount of such new species was considerably high. For example, the seven compounds that represent more than 80% of the composition of the initial EO for experiment L02 only add to 30% for the final boiler fraction. Of course, this error was propagated when the problem of data reconciliation was solved. For that reason, there is an error due to the extrapolation of this current for L02 which is clearly observed in the data.

5.3. Extension to other EOs

In order to apply and extend the methodology used in this manuscript to other EO, possibly with a greater number of compounds, Fig. 8 shows a block diagram with information and procedures necessary to achieve the modeling and validation of batch distillation data. Of course, it is essential to know the composition of the EO, for which mass spectrometry coupled to gas chromatography (GC–MS) is convenient. A quantification strategy should be selected, preferably using external calibration (Cuadros-Rodrguez et al., 2007). GC-FID analysis should be used for EO components quantitation. More compounds will require different calibration curves, so a convenient strategy for quantification would be to group the compounds by chemical families and quantify such groups by only measuring one representative molecule. The compositions are estimated with the calibration curves. This procedure is developed together with the experimental batch distillation, which must consider how to deal with the losses, flooding and overheating.

Data reconciliation is inevitable if all EO compounds are not quantified. Regarding computation, the developed algorithm for data reconciliation was designed for a general number of compounds, as long as the input data are arranged as shown in Eqs. (1) and (2) (mass flows and compositions, respectively). We think that this is a sufficiently general form to deal with similar distillation problems, where available experimental data correspond to concentration of each component in several streams (of known mass). For distillation modeling, it is necessary to solve the material and energy balances together with vapor liquid equilibria. This requires knowing the thermodynamic properties of the participating species, and selecting a model to calculate activity coefficients. Computational resources are also necessary; in our case, the distillation model was solved in `Python` by building a class, aiming to deal with a general batch distillation problem (with k components and N_p equilibrium stages) using UNIQUAC to

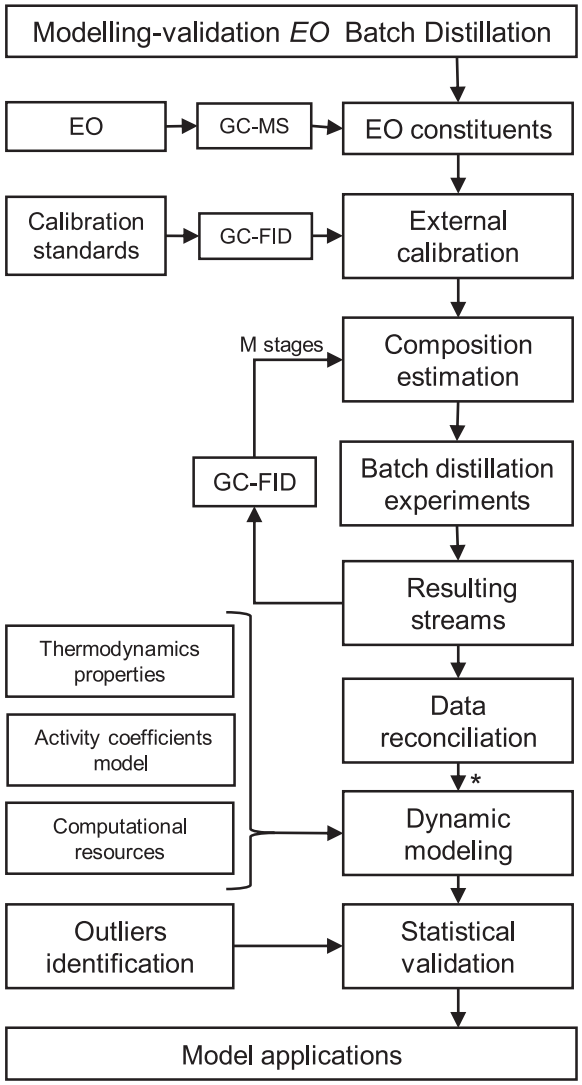

Fig. 8. Block diagram of methodology to modelling EO batch distillation used in this work.* Model is fed with reconciled data, not with experimental ones.

model activity coefficients. As long as the UNIQUAC binary interaction parameters are available, the batch rectification process of different essential oils can be simulated using the developed tool.

On the other hand, statistical tools are used to identify outliers and validate the data. The last step in the diagram is labeled as model applications to recall that models are used in dynamic optimization strategies applied in a wide number of domains of chemical engineering computing. These include off-line applications like optimal control, nonlinear parameter estimation, and dynamic optimization of distillation operation (Vassiliadis et al., 1994a; 1994b; Kameswaran and Biegler, 2006).

Finally, we remark that when designing a new batch distillation process, processing more than one EO is advisable for profitability issues, which implies the aforementioned dynamic optimization techniques as well as operation scheduling algorithms (Zamar et al., 2005).

6. Conclusions

Nine different EOs of *Lippia origanoides* were rectified by batch distillation in a microdistillation plant. The reconciled bottom and top mass compositions of the distilled fractions were compared with the results obtained from the developed dynamic distillation model. The results show that it is possible to describe the composition of the collected fractions from the EOs with fair accuracy, as demonstrated by the obtained r^2 (0.81 - 0.94) and *MSE* (0.013 - 0.003). The error in the prediction of compositions increases with overheating in the feeding plate because degradation products in the bottom fraction are generated. Distillation of EOs with high content of volatile compounds, such as L02 or L07, were more susceptible to mass losses, causing uncertainty in the measurement of light fractions, and outliers with respect to the fractions predicted by the distillation model. Finally, the developed methodology is intended to be used not only to predict the experimental composition data collected in this work, but also to decide on the operating conditions to be used in order to obtain enriched fractions from others EOs, which are of interest as raw materials for perfumery, household and pharmaceutical industries.

Declaration of Competing Interest

The authors declare that they have no known competing financial interests or personal relationships that could have appeared to influence the work reported in this paper.

CRediT authorship contribution statement

Julián Arias: Investigation, Supervision, Validation, Formal analysis. **Daniel Casas-Orozco:** Software, Visualization, Methodology, Data curation, Formal analysis, Writing - original draft. **Andrés Cáceres-León:** Investigation, Visualization, Data curation, Methodology. **Jairo Martínez:** Conceptualization, Writing - review & editing, Supervision, Funding acquisition. **Elena Stashenko:** Writing - review & editing, Supervision, Funding acquisition. **Aída-Luz Villa:** Writing - review & editing, Supervision.

Acknowledgments

JA and DCO acknowledges the support of Departamento Administrativo de Ciencia, Tecnología e Innovación de Colombia (COLCIENCIAS) through the PhD Scholarship, Call 567 of 2012, and Universidad Industrial de Santander (UIS), Bucaramanga, Colombia. DCO and ALV acknowledge financial support from Universidad de Antioquia (UdeA), Medelln, Colombia.

Supplementary material

Supplementary material associated with this article can be found, in the online version, at doi:10.1016/j.compchemeng.2020.106738

References

Abrams, D.S., Prausnitz, J.M., 1975. Statistical thermodynamics of liquid mixtures: a new expression for the excess Gibbs energy of partly or completely miscible systems. AIChE J. 21 (1), 116–128. doi:10.1002/aic.690210115.

Alighiri, D., Eden, W.T., Cahyono, E., Supardi, K.I., 2018. Quality improvement by batch vacuum distillation and physicochemical characterization of clove leaf oil in central java, indonesia. J. Phys. Conf. Ser. 983 (1), 12163. doi:10.1088/1742-6596/983/1/012163.

Almeida, R.N., Soares, R.d.P., Cassel, E., 2018. Fractionation process of essential oils by batch distillation. Brazilian J. Chem. Eng. 35 (03), 1129–1140.

Andersson, C., Führer, C., Åkesson, J., 2015. Assimulo: a unified framework for ODE solvers. Math. Comput. Simul. 116, 26–43. doi:10.1016/j.matcom.2015.04.007.

Asadi, S., 2014. Multicomponent distillation modeling of an essential oil by the SRK and PSRK state equations. IJCCE 33 (3), 77–82.

Beneti, S.C., Rosset, E., Corazza, M.L., Frizzo, C.D., Di Luccio, M., Oliveira, J.V., 2011. Fractionation of citronella (*Cymbopogon winterianus*) essential oil and concentrated orange oil phase by batch vacuum distillation. J. Food Eng. 102 (4), 348–354. doi:10.1016/J.JFOODENG.2010.09.011.

Bonsfills, A., Puigjaner, L., 2004. Batch distillation: simulation and experimental validation. Chem. Eng. Process. Process Intensif. 43 (10), 1239–1252. doi:10.1016/J.CEP.2003.11.009.

Castillo-Herrera, G.A., García-Fajardo, J.A., Estarrón-Espinosa, M., 2007. Extraction method that enriches phenolic content in oregano (*Lippia graveolens* h.b.k.) essential oil. J. Food Process Eng. 30 (6), 661–669. doi:10.1111/j.1745-4530.2007.00134.x.

Cuadros-Rodrguez, L., Bagur-Gonzlez, M.G., Snchez-Vias, M., Gonzlez-Casado, A., Gmez-Sez, A.M., 2007. Principles of analytical calibration/quantification for the separation sciences. J. Chromatogr. A 1158 (1), 33–46. doi:10.1016/j.chroma.2007.03.030. Data Analysis in Chromatography.

Distefano, G.P., 1968. Mathematical modeling and numerical integration of multicomponent batch distillation equations. AIChE J. 14 (1), 190–199. doi:10.1002/aic.690140132.

Diwekar, U., 2012. Batch Distillation, 2 CRC Press, Boca Ratón, FL.

Diwekar, U.M., Madhavan, K.P., 1991. Multicomponent batch distillation column design. Ind. Eng. Chem. Res. 30 (4), 713–721. doi:10.1021/ie00052a014.

Domenech, S., Enjalbert, M., 1974. Modele mathematique d'une colonne de rectification discontinuei. etablissement du modele. Chem. Eng. Sci. 29 (7), 1519–1528. doi:10.1016/0009-2509(74)87002-8.

dAntuono, L.F., Galletti, G.C., Bocchini, P., 2000. Variability of essential oil content and composition of *Origanum vulgare* l. populations from a north mediterranean area (liguria region, northern italy). Ann. Bot. 86 (3), 471–478.

Fang, T., Goto, M., Sasaki, M., Hirose, T., 2004. Combination of supercritical CO2 and vacuum distillation for the fractionation of bergamot oil. J. Agric. Food Chem. 52, 5162–5167. doi:10.1021/JF049895F.

Farah, A., Afifi, A., Fechtal, M., Chhen, A., Satrani, B., Talbi, M., Chaouch, A., 2006. Fractional distillation effect on the chemical composition of moroccan myrtle (*myrtus communis*l.) essential oils. Flavour Fragr. J. 21 (2), 351–354. doi:10.1002/ffj.1651.

Farhat, S., Czernicki, M., Pibouleau, L., Domenech, S., 1990. Optimization of multiplefraction batch distillation by nonlinear programming. AIChE J. 36 (9), 1349–1360. doi:10.1002/aic.690360908.

Fuentes, J.L., Garcia Forero, A., Quintero Ruiz, N., Prada Medina, C.A., Rey Castellanos, N., Franco Nino, D.A., Contreras Garcia, D.A., Cordoba Campo, Y., Stashenko, E.E., 2017. The sos chromotest applied for screening plant antigenotoxic agents against ultraviolet radiation. Photochem. Photobiol. Sci. 16, 1424–1434. doi:10.1039/C7PP00024C.

García, A.N., Loría, J.C., Marín, A.R., Quiroz, A.V., 2014. Simple multicomponent batch distillation procedure with a variable reflux policy. Brazilian J. Chem. Eng. 31 (2), 531–542. doi:10.1590/0104-6632.20140312s00001590.

Habsari, R.A., Warsito, Noorhamdani, 2018. Chemical composition of oil fraction kaffir lime (*citrus hystrix* dc) as antibacterial activity of *E. coli*. J. Pure App. Chem. Res 7 (1), 32–38. doi:10.21776/ub.jpacr.2018.007.01.352.

Hairer, E., Wanner, G., 1991. Solving Ordinary Differential Equations: Stiff and Differential-Algebraic Problems, 2 Springer, Leipzig.

Hernandes, C., Pina, E., Taleb contini, S., Bertoni, B., Cestari, I., Espanha, L., Varanda, E., Camilo, K., Martinez, E., Frana, S., Pereira, A., 2017. *Lippia origanoides* essential oil: an efficient and safe alternative to preserve food, cosmetic and pharmaceutical products. J. Appl. Microbiol. 122 (4), 900–910. doi:10.1111/jam.13398.

Hindmarsh, A.C., Brown, P.N., Grant, K.E., Lee, S.L., Serban, R., Shumaker, D.E., Woodward, C.S., 2005. Sundials. ACM Trans. Math. Softw. 31 (3), 363–396. doi:10.1145/1089014.1089020.

Kameswaran, S., Biegler, L.T., 2006. Simultaneous dynamic optimization strategies: Recent advances and challenges. Comput. Chem. Eng. 30 (10), 1560–1575. doi:10.1016/j.compchemeng.2006.05.034. Papers form Chemical Process Control VII.

Kenig, E.Y., Blagov, S., Gorak, A., Sorensen, E., 2014. Modeling of Distillation Processes. Academic Press, Boston, pp. 383–436.

Kister, H.Z., 2010. Distillation Troubleshooting. Wiley-Blackwell doi:10.1002/9780471690726.ch3.

Knopf, F.C., 2012. Modeling, Analysis and Optimization of Process and Energy Systems. John Willey & Sons, Inc., Hoboken, NJ.

Lopes, D., Raga, A.C., Stuart, G.R., de Oliveira, J.V., 2003. Influence of vacuum distillation parameters on the chemical composition of a five-Fold sweet orange oil (*citrus sinensis*osbeck). J. Essent. Oil Res. 15 (6), 408–411. doi:10.1080/10412905.2003.9698624.

Low, K.H., Sorensen, E., 2004. Simultaneous optimal design and operation of multipurpose batch distillation columns. Chem. Eng. Process. Process Intensif. 43 (3), 273–289. doi:10.1016/S0255-2701(03)00123-5.

Macedo, H.D., Oliveira, J.N., 2013. Typing linear algebra: a biproduct-oriented approach. Sci. Comput. Program. 78 (11), 2160–2191. doi:10.1016/j.scico.2012.07.012.

Madrid Garcs, T.A., Parra Suescun, J.E., Lpez Herrera, A., 2017. La inclusin de aceite esencial de organo (*lippia origanoides*) mejora parmetros inmunolgicos en pollos de engorde. Biotec. Sect. Agrop. y Agroind. 15, 75–83.

Mar, J.M., Silva, L.S., Azevedo, S.G., Frana, L.P., Goes, A.F., dos Santos, A.L., de A. Bezerra, J., de Cssia S. Nunomura, R., Machado, M.B., Sanches, E.A., 2018. *Lippia origanoides* essential oil: an efficient alternative to control *aedes aegypti, tetranychus urticae* and *cerataphis lataniae*. Ind. Crops Prod. 111, 292–297. doi:10.1016/j.indcrop.2017.10.033.

Miller, J.N., Miller, J.C., 2005. Statistics and Chemometrics for Analytical Chemistry. Pearson Education.

Milojević, S., Glišić, S.B., Skala, D.U., 2010. The batch fractionation of *juniperus communis*l. essential oil: experimental study, mathematical simulation and process economy. Chem. Ind. Chem. Eng. Q. 16 (2), 183–191. doi:10.2298/CICEQ100317026M.

Montgomery, D.C., Runger, G.C., 2010. Applied statistics and probability for engineers, 3 John Wiley & Sons.

Mujtaba, I.M., 2004. Batch distillation -Design and operation. Imperial College Press, London.

Mujtaba, I.M., Macchietto, S., 1998. Holdup issues in batch distillation-binary mixtures. Chem. Eng. Sci. 53 (14), 2519–2530. doi:10.1016/S0009-2509(98)00088-8.

Neira, L., Mantilla, J., Stashenko, E., Escobar, P., 2018. Toxicidad, genotoxicidad y actividad anti-*Leishmania* de aceites esenciales obtenidos de cuatro (4) quimiotipos del género *lippia*. Bol. latinoam. Caribe plantas med. aromt. 17 (1), 68–83.

O'Leary, N., Denham, S.S., Salimena, F., Múlgura, M.E., 2012. Species delimitation in lippia section *Goniostachyum* (verbenaceae) using the phylogenetic species concept. Bot. J. Linn. Soc. 170 (2), 197–219. doi:10.1111/j.1095-8339.2012.01291.x.

Oliveira, D.R., Leito, G.G., Bizzo, H.R., Lopes, D., Alviano, D.S., Alviano, C.S., Leito, S.G., 2007. Chemical and antimicrobial analyses of essential oil of *lippia origanoides* h.b.k. Food. Chem. 101 (1), 236–240. doi:10.1016/j.foodchem.2006.01.022.

Ortiz, R.E., Aafanador, G., Vasquez, D.R., Ariza, C., 2017. Efecto del aceite esencial de organo sobre el desempeo productivo de ponedoras y la estabilidad oxidativa de huevos enriquecidos con cidos grasos poliinsaturados. Rev. Med. Vet. Zoot. 64, 61–70.

Özyurt, D.B., Pike, R.W., 2004. Theory and practice of simultaneous data reconciliation and gross error detection for chemical processes. Comput. Chem. Eng. 28 (3), 381–402. doi:10.1016/j.compchemeng.2003.07.001.

Perini, J.F., Silvestre, W.P., Agostini, F., Toss, D., Pauletti, G.F., 2017. Fractioning of orange (*Citrus sinensis* l.) essential oil using vacuum fractional distillation. Sep. Sci. Technol. 52 (8), 1397–1403. doi:10.1080/01496395.2017.1290108.

Perry, R., Green, D., Maloney, J., 1999. Perry's chemical engineer's handbook, 7 McGraw-Hill Book.

Petersen, K.B., Pedersen, M.S., 2012. The Matrix Cookbook. Technical University of Denmark, Copenhaguen.

Pires, V.P., Almeida, R.N., Wagner, V.M., Lucas, A.M., Vargas, R.M.F., Cassel, E., 2019. Extraction process of the *achyrocline satureioides* (lam) DC. essential oil by steam distillation: modeling, aromatic potential and fractionation. J. Essent. Oil Res. 31 (4), 286–296. doi:10.1080/10412905.2019.1569564.

Prez Zamora, C.M., Torres, C.A., Nuez, M.B., 2018. Antimicrobial activity and chemical composition of essential oils from verbenaceae species growing in south america. Molecules 23 (3). doi:10.3390/molecules23030544.

Ríos, N., Stashenko, E.E., Duque, J.E., 2017. Evaluation of the insecticidal activity of essential oils and their mixtures against *Aedes aegypti* (diptera: culicidae). Rev. Bras. entomol. 61 (4), 307–311.

Salomone, H.E., Chiotti, O.J., Iribarren, O.A., 1997. Short-Cut design procedure for batch distillations. Ind. Eng. Chem. Res. 36 (1), 130–136. doi:10.1021/ie950458n.

Santos-Gomes, P.C., Fernandes-Ferreira, M., 2001. Organ- and season-Dependent variation in the essential oil composition of *salvia officinalis*l. cultivated at two different sites. J. Agric. Food Chem. 49, 2908–2916. doi:10.1021/JF001102B.

Sarrazin, S.L.F., da Silva, L.A., de Assuno, A.P.F., Oliveira, R.B., Calao, V.Y.P., da Silva, R., Stashenko, E.E., Maia, J.G.S., Mouro, R.H.V., 2015. Antimicrobial and seasonal evaluation of the carvacrol-chemotype oil from *Lippia origanoides* kunth.. Molecules 20 (2), 1860–1871. doi:10.3390/molecules20021860.

Shaw, A.C., 1951. The essential oil of *Tsuga canadensis* (l.) carr. J. Am. Chem. Soc. 73 (6), 2859–2861. doi:10.1021/ja01150a128.

da Silva, A.P., Silva, N., Andrade, E.H.A., Gratieri, T., Setzer, W.N., Maia, J.G.S., da Silva, J.K.R., 2017. Tyrosinase inhibitory activity, molecular docking studies and antioxidant potential of chemotypes of *Lippia origanoides* (verbenaceae) essential oils. PLoS ONE 12 (5), e0175598. doi:10.1371/journal.pone.0175598.

Silvestre, W., Agostini, F., Muniz, L., Pauletti, G., 2016. Fractionating of green mandarin (*citrus deliciosa* tenore) essential oil by vacuum fractional distillation. J. Food Eng. 178, 90–94. doi:10.1016/J.JFOODENG.2016.01.011.

Smith, J.M., Ness, H.C.V., Abbott, M., Ness, H.V., 2000. Introduction to Chemical Engineering Thermodynamics, 7th ed. McGraw Hill.

Soares, B.V., Cardoso, A.C.F., Campos, R.R., Gonalves, B.B., Santos, G.G., Chaves, F.C.M., Chagas, E.C., Tavares-Dias, M., 2017. Antiparasitic, physiological and histological effects of the essential oil of *lippia origanoides* (verbenaceae) in native freshwater fish *colossoma macropomum*. Aquaculture 469, 72–78. doi:10.1016/j.aquaculture.2016.12.001.

Sorensen, E., 1994. Studies on Optimal Operation and Control of Batch Distillation Columns. University of Trodheim Phd thesis in engineering.

Stashenko, E.E., Martnez, J.R., Ruz, C.A., Arias, G., Durn, C., Salgar, W., Cala, M., 2010. *Lippia origanoides* chemotype differentiation based on essential oil gcms and principal component analysis. J. Sep. Sci. 33 (1), 93–103. doi:10.1002/jssc.200900452.

Stuart, G.R., Lopes, D., Oliveira, J.V., 2001. Deterpenation of brazilian orange peel oil by vacuum distillation. J. Am. Oil Chem. Soc. 78 (10), 1041–1044. doi:10.1007/s11746-001-0385-x.

Sundaram, S., Evans, L.B., 1993. Synthesis of separations by batch distillation. Ind. Eng. Chem. Res. 32 (3), 500–510. doi:10.1021/ie00015a013.

Tamhane, A.C., Mah, R.S.H., 1985. Data reconciliation and gross detection in chemical process error networks. Technometrics 27 (4), 409–422.

Telci, I., Demirtas, I., Sahin, A., 2009. Variation in plant properties and essential oil composition of sweet fennel (*Foeniculum vulgare* mill.) fruits during stages of maturity. Ind. Crops Prod. 30 (1), 126–130. doi:10.1016/J.INDCROP.2009.02.010.

Vassiliadis, V.S., Sargent, R.W., Pantelides, C.C., 1994. Solution of a class of multistage dynamic optimization problems. 1. problems without path constraints. Ind. Eng. Chem. Res. 33 (9), 2111–2122. doi:10.1021/ie00033a014.

Vassiliadis, V.S., Sargent, R.W., Pantelides, C.C., 1994. Solution of a class of multistage dynamic optimization problems. 2. problems with path constraints. Ind. Eng. Chem. Res. 33 (9), 2123–2133. doi:10.1021/ie00033a015.

Wächter, A., Biegler, L.T., 2006. On the implementation of an interior-point filter line-search algorithm for large-scale nonlinear programming. Math. Program. 106 (1), 25–57. doi:10.1007/s10107-004-0559-y.

Wankat, P.C., 2012. Separation process engineering, 3rd Prentice Hall, New Jersey.

Zamar, S.D., Salomone, E., Iribarren, O.A., 1998. Shortcut method for multiple task batch distillations. Ind. Eng. Chem. Res. 37, 4801–4807. doi:10.1021/IE9800795.

Zamar, S.D., Salomone, H.E., Iribarren, O.A., 2005. Operation planning in the rectification of essential oils. J. Food Eng. J 69 (2), 207–215. doi:10.1016/J.JFOODENG.2004.07.019.

Appendix E. International Patent 2

(12) SOLICITUD INTERNACIONAL PUBLICADA EN VIRTUD DEL TRATADO DE COOPERACIÓN EN MATERIA DE PATENTES (PCT)

(19) Organización Mundial de la Propiedad Intelectual
Oficina internacional

(43) Fecha de publicación internacional
05 de julio de 2018 (05.07.2018)

W I P O I P C T

(10) Número de publicación internacional
WO 2018/122654 Al

(51) Clasificación internacional de patentes:
C11B 9/02 (2006.01)

(21) Número de la solicitud internacional:
PCT/IB20 17/057862

(22) Fecha de presentación internacional:
13 de diciembre de 2017 (13.12.2017)

(25) Idioma de presentación: español

(26) Idioma de publicación: español

(30) Datos relativos a la prioridad:
NC2016/0005880
27 de diciembre de 2016 (27.12.2016) CO

(71) Solicitante: **UNIVERSIDAD INDUSTRIAL DE SAN¬ TANDER** [CO/CO]; CRA 13-A #28-38 Bufete 230, Bogotá, 11031 1 (CO).

(72) Inventores: **STASHENKO, Elena;** CRA 13-A # 28-38 Bufete 230, Bogotá, 1103 11 (CO). **DURAN GARCÍA, Diego Camilo;** CRA 13-A # 28-38 Bufete 230, Bogotá, 1103 11 (CO). **MARTINEZ MORALES, Jairo René;** CRA 13-A # 28-38 Bufete 230, Bogotá, 1103 11 (CO). **CORDOBA CAMPO, Yuri;** CRA 13-A # 28-38 Bufete 230, Bogotá, 1103 11 (CO). **ARIAS VELANDIA, Anderson Julián;** CRA 13-A # 28-38 Bufete 230, Bogotá, 1103 11 (CO). **MEJIA MEDINA, Jesica Julieth;** CRA 13-A # 28-38 Bufete 230, Bogotá, 1103 11 (CO). **TAVERA REYES, Camilo Andrés;** CRA 13-A # 28-38 Bufete 230, Bogotá, 1103 11 (CO).

(74) Mandatario: **MAYA RODRIGUEZ, Carlos Orlando** et al; CRA 13-A # 28-38 Bufete 230, Bogotá, 1103 11 (CO).

(81) Estados designados *(a menos que se indique otra cosa, para toda clase de protección nacional admisible):* AE, AG, AL, AM, AO, AT, AU, AZ, BA, BB, BG, BH, BN, BR, BW, BY, BZ, CA, CH, CL, CN, CO, CR, CU, CZ, DE, DJ, DK, DM, DO, DZ, EC, EE, EG, ES, FI, GB, GD, GE, GH, GM, GT, HN, HR, HU, ID, IL, IN, IR, IS, JO, JP, KE, KG, KH, KN, KP, KR, KW, KZ, LA, LC, LK, LR, LS, LU, LY, MA, MD, ME, MG, MK, MN, MW, MX, MY, MZ, NA, NG, NI, NO, NZ, OM, PA, PE, PG, PH, PL, PT, QA, RO, RS, RU, RW, SA, SC, SD, SE, SG, SK, SL, SM, ST, SV, SY, TH, TJ, TM, TN, TR, TT, TZ, UA, UG, US, UZ, VC, VN, ZA, ZM, ZW.

(84) Estados designados *(a menos que se indique otra cosa, para toda clase de protección regional admisible):* ARIPO

(54) **Title:** METHOD FOR MAKING FULL USE OF LIPPIA ORIGANOIDES

(54) **Título:** PROCESO DE APROVECHAMIENTO INTEGRAL DE LIPPIA ORIGANOIDES

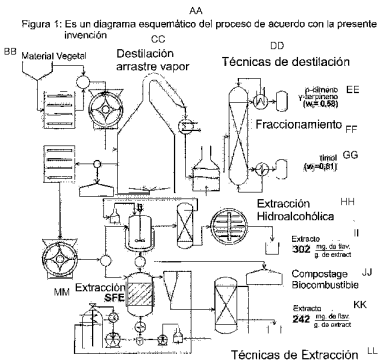

AA Figure 1: Schematic diagram of the method according to the present invention
BB Plant Material
CC Steam distillation
DD Distillation techniques
EE p-cymene
y-terpinene
(wi=0.58)
FF Fractionation
GG thymol
(wi=0.81)
HH Hydroalcoholic Extraction
II Extract
mg flav
g extract
JJ Biofuel Composting
KK Extract
mg flav
g extract
LL Extraction Techniques
MM SFE Extraction

(57) **Abstract:** The present invention relates to methods for extracting, separating and purirying compounds of interest obtained from essential oils and plant extraets, in a continuous process.

(57) **Resumen:** La presente invención se relaciona con métodos para extraer, separar y purificar compuestos de interés obtenidos a partir de aceites esenciales y extractos de plantas en un proceso se lleva a cabo de manera continua.

WO 2018/122654 A1

[Continúa en la página siguiente]

(BW, GH, GM, KE, LR, LS, MW, MZ, NA, RW, SD, SL, ST, SZ, TZ, UG, ZM, ZW), euroasiática (AM, AZ, BY, KG, KZ, RU, TJ, TM), europea (AL, AT, BE, BG, CH, CY, CZ, DE, DK, EE, ES, FI, FR, GB, GR, HR, HU, IE, IS, IT, LT, LU, LV, MC, MK, MT, NL, NO, PL, PT, RO, RS, SE, SI, SK, SM, TR), OAPI (BF, BJ, CF, CG, CI, CM, GA, GN, GQ, GW, KM, ML, MR, NE, SN, TD, TG).

Publicada:

— *con informe de búsqueda internacional (Art. 21(3))*
— *con reivindicaciones modificadas y declaración (Art. 19(1))*

PROCESO DE APROVECHAMIENTO INTEGRAL DE *Lippia origanoides*

CAMPO DE LA INVENCIÓN

La presente invención se relaciona con métodos para extraer, separar y purificar compuestos de interés obtenidos a partir de aceites esenciales y extractos de plantas.

ANTECEDENTES DE LA INVENCIÓN

Las plantas son una fuente de una gran cantidad de compuestos con múltiples usos a nivel industrial. Industrias de cosméticos, alimentos, fármacos así como la pecuaria, agrícola, veterinaria entre otras se ven beneficiadas por la gran cantidad de compuestos que es posible obtener de las plantas.

Por tal motivo, desde tiempos inmemoriales, se han desarrollado diferentes procesos para extraer y purificar compuestos a partir de las plantas. Estos procesos consisten en su mayoría en operaciones unitarias independientes que buscan aislar de manera separada las moléculas de interés. Los procesos no siempre logran separar y purificar de manera eficiente múltiples compuestos valiosos de una misma matriz, ya que la obtención de un compuesto de interés en particular, en algunos casos, causa la degradación de otro.

Puesto que es de particular interés para las industrias antes mencionadas aprovechar al máximo la materia prima, con el fin de obtener más y mejor producto. Se hace necesario desarrollar procesos industriales continuos que permitan aprovechar integralmente a las plantas, de tal manera que su extracción se pueda llevar a cabo dependiendo de las familias de compuestos a extraer.

Una planta que resulta de particular interés, debido al rendimiento y variedad de los compuestos que se pueden obtener junto con el número de industrias que los usan, es la *Lippia origanoides.* La presente invención resuelve el

aprovechamiento integral de la *Lippia origanoides* como materia prima para la obtención de productos naturales, requeridos por diversa industrias (cosmética, alimentos, farmacéutica, pecuaria, agrícola, veterinaria, entre otras).

FIGURAS

Figura 1 Es un diagrama esquemático del proceso de acuerdo con la presente invención.

BREVE DESCRIPCION DE LA INVENCION

La presente invención se relaciona con el diseño de un proceso que permite la extracción, separación y purificación de compuestos de interés presentes en *Lippia origanoides.* La configuración de operaciones unitarias, correspondientes a los métodos verdes de destilación y extracción descritos en el proceso, de acuerdo con la presente invención, proporcionan alto valor agregado a los productos mediante la posibilidad de concentrar tres familias de moléculas de interés: fracción liviana de aceite esencial compuesta por precursores de fenilpropanos, fracción compuesta por fenilpropanos con actividad biológica y fracción de extracto compuesto por flavonoides.

El proceso está orientado a aislar los componentes más valiosos como timol, carvacrol, p-cimeno, gamma terpineno, pinocenbrina y naringenina de la planta, con el propósito de obtener productos con concentraciones de familia de compuestos entre el 80 y 99 %. La manera como está dispuesto el desarrollo permite obtener mayores cantidades de fenilpropanos y flavonoides presentes en la planta por unidad de medida de la materia prima. Todos los residuos de la planta como resultado de las etapas de extracción son aprovechados como subproductos o son reutilizados en el proceso.

Es, por lo tanto, un objeto de la presente invención, proporcionar un proceso donde existe un fraccionamiento *in* situ. Es también, un objeto de la presente invención, proporcionar un proceso en donde este fraccionamiento se lleve a cabo durante la etapa de destilación. Es además un objeto de la presente invención, el proporcionar elementos de decisión para determinar si la extracción inicial del material vegetal se debe efectuar mediante arrastre vapor o mediante hidrodestilación.

El proceso de acuerdo con la presente invención permite obtener extractos y aceites esenciales de *Lippia origanoides* con mayor valor agregado debido a que permite concentrar los compuestos más valiosos presentes en la planta como lo son los fenilpropanos timol y carvacrol, sus precursores p-cimeno y gama-terpineno, así como flavonoides.

Por último, es un objeto de la presente invención el proporcionar un proceso de aprovechamiento integral de *Lippia origanoides* el cual reutiliza la biomasa residual de la planta en el mismo proceso de obtención de aceites esenciales y extractos.

DESCRIPCIÓN DETALLADA DE LA INVENCIÓN

De acuerdo con lo establecido arriba, el proceso de esta invención está orientado a aislar los componentes más valiosos como timol, carvacrol, p-cimeno, gamma terpineno, pinocenbrina y naringenina de la planta, para obtener productos de concentración entre el 80 y 99 %. La manera como está dispuesto el desarrollo permite obtener mayores cantidades de fenilpropanos y flavonoides presentes en la planta por unidad de medida de la materia prima. Todos los residuos de la planta como resultado de las etapas de extracción son aprovechados como subproductos o son reutilizados en el proceso.

El proceso de extracción de productos naturales a partir de *Lippia origanoides* de acuerdo con la presente invención, está enfocado en incrementar el valor agregado del aceite y extracto de la planta. Los fenilpropanoides timol y carvacrol

junto con sus precursores biosintéticos p-cimeno y gamma-terpineno además de los flavonoides pinocembrina y naringenina, entre otros, son compuestos con gran bioactividad que se aislan mediante el presente desarrollo.

El proceso comienza con la entrada del material vegetal de *Lippia origanoides* con humedad conocida. De acuerdo con la humedad y el interés de los productos del proceso, se decide si la materia prima debe ser o no secada. El material vegetal fresco o seco es sometido a un tratamiento de reducción de tamaño de partícula. Los valores determinados de tamaño de partícula están entre 0,5 y 5 cm.

El material vegetal con tamaño de partícula reducido, se carga a un equipo de destilación, donde se lleva a cabo la separación del aceite esencial. El proceso de destilación puede ser por arrastre con vapor o por hidrodestilacion, dos metodologías conocidas para la obtención de aceites esenciales.

La densidad de carga del material vegetal en el equipo de destilación está entre 200 y 320 kg/m^3. Cuando el método de destilación es por arrastre con vapor la presión de vapor de la caldera y el flujo de vapor es de 50-1 10 psi 0,8-1 .5 L/min. Con el método de destilación por hidrodestilacion la cantidad de calor suministrada al sistema debe ser la necesaria para mantener el flujo de vapor entre 0,8 y 1 L/min. El proceso de destilación se lleva a cabo entre 60 y 150 minutos, dependiendo de la cantidad de aceite que posea la matriz. El aceite mezclado con el agua condensada se fracciona en el tiempo, el aceite recolectado en los 10 - 20 primeros minutos corresponde a la fracción liviana. Esta fracción corresponde al producto más volátil enriquecido en precursores de fenilpropanos tales como p-cimeno y gamma-terpineno. (w_i = 0,5-0,6). Después de colectada la fracción liviana, el aceite esencial obtenido del destilador corresponde a la fracción pesada, una mezcla con mayor contenido de fenilpropanos timol y carvacrol que la llamada fracción liviana. La misma metodología se emplea cuando el proceso se realiza por hidrodestilacion, incrementando el tiempo de recolección hasta 30 minutos.

El aceite es separado del hidrolato en un decantador o sistema de vasos comunicantes. El hidrolato, que es una mezcla muy aromática de moléculas presentes en la *Lippia origanoides* que se disolvieron en el agua, es reutilizado en el proceso de destilación y posteriormente recuperado como subproducto. Una vez que el aceite esencial correspondiente a la fracción pesada es decantado, se introduce a una columna de destilación fraccionada en donde los fenilpropanos son concentrados a valores de fracción másica (w_i=0,8-1) en el fondo de la columna. Los condensados obtenidos en esta etapa de destilación fraccionada, se colectan en tope de la columna y son ricos en los precursores p-cimeno y gamma-terpineno. Por tal razón este producto se mezcla con la fracción volátil obtenida en los 10-30 primeros minutos de destilación por arrastre vapor o hidrodestilación, según sea el caso. Si la concentración de los fenilpropanos presentes en el aceite es mayor de 75% el proceso de fraccionamiento no se realiza, en su remplazo se realiza un proceso de cristalización lenta a -15°C, que mediante la disminución paulatina de la temperatura y la adición de un cristal de timol o carvacrol dependiendo del quimiotipo, se logra concentrar la fracción másica de fenilpropano por encima de 0,9.

El material vegetal destilado es nuevamente secado y extraído por dos diferentes técnicas: la extracción hidroalcohólica y la extracción con dióxido de carbono supercrítico, dependiendo del tipo del flavonoide requerido, glucosidado o no. Con estas técnicas, ya conocidas, se obtienen concentraciones de flavonoides de 300-320 y 240-260 mg de flavonoides por gramo de extracto respectivamente.

Extracto supercrítico enriquecido en flavonoides de 300-320 mg de flavonoides por gramo y 240-260 mg de flavonoides por gramo se obtienen en la etapa extractiva correspondiente al proceso de extracción supercrítica, una vez que el material vegetal ya ha sido destilado. Esta técnica se diferencia de las destilativas en que no se utiliza un solvente que solubiliza al extracto. Este producto es viscoso y no líquido ni volátil como la Fracción volátil enriquecida en precursores p-cimeno y gamma-terpineno o la Fracción pesada enriquecida con fenilpropanoides timol y carvacrol.

Todos los parámetros de diseño como flujos, presiones, temperatura de cada etapa del proceso se optimizan dependiendo de las condiciones de la planta.

Los productos y subproductos del proceso con sus aplicaciones se presentan en la siguiente tabla:

Tabla 1. Productos y subproductos obtenidos del aprovechamiento integral de *Lippia origanoides.*

	Descripción	**Utilidad**
Productos	Fracción volátil enriquecida en precursores p-cimeno y gamma-terpineno. (w_i = 0,5-0,6)	Insumo de perfumería, aporte de notas cítricas.
	Fracción pesada enriquecida con fenilpropanoides timol y carvacrol (w_i=0,8-1)	Insumo para la industria cosmética y de aseo personal (enjuague bucal, jabones). Insumo para la industria alimenticia. Insumo para industria farmacéutica. Insumo para promotores de crecimiento animal (avícola, porcino, otros)
	Extracto hidroalcohólico enriquecido en flavonoides glucosídicos 300-320 mg flav/g	Insumo de la industria cosmética y de alimentos como antioxidante estable.
	Extracto supercrítico enriquecido en flavonoides 240-260 mg flav/g	Insumo de la industria de cosméticos y alimentos como antioxidante menos estable.

Subproductos	Hidrolato	Recirculación en el proceso de hidrodestilación. Base para la industria de ambientadores. Biorepelentes y bioplaguicidas agrícolas.
	Biomasa residual	Reutilización en el proceso como biocombustible o como abono compostado para cultivos de la misma planta u otras.

Si bien hasta ahora se ha realizado una descripción de una de las modalidades preferidas de la invención, la misma no tiene carácter limitante puesto que la invención solo es limitada por las reivindicaciones a continuación. El experto con habilidad en la materia entenderá que es posible realizar cambios y modificaciones al proceso divulgado en la presente solicitud. Este también puede ser modificado en sus condiciones o etapas sin alejarse del espíritu de la invención.

REIVINDICACIONES

1. Proceso para la extracción de compuestos de interés de plantas, caracterizado porque comprende los pasos de:

a. Reducir el material vegetal a un tamaño de partícula adecuado;

b. Cargar el material vegetal del paso a) en un equipo de destilación;

c. Someter el material vegetal a una primera destilación;

d. Separar los destilados en una fracción liviana y una fracción pesada;

e. Secar el material vegetal del paso c); y

f. Someter el material del paso e) a una extracción con solventes para recuperar otros compuestos;

Caracterizado porque, el proceso se lleva a cabo de manera continua.

2. Proceso de acuerdo con la reivindicación 1, caracterizado porque en el paso a) el tamaño de partículas está entre 0,5 cm y 5 cm.

3. Proceso de acuerdo con la reivindicación 1, caracterizado porque el paso c) se puede realizar mediante un proceso de arrastre con vapor.

4. Proceso de acuerdo con la reivindicación 1, caracterizado porque el paso c) se puede realizar mediante un proceso de hidrodestilación.

5. Proceso de acuerdo con la reivindicación 1, caracterizado porque el paso c) comprende una etapa c1) separar durante los primeros 10 - 30 minutos una fracción liviana mezclada con agua.

6. Proceso de acuerdo con la reivindicación 5, caracterizado porque la fracción obtenida en el paso c1) comprende una fracción volátil enriquecida en precursores de fenilpropanos p-cimeno y gamma-terpineno.

7. Proceso de acuerdo con la reivindicación 1, caracterizado porque la fracción liviana obtenida en el paso d) se combina con la fracción liviana obtenida en el paso c1).

8. Proceso de acuerdo con la reivindicación 7, caracterizado porque la fracción pesada es pasada a una columna de fraccionamiento.

9. Proceso de acuerdo con la reivindicación 7, caracterizado porque la fracción pesada es sometida a un proceso de cristalización.

10. Proceso de acuerdo con la reivindicación 1, caracterizado porque el paso f) se realiza con mezcla hidroalcohólica.

11. Proceso de acuerdo con la reivindicación 1, caracterizado porque el paso f) se realiza con dióxido de carbono supercrítico y etanol.

12. Proceso de acuerdo con la reivindicación 1, caracterizado porque el hidrolato obtenido en el paso c se recircula durante el proceso y al final del proceso se colecta como subproducto útil para fabricar ambientadores, bioplaguicidas, repelentes, entre otros.

13. Proceso de acuerdo con la reivindicación 1, caracterizado porque el material vegetal extraído en el paso f es utilizado como subproducto para compostaje o biocombustible útil como fuente de energía para el proceso.

REIVINDICACIONES MODIFICADAS
recibidas por la oficina Internacional el 20 Abril 2018 (20.04.2018)

1. Proceso para la extracción de compuestos de interés de *Lippia origanoides,* caracterizado porque comprende los pasos de:

a. Reducir el material vegetal de *Lippia origanoides* a un tamaño entre 0,5 cm y 5 cm;

b. Cargar el material vegetal del paso a) en un equipo de destilación;

c. Someter el material vegetal a una primera destilación;

d. Separar los destilados en una fracción liviana y una fracción pesada;

e. Secar el material vegetal del paso c); y

f. Someter el material del paso e) a una extracción con solventes para recuperar otros compuestos;

Caracterizado porque, el proceso se lleva a cabo de manera continua.

2. Proceso de acuerdo con la reivindicación 1, caracterizado porque el paso c) se puede realizar mediante un proceso de arrastre con vapor.

3. Proceso de acuerdo con la reivindicación 1, caracterizado porque el paso c) se puede realizar mediante un proceso de hidrodestilación.

4. Proceso de acuerdo con la reivindicación 1, caracterizado porque el paso c) comprende una etapa c1) separar durante los primeros 10 - 30 minutos una fracción liviana mezclada con agua.

5. Proceso de acuerdo con la reivindicación 5, caracterizado porque la fracción obtenida en el paso c1) comprende una fracción volátil enriquecida en precursores de fenilpropanos p-cimeno y gamma-terpineno.

6. Proceso de acuerdo con la reivindicación 1, caracterizado porque la fracción liviana obtenida en el paso d) se combina con la fracción liviana obtenida en el paso c1).

7. Proceso de acuerdo con la reivindicación 6, caracterizado porque la fracción pesada es pasada a una columna de fraccionamiento.

8. Proceso de acuerdo con la reivindicación 6, caracterizado porque la fracción pesada es sometida a un proceso de cristalización.

9. Proceso de acuerdo con la reivindicación 1, caracterizado porque el paso f) se realiza con mezcla hidroalcohólica.

10. Proceso de acuerdo con la reivindicación 1, caracterizado porque el paso f) se realiza con dióxido de carbono supercrítico y etanol.

11. Proceso de acuerdo con la reivindicación 1, caracterizado porque el hidrolato obtenido en el paso c se recircula durante el proceso y al final del proceso se colecta como subproducto útil para fabricar ambientadores, bioplaguicidas o repelentes.

12. Proceso de acuerdo con la reivindicación 1, caracterizado porque el material vegetal extraído en el paso f) es utilizado como subproducto para compostaje o biocombustible útil como fuente de energía para el proceso.

DECLARACION CONFORME AL ARTÍCULO 19.1

Se corrige la reivindicación 1, limitando el proceso a la especie *Lippia orígánoides* con una primera etapa de reducción de tamaño entre 0,5 cm y 5 cm.

Se elimina la reivindicación 2 que reclamaba el tamaño entre 0,5 cm y 5 cm del material vegetal y se incorpora en la reivindicación 1.

Se reemplazan entonces las reivindicaciones iniciales 1 a 13 por las reivindicaciones corregidas 1 a 12. Las reivindicaciones presentadas definen el proceso cuya protección se solicita en la descripción en concordancia también con la figura 1 y con los ejemplos presentes en la descripción. Las reivindicaciones corregidas son claras, concisas y se limitan a la planta *Lippia orígánoides* fundamentándose enteramente en la descripción.

Por otro lado, la figura 1 esta descrita en el capítulo descriptivo; pero para mayor claridad se explica el proceso de acuerdo con el esquema de la figura 1 así:

El proceso comienza con la entrada del material vegetal (1) tomado de la planta *Lippia orígánoides.* La biomasa, es secada en el horno (2). El material es sometido a un tratamiento de reducción de tamaño de partícula en el molino (3). El material vegetal con tamaño de partícula reducido se carga a un alambique de destilación (4) para separar el aceite esencial. El aceite es separado del hidrolato en un decantador Florentino (5). La fracción pesada decantada se introduce a una columna de destilación fraccionada (6), en donde los fenilpropanos son concentrados. Los fenilpropanos productos de destilación se solidifican en el cristalizador (7).

El material vegetal destilado es nuevamente secado en el horno (8) y molido en el molino (9). Aquí, es posible usar dos metodologías de extracción. a) Extracción hidroalcohólica del material vegetal, donde agua y etanol se mezclan en el extractor agitador (10). Un separador *flash* (11) separa el etanol de la mezcla. Finalmente, las moléculas son concentradas en un liofilizador (12). El etanol y agua son reintegrados al extractor agitado (10). b) La extracción con dióxido de carbono supercrítico y etanol, donde el material vegetal se extrae con una corriente de CO2 y etanol proveniente de las bombas de alta presión (13) y (14). La extracción ocurre en un extractor de alta presión (15). El CO2 es separado de la mezcla en el ciclón (16) y reintegrado al proceso mediante el sistema de recirculación (17). La mezcla etanol y extracto se separa en la unidad *flash* (18). El etanol evaporado es reintegrado a la bomba (14) completando el ciclo. El extracto es colectado puro en el fondo de la destilación *flash.* El material vegetal despojado del aceite esencial y el extracto es compostado en las piscinas (19) o bien secado para completar así su aprovechamiento como abono o biocombustible.

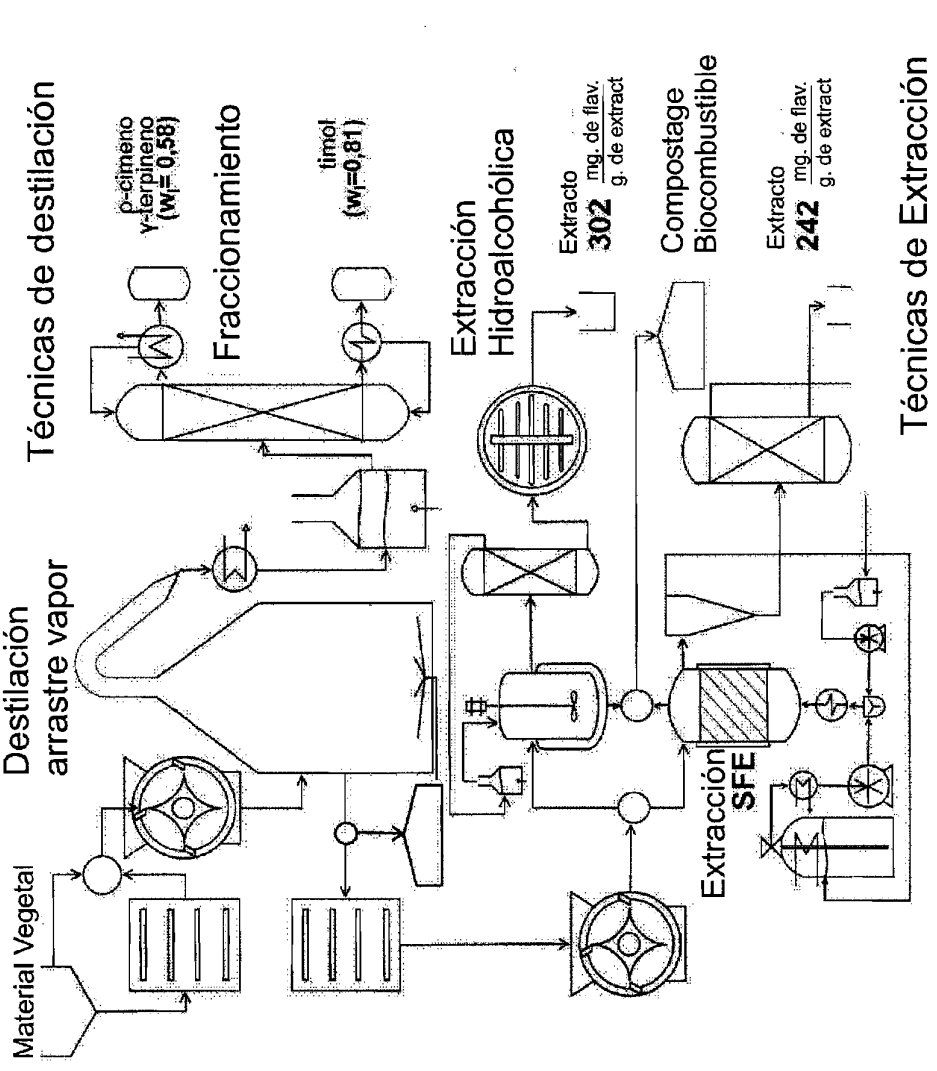

Figura 1: Es un diagrama esquemático del proceso de acuerdo con la presente invención

INTERNATIONAL SEARCH REPORT

International application No.
PCT/IB2017/057862

A. CLASSIFICATION OF SUBJECT MATTER

C11B9/02 (2006.01)

According to International Patent Classification (IPC) or to both national classification and IPC

B. FIELDS SEARCHED

Mínimum documentation searched (classification system followed by classification symbols)
C11B

Documentation searched other than mínimum documentation to the extent that such documents are included in the fields searched

Electronic data base consulted during the international search (ñame of data base and, where practicable, search terms used)

EPODOC, INVENES, WPI, XPESP, INTERNET

C. DOCUMENTS CONSIDERED TO BE RELEVANT

Category*	Citation of document, with indication, where appropriate, of the relevant passages	Relevant to claim No.
A	VÁSQUEZ CARREÑO, D.A. El orégano de monte (Lippia origanoides) del Alto Patía: Efecto del método de obtención de sus extractos sobre la composición y la actividad antioxidante de los mismos. 2012 [on line] [retrieved the 05/03/2018]. Retrieved from Internet <URL: http://www.bdi<ncal.ur:ai.edu.cO/9018/1/19751420[2.pdf>	1-13
A	STASCHENKO, E., et al. Comparison of different extraction methods for the analysis of volatile secondary metabolites of Lippia alba (Mill.)N.E. Brown, grown in Colombia, and evaluation of its in vitro antioxidant activity. Journal of Chomatography A, 2004, N° 1025, Pages 93-103 [on line] [retrieved on 05/03/2018]. Abstract. Retrieved from DataBase XPESP.	1-13

☐ Furfher documents are listed in the continuation of Box C. ☐ See patent family annex.

* Special categories of cited documents:
"A" document defining the general state of the art which is not considered to be of particular relevance.
"E" earlier document but published on or after the international filing date
"L" document which may throw doubts on priority claim(s) or which is cited to establish the publication date of another citation or other special reason (as specified)
"O" document referring to an oral disclosure use, exhibition, or other means.
"P" document published prior to the international filing date but later than the priority date claimed
"T" later document published after the international filing date or priority date and not in conflict with the application but cited to understand the principie or fheory underlying the invention
"X" document of particular relevance; the claimed invention cannot be considered novel or cannot be considered to involve an inventive step when the document is taken alone
"Y" document of particular relevance; the claimed invention cannot be considered to involve an inventive step when the document is combined with one or more other documents , such combination being obvious to a person skilled in the art
"&" document member of the same patent family

Date of the actual completion of the international search	Date of mailing of the international search report
06/03/2018	**(08/03/2018)**
Ñame and mailing address of the ISA/ OFICINA ESPAÑOLA DE PATENTES Y MARCAS Paseo de la Castellana, 75 - 28071 Madrid (España) Facsímile No.: 91 349 53 04	Authorized officer J. López Nieto Telephone No. 91 3498426

Form PCT/ISA/210 (second sheet) (January 2015)

INFORME DE BÚSQUEDA INTERNACIONAL

Solicitud internacional nº
PCT/IB2017/057862

A. CLASIFICACIÓN DEL OBJETO DE LA SOLICITUD
C11B9/02 (2006.01)

De acuerdo con la Clasificación Internacional de Patentes (CIP) o según la clasificación nacional y CIP.

B. SECTORES COMPRENDIDOS POR LA BÚSQUEDA

Documentación mínima buscada (sistema de clasificación seguido de los símbolos de clasificación)
C11B

Otra documentación consultada, además de la documentación mínima, en la medida en que tales documentos formen parte de los sectores comprendidos por la búsqueda

Bases de datos electrónicas consultadas durante la búsqueda internacional (nombre de la base de datos y, si es posible, términos de búsqueda utilizados)
EPODOC, INVENES, WPI, XPESP, INTERNET

C. DOCUMENTOS CONSIDERADOS RELEVANTES

Categoría*	Documentos citados, con indicación, si procede, de las partes relevantes	Relevante para las reivindicaciones n°
A	VÁSQUEZ CARREÑO, D.A. El orégano de monte (Lippia origanoides) del Alto Patía: Efecto del método de obtención de sus extractos sobre la composición y la actividad antioxidante de los mismos.. 2012 [en línea] [recuperado el 05/03/2018]. Recuperado de Internet <URL: http://www.bdigital.unal.edu.co/9018/1/19751420122.pdf>	1-13
A	STASCHENKO, E., et al. Comparison of different extraction methods for the analysis of volatile secondary metabolites of Lippia alba (Mill.)N.E. Brown, grown in Colombia, and evaluation of its in vitro antioxidant activity. Journal of Chomatography A, 2004, N° 1025, Páginas 93-103 [en línea] [recuperado el 05/03/2018]. resumen. Recuperado de Base de datos XPESP.	1-13

□ En la continuación del recuadro C se relacionan otros documentos

☐ Los documentos de familias de patentes se indican en el anexo

* Categorías especiales de documentos citados:

"A" documento que define el estado general de la técnica no considerado como particularmente relevante.

"E" solicitud de patente o patente anterior pero publicada en la fecha de presentación internacional o en fecha posterior.

"L" documento que puede plantear dudas sobre una reivindicación de prioridad o que se cita para determinar la fecha de publicación de otra cita o por una razón especial (como la indicada).

"O" documento que se refiere a una divulgación oral, a una utilización, a una exposición o a cualquier otro medio.

"P" documento publicado antes de la fecha de presentación internacional pero con posterioridad a la fecha de prioridad reivindicada.

"T" documento ulterior publicado con posterioridad a la fecha de presentación internacional o de prioridad que no pertenece al estado de la técnica pertinente pero que se cita por permitir la comprensión del principio o teoría que constituye la base de la invención.

"X" documento particularmente relevante; la invención reivindicada no puede considerarse nueva o que implique una actividad inventiva por referencia al documento aisladamente considerado.

"Y" documento particularmente relevante; la invención reivindicada no puede considerarse que implique una actividad inventiva cuando el documento se asocia a otro u otros documentos de la misma naturaleza, cuya combinación resulta evidente para un experto en la materia.

"&" documento que forma parte de la misma familia de patentes.

Fecha en que se ha concluido efectivamente la búsqueda internacional.	Fecha de expedición del informe de búsqueda internacional.
06/03/2018	**08 de marzo de 2018 (08/03/2018)**
Nombre y dirección postal de la Administración encargada de la búsqueda internacional OFICINA ESPAÑOLA DE PATENTES Y MARCAS Paseo de la Castellana, 75 - 28071 Madrid (España) N° de fax: 91 349 53 04	Funcionario autorizado J. López Nieto N° de teléfono 91 3498426